INFLUENCES OF STIMULUS CHARACTERISTICS AND OCULAR SURFACE CONDITIONS ON NON-INVASIVE CORNEAL SENSITIVITY MEASUREMENT

Daniela Sonja Nosch

School of Optometry and Vision Sciences

Cardiff University

This thesis is presented in fulfillment of the requirements for the Degree of Doctor of Philosophy in Cardiff University

2015

ABSTRACT

Purpose: To *i)* investigate the stimulus characteristics of the Belmonte OPM pneumatic aesthesiometer *in vitro* and *in vivo; ii)* explore the relationship between corneal sensitivity threshold (CST), spontaneous eye blink rate (SEBR), ocular surface temperature (OST) and tear film quality, using the non-contact aesthesiometer (NCCA), and *iii)* investigate the relationship between heating and cooling of the ocular surface on CST (with the NCCA).

Methods: Stimulus flow rate (airflow meter), air stimulus volume (air capture) and force (weight scales) were recorded *in vitro*. Stimulus temperature was measured *in vitro* (using thermocouples) and *in vivo* (via a thermal infrared camera). SEBR, CST, OST, non-invasive tear break-up time (NIBUT) and lipid pattern of the tear film were recorded. CST (using NCCA), OST and tear film quality were obtained at baseline, and after increasing and decreasing OST, using heated goggles or cooling gel mask, respectively, until OST baseline level was reached again. OST was recorded during stimulus presentation at CST, immediately after heating and cooling of the ocular surface.

Conclusions: Stimulus characteristics measured *in vitro* showed little variability and may therefore be considered as reliable. Stimulus temperature recorded *in vivo* showed that a change in stimulus flow rate produced a small, but statistically significant effect on OST. Consequently, this air stimulus may not be exclusively 'mechanical', and may provoke an additional response from temperature sensitive C fibres. A moderate correlation between corneal sensitivity and blink frequency was established, and a strong correlation between tear film quality, SEBR and OST was obtained, emphasising that ocular surface condition represents one important trigger for the initiation of a blink.

After both an increase and a decrease of OST, a greater localised OST decrease was required at CST, indicating that heating or cooling of the ocular surface may affect the nervous activity / sensitivity of cold thermoreceptors in the superficial cornea.

This work has not been submitted in substance for any other degree or award at this or any other university or place of learning, nor is being submitted concurrently in candidature for any degree or other award.

June 5th 2015, Daniela Sonja Nosch

This thesis is being submitted in partial fulfillment of the requirements for the degree of PhD

June 5th 2015, Daniela Sonja Nosch

This thesis is the result of my own independent work/investigation, except where otherwise stated. Other sources are acknowledged by explicit references. The views expressed are my own.

June 5th 2015, Daniela Sonja Nosch

I hereby give consent for my thesis, if accepted, to be available online in the University's Open Access repository and for inter-library loan, and for the title and summary to be made available to outside organisations.

June 5th 2015, Daniela Sonja Nosch

TABLE OF CONTENTS

LIST OF FIGURES

LIST OF TABLES

ACKNOWLEDGEMENTS

Huge thanks go to my principal supervisors, Prof. Paul Murphy and Dr. Heiko Pult, for their encouragement, positive thinking, advice and guidance throughout my PhD. Special thanks also go to my associate supervisors, Prof. Christine Purslow and Dr. Julie Albon. They have all been wonderful in sharing their great experience and valuable knowledge.

I am very grateful to my dear husband Beat for his love and patience throughout the PhD period – his understanding and encouragement have been endless.

I would like to thank all the staff, students and friends who took the time to sit in as subjects several times for my clinical experiments.

I am also very grateful to Prof. Roland Joos who guided me through challenging statistical analyses with his tremendous expertise.

LIST OF ABBREVIATIONS

Ach	acetylcholine
ASIC	acid-sensing ion channel
GFR	glial cell-derived neurotrophic factor receptor
CGRP	calcitone gene-related peptide
CL	contact lens
CMR1	cold menthol receptor type 1
CNTF	ciliary neurotrophic factor
CST	(central) corneal sensitivity threshold
DED	dry eye disease
Dk	diffusion coefficient (oxygen permeability)
DEG	degenerin sodium channel
EW	extended wear
GDNF	glial cell-derived neurotrophic factor
GP	gas permeable
HEMA	hydroxyethylmethacrylate
IBI	inter-blink interval
IVCM	*in vivo* confocal microscopy
LASIK	*in situ* keratomileusis
LFU	lacrimal functional unit
LIPCOF	lid parallel conjunctival folds
NCCA	non-contact corneal aesthesiometer
NGF	nerve growth factor
NIBUT	non-invasive tear break-up time
NHC	noxious heat channel
OPM	ocular pain meter (Belmonte air gas aesthesiometer)
OSDI	ocular surface disease index
OST	ocular surface temperature
PMMA	polymethylmethacrylate
PRK	photorefractive keratectomy
RGP	rigid gas permeable
SEBR	spontaneous eye blink rate

SP	substance P
TBUT	tear break-up time
TRPM8	transient receptor potential menthol 8
VIP	vasoactive intestinal polypeptide
VR	vanilloid receptor

CHAPTER 1

Introduction and literature review

1.1 Introduction

Corneal sensitivity represents a neurological response from the free nerve endings within the epithelium. They are sensitive to mechanical, electrical, chemical or thermal stimuli and hence have a protective function for the cornea: mechanical stimulation evokes sensations of touch and pain, electrical stimulation leads to pain and irritation, cold thermal stimulation gives rise to a 'cooling' sensation, hot thermal stimulation causes irritation, and chemical stimulation (CO_2) is experienced as a burning or stinging pain.

Corneal nerves play an important role in cell growth and proliferation of epithelial cells, wound healing and repair.[1,2] They regulate this process by releasing trophic neuropeptides, such as substance P (SP) and calcitonin gene-related peptide (CGRP).[3-6] In experimental studies, corneal denervation has been reported to result in epithelial changes: increased permeability, decreased proliferation, changed appearance and delayed wound healing.[7,8] Therefore, intact corneal innervation is required to maintain the integrity of a normal corneal epithelium.

In addition to their essential role in maintaining a healthy ocular surface, it has been proposed that thermal nerve endings serve the cornea to detect thinning or breaks in the pre-ocular tear film as part of the normal blink process.[9,10] As a result of evaporation, the open eye experiences a slight reduction in surface temperature across the cornea and conjunctiva.[11] Murphy et al. postulated that sensory corneal and conjunctival nerves detect greater temperature changes caused by localised tear film thinning, and consequently initiate a blink.[12] This would reform the tear film and re-stabilise the pre-ocular tear film temperature.

Many published studies are based on measurements using the Cochet-Bonnet aesthesiometer, which is criticised for its many shortfalls.[13-18] The development of air gas aesthesiometers has permitted separate application of controlled mechanical pulses, irritant chemical stimuli and hot (or cold) air pulses onto the ocular surface.[14,19] The

Belmonte aesthesiometer was the first instrument to deliver chemical (CO_2), thermal, and mechanical stimuli to the ocular surface at different temperatures.[19] This novel method of ocular surface sensitivity measurement has been developed to enable the assessment of corneal nerve function by subjectively measuring the corneal sensitivity threshold of healthy eyes, with the purpose of learning more about the extent of loss and recovery of corneal nerve function after surgery, during and after disease, and with contact lens wear. However, there are some discrepancies between different research groups as to what temperature the air stimulus should be, in order to deliver a mechanical stimulus.[19-21] Furthermore, it is unclear if a true threshold for mechanical corneal sensitivity can be established with the aid of an air gas aesthesiometer with increasing levels of airflow rates, since this would require that a localised corneal temperature change be excluded. This would be difficult to obtain, since there is a cooling effect from the airflow caused by localised evaporation from the tear film.[22]

It has been hypothesised that corneal sensitivity must play an important role in triggering involuntary blinks, because it has been shown that the blink rate reduces when corneal sensation is blocked with a local anaesthetic.[10,23,24] Is involuntary spontaneous blinking, determined by a local corneal reflex that is dependent on corneal sensitivity, possibly triggered by ocular surface cooling when the tear film progressively evaporates, as proposed by some researchers?[25,26] However, the mechanisms involved in the initiation of an eye-blink are complex, as the local ocular sensory input only represents one trigger, next to other external influences and internal factors that are under cortical control.[27,28]

Electrophysiological recordings from the cat and guinea pig cornea have shown that cold thermoreceptors exhibit a spontaneous firing rate of nerve impulses at a normal ocular surface temperature (34-35°C) and that they increase the frequency and amplitude of their impulse activity when temperature decreases.[29,30] However, upon warming of the ocular surface, cold thermoreceptors are silenced.[29,31] A fraction of polymodal fibres have been shown to also increase their firing rate when corneal temperature is reduced to less than 29°C.[32,33] These nerve responses offer a possible pathway for an ocular cooling stimulus, however, it is unclear if localised heating or

cooling of the ocular surface affects the sensitivity of these thermoreceptors in the superficial cornea.

This thesis aims to answer the following three questions:
1) Does the Belmonte OPM aesthesiometer provide a reliable stimulus to obtain accurate and reapeatable corneal sensitivity measurements? Specifically, whether cooling and mechanical sensitivity thresholds can be obtained separately.
2) Can a correlation between corneal sensitivity and blink frequency be established, which would confirm that ocular surface condition represents an important trigger for the initation of a blink?
3) Is ocular surface sensation affected by heating and/or cooling of the ocular surface, similarly to cutaneous cold-sensitive receptors?

The following literature review will cover the specific background knowledge relevant to the contents of this thesis:

1.2 Corneal and conjunctival innervation

Corneal innervation originates from the ophthalmic branch of the trigeminal nerve. The ophthalmic nerve branches into the frontal, lacrimal and nasociliary nerve. The long posterior ciliary nerve branching off the nasociliary nerve penetrates the posterior of the eye and passes between the sclera and choroid, in order to supply the cornea, the iris, the sensory fibres to the ciliary body, the trabecular meshwork and the sclera (Figure 1.1). It has been shown, in some cases, that the inferior cornea may also receive some innervation from the maxillary branch of the trigeminal nerve.[1]

Sensory conjunctival innervation is supplied from various sensory branches of the trigeminal nerve: the lacrimal and frontal branches of the ophthalmic nerve are thought to innervate the superior bulbar conjunctiva.[34] The lateral and medial conjunctiva are innervated by the lacrimal nerve and the infratrochlear division of the nasociliary branch of the ophthalmic nerve.[34] There is some dispute as to whether the inferior conjunctiva is supplied by the infraorbital division of the maxilliary nerve, or by the lacrimal nerve.[35]

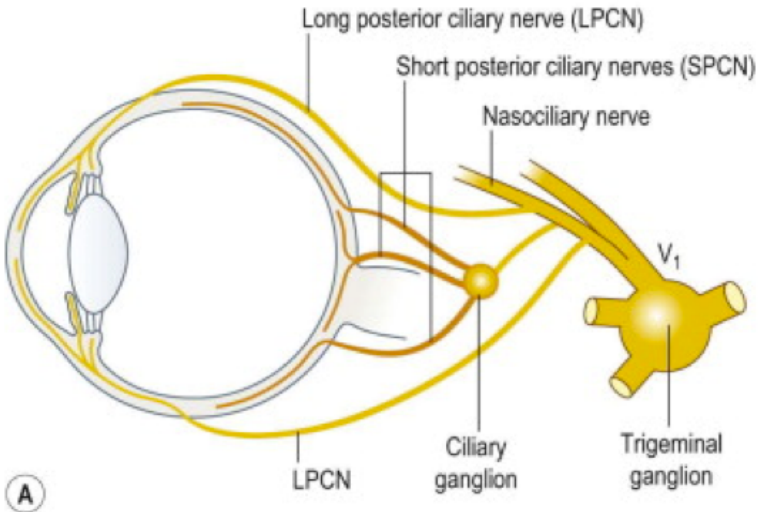

Figure 1.1: Corneal Innervation (Adler's Physiology of the Eye, 2011)[36]

1.3 Corneal anatomy

The cornea is the transparent and avascular outer surface of the eye, through which all light rays travel to form an optical image on the retina. It is therefore essential that its surface is regular and smooth to maximise the eye's visual potential and to minimise any unwanted interference that would cause scattering or deviation of the transmitting light rays.

On average, the cornea has a horizontal diameter of 11.7mm and a mean central thickness of 0.54±0.03mm,[37] increasing to approximately 0.65mm peripherally.[38] The corneal surface is spherical within a central radius of 3mm, but flattens progressively in the periphery to assume an elliptical shape. Its functions are to protect the interior ocular structures and to provide 70% of the refractive power of the eye. The cornea consists of five layers: the epithelium, Bowman's layer, the stroma, Descemet's membrane and the endothelium (Figure 1.2).

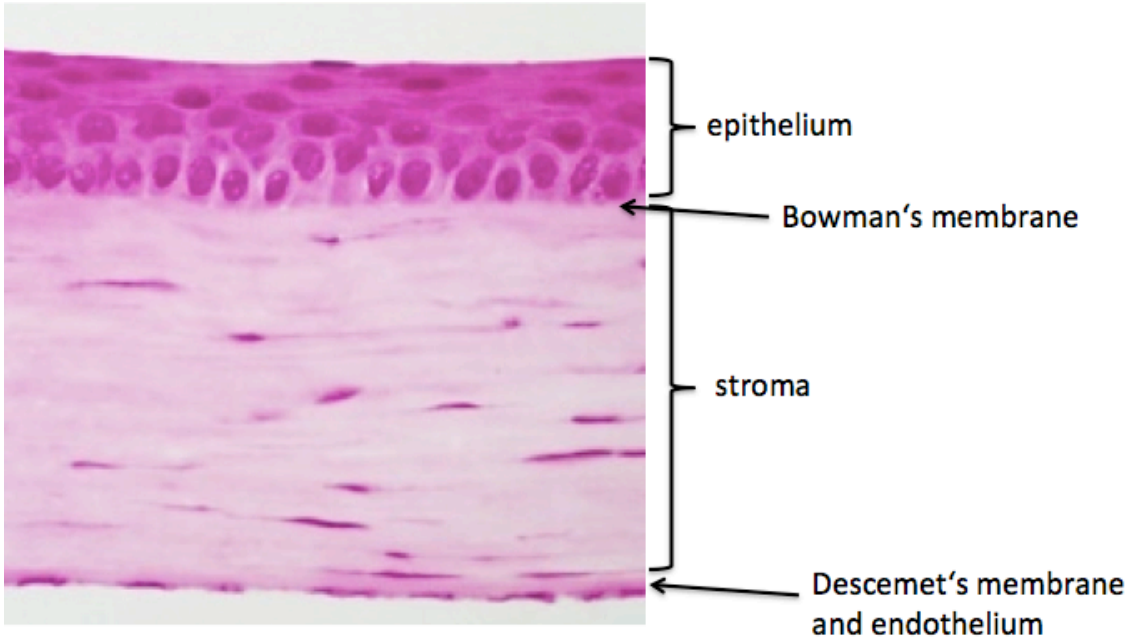

Figure 1.2: The human cornea http://www.sciencephoto.com/images/imagePopUpDetails.html?pop=1&id=804240035&pviewid=&country=67&search=&matchtype=FUZZY; accessed 2011 – 15.02.11. Science Photo Library).

1.3.1 The corneal epithelium

The epithelium is formed as a non-keratinised stratified squamous layer and is five to seven cells thick, measuring about 50μm.[39] It thickens in the periphery and is continuous with the conjunctival epithelium at the limbus. It consists of a superficial or outer squamous layer (two cells thick), a middle or wing layer (two to three layers), and a deeper basal cell layer (a single layer of columnar cells; Figure 1.3).[40] Epithelial cells migrate from the inner to the outer layer, as newly formed cells in the basal layer, derived from limbal stem cell population, push them up and outward. Having reached the outer surface, they lose their attachments and are sloughed into the tear film.[41] Tight junctions between the superficial cells form a barrier function to the tear film.[42] These junctions have to be broken before the cells can be sloughed. Additional adhesion between the cells is provided by numerous desmosomes. The Golgi complex is more prominent in the basal layer.[43] On the outer surface, there are microvilli (fingerlike projections) and microplicae (ridgelike projections).[44] Adhering to the microvilli is a glycocalyx (secreted by the surface epithelial cells), which contains mucin-like substances that are important for the spreading and attachment of the pre-corneal tear film.[38] The wing cells have winglike lateral processes, are polyhedral, and have convex

anterior surfaces and concave posterior surfaces that fit over the basal cells. They form the intermediate epithelial layer and represent a network consisting of intermediate filaments and few microtubules.[43] They also contain free glycogen granules and sparse mitochondria. The wing cells become increasingly flattened that occurs during the transition from the thicker basal cells to the flattened superficial cells. The basal cells have a columnar shape and contain oval-shaped nuclei displaced towards the apex oriented at right angles to the surface. Around their nuclei, there are some mitochondria and, less prominently, a Golgi complex.[43] They also contain a large number of filaments and glycogen granules. Basal cells are joined together by zonula adherens and gap junctions. Their basal surface attaches to the underlying basement membrane (basal lamina) via hemidesmosomes. Anchoring fibrils pass from these junctions through Bowman's layer into the stroma.[45]

1.3.1.1 Epithelial replacement

As mentioned above, the surface cells are continually being shed into the tear film and their replacement is essential for the maintenance of the smooth corneal surface. This renewal of the epithelium involves cell division, migration, differentiation, and senescence.[36] Cell proliferation occurs in the basal layer. Basal cells move up to become wing cells, and wing cells move up to become surface cells. Only the cells in contact with the basement membrane are able to divide and they lose this ability when they are displaced upwards into the wing cell layer.[46] The stem cells are located in a 0.5 to 1.0mm wide band around the corneal periphery at the limbus and represent the source for renewal of the corneal basal cell layer. Basal cells migrate slowly from the periphery toward the centre of the cornea.[47,48] The epithelium renews itself every seven days.[41,49] The corneal epithelial tissue heals rapidly: minor abrasions within hours and larger ones often overnight. However, the healing and complete replacement of the basement membrane and hemidesmosomes may take months.[50,51]

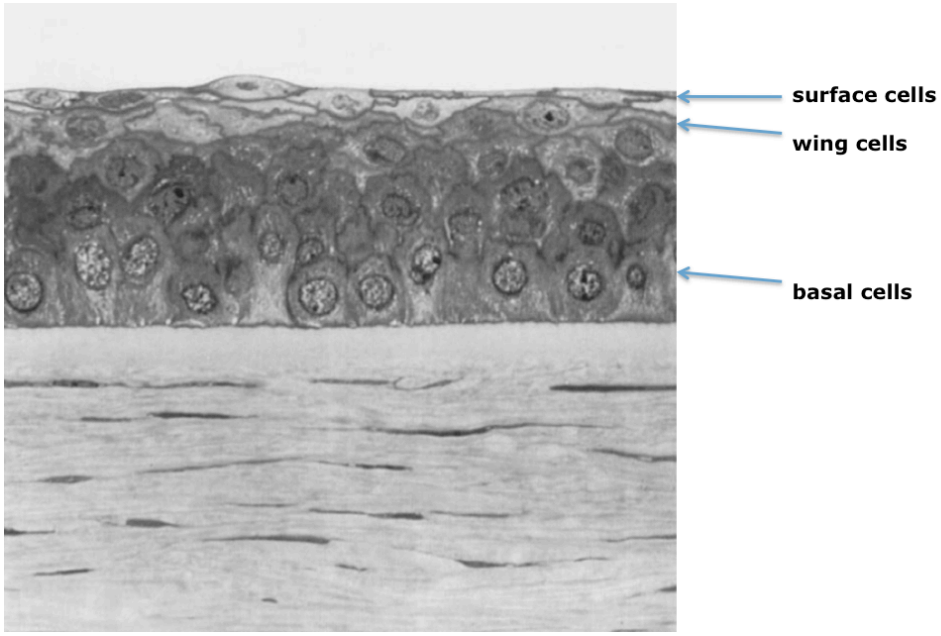

Figure 1.3: The corneal epithelium and Bowman's layer, from Beuerman and Pedroza (1996)[43]

1.3.2 Bowman's layer

Bowman's layer represents an amorphous band of fibrillar material of collagen embedded in a proteglycan matrix.[43] It is approximately 40 to 60nm thick, and its function is unknown.[38] There have been some suggestions that it provides a stabilising element in the cornea.[38] It delivers a foundation for the epithelium, and represents a boundary to the underlying stroma, but is unable to regenerate.[52] Hemidesmosomes running across Bowman's layer enable a strong adherence of the epithelium to the stroma.

1.3.3 The corneal stroma

The stroma consists of stacked lamellae which represent 90% (approx. 0.488mm) of the thickness of the corneal thickness (Figure 1.4).[43] It contains keratocytes, fibroblastic cells capable of producing collagen and other extracellular matrix molecules, and neural tissue with associated Schwann cells.[43] Keratocytes are responsible for stromal maintenance. If an insult occurs, they transform to become myofibroblastic and increase the production of stromal collagen. Their density decreases from the superficial to deep stroma and increases from the centre to periphery. Keratocytes display a large nucleus with long slender processes extending from the cell body. The collagen fibrils that make up the stroma are packed in 200-250 lamellae.[38] All lamellae cross the cornea from

limbus to limbus, and individual fibrils are separated by proteoglycans (keratan sulphate and dermatan sulphate). Proteoglycans are macromolecules consiting of a core protein with one or more attached glycosaminoglycan side chains. Glycosaminoglycans are hydrophilic, negatively charged carbohydrate molecules located at specific sites around each collagen fibril. They attract and bind with water, maintaining the precise spatial relationship between individual fibrils.[53] In the posterior stroma, are arranged preferrably in vertical and horizontal directions, whereas in the anterior stroma they are angled at small angles to each other (Figure 1.5).[43] This particular arrangement of collagen imparts a high tensile strength for corneal protection.

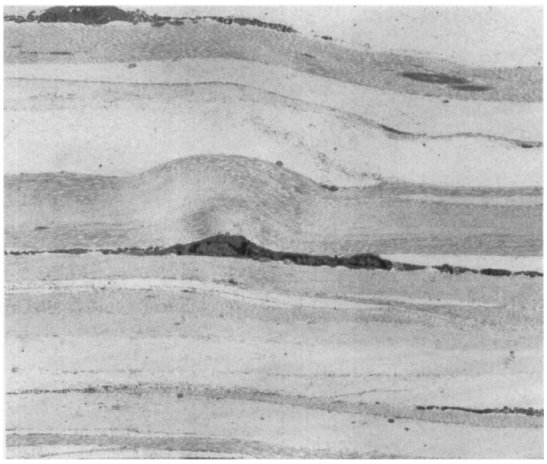

Figure 1.4: The collagenous layers of the corneal stroma, from Beuerman and Pedroza (1996)[43]

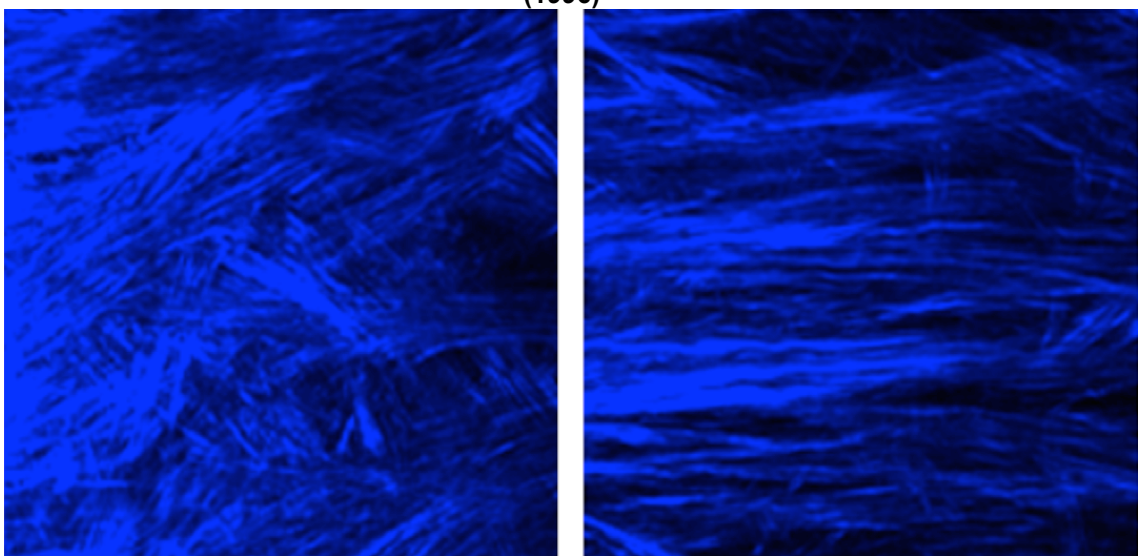

Figure 1.5: Arrangement of collagen fibres in the peripheral mid-(left) and posterior stroma (right), from Kamma-Lorger et al. (2010)[54]

1.3.4. Descemet's membrane and the corneal endothelium

Descemet's membrane is a thick, basal lamina secreted by the endothelium. It consists of an anterior, banded portion and a posterior, non-banded portion. At birth it is 3-4μm thick, the posterior non-banded portion increases in thickness throughout life to reach a total thickness of 10-12μm in the adult.[55] The method of attachment between Descemet's membrane and the neighbouring layers is poorly understood. The attachment sites between the stroma and Descemet's membrane are relatively weak, and so the membrane can be detached easily from the posterior stroma.[56] Hemidesmosomes as anchoring fibrils cannot be seen in Descemet's,[57] hence the adhesions between Descemet's membrane and the endothelium are not typical hemidesmosomes.[58]

The endothelium is a unique, single layer of 400,000 cells that are 4-6 μm thick.[43] These cells have a hexagonal shape and are approximately 20 microns wide (Figure 1.6).[43]

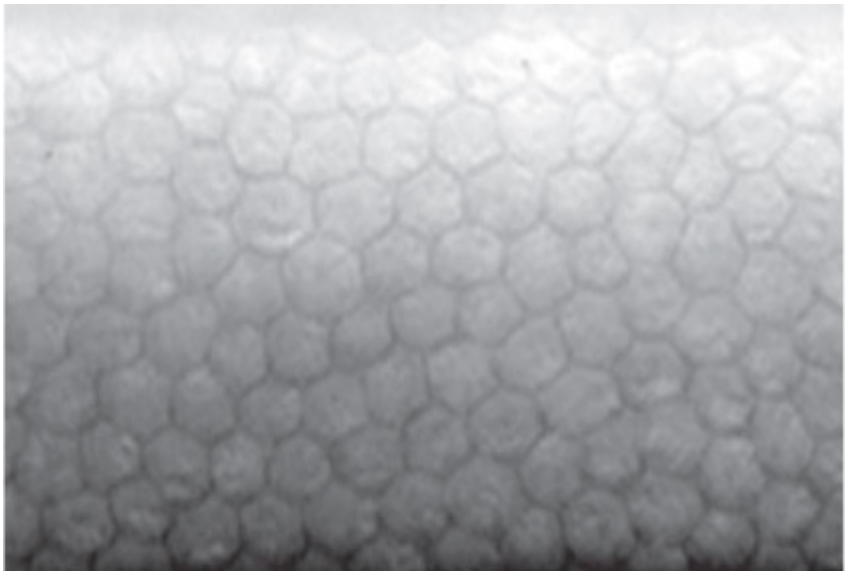

Figure 1.6: Hexagonally shaped cells of the single-layered endothelium (<http://www.scielo.br/img/revistas/pvb/v28n9/06f1.jpg>. Accessed 2011 15.02.11)

The endothelium does not regenerate in primates. When cells are lost, neighbouring cells enlarge to fill the gaps and to maintain tight contact to surrounding cells. Endothelial cells contain a large circular or lobulate nucleus and a cytoplasm rich in organelles, such as mitochondria, elaborate and smooth endoplasmic reticulum, and a prominent Golgi complex. Endothelial cells are responsible for a high ion transport, via an endothelial pump which acts to maintain corneal transparency.[59,60]

1.4 Corneal nerve architecture

The classic understanding of corneal nerve architecture is of a circular limbal plexus, from which radial branches extend into the cornea towards the central area. However, non-invasive *in vivo* confocal microscopy (IVCM) has also made it possible to gain a better understanding of the nerve architecture of the living human cornea.[61] Patel and Ghee created a montage of 315 pictures of the sub-basal nerve complex (located between Bowman's layer and the basal epithelium), obtained with IVCM (Figure 1.7).[62] They observed an arrangement in a radial pattern in three healthy subjects, converging toward an area approximately 1 to 2 mm infero-nasally to the central cornea, with a clockwise whorl or vortex pattern (whorl-like complex) in the area of convergence.

These findings were later confirmed by He et al. and Lum et al.[63,64]

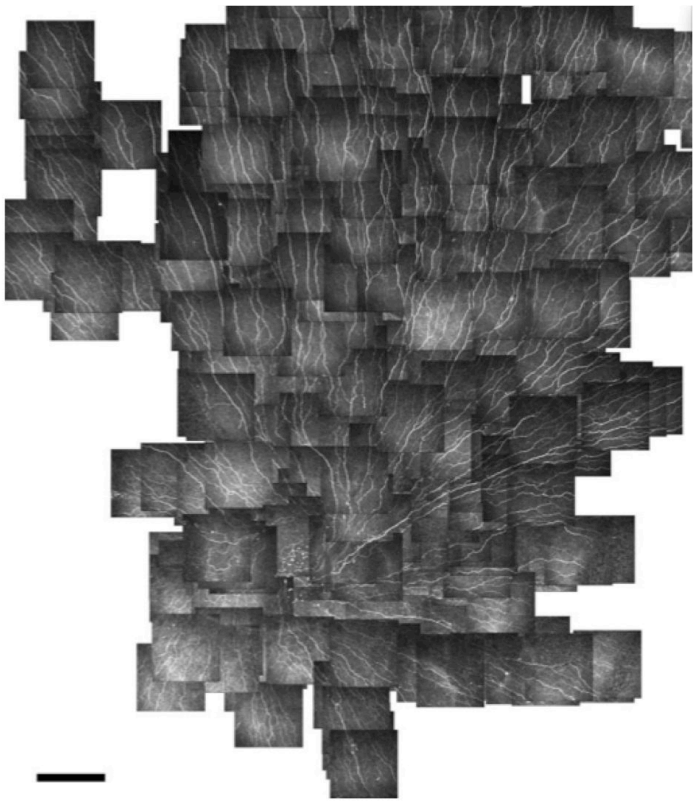

Figure 1.7: Map of the epithelial subbasal nerve complex (Patel and Ghee, 2005).[62]

The subepithelial nerve plexus lies at the interface between Bowman's layer and the anterior stroma. Stromal nerves enter from the sclera or ciliary body and penetrate the stroma in a radial pattern.[63] Some of these nerves are connected at the central area and

form a stromal nerve network (Figure 1.8). A small proportion of these nerves even reach the epithelium.[63]

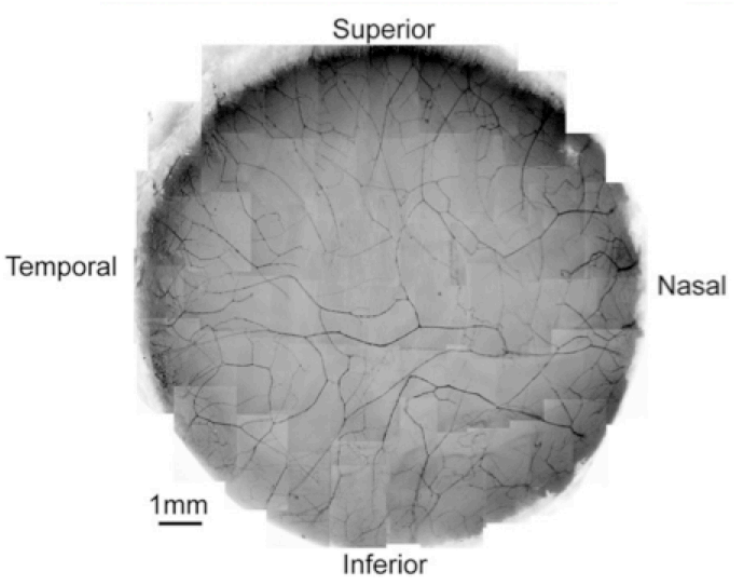

Figure 1.8: Whole mount view of human corneal stromal nerve network (He et al., 2010).[63]

1.5 Ultrastructure of corneal and conjunctival nerves

Twelve to sixteen bundles of myelinated and unmyelinated axons (each containing 900-1200 axons) enter the cornea radially from the limbus into the anterior and mid-stroma.[65] They lose their myelination within 1-2 mm of the limbus and continue into the cornea surrounded only by Schwann cell sheaths.[43,66] Keratocytes have been identified in close proximity to the nerve fibres, which they occasionally enwrap.[1] On their way to the apex, they divide at the mid-stromal level and send fibres anteriorly bending 90° to penetrate Bowman's layer at about 400 sites throughout the peripheral and central cornea.[66] The large nerve bundles divide into several smaller ones, which then bend again at 90° and run beneath the basal epithelial cell layer. Here they divide further and are interconnected with peripheral nerves that enter the basal epithelium from the limbus to form the sub-basal epithelial plexus between the basal epithelial cell layer and Bowman's layer.[67] There is a mixture of straight and beaded nerve fibres. Only individual beaded fibres separate from the sub-basal bundles and course obliquely between the basal cells into the more superficial epithelial cell layers where they eventually terminate at the level of the wing cells.[1]

The nerve fibres are of two types and are arranged according to their type:
Myelinated Aδ fibres run parallel and deeper (within the basal cell layer) below the corneal surface, and are smaller in diameter (Type II in Figure 1.9 and Figure 1.10).[1] They are straight, fast-adapting nerves with a high conduction velocity (mean 6 m/s). They are proposed to respond to mechanical stimuli, and may also be polymodal nociceptors.[29,68-71]

Unmyelinated C fibres run upward from the epithelial plexus towards the surface, traversing the epithelium and approaching the surface within 5μm (Type I in Figure 1.9 and Figure 1.11). They are large, beaded nerves that conduct nerve impulses at a much lower velocity of 2m/s. They respond to thermal and/or chemical stimuli. Many of them have been found to be polymodal and, hence, respond to near-noxious mechanical energy as well.[29,31,66,70]

However, the complete understanding of the functional properties of these different corneal nerve fibres still remains incomplete.

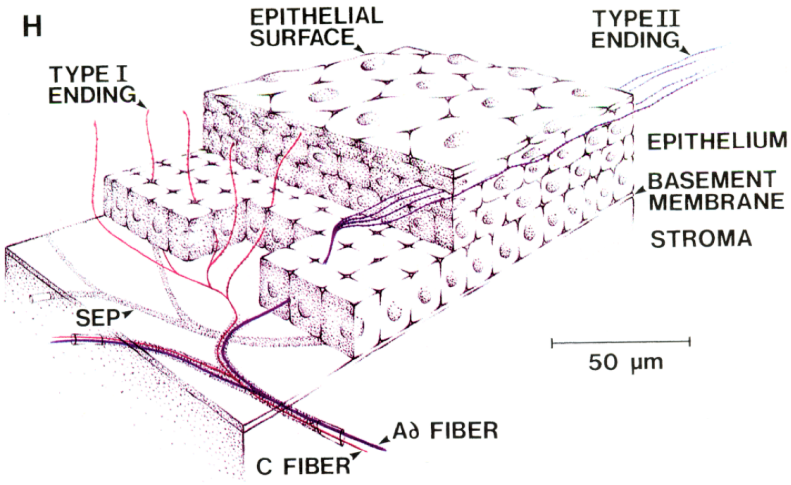

Figure 1.9: Fibre-type specific nerve ending morphology, from McIver and Tanelian (1993).[68]

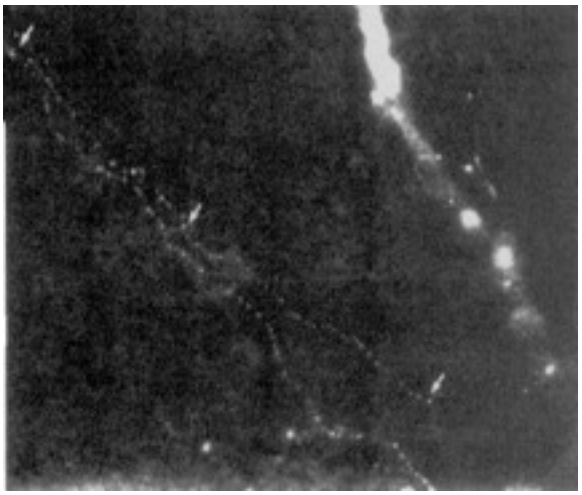

Figure 1.10: Aδ fibres running parallel to corneal surface, from MacIver and Tanelian (1993).[68]

Figure 1.11: Cross-section of C fibres, from McIver and Tanelian (1993).[68]

Most of the conjunctival fibres are unmyelinated and terminate beneath the epithelium in the substantia propria, as free nerve endings.[35] Some rare fibres seem to pass through the basal lamina and terminate within the epithelium.[72] In addition, corpuscular nerve endings were first described by Krause in 1859.[73] These Krause corpuscles have a round or oval encapsulated structure, served by one to three myelinated fibres that lose their myelin sheath before entering the body of the corpuscle. Lawrenson and Ruskell examined cadaver eyes with use of light and electron microscopy and found a high concentration of these corpuscular nerve endings within a narrow, 1.00mm wide, annular zone of limbal conjunctiva, located approximately 0.5mm from the

corneoscleral margin.[74] The function of such complex sensory nerve endings is as yet unknown, however, they may represent receptors for particular sensory modalities.

1.6 Corneal and conjunctival nerve density and receptive field sizes

In vivo confocal microscopy (IVCM) has become a popular method for imaging the cornea.[75-78] Using IVCM, Müller et al calculated that approximately 5400-7200 nerve bundles are present in the sub-basal epithelial plexus.[65] Assuming that each nerve fibre bundle has many side branches, each containing 3-7 individual axons, they estimated the total number of axons to be 19,000-44,000. The total number of nerve endings is not known yet, but it is believed that each nerve fibre has at least 10-30 nerve terminals, which would amount to total number of 315,000 to 630,000.[1,65]

The corneal epithelium is believed to be the most densely innervated tissue in the human body:[1,79] 20 to 40 times more than in tooth pulp and 300-600 times more than skin.[79] Innervation density is greatest at the corneal apex and decreases towards the limbus.[65,79]

From sensory recordings mostly in rabbits and cats, it has been shown that nerve receptive field sizes are large and overlap extensively.[31,69,70] This gives a large amplification effect to a foreign body stimulus, but affects the ability to localise stimuli on the cornea, as a single stimulus will stimulate many receptive fields.[80]

Compared to the cornea, conjunctival innervation is sparse and decreases in density away from the limbus.[81] Consequently, its mechanical sensitivity is lower than the cornea's.[82,83] The edge of the eyelid has been shown to be more sensitive to mechanical stimulation than the bulbar conjunctiva.[82,84]

1.7 The role of nerves in the maintenance of a healthy cornea

Corneal nerves play an important role in maintaining a healthy ocular surface, through their involvement in cell growth and proliferation of epithelial cells, wound healing and repair.[1,2] Dysfunction of corneal innervation produces a degenerative condition known

as neurotrophic keratitis, which is characterised by non-healing epithelial defects and eventual stromal melting. The causes for this condition include desiccation of the corneal surface as a consequence of diminished lacrimal secretions, impaired corneal sensitivity leading to a prolonged blink rate, abnormal epithelial cell metabolism and, hence, inadequate protection against trauma, drying, and infection, as well as a loss of trophic influences supplied by corneal nerves.[85-87] Animal studies gave some insight into how corneal denervation causes morphological and metabolic epithelial disturbances. As a result of ocular nerve injury, squamous epithelial cells at the ocular surface become swollen, and slough off at an accelerated rate into the tear film.[88-90] Multiple punctate epithelial defects appear. Underlying these surface effects, a cascade of metabolic changes occurs: the wing and basal cell layers show a loss of tonofilaments, cells become abnormally rounded and intercellular spaces become larger.[88,91,92] Basal epithelial cell mitogenesis decreases, the epithelium thins.[93-96] Furthermore, the epithelium may become more permeable, it stores less cellular glycogen, takes up less oxygen, and shows an altered hypoxic swelling response.[89,96,97] Corneal denervation also inhibits corneal wound healing, giving rise to spontaneous epithelial erosions in newly healed corneas.[8,88,98]

How exactly do corneal nerve fibres maintain a healthy cornea and how do they promote wound healing after eye injuries?

In vitro co-culture studies suggest that neurons and corneal epithelial cells support one another trophicly through the mutual release of soluble substances: trigeminal neurons release neurotransmitters and neuropeptides, thus stimulating corneal epithelial cell growth, proliferation, differentiation, and type VII collagen production.[7,99] Corneal epithelial cells release soluble factors, such as nerve growth factor (NGF) and glial cell-derived neurotrophic factor (GDNF), to promote neurite extension and survival.[100-102] Stromal keratocytes also produce neurotrophins.[103,104] The movement of the eyelid over the cornea during blinking, and desiccation of the ocular surface stimulate the release of neurochemicals from the corneal nerve terminals.[1,105] The question has been posed whether patients with impaired corneal innervation due to herpetic keratitis, diabetes, prolonged contact lens wear, advanced age or refractive surgery are more at risk of developing a compromised epithelium and hence, of ulceration, due to a reduced trophic support provided by corneal nerves and the tear film.[106]

In addition to their essential role in maintaining a healthy ocular surface, it has been proposed that they also play an important role in maintaining the resting tear flow (as well as triggering lacrimation in the presence of a foreign body), as their afferent impulses from the ocular surface lead to a reflex response:[107] the thermal nerve endings serve the cornea to detect thinning or breaks in the pre-ocular tear film.[9,10] Between spontaneous eye blinks evaporation occurs and the open eye experiences a slight reduction in surface temperature across the cornea and conjunctiva.[11] The sensory maintenance of the tear film will be discussed in more detail in section 1.12.

1.8 Neuropeptides and neurotransmitters

Corneal axons appear morphologically homogenous when they are visualised using histology or electron microscopy techniques. However, immunohistochemical techniques have indicated different neuropeptides within the cell soma and peripheral axonal fibres of corneal neurons, suggesting that they are functionally heterogenous. Dense networks of the neuropeptide, substance P (SP), have been demonstrated.[108,109] A number of publications suggest that SP contributes to regeneration and wound healing of the corneal epithelium: It stimulates corneal epithelial cell proliferation,[99,110] migration[4] and adhesion.[111-113] SP is present in the normal cornea, together with SP-specific (NK1) receptors on epithelial cells.[114-116] SP can also be found in normal tears, and its concentration decreases in patients with herpetic keratitis and other types of fifth nerve palsy.[117] However, some of its actions only occur through its synergistic interactions with other growth factors such as insulin-like growth factor-1 (IGF-1).[3,111,116,118-120] Furthermore, SP promotes epithelial cell adhesion and migration by enhancing the expresion of adhesion molecules and cytoskeletal proteins, such as E-cadherin and alpha 5 integrin.[111-113] The latter represents a sub-unit of the fibronectin receptor, which enhances epithelial cell adhesion to fibronectin. Fibronectin is deposited at the corneal wound site after epithelial erosion and provides a temporary matrix for epithelial migration. Several trials have been carried out to explore the therapeutic benefits of topical SP to treat neurotrophic keratopathy and were successful in cases where conventional treatment failed.[5,121-123] Calcitone gene-related peptide (CGRP) is often found together with SP and plays a similar role in epithelial renewal and wound repair: many epithelial corneal nerves are CGRP-positive,[124] it is present in normal tears,[125] and there are many CGRP receptors on corneal and limbal epithelial cells.[126,127]

However, there is no agreement as to the degree of its involvement in corneal wound healing.[3,4,128,129] There is some suggestion that it may support chemo-attraction of neutrophils to sites of acute inflammation at the corneal surface.[127] Norepinephrine is present in the tear film and aqueous humour.[130-134] It has been shown to stimulate corneal epithelial cell proliferation and migration.[94,99,135-137] However, the human cornea only receives a sparse sympathetic innervation,[99,135-138] so the extent of its involvement in corneal maintenance and wound healing in the human eye is not clear. Several studies have shown that the administration of exogenous norepinephrine to cultured human corneal epithelial cells stimuates cell proliferation, migration, and transcellular ion transport process.[91,139-142] Acetylcholine (Ach) is present in the corneal epithelium in high concentrations. Several *in vitro* studies have shown that it supports epithelial metabolism in many ways: stimulation of epithelial cell DNA synthesis,[131,143] activation of the phosphoinositidyl cycle,[131,133] cholinergic simulation of non-corneal epithelial cells,[144,145] cell-to-cell and cell-to-substrate adhesion, and cell motility.[144,145] The role of Vasoactive Intestinal Polypeptide (VIP) is not clear yet. There is some suggestion that VIP stimulates corneal epithelial cell production of nerve growth factors.[1] Neurotensin has been shown to have trophic effects on corneal keratocytes.[146] Met-enkephalin (opioid growth factor) is present in small numbers of corneal nerve fibres. It is supposed to help modulate repair and regeneration of the ocular surface epithelium in a receptor-mediated fashion.[1] Neurotrophins represent a number of structurally-related proteins. In their mature state, they bind to and activate transmembranous receptors, Tyrosine kinase (Trk) receptors in particular.[147,148] Binding to these Trk receptors initiates a signal transduction cascade and leads to gene transcription. Mice studies have shown that Trk receptors are essential for the survival of sensory nerves in the cornea.[149]

Nerve growth factor (NGF) has anti-inflammatory and healing–promoting properties to the extent that when administered, it can cure non-healing epithelial defects and stromal ulceration.[150,151] NGF is critical for corneal nerve survival and maintenance, as well as axonal branching and elongation, neuronal sprouting, and regeneration following nerve damage.[6,104,152,153] Ciliary neurotrophic factor (CNTF) has recently been shown to be released in response to oxidative stress by corneal endothelial cells.[154] It stimulates VIP synthesis which seems to protect endothelial cells from oxidative stress.[155] Glial cell-derived neurotrophic factor (GDNF) binds to the glial cell-derived neurotrophic factor

receptor (GFR) alpha 1, and they are both present in the corneal epithelium. They enhance migration of corneal epithelial cells and stimulate epithelial proliferation.[156]

1.9 Neuro-receptors in the cornea and conjunctiva

Until the mid-19th century, corneal sensory receptors were thought to be purely nociceptive (detecting pain) and only able to produce a small variation in the sensation experienced. In 1956, Lele and Weddell published a detailed summary of previous researchers who applied thermal stimuli using heated and cooled hair, warm and cold water through thin glass tubes, metal surgical probes kept in hot or cold water, cocaine, or metal knobs at different temperatures.[157] Depending on their study design, they arrived at different conclusions: already in 1878, Fuchs (1878) was able to show that the cornea was able to sense different temperatures, by applying button-like expansions on the end of metal surgical probes kept in hot or cold water.[157] Molter (1879) was able to report sensations of touch, warmth, cold and pain (using water at different temperatures as the stimulus, applied to the cornea though thin glass tubes).[157] Donaldson (1885) used cocaine as a stimulus and showed that the cornea was able to distinguish warmth and cold.[157] Dessiur (1892) came to similar conclusions delivering small metal knobs at different temperatures.[157] Bonamico (1905) and Stein (1925) also found the cornea to be sensitive to touch, warmth, cold and pain.[157] Von Frey (1894, 1895 and 1922), however believed that the cornea would only be able to perceive pain (using horse hairs).[157]

1.10 Electrophysiology of the cornea and conjunctiva

Sensory nerve terminals convert energy from various stimulus modalities into action potentials, which are propagated along the nerve fibre.

Electrophysiological studies were carried out in order to record the magnitude, frequency and velocity of such signals. In 1959, Lele and Weddell carried out electrophysiological studies on cats and detected corneal sensory fibres with different diameters for different stimulus modalities (mechanical and thermal) and suggested that there may be four categories of nerves.[158] Many more studies followed and confirmed that there are different functional types of corneal sensory fibres, outlined below (Figure 1.12).[29,31,33,68-70,159-161]

1.10.1 Corneal mechanoreceptors

These receptors are similar to cutaneous Aδ mechanoreceptors and respond only to mechanical stimulation, such as a brief or sustained indentation of the corneal surface or stimuli moving across the surface.[2,69] However, because of their high density over a small area, they have a much lower threshold (about 0.6 mN in cats[2]), than mechano-nociceptor fibres of the skin.[2,159,162] They are classified as 'phasic sensory receptors' because they can signal the onset of a stimulus and adapt readily when it is sustained.[2,31,33,69] Hence, they are more suitable for detecting a stimulus than encoding its intensity and velocity.[29,33,70] Acosta et al carried out electrophysiological and psychophysical experiments in cats and humans and confirmed that mechanosensory units could not respond to an increase in mechanical stimulation, and suggested that stimulus intensity may be encoded by polymodal units.[32]

According to cat studies, mechanoreceptors account for about 20% of the corneal sensory nerve fibres[1] and 70% in the rabbit.[31]

The receptive fields were shown to be round, or oval, and large.[33] In the rabbit, most mechano-receptors covered 10-20 mm^2 (5-10%) according to Tanelian and Beuerman, and 4-6mm^2 according to MacIver and Tanelian of the total ocular surface,[31,69] while in cats, Belmonte et al. measured a vertical axis of 11.5mm.[70]

1.10.2 Corneal polymodal receptors

Polymodal nociceptors that resemble those present in skin have been found in the cat and are believed to represent about 70% of all corneal sensory fibres.[29,70] They respond to near-noxious mechanical energy, but also sense heat, endogenous and exogenous chemical stimuli. The majority are C fibres, although some polymodal Aδ fibres have been found.[1,32] They discharge continuous and irregular nerve impulses lasting as long as the duration of the stimulus. Their firing frequency corresponds to the amount of stimulus intensity. Their mechanical threshold is slightly lower than that of pure mechanoreceptors, however they only respond to heat over 39-40°C. In cat studies, some polymodal fibres have also shown an increased firing rate when the stimulus temperature was decreased below 29°C.[32,33] When exposing cat corneas to increasing

concentrations of CO_2, no differences between C and Aδ fibres regarding their firing frequency could be detected, although C fibres had longer response latencies and were slower to reach their peak firing rate.[163]

The receptive field size along the vertical axis was found to be 4.9mm for C fibres and 8.2mm for Aδ fibres in cats.[29,70] When exposed to chemical stimulation, the receptive fields were measured of 4.4mm and 5.9 mm for C and Aδ fibres, respectively.[163]
Tanelian and Beuerman examined rabbits for polymodal fibres, but could only find bimodal Aδ nociceptors that were responsive to mechanical and heating stimulation such as corneal mechano-heat receptors.[31,69,164]

1.10.3 Corneal mechano-heat receptors

A sub-type of corneal Aδ fibres, which are only sensitive to mechanical and heating, but not to chemical stimulation, could be found in the rabbit and cat.[31,69,70] They had higher mechanical thresholds and sensed an increase in temperature above 39°C in the rabbit and 43°C in the cat. Their receptive fields were shown to be large and, because of their similar response profile, they could also be polymodal receptors with higher chemical thresholds.[70] Belmonte et al found the receptive field size to be 8.5mm along the vertical axis.[70]

1.10.4 Corneal cold receptors

According to cat and rabbit studies, 10-15% of the corneal nerve fibres are cold-sensitive receptors, of which some may be Aδ fibres, but the majority are C fibres.[29,31,69]
The presence of corneal cold receptors was also confirmed in guinea pigs.[30] They are tonically active at resting temperature, however their discharge frequency increases when the temperature reduces to 33°C and decreases again with rising temperature.[29-31]
Evaporation at the corneal surface, blowing of cold air onto the cornea and applying cold solutions also reduce corneal temperature that consequently increases their firing rate. Upon warming, cold receptor fibres were silenced in cats, and MacIver and Tanelian observed a 50% decrease in firing frequency when rabbit corneae temperatures were increased from 35° to 37°C.[69] However, corneal cold receptors also ceased to respond if the cornea was cooled down below 5°C.[29] Acosta et al. observed in cat

corneas that cold-sensory fibres were activated proportionally to the temperature reduction.[32] The minimum amount of temperature change they are able to sense in cats, is believed to be 0.1°C or even less.[29]

In the rabbit, a greater overlap of receptive fields was observed in the centre of the cornea.[31] Gallar et al. found the receptive field sizes in cats to vary considerably between 2 and 9mm, with a mean value of 3.7mm.[29]

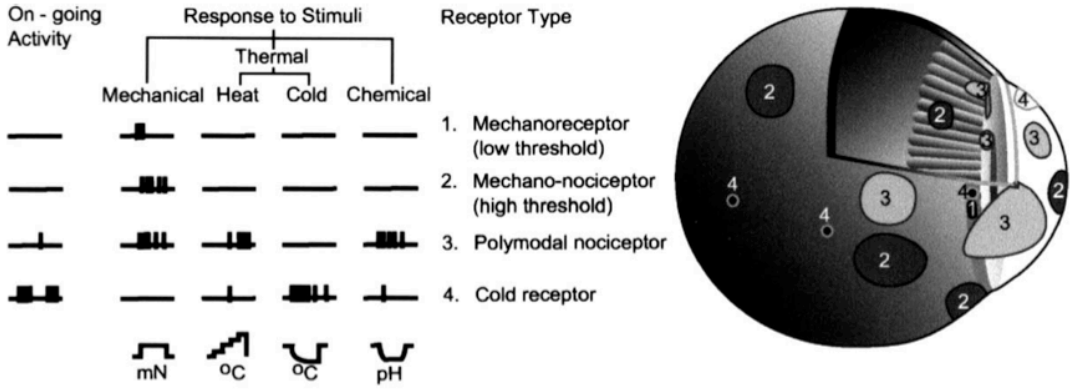

Figure 1.12: Functional types of sensory neurons innervating the eye (Belmonte et al., 2004)[2]

1.10.5 Conjunctival receptors

Very few electrophysiological studies have sought to identify sensory receptor types in the conjunctiva. However, they have identified the same main functional classes of sensory afferents, such as mechano-nociceptors, polymodal nociceptors and cold receptors, in the limbal area and bulbar conjunctiva.[2] The majority of conjunctival sensory neurons that could be recorded in the guinea pig were mechanosensory (70%), with fewer polymodal (23%) and cold sensitive neurons (7%).[165]

The receptive fields of corneal fibres near the limbus were found to overlap onto the conjunctiva. A small number of mechano-sensory fibres, with receptive field sizes of approximately 1mm diameter, were found in the cat in close proximity to the cornea,[166] whilst the receptive field sizes of conjunctival mechano-receptors elsewhere were measured to be 2-3mm.[165] Polymodal conjunctival fibres were found with medium size receptive fields of 2-3mm diameter and cold receptors with receptive field sizes of slightly more than 2mm, close to the limbal area.[165,166]

1.11 Psychophysics

1.11.1 Corneal and conjunctival sensations

The development of gas aesthesiometers has permitted separate application of controlled mechanical pulses, irritant chemical stimuli and hot (or cold) air pulses onto the ocular surface.[14,19] Hence, it has been possible to carry out psychophysical studies and explore the sensation evoked by each type of stimulus in more detail.

Mechanoreceptors may produce a sharp sensation of pain following a mechanical contact with the corneal surface. Humans are able to feel sensation proportional to stimulus intensity: however, the threshold for mininum sensation varies greatly between subjects using a gas aesthesiometer.[32] Mechanical stimulation close to the threshold level may also be perceived as warm or cold, hence temperature sensations associated with mechanical sensation are not clearly defined yet.[32]

Polymodal and mechano-nociceptors contribute to the sharp mechanical pain that arises when the cornea is acutely exposed to mechanical force, but they are also responsible for nerve impulse activity caused by chemical irritation, heat or noxious cold.[33]
Sustained sensations of pain may also be caused by locally released mediators during inflammation that also stimulate polymodal nociceptors.[2]

Chemical stimulation leads to a decrease in corneal pH and is sensed as mildly stinging.[163,167] According to Chen et al, the threshold for sensation in humans is 38.7±2.5%, with a 3s stimulation duration. They noted a relationship between CO_2 concentration and the magnitude of the evoked sensation, which also corresponded to nociceptor activity in cats.[163] With increasing CO_2 concentration, the sensation may change into a burning pain and warming rather than cooling, but both of low magnitude.[32] The sensation felt when exposed to heat has been described as very similar to chemical stimulation.[168,169] This supports the assumption that thermal and chemical pain are encoded by the same population of polymodal afferents, as in skin and other tissues.[170-172]

An increase in cold receptor activity creates a conscious sensation of cooling.[32,173] According to Acosta et al., cold stimulation has a well-defined profile, clearly distinguishable from other stimulus modalities: changes in stimulus intensity were well detected and correlated closely with the magnitude of the cooling component.[32] Murphy et al. calculated the minimum perceivable amount of cooling in the central cornea to be 0.3°C.[173] Acosta et al. (2001) explored the effect of menthol and reported an immediate sensation of cooling and mild irritation, which is sometimes followed by a feeling of light discomfort and, occasionally, with burning.[32] Shortly after menthol instillation, no response to cooling could be recorded in humans, and in cats the cooling response was reduced. However, no changes to thermal or chemical responsiveness of the polymodal units could be detected.[32] From electrophysiological and psychophysical experiments carried out in cats and humans respectively, Acosta et al. postulated that Aδ mechanosensory and polymodal fibres mediate sensations of stinging pain, while C fibres evoke burning pain sensations.

How do sensations compare between cornea and conjunctiva?

Acosta et al. (2001) reported that the intensity of sensation of stinging and burning pain was felt to be weaker coming from the conjunctiva than from the cornea.[174] With chemical stimulation, they made similar observations regarding irritation and burning pain sensation, however stinging pain, warming and cooling were perceived equally well by the conjunctiva and cornea.[174] Regarding thermal stimulation, the sensations of irritation and stinging were felt less by the conjunctiva, whereas the warming and cooling components were perceived equally well.[174]

1.11.2 Corneal psychophysical sensory channels

Feng and Simpson (2004) proposed that there are at least five corneal psychophysical sensory channels mediating cold, heat, mechanical, chemical and histamine-type substance modalities.[175] With mechanical and chemical stimulation at different temperatures they could show different qualities of sensations (using the Belmonte pneumatic aesthesiometer): temperature changes had no effect on chemical or mechanical thresholds, however chemical thresholds were considerably lower with additional mechanical stimulation and vice-versa.

They concluded that psychophysical channels are not completely independent, but interact due to sharing of molecular and neuro-receptors. Thus, a subject with good mechanical sensitivity can be expected to have good thermal sensitivity.

1.12 Molecular receptors mediating the neuro-receptor response

Several different molecular receptors being expressed by trigeminal neurons could be shown with molecular biological techniques.[176,177] It is believed that they provide the substrate for corneal psychophysical channels.[175]

1.12.1 Mechanical stimulation

Mechanically sensitive receptors, such as the degenerin/epithelial sodium channel (DEG/ENaC) family, mediate mechanical sensitivity.[175]

1.12.2 Thermal stimulation (cooling and warming)

Cold stimulation is processed by cold menthol receptor type 1 (CMR1) / transient receptor potential menthol 8 (TRPM8), which responds from 8°C to 30°C and is expressed on trigeminal ganglion C fibers.[178,179] It has also been proposed that a complex interaction exists between ion channels that are expressed on the cold neurons and produce the cooling sensation.[180]

A corneal noxious heat channel (NHC) mediates thermal pain, and its possible substrate may be the vanilloid receptor (VR)-1, which is expressed on Aδ and C fibers.[176]

1.12.3 Chemical stimulation

CO_2 dissolves in the tears to release hydrogen ions that can mimic tissue acidosis characterising infection, ischemia and inflammation.[20] C fibres are stimulated, possibly mediated by the vanilloid receptor 1(VR1) and/or acid-sensing ion channels (ASICs).[20,177] Feng and Simpson (2004) speculated that mechanical stimuli activate all populations of fibres (mechanosensory Aδ, polymodal Aδ and polymodal C fibres), but CO_2 activates only polymodal fibres. Possibly, short-lasting mechanical stimuli activate the predominantly faster Aδ fibres and CO_2 recruits the slower polymodal C fibres, as

the mechanical sensation is transient during stimulus presentation and disappears, but after CO_2 stimulation, sensation is delayed and persistent after stimulus presentation.

1.13 Corneal adaptation to mechanical, cooling and chemical stimulation

Adaptation is defined as 'the decrease in the magnitude of sensation or in neural response during a sustained stimulation at a constant intensity'.[181] It has been demonstrated in sensory systems, such as olfaction,[182] audition,[183] and the somatosensory systems in the tooth pulp[184] and skin.[181] It is believed that the adaptation process limits further injury.[185] Sensitisation represents an alternative response to repeated noxious stimulation.[13] Both, adaptation and sensitisation have been shown to take place in the eye.[33,70] So far, only one study has been published investigating corneal adapatation and sensitisation in humans:[185] Chen et al could show corneal adaptation to suprathreshold (with increased intensity) mechanical and cooling stimulation, and to chemical stimulation at threshold CO_2 concentration. They attributed these different findings with chemical stimulation to the difference in pneumatic stimuli and how they interact with the tear film and ocular surface, differences between receptor types and underlying sensory channels and functional differences in the central nervous system.[185]

1.14 Sensory maintainance of the tear film

As mentioned before, the corneal sensory nerves are believed to play an important role in maintaining the resting tear flow, as their afferent impulses from the ocular surface lead to a reflex response,[107] best described by the lacrimal functional unit (LFU): an integrated system comprising the ocular surface tissues (cornea, corneal limbus, conjunctiva, conjunctival blood vessels, and eyelids), the tear secreting components (main and accessory lacrimal glands, meibomian glands, conjunctival goblet, and epithelial cells), and the sensory and motor nerves that connect them.[186-188] It represents a complex network connecting the sensory tissues and the secretory glands that provide homeostasis on the ocular surface. Hence, the LFU reacts to external, endocrine and central neuronal influences, in order to protect the ocular surface and to ensure its health.[189,190] It is tightly controlled by the neural input from the ocular surface tissues.

Subconscious stimulation of the corneal nerve endings triggers afferent impulses, which integrate the central nervous system and the paraspinal sympathetic tract: the trigeminal sensory fibres run from the ocular surface (in particular from the cornea) to the superior salivary nucleus in the pons, from where efferent fibres pass, in the nervus intermedius, to the sphenopalatine ganglion (Figure 1.13). From there, they run to the lacrimal gland, the nasopharynx, and the vessels of the orbit, to stimulate secretion of the healthy tear film.

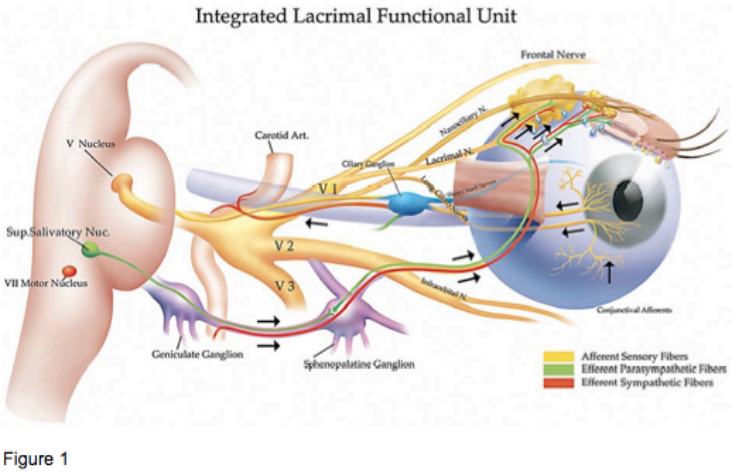

Figure 1.13: The integrated Lacrimal Functional Unit (Stern et al., 2013)[191]

Tear film stability is carefully balanced by the interaction between the amount of tear film secretion, adequate tear clearance and tear composition.[189] The initial compensatory reflex mechanism to ocular surface irritation represents reflex tear secretion. However, if the tear film is impaired over a prolonged period, inflammation and a decrease in corneal sensation will occur and eventually compromise the tear reflex response, causing an even greater tear film instability.[189]

The blink reflex is controlled by the afferent neural pathway via trigeminal sensory fibres arising from the ocular surface and efferent somatic pathway of the facial (seventh) cranial nerve.[189]

1.15 The tear film

The ocular surface is covered by the tear film. The aqueous tears are secreted by the main and accessory lacrimal glands. When the eye opens, the tears form the preocular tear film and the tear menisci during the upstroke of the blink.[192-194] The precorneal tear film is estimated to be approximately 3μm in thickness.[195,196] The menisci at the interface between the lid margins and the surface of the globe provide the route by which the tears reach the lacrimal puncta and canaliculi and then enter the nasolacrimal system.

The thin, outermost lipid layer of the tear film was measured to have a thickness of 50 to 100nm,[197,198] and forms the barrier between the environment and the eye. The lipid layer is mainly secreted by the meibomian glands.[192] Its main function is to retard evaporation from the ocular surface,[199,200] and to prevent the overspill of tear fluid onto the eyelids and, hence, the contamination of the tear film by skin lipids.[201,202]

The aqueous phase of the tear film makes up the bulk of the tear film thickness.[192] It is primarily secreted by the main lacrimal gland and accessory lacrimal glands of Krause and Wolfring, and additional fluid and electrolytes are secreted by the ocular surface epithelial cells.[203] The tear flow rate is dependent on sensory stimulation and may vary considerably, depending on the demands of the external environment. The aqueous phase is responsible for nurturing and protecting the epithelia, by providing a medium for the transfer of oxygen and nutrients to the avascular corneal tissue, conveying signals between the structures bathed in aqueous, and flushing away epithelial debris, toxins and foreign bodies.[204] Electrolytes in the aqueous phase maintain epithelial tear film stability, and their amount determines the osmolarity and regulates pH of the tear fluid.[204] Aqueous layer proteins contribute to ocular surface defence[205] and maintenance of tear film stability.[201] Additional antioxidants and growth factors additionally help in epithelial regeneration and wound healing.[206]

The aqueous phase of the tear film also contains soluble, gel-forming mucins, produced by goblet cells.[207,208] They play an important role in the removal of pathogens and debris from the ocular surface, the smoothing of the ocular surface, and for the

protection of the surface through lubrication, from the blink, and from environmental insult.[204] Another type of mucin, the transmembrane mucins, contribute to form the glycocalyx. They are anchored to the apical plasma membrane of the corneal and conjunctival epithelial cells and can interact with multiple proteins.[204]

1.16 Blinking and the ocular surface

Eye blinking is a fast eyelid movement that closes and opens the palpebral fissure. For a blink to occur, the antagonistic muscles of the levator palpebrae superioris and the orbicularis oculi alternately contract in a push-pull fashion:[209-211] The eyelid closes due to a burst activation of orbicularis oculi motor-neurons and a brief inhibition of the tonic activity of levator palpebrae superioris motor-neurons. Thereafter, the orbicularis oculi action ceases, and for a short moment both muscles are inactive. Subsequently, when the downward lid movement stops, the orbicularis oculi muscle takes up its tonic activity again and the eyelid reopens as a result of contraction in the levator palpebrae superioris.[210-214] When the eyes are open, there is a balanced level of tonic activity in both muscles.

There are three types of blinks: spontaneous endogenous, reflex (both involuntary) and voluntary. Reflex and spontaneous blinks represent a response to different trigeminal, visual and acoustic stimuli, whereas spontaneous blinks occur unconsciously, without any evident stimulus.

1.16.1 Innervation of eye blinking

The afferent pathway of the involuntary blink reflex runs along small unmyelinated and myelinated fibres in the long ciliary branch of the ophthalmic division of the trigeminal nerve to the pons, then into the medullar oblongata along the spinal trigeminal tract in the lateral medullary region, and they terminate on cells of the ipsilateral spinal nucleus of the trigeminal nerve.[215] The efferent pathway is conveyed by the somatic fibres of the facial nerve.[215] The exact pathway leading from the supraorbital branch of the sensory trigeminal nerve to the ipsilateral facial nucleus in the pons is still unknown.[216] Since the reflexes arising from the cornea run through the medulla oblongata before connecting with the ipsilateral and contralateral facial nucleus, it has been postulated

that the corneal reflex and the blink reflex use similar trigemino-facial connections.[216] It has been proposed that involuntary spontaneous blinking is influenced by a local corneal reflex that is dependent on corneal sensitivity, possibly triggered by ocular surface cooling when the tear film progressively evaporates.[25,217]

1.16.2 Types of eye blinks (complete, incomplete, 'overblink' and 'twitch')

Spontaneous blinks can be described as complete or incomplete, as 'twitch blinks' and 'overblinks'. The twitch blink has been described as a small, almost undetectable movement of the upper eyelid. Abelson and Holly defined a blink as complete if the upper eye lid touches the lower eyelid, occluding the palpebral fissure.[218] They described it as incomplete, when the upper lid covered less than two thirds of the cornea during the downward movement.[218] Pult et al. recorded the blinking behaviour additionally from a temporal-inferior view and noted that some blinks, appearing to be complete with a frontal view, were in fact not complete from the temporal-inferior view. They defined these blinks as being almost complete. Incomplete and almost incomplete blinks have been reported to occur frequently,[218-221] and they can result in dry eye and exposure keratopathy.[222] Pult et al. noted a significant correlation between almost complete blinks and lid paraellel conjunctival folds (LIPCOF) Sum ($r=0.649$; $p<0.001$) and the ocular surface disease index (OSDI) score ($r=0.570$; $p<0.001$).[221] The presence of LIPCOF may have a causative effect on incomplete blinking, as they may create a physical barrier between the lid margins, and it may also present as a consequence of incomplete blinking due to mucin deficiency, resulting in a higher blink rate (and hence a higher ratio of incomplete blinks) and increased friction with the ocular surface.[221] Other causes for incomplete and/or infrequent blinking include dermatochalasis (a result of the effort of the brow opposing the blink reflex),[223] eyelid laxity (age-related degenerative changes, trauma or floppy eyelid syndrome), facial palsies, lagophthalmus, proptosis, concentrated visual tasks and VDU work.[224]

Korb et al.[225] noticed that there was no central touch between the upper and lower lid during a blink. Pult et al.[226] confirmed this and described these blinks as 'overblinks', indicating the position of the upper lid anterior to the lower lid on closure during a blink

on normal groups of subjects. This preventing a contact between the central portion of the lid margins during spontaneous blinking. They observed this 'overblink' in all participating subjects, irrespective of whether the blinks were complete, incomplete, or almost complete. As the lipids secreted by the meibomian glands were still observed to spread of the tear film during blinking, they assumed that the tear film reservoir behind the upper lid must be still able to fuse with the tear meniscus of the lower lid when the upper lid reaches its lowest point during the blink.[226]

1.16.3 Blink rate

The number of blinks performed over a certain time period represents the blink rate and describes the number of blinks recorded per minute.

A normal blink rate is considered to be 10-16 blinks per minute:[227] King and Michels measured 12.0 blinks per min.,[228] Carney and Hill found on average 12.6 blinks per min. with a marked individual variation,[229] Collins et al. observed a mean of 24.0 blinks per minute,[10] Zaman et al. measured on average 11.9 blinks per minute,[230] and Pult et al. reported a mean of 14.9 blinks per min.[221] Blink rate has been shown to be higher in females than in males.[218-221] Several studies could not find any change of SEBR in elderly subjects.[230-233] However, it has been proposed that the blink kinematics change with age, due to the decrease in palpebral fissure width as a result of ptosis and a weakness of the levator palpebrae superioris and/or the Müller's muscle, leading to a decrease in blink amplitude and peak velocity.[231] The increase in blink duration has also been explained by the age-related loss of substantia nigra dopamine neurons.[234]

1.16.4 Interblink time intervals (IBI)

Eyeblink activity may also be described with the distribution of the interblink interval (IBI), as the frequency of blinking of an individual may not necessarily be distributed in a symmetrical manner, but may be skewed. Indeed, Ponder and Kennedy noticed that the IBI were quite variable between subjects and distinguished four patterns:[235] J-shaped (positively skewed; large number of short IBI and a steadily decreasing number of longer IBI), irregular plateau, bimodal and symmetrical. There have been some conflicting results between various studies regarding which of the IBI patterns occurs

the most frequently in a normal subject group: Ponder and Kennedy[235] as well as Zaman and Doughty[236] observed the positively skewed IBI pattern to occur the most frequently, whereas Carney and Hill[229] noted a positive skew in all their study subjects. Zaman and Doughty estimated the proportion of symmetrical IBI patterns based on their study group to be greater than did Ponder and Kennedy.

1.16.5 Duration of a spontaneous blink

The down phase of a blink is considered to be faster than the up phase, with typical durations of 60ms. and 180ms., respectively.[209]

The closing portion consists of a slow phase of accelerating velocity during the inhibition of the levator palpebrae superioris, a fast phase during the increased activity of the orbicularis oculi muscle, and a decelerating slower phase ending in complete closure.[216] The reopening portion consists of an initial rapid return from full closure, followed by progressively slower motion as the lids return to the baseline position.[216]
The relationship between the amplitude and the peak velocity is considered to be linear.[209,231,237,238]

1.16.6 Vision suppression during eye blinks

During an eye blink, the pupil is occluded, causing a momentary diminution in retinal luminance. Since these blackout periods are not perceived, there must be a momentary disruption of visual input to the brain several times per minute. This so-called blink suppression has been shown in a number of experiments.[239-242]

1.16.7 Blinking and the integrity of the ocular surface

Blinking plays an important role in the maintenance of the integrity of the ocular surface, by contributing to the maintenance of the ocular surface moisture, the drainage of tears, the expression of lipids from meibomian glands, and the spreading of tear lipids across the pre-corneal tear film.[243-247]

The eye-blink spreads tears over the cornea and the conjunctiva, promoting stability to the tear film. Upon downward movement of the upper lid during a blink, the temporal

portions of both lids meet first, which pushes the tear film into the tear menisci whilst excess tears and debris are being moved towards the drainage puncta.[245] Still during the early phase of lid closure, the lid margins meet at the puncta regions and close off the punctual openings with a significant amount of pressure. Upon further closure of the lids, fluid present within the punctum and lacrimal canaliculi is then forced down into the lacrimal sac.[245] The negative pressure in the lacrimal sac resulting from the subsequent eye opening then draws any excess tears from the menisci into the sac.[245]

Blinking is hence vital in maintaining optical performance, ocular surface health and tear film drainage.[28,248] Hence, infrequent and/or ineffective blinking can be involved in the development of dry eye disease (DES), as a result of insufficient tear clearance and evaporative tear loss. However, an increased SEBR is also frequently observed in DES, representing a physiological adaptation to reduced tear film stability.[249]

1.16.8 Influences on eye blinking behaviour and the trigger of a blink

1.16.8.1 Cortical control of blink rate

The eye blink rate is greatly variable and under cortical control.[27] It is strongly influenced by external factors, psychologic and physiologic influences, and activity-related factors.[27] Blink rate increases during anxiety,[250] as a result of depression, [251] visual fatigue,[252,253] sleep deprivation,[254-257] driving,[258] or flying,[259] and tasks that require speech.[233,260,261] It is reduced during reading[261,262] or when concentrating on a text on a video display:[9,263-265] the more difficult the task, the greater the resulting blink inhibition will be. Conversation, anger and excitement markedly increase the blink rate.[28,227] Furthermore, neurological and psychiatric diseases have an influence, as Cruz et al. reviewed:[28] Blink rate is recognised as a clinical marker of central dopaminergic activity: a low blink rate could be recorded in conditions with hypodopamine activity (e.g. Parkinson disease, progressive supranuclear palsy and attention deficit/hyperactivity disorder). Blink rate was found to be high in conditions with hyperdominergic activity (e.g. Huntington disease, schizophrenia, or focal dystonia and neuro-developmental conditions). Alcohol abuse[235] and recreational cocaine use[266] were shown to decrease SEBR.

1.16.8.2 The influence of ocular surface conditions on blink rate

Despite the cortical control, ocular surface conditions have been associated with blink rate: it may be influenced by tear film quality,[23,267] as it was shown to be higher in dry eye patients than that of the normal population,[9,23,249] and which can be influenced by use of artificial tears and protective eyeglasses.[249] Nakamori et al. recorded a higher blink rate in patients with dry eye disease of 34.1±2.4 per min as supposed to normals with to 20.1±1.6 per min.[23] Also, the maximum time during which a person can keep their eyes open was shown to be decreased among dry eye patients.[23] Ocular surface damage has been shown to increase the blink rate.[268]

Topical anaesthesia has been shown to reduce, but not to abolish blink rate.[10,23,24,269] Situ et al. established a weak to moderate correlation between NIBUT and ocular surface sensation in patients with dry eyes (r=0.31 for cornea, r=0.40 for conjunctiva; air gas aesthesiometry).[270] No previous study could establish a correlation between corneal sensitivity and blink rate: Ntola observed a correlation of r=0.236 without statistical significance (p=0.315), having excluded subjects with a TBUT <8 seconds.[271] Collins et al. could show that infrequent blinking can result from diminished corneal sensitivity, however they could only establish a moderate correlation without statistical significance (r=0.56, p>0.10).[10] However, the blink rate was recorded whilst the subjects were involved in conversation, which may have artificially increased blink rate. Also, their sample group comprised only nine subjects. Doughty et al. also investigated the correlation between tactile ocular surface sensitivity (Cochet Bonnet aesthesiometer) and blink rate, whereby they recorded the blink rate during 5 mins. in silence, without any visual stimulation for the participating subjects.[272] They could not establish any correlation between central corneal tactile threshold and blink rate, however for the conjunctival tactile threshold, they found an inverse moderate relationship: the lower the conjunctival sensitivity, the higher blink rate was found to be (r=0.588, p<0.001). These surprising results can be questioned, as the Cochet Bonnet aesthesiometer has been shown to have many limitations, most importantly a truncated stimulus range and imprecise stimulus application.[14] It may therefore not be sensitive enough for subtle sensitivity differences in normal subjects. Furthermore, a blink rate without any visual

stimulation at all may not necessarily be natural. Other research also showed a strong relationship between corneal sensation and tear film drying dynamics.[273]

Several investigations found significant negative correlations between TBUT (with use of flourescein) and blink rate:[267,274,275] Yap et al. found a strong and statistically significant correlation of $r=0.69$ ($p<0.01$), whereby the patients were filmed with a hidden camera during a period of 5 minutes whilst waiting in the exam room.[267] Al-Abdulmunem also observed a strong correlation in 159 healthy students when they recorded their blink rate by observation in a lecture theatre ($r=0.74$, $p<0.05$).[274] Collins et al. established a moderate correlation between TBUT and blink frequency, however without statistical significance ($r=0.38$, $p>0.10$). Prause and Norn found a weak to moderate correlation between TBUT and blink frequency ($r=0.33$; $p<0.05$) for normals and a stronger, moderate effect for patients with Sjögrens syndrome ($r=0.58$; $p<0.05$).[275] However, they measured blink rate during reading, which may have had an inhibitory effect. Tsubota and Nakamori observed an influence of ocular surface area on blink rate,[276] however these results were disputed by Zaman et al., who could not find any correlation between ocular surface area and spontaneous eyeblink activity in elderly Caucasians.[230]

Acosta et al., as well as Nakamori et al., were able to decrease blink rate during computer work with the use of artificial tears,[23,277] which supports the hypothesis that sensory input from the corneal and conjunctival sensory fibres modulates the neural circuits involved in spontaneous blinking. They concluded that blink rate at rest might be partially influenced by extrinsic factors, such as ocular surface conditions, whereas a low SEBR induced by the performance of an attentive task may be mainly governed by intrinsic neural mechanisms. The resulting strong inhibition of neural blinking mechanisms during the computer task is stronger than the sensory input from the cornea and conjunctiva. It has been suggested that spontaneous blinking originates in the central nervous system and is modulated by internal factors such as fine motor controls, speech centres, emotional and psychological states, cognition and attention.[24] Thus, both central and neural control and local ocular sensory input may jointly act to stimulate blinks.

1.16.8.3 The effect of contact lens (CL) wear on blink rate

CL wear may increase or decrease blink rate, depending on whether it causes irritation (such as mechanical effects or end of day dryness) by its presence, or, as with a soft CL, it may dampen the activity of the superficial nerve endings on the corneal surface with the aid of a thin tear film layer between the ocular surface and the back surface of the CL. Hence, conflicting reports on the effect of CL on blink rate have been published: Holly found soft CL wear to decrease blink rate,[278] while Carney et al. observed an increase in blink rate with soft CL wear[279] and Hill et al. with hard CL wear.[280] There is a general agreement on the increased proportion of incomplete blinks during CL wear.[10,278]

1.16.8.4 Lid abnormalities and SEBR

A facial nerve palsy leads to a variable orbicularis oculi muscle impairment, which may partially, or even completely abolish blink activity in severe cases.[281] Blepharospasm, characterised by involuntary bilateral closure of eyelids, causes an increased blink rate that is higher during rest conditions than during conversation.[282] Graves' upper eyelid retraction (the most common and prominent signs of Graves' orbitopathy) causes infrequent and incomplete blinking, as well as a reduced blinking amplitude.[283] Due to the high position of the upper lid margin, three-quarters of the blinks have been reported as not being able to reach the pupil centre.[28] Interestingly, the blink rate of patients has not been observed to increase as a consequence of lid retraction.[28]

1.17 Measurement of ocular surface sensation

In the late 19th and beginning of the 20th century, various researchers used hairs, warm and cold water through thin glass tubes, metal surgical probes kept in hot or cold water, cocaine, and metal knobs at different temperatures, in order to measure corneal sensitivity.

Today, the **Cochet-Bonnet aesthesiometer** is the most widely-used aesthesiometer (Figure 1.14). It is based on the concept of Von Frey in 1894, who measured corneal sensitivity with various lengths of calibrated horse hairs attached to a glass rod.[13] Varying pressures can be applied to the cornea with a fine nylon filament, 6cm in length

and 0.08 or 0.12mm in diameter, by varying its length to produce different intensities of stimulus on the ocular surface.[13] It has, however many limitations:

- The stimulus is invasive, causing an abrasion to the epithelial surface, which may alter threshold,[13] and should not be used when the epithelium is compromised.
- The pressure required to produce punctuate staining is less than that required to cause a sensation.[14-16]
- The nylon filament is seen by the subject and may cause apprehension – this may affect threshold, as it has been shown to be higher when measurements are taken in the dark and the subject cannot see the nylon filament.[15]
- A limited stimulus range with the 0.12mm thread, as it excludes high corneal sensitivity (gives artificially high threshold) and low conjunctival sensitivity.[17]
- Alignment of stimulus is difficult, as the stimulus cannot be easily seen against the ocular tissue.
- Estimation of precise force applied is difficult, especially as the results vary greatly if the required 5° angle of the bend in the nylon thread is not achieved.[18] This leads to poor repeatability of the stimulus pressure.
- Ambient humidity affects the degree of bend of the nylon filament.[182] Furthermore, its flexibility will alter with repeated use.

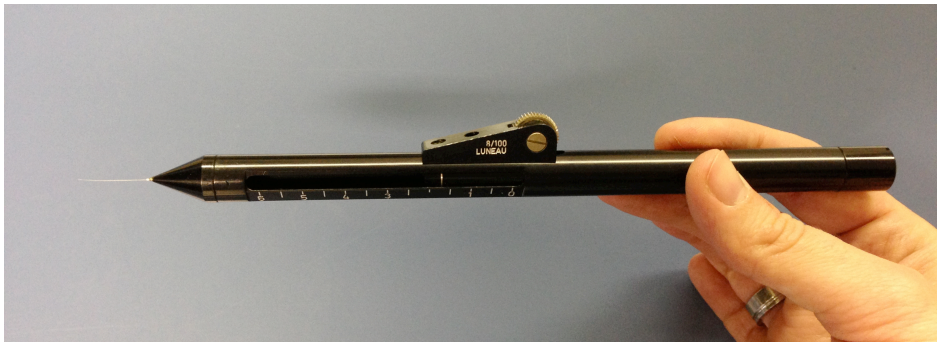

Figure 1.14: The Cochet-Bonnet aesthesiometer

In order to overcome these shortfalls of the Cochet-Bonnet aesthesiometer, the non-contact corneal aesthesiometer (NCCA) by Murphy et al,[14] a similar design by Vega et al.,[284] and the Belmonte aesthesiometer[19] (a modified version of the Belmonte design) were developed.[21,284]

With the **NCCA**, a pulse of pressurised air stimulates the ocular surface in a well-controlled, repeatable and consistent manner. The laminar airflow can be well maintained by manual control through a valve, and its pressure is monitored with an electronic sensor measuring in millibars. The best diameter of the stimulus air-jet was found to be 0.5mm, representing the best compromise between limiting airflow dispersion and ease of setting the stimulus pressure. Three different acceptable stimulus durations were chosen: 0.5, 0.9 and 1.5 seconds. 0.9 sec. was chosen as the optimum duration, as 0.5 secs was thought to be too quick for less vigilant subjects, and the 1.5 secs duration could possibly cause unnecessary drying of the tear film over repeated applications. The optimum working distance was chosen to be 1.0cm, since at 1.5cm the ocular surface would be close to the region where the air-flow degenerated into turbulence, and at 0.5cm the ocular surface might be affected by the back flow of the air from the surface. A temperature change to the cornea was noted, as the stimulus air pulse was sent to the eye at room temperature. The temperature of the cornea has been recently measured to be 35±1.1ºC,[285] and the NCCA has therefore a cooling effect on the ocular surface. Murphy et al. concluded that the stimulus could be localised to small areas of the corneal surface.[14] The stimulus modality was thought to be primarily due to the rate of temperature change, although the exact modality of the stimulus was not known. The overall corneal area covered by the air jet, which experienced the cooling effect, was described as being $3mm^2$.

Does the airflow emitted from the NCCA mainly change the temperature of the corneal surface, or is it also able to deform the corneal surface?

Murphy et al demonstrated the former with an experiment using a thermal camera to measure the temperature change induced on the cornea with increasing stimulus pressure.[22] The reduction in corneal temperature increased as the stimulus pressure (or airflow rate) increased. They concluded that the cooling of the tear film was related to the process of evaporation. The airflow striking the corneal surface increased the rate of evaporation from the tear film by altering the humidity equilibrium of the air above the cornea and by removing any evaporated water molecules from the vicinity. Energy is removed from the tear film at the stimulus location by means of evaporation, and its temperature drops.[22] Murphy et al also tried to find out if there was a mechanical deformation component.[22] However, they could not demonstrate any distortion in the

tear film after sending a high-pressure airflow onto the corneal surface (5mbars). They concluded that the surface distortion component of the stimulus must be very small, compared with the very clear temperature change component.

The **Belmonte Aesthesiometer** was the first instrument to deliver chemical (CO_2), thermal, as well as mechanical stimuli to the ocular surface at different temperatures,[19] since stimulus temperature affects different sensory receptors on the ocular surface (Figure 1.15). The instrument consists of two cylinders of gas: one containing medical grade compressed air and one 98.5% CO_2 mixed with air. The gas cylinders are connected via two pressure regulators and two uni-directional regulators to an electronic proportionally-directional, control valve. This adjusts the flow of gas, producing mixtures with a controlled proportion of CO_2 and air. The final flow of the gas mixture is adjusted with a flow meter and supplied to the probe of internal diameter 0.5mm, mounted in a modified non-contact tonometer.

The stimulus nozzle contains a temperature controling device (a thermode, a servo-regulater, and a Peltier cell), and its diameter was chosen to be 0.5mm. It warms the flowing gas and contains a three-way solenoid valve to direct the output of gas. The effective temperature of the stimulus on the eye can be varied between room temperature (20°C) and 34°C. The temperature sensor provides feedback to maintain a steady temperature independent of air flow and ambient temperature. The effective on-eye temperature was calibrated across the range of available flow rates, for nominal temperatures of 20°C and 34°C. There was no significant temperature variation across flow rates and there was no demonstrable reduction in temperature or increased variability with increased flow rates, for 1 second and 2 seconds pulse durations. The stimulus temperatures were selected to provide a mechanical stimulus without a thermally cooling effect (34°C) and a mechanical stimulus with maximum cooling effect (20°C). Using the current instrument design without an additional cooling device, air pulses could not be delivered at temperatures lower than 20°C.

During stimulation, the gas is transiently directed towards the tip of the probe by means of a pulse generator that changes the direction of flow in the electronic valve. This produces a pulse of gas in the tip of the probe with a defined duration, CO_2

concentration, temperature, and flow rate. Stimulus duration ranged between 1–3 seconds, with a precision of 0.1 second.

The distance between the cornea and probe tip was set at 5mm. The stimulus air-jet is mounted on a slit-lamp holder and enables the practitioner to position it onto the corneal apex. Threshold measurements are carried out in terms of flow of gas, in millimetres per minute.

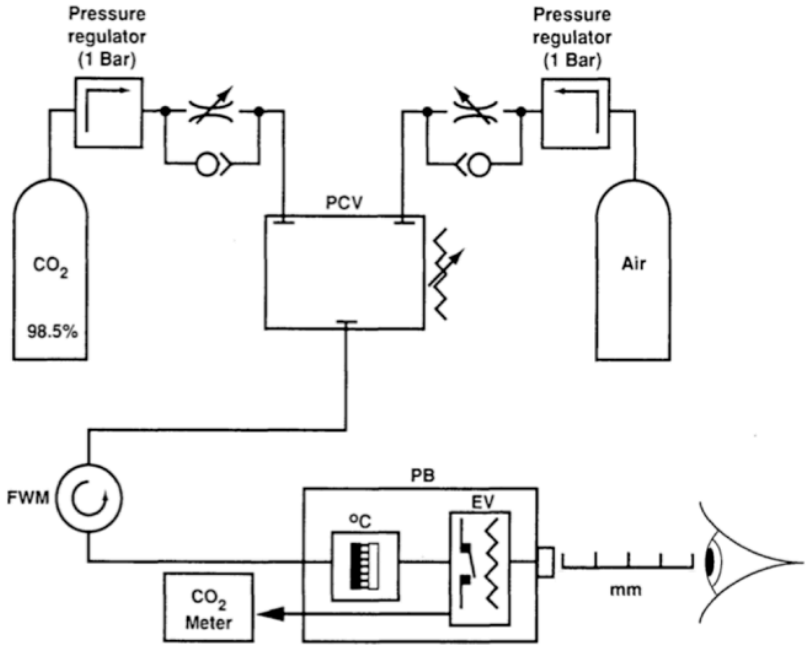

Figure 1.15: Schematic drawing of the Belmonte aesthesiometer.[14] PCV: proportional directional control valve; FWM: flowmeter; PB: probe mounted in a slit-lamp holder; EV: three-way solenoid valve to direct output of gas;

The **CRCERT-Belmonte Aesthesiometer** is a modified version of the Belmonte Aesthesiometer.[21] The CO_2 flow control meter was converted and recalibrated for air, in order to increase the maximum flow from previously 200ml/min to 400ml/min. Precise positioning of the stimulus on the central cornea was achieved by two laser pointers that helped finding the correct working distance when stimulating non-reflective locations on the ocular surface. Moveable fixation lights were mounted on the instrument housing in order to enable alterations of stimulus location.

1.18 Methods of limits as choice of psychophysical measurement

The minimum level of stimulus intensity before a sensory receptor will respond, is known as the absolute threshold. Since there is always some level of fluctuating electrical activity in the nervous system, the threshold level will change from one moment to the next. Hence, the threshold of detection is considered to occur at the stimulus intensity at which 50% of presentations are detected.[286]

The method of limits – also called the double staircase technique - is an efficient and less time consuming procedure, which has been shown to be the most accurate measurement protocol, as it allows a more rapid assessment and a reduction of possible subject fatigue, when measuring the central corneal threshold using the NCCA aesthesiometer.[287] With this method, stimuli are first presented well above or below the threshold, after which the stimulus intensity is changed in small equal amounts until the boundary of sensation is obtained, either in an ascending or descending fashion. In an ascending order series, the starting stimulus intensity is below threshold and the intensity is subsequently increased by the same set amount until the subject can detect it. In a descending order series, the starting stimulus intensity is well above threshold and the intensity is gradually decreased until the subject can no longer perceive it. The transition point for each the ascending and descending order series represents the threshold and the average of all transition points is considered to be the absolute threshold.[286] In order to avoid the error of expectation and the error of habituation, the starting point of the stimulus should be varied in each order series, so that neither the observer nor the patient will be able to judge the number of steps required to achieve the threshold.

1.19 Physiological variation in ocular surface sensitivity

It is generally agreed that the bulbar conjunctiva is less sensitive to mechanical, chemical and thermal stimuli, than the central cornea.[20,21,81,82,174,284,288,289] This difference is expected, since the cornea shows a considerably higher innervation density than the conjunctiva.[65,66,79,81,290] Fewer studies have investigated conjunctival sensitivity and all were carried out with use of the Cochet Bonnet aesthesiometer (0.12mm

filament). In 1973, Norn measured the sensitivity in 18 areas of the tarsal and bulbar conjunctiva and the lid margins ('behind the cilia, but in front of the conjunctiva') on 102 eyes and observed no difference within the tarsal and bulbar conjunctiva, but a significantly higher sensitivity at the lid margins (similar thresholds for upper and lower lid) and the caruncle.[82] McGowan et al. also investigated the sensitivity at the lid margins (n=30) by measuring at two separate points of the eyelid margin and palpebral conjunctiva for upper and lower lids.[84] They found the sensitivity to be higher at the inner edge of the lid margin (now called 'lid wiper') than on the lower eyelid margin-surface (mid-way between the eyelashes and the tarsal gland openings) and the palpebral conjunctiva. In contrast to Norn, they measured the sensitivity to be greater on the lower than the upper lid, although this could have been associated with any eyelid manipulation and tear film drying caused by the full eversion of the upper lid. Golebiowski also observed a higher sensitivity on the lower compared to the upper lid margin, at the level with the opening of the meibomian glands, slightly anterior to the lid wiper and Marx line (n=27; use of the Cochet Bonnet aesthesiometer), and established a significant relationship between tear osmolarity and lid sensitivity.[291] More recently, Navascues-Cornago et al. confirmed a greater sensitivity at the marginal conjunctiva (at level of the lid wiper), compared to the bulbar and tarsal conjunctiva, however no difference between the upper and lower lid of the marginal conjunctiva (n=35).[290] Instead, they observed a higher sensitivity at the the tarsal conjunctiva of the upper eyelid than that of the lower eyelid.

Researchers using the Cochet-Bonnet aesthesiometer generally agreed that corneal sensitivity was highest in the central cornea, compared to peripheral corneal locations.[12,13,21,81,83,288,292-294] However, when using the pneumatic Belmonte aesthesiometer, Situ et al. could not measure significantly different chemical, cool and mechanical sensitivity thresholds when comparing central, nasal and temporal corneal locations.[295] Their results were similar to Murphy et al. who received only small differences in sensitivity thresholds across the cornea, using a pneumatic cooling stimulus.[12] Stapleton et al. also could not report any difference in sensitivity comparing the central and inferior cornea.[21] Yet, Patel et al. using the cooling stimulus of the NCCA measured corneal sensitivity to be significantly higher in the centre than in its periphery.[296] They examined a large sample size (n=56, compared to n=15 in the Situ et

al. study) and noted a higher central corneal sub-basal nerve density with confocal microscopy. Murphy et al. measured corneal sensitivity to be lowest in the superior cornea, and the nasal cornea to be most sensitive, followed closely by the temporal cornea.[12] Using the Cochet-Bonnet aesthesiometer, Roszkowska et al. found the temporal cornea to be more sensitive than the nasal cornea, and the inferior region to be more sensitive than the superior area.[292] However, these differences in the peripheral parts may only be small according to some studies.[292,297] Patel et al. measured the temporal mid-periphery to be more sensitive than other peripheral corneal locations.[296]

According to several studies, ocular surface sensitivity decreases with age.[81,83,292,298-301] However, there is some uncertainty as to the precise age at which the decrease becomes significant, or whether it occurs at all. Using the Cochet-Bonnet aesthesiometer, Millodot *et al.* found that this decrease is detectable at the age of 50, or later.[83,292,301] Murphy et al. used the NCCA and measured a decrease after the age of 30.[300] It has been suggested that the reduction in sensitivity was due to decreased sub-basal nerve density with increasing age.[302] However, some researchers did not report any age-related changes in corneal sensitivity.[303,304] Golebiowski noted a significant reduction in corneal threshold with age for females, but not for males.[288]

Several researchers observed a drop in corneal sensitivity overnight, with a gradual recovery throughout the day.[21,305,306] Du Toit et al. reported a variation of 35% in central corneal sensitivity (using air gas aesthesiometry) with a 3.9% variation in central corneal thickness over 24 hours.[306] They concluded that corneal sensitivity correlates with an increase in corneal thickness, caused by overnight-oedema. It has been proposed that this corneal sensitivity drop is due to corneal swelling caused by a reduced oxygen tension at the epithelial surface during eye closure. The degree of reduction in sensitivity is supposed to be related to the duration of eye closure.[307] It was suggested that baseline central corneal sensitivity and thickness return to baseline readings 7 hours after awakening.[306] Stapleton et al. measured mechanical corneal and conjunctival sensitivity at 10am and 6 hours later, in the afternoon:[21] with a stimulus temperature of 20°C, their measurements were unaffected by the time of day. However, with a stimulus temperature of 34°C, they found higher sensitivity measurements in the afternoon for the cornea (13% variation), but not for the conjunctiva. The conjunctiva is

likely to be less susceptible to the effects of hypoxia because of its vascular nature. It also has to be remembered that the morning measurements were not taken immediately after awakening.

Conflicting results have been published on the effect of iris colour on corneal sensitivity: Millodot used the Cochet-Bonnet aesthesiometer and found blue eyes to be considerably more sensitive than brown eyes.[308] Acosta et al. measured similar mechanical thresholds for brown and green eyes (using the Belmonte aesthesiometer), but lower threshold values for blue eyes.[83] However, they examined a smaller sample group of blue and green eyes than that of brown eyes. Lawrenson and Ruskell could not observe any difference in limbal touch sensitivity between differently coloured irides either.[81]

Some studies have found an increased,[288,304] and some a decreased corneal sensitivity in females compared to males.[294] It is possible that hormonal changes in the menstrual cycle are responsible for more fluctuations in females.[298,309] Acosta et al. received lower mechanical, but not chemical thresholds for pre-menopausal women than men of the same age group.[83] However, several studies have found no difference at all between genders.[292,299,300,303] Golebiowski et al. could not detect any gender differences in corneal sensitivity in long term low and high Dk/t extended CL wear, however they did note higher levels of conjunctival sensitivity in females, which they attributed to the fact that the conjunctiva is vascularised and therefore more susceptible to differences in hormone levels, which in other sensory systems have been suggested to influence the mediation of sensitivity.[310-312]

1.20 The influence of systemic and ocular conditions on ocular surface sensation

Diabetes, herpes simplex virus keratitis, corneal ulcers, keratoconus, corneal dystrophies, albinism and trachoma have been shown to decrease corneal sensitivity.[313-317] According to some studies using the Cochet-Bonnet aesthesiometer, corneal sensitivity decreases progressively in diabetes and has been attributed to the sensory deficit as a consequence of polyneuropathy.[298,314,318] Murphy et al used the NCCA and agreed that corneal sensitivity is reduced in older diabetic patients, but could not establish a relationship between corneal sensitivity and duration of diabetes.[300]

The mechanisms that lead to symptoms of dry eye disease (DED) are not clearly understood yet. Their presence indicates the activation of nociceptors on the ocular surface,[2] as a result of tear hyper-osmolarity, reduced tear film break-up time, reduced tear volume, and/or reduced expression of mucins, inflammatory mediators and hyper-sensitivity of nociceptive sensory nerves.[189] Conflicting findings have been published regarding the effect of dry eye on corneal sensitivity. Some studies using the Cochet-Bonnet aesthesiometer[319-322] and the Belmonte aesthesiometer[299,302,323] report corneal sensitivity to decrease in subjects with dry eyes. Xu et al. and Adatia et al. observed a correlation between increased staining (fluorescein and lissamine green) and decreased levels of corneal sensitivity, and argued that this reflected the severity of DED. They speculated that an adaptation process would take place with prolonged erosion and irritation of the ocular surface, elevating the threshold for pain. Bourcier et al. and Benitez-del-Castillo et al. also measured increased mechanical, chemical and thermal thresholds in patients with dry eyes.[299,302,323] Hosal et al. noted reduced corneal sensitivity in Sjögren's patients and thickened sub-epithelial nerves in this patient group, using confocal microscopy.[322] Yet, several research groups have measured higher levels of corneal sensitivity to cooling and mechanical stimulation in dry eyes, using the Belmonte aesthesiometer.[270,303,324,325] De Paiva et al. speculated that the tight junctions of epithelial cells were disrupted or that they were desquamated.[303] They reasoned that inflammatory mediators associated with dry eye could have caused hyper-sensitivity of the corneal nerve endings. Yet, they could not measure any change in sensitivity to chemical stimulation. Tuisku et al. also observed nerve sprouting and thickened stromal nerves (using confocal microscopy), along with hyper-sensitivity in patients with Sjögren's syndrome.[324] Situ et al. established an inverse correlation between the corneal and conjunctival thresholds and staining and dry eye symptoms: the more symptoms, the higher the corneal sensitivity to mechanical and cooling stimulation was.[325] Surprisingly, they obtained higher conjunctival than corneal sensitivity in symptomatic patients and speculated that the sensory processing of the conjunctiva may be more impaired in dry eye conditions.[270] Recently, Golebiowski et al. measured an increased sensitivity of the lower lid margin (at the level of the meibomian gland openings) in patients with hyper-osmolar tears, using the Cochet Bonnet aesthesiometer.[291] They proposed that the stagnation of tears on the lower lid

margin may have caused a chemical irritation of the lid margin tissue, as a consequence of inflammatory mediators.

These contradictory reports on corneal sensitivity in dry eye conditions could indicate that there may be a continuum in compensation to this disease process: in the early stages there is hyper-sensitivity, as a result of sensitisation of the sensory nerves, which may gradually turn into hypo-sensitivity, reflecting sensory nerve damage:[325] During the early stage of DED increased evaporation, hyper-osmolarity and the consequently thinner tear film give rise to a cooling of the ocular surface: the cold sensitive nerve fibres in the sub-basal nerve complex increase their firing rate.[2] Electrophysiological studies on the cat cornea have shown that these cold fibres may detect smallest temperature differences of ±0.1°C,[29] which in turn lead to a cooling sensation.[32,173] In further stages of DED, the polymodal nociceptors react to injury and inflammatory mediators, which are secreted as a consequence of reduced tear secretion and a changed tear film quality.[2,166] As a result, the morphology of the sub-basal nerve complex changes,[302] as well as due to age-related degenerative changes, which in turn leads to a decrease in ocular surface sensation. However, the sensation of pain may continue, as the damaged nerve fibre endings in the cornea and conjunctiva may react sporadically and irregularly.[326] Also, secondary hyperalgesia (increased responsiveness to pain) and allodynia (pain from stimuli which are not normally painful) may develop, as they may appear in chronic neurological diseases.[326]

1.21 Other influences on ocular surface sensation: topical drugs, surgery and contact lens wear

Topical anaesthetics reduce corneal sensitivity, as do non-steroidal anti-inflammatory agents.[284,327,328] Non-steroidal anti-inflammatory drugs (NSAIDs) inhibit cyclo-oxygenase which mediates the breakdown of arachidonic acid in order to produce inflammatory mediators, such as prostaglandins.[329] Acosta et al observed a significant reduction in sensation intensity of mechanical, thermal and chemical stimuli (using the Belmonte gas aesthesiometer) after 0.1% diclofenac sodium, and only a slight decrease in sensation perceived after 0.03% flurbiprofen instillation.[329]

All ocular surgery involving the cornea, such as cataract surgery,[96] keratoplasty (lamellar and penetrating) and refractive surgery (LASIK, PRK, refractive keratectomy)[323,330-334] affect corneal sensitivity. As the neurons regenerate after refractive surgery, corneal sensibility gradually returns.[335-339] The reported duration of recovery varies greatly between different published studies and depending on the refractive procedure applied. Some studies report normal or near to normal corneal sensitivity levels after only six to nine months with the Cochet-Bonnet[323,330,331] and the NCCA,[340] but in another study Murphy et al. could not show full recovery of corneal sensitivity to a pre-operative level after one year, also using the NCCA.[332] Gallar et al. could observe corneal sensory disturbances even two years after LASIK, using the Belmonte aesthesiometer.[333]

As a consequence of penetrating keratoplasty, nerve fibers are severed on their course from the periphery to the centre of the cornea. Using confocal microscopy, Darwish et al. could not observe any sub-basal nerves one year after keratoplasty,[340] and Richter et al. detected some only two years after the procedure.[341] Tervo et al. used histochemical techniques and reported that the architecture and density of corneal nerves had not fully recovered three years after keratoplasty.[342] Using the Cochet-Bonnet aesthesiometer, Richter et al. measured no or considerably reduced corneal sensitivity 12 months post-operatively,[341] Mathers et al. could not measure any corneal sensitivity until 18 months after penetrating keratoplasty,[343] and Ruben and Colebrook, as well as Stamer et al., found that it had still not fully recovered three years post-operatively.[344,345] Surprisingly, Darwish et al. recorded full recovery of corneal sensitivity 12 months following penetrating keratoplasty using the NCCA, although sub-basal regeneration could not be observed at that stage.[340]

In earlier studies applying tactile stimulation, a reduction in ocular surface sensitivity was observed following contact lens (CL) wear, associated with duration of CL wear (particularly with PMMA and RGP CLs),[346-349] lens type,[350,351] and oxygen permeability.[294,352] However, with the newer silicone hydrogel (SH) CLs, no change or even a slight increase in sensitivity was observed, using air gas aesthesiometry.[21,353] The following mechanisms have been proposed to cause a change in ocular surface sensitivity in CL wear:[354] metabolic impairment of the cornea due to decreased oxygen

transmission,[294,351,355] sensory adaptation to mechanical stimulation[356,357] and corneal acidosis.[358]

1.22 Summary of the literature review

The Belmonte OPM aesthesiometer is the first commercially available instrument that uses a pulse of pressurised air directed through an air-jet located close to the eye to stimulate the ocular surface using a cooling stimulus, which can be heated to give a mechanical or warming stimulus, or mixed with CO_2 to provide a chemical stimulus. It was designed to overcome the shortfalls of the currently most widely used Cochet-Bonnet aesthesiometer. However, as a relatively new instrument, little is known of its stimulus consistency or of its stimulus characteristics. Depending on which type of nerve endings in the cornea or ocular surface that the examiner wishes to excite, different stimulus temperatures can be chosen: a cooling stimulus with a temperature lower than ocular surface temperature (OST) will excite the temperature sensitive C fibres, whereas an air gas stimulus equal to OST should be sensed by the mechanically sensitive Aδ fibres when a sufficient degree of corneal deformation can be produced by the air gas stimulus. However, it has not been established yet, what exact temperature the air stimulus of the OPM should be, in order to deliver a mechanical stimulus, and indeed, if a truly mechanical stimulus can be generated with an air gas aesthesiometer.

Blinking plays an important role in the maintenance of the integrity of the ocular surface, by contributing to the maintenance of the ocular surface moisture, the drainage of tears, the expression of lipids from meibomian glands, and the spreading of the tear lipids across the pre-corneal tear film. However, it is not clear, what role corneal sensitivity and tear film quality play in triggering a blink.

Electrophysiological recordings from the cat and guinea pig cornea have shown that cold thermoreceptors exhibit a spontaneous firing rate of nerve impulses at a normal ocular surface temperature (34-35°C) and that they increase the frequency and amplitude of their impulse activity when temperature decreases. However, upon warming of the ocular surface, cold thermoreceptors are silenced and polymodal nociceptors are being activated at temperatures over 39-40°C. A fraction of polymodal fibres have been shown to also increase their firing rate when corneal temperature is

reduced to less than 29°C. It has not been shown yet, what the effect of heating and cooling of the ocular surface, combined with the resulting changes in tear film quality on ocular surface sensation in response to an air gas stimulus may be. Will there be an enhanced or a reduced neural response of the temperature-sensitive nerves in the superficial cornea?

1.23 Thesis Hypotheses and Aims

1) The Belmonte OPM aesthesiometer provides a reliable stimulus regarding air stimulus volume, flow rate, force and temperature to obtain accurate and repeatable corneal sensitivity measurements, whereby a cooling and mechanical sensitivity threshold can be obtained separately.

The specific aims of each chapter:
Chapter 2: To evaluate if the Belmonte OPM pneumatic aesthesiometer provides a reliable stimulus to obtain accurate and repeatable corneal sensitivity measurements.

Chapter 3: To record stimulus temperature measurement of the Belmonte air gas aesthesiometer ('Ocular pain meter') *in vitro* and *in vivo.*

2) A correlation between corneal sensitivity and blink frequency is expected, confirming that ocular surface condition represents one important trigger for the initiation of a blink.

Specific chapter aim:
Chapter 4: To explore the relationship between corneal sensation, blinking (spontaneous eye blink rate and inter-blink interval), ocular surface temperature, tear film quality (non-invasive tear break up time and lipid pattern) and degree of iris pigmentation, using the cooling stimulus of the non-contact corneal aesthesiometer (NCCA).

3) Ocular surface sensation is not expected to change following a heating and / or a cooling procedure of the ocular surface, similarly to cutaneous cold-sensitive receptors, whose thermal detection threshold has not been observed to change to an increased or decreased level of impulse frequency induced by temperature change.

Specific chapter aims:
Chapters 5 and 6: To investigate the relationship between heating and cooling of the ocular surface on ocular surface sensation, using the cooling stimulus of the NCCA.

CHAPTER 2

Verification of the stimulus characteristics of the Belmonte OPM aesthesiometer

The Belmonte Ocular Pain Meter aesthesiometer (OPM; Deriva Global S.L., Valencia, Spain) is a new instrument, developed from the laboratory instrument of Belmonte et al.[19] It uses a pulse of pressurised air directed through an air-jet located close to the eye to stimulate the ocular surface using a cooling stimulus, which can be heated to give a mechanical or warming stimulus, or mixed with CO_2 to provide a chemical stimulus (Figure 1.15, Chapter 1.17). It is the first commercially available instrument to deliver this range of stimuli and thereby stimulate the different sensory receptors on the ocular surface (Figure 2.1). The OPM was designed to overcome the shortfalls of the currently most widely-used Cochet-Bonnet aesthesiometer. However, as a new instrument, little is known of its stimulus consistency or of its stimulus characteristics. For the purpose of the following experiments, only the air stimuli with different temperature and airflow rate settings will be considered.

Figure 2.1: The Belmonte OPM aesthesiometer, showing the arrangement for adjusting the positioning of the stimulus air-jet.

The range of airflow rates available from the OPM is 0-200ml/min, with the lowest level of airflow rate that a subject can sense 50% of the time taken to represent their threshold for ocular surface sensitivity. It is also possible to choose different stimulus temperatures, depending on which type of nerve endings in the cornea or ocular surface that the examiner wishes to excite: a cooling stimulus with a temperature lower than ocular surface temperature (OST) will excite the temperature sensitive C fibres, whereas an air gas stimulus equal to OST should be sensed by the mechanically sensitive Aδ fibres when a sufficient degree of corneal deformation can be produced by the air gas stimulus. Normal OST has been shown to range from 32.9-36°C.[285]

There are some discrepancies between different research groups as to what temperature the air stimulus should be, in order to deliver a mechanical stimulus: Feng and Simpson, as well as Stapleton et al., recommended a stimulus temperature of 50°C,[20,21] and in 1999, Belmonte et al. also used 50°C.[19] However, the manufacturers of the OPM recommend 43°C, which equates to a temperature increase of 19°C above a room temperature of 24°C (OPM User Manual, Deriva Global S.A.). The OPM used for the following experiments has been additionally equipped with a temperature sensor that was fitted on the outside of the instrument housing for measurement of ambient room

temperature. Stimulus temperature can be regulated by the choice of 'delta', which ranges from 3 to 60°C. 'Delta' represents the number of degrees (°C) by which the OPM will heat the air gas stimulus above the ambient temperature indicated by the external thermometer attached to the instrument. For ocular surface sensitivity measurement, the subject is seated in front of the exit nozzle of the OPM at a certain distance. Different distances are recommended by different research groups, using different builds of aesthesiometers: Murphy et al. used a distance of 1cm with the NCCA,[14] Stapleton et al. used a distance of 4mm using the CRCERT Belmonte aesthesiometer,[21] Situ et al. applied a distance of 5mm also using a Belmonte aesthesiometer,[353] and Gallar et al. chose a distance of 5mm, using the Belmonte aesthesiometer.[359] The preference for stimulus duration also varies: Stapleton et al. used stimulus durations of 1-3s,[21] Situ et al. applied 2s,[353] Gallar et al. preferred 3s,[359] and Murphy et al. selected 1s.[14]

A key component of the stimulus characteristics of the OPM depends on the consistency with which the instrument produces each stimulus air-pulse. This chapter reports on a series of experiments that were carried out to verify the following stimulus characteristics: air stimulus volume, air stimulus flow rate, air stimulus force, and air stimulus temperature.

2.1 Verification of stimulus flow rate

The first physical parameter of the OPM stimulus considered was the stimulus flow rate. In the instrument this is controlled by a flowmeter built into the machine ('FWM' in Figure 2.1). Stimulus flow rate is the primary stimulus characteristic, and the recorded output for sensation from the OPM is recorded in airflow (ml/min). Understanding this parameter is therefore important, as it gives a direct indication of the level of sensitivity measured on the ocular surface. The aim of this experiment was to verify the rate of airflow generated by the OPM.

2.1.1 Methods

A microbridge mass airflow sensor (AWM3000 series with performance characteristics @10.01±0.01 VDC; sensitivity to low flows of 30-1000ml/min; Honeywell, Freeport, Illinois, USA) was attached to the exit nozzle of the OPM (Figure 2.2). The sensor, a superconductor, operates on the theory that airflow directed across the surface of the sensing element causes heat transfer, and therefore temperature change, which is converted by the superconductor into an electric current. Output voltage varies in proportion to the mass of air flowing through the sensor's inlet and outlet ports.

The output voltage of air gas stimuli was recorded for OPM airflow rates of 30, 60, 100, 150 and 200ml/min, to represent the typical test airflows used when locating the sensation threshold. Airflow rates lower than 30ml/min could not be measured, as they were below the airflow sensor's sensitivity range. Stimulus duration was kept at 5s and all measurements were carried out five times.

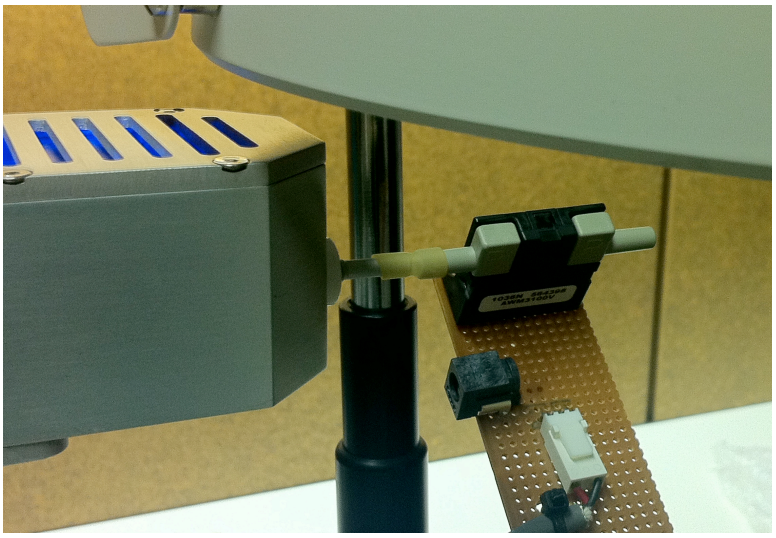

Figure 2.2: The airflow sensor connected to the exit nozzle of the OPM.

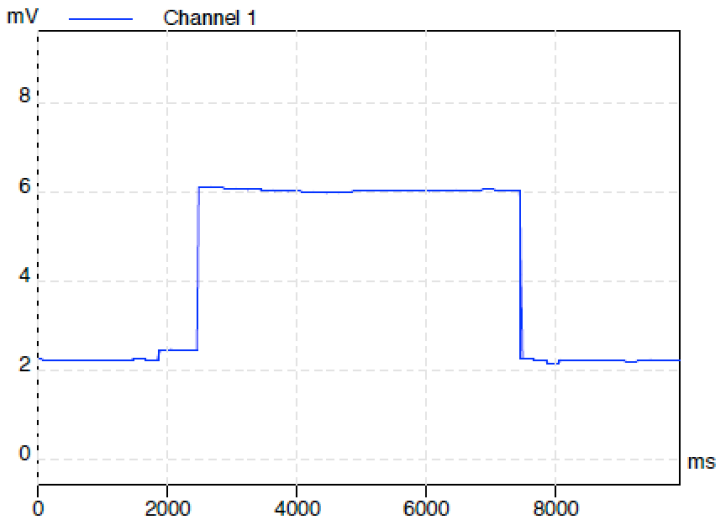

Figure 2.3: Example for a voltage output with an airflow rate of 100ml/min and a stimulus duration of 5s.

2.1.2 Results

Output voltage produced by each level of airflow rate was consistent, with little variability noted (Table 2.1). When plotted, the relationship was found to be quadratic polynomial (r= 0.996, Figure 2.4).

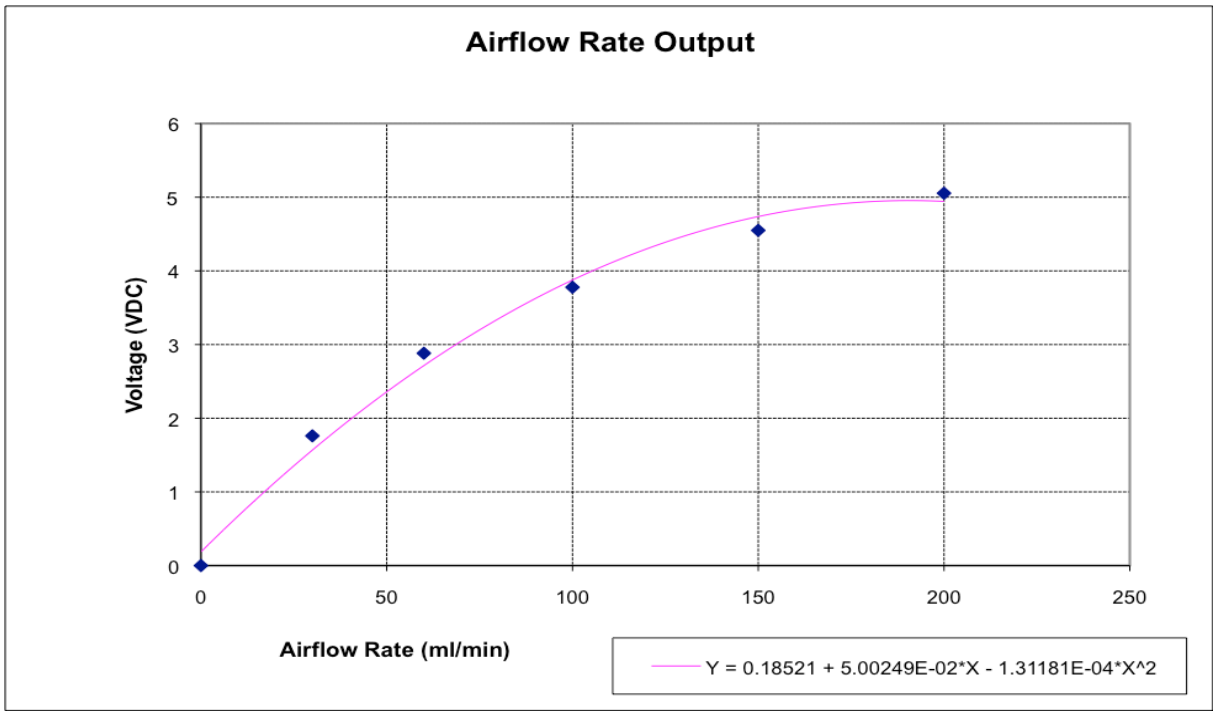

Figure 2.4: Polynomial relationship between the airflow rate (ml/min) and the voltage (VDC)

The voltage values were converted into airflow rates, according to the manufacturer's (Honeywell, USA) regression formula: y=A+B*x, whereby y=voltage (VDC), A=1.5004, B=0.0195 and x=airflow rate. Each of the five measurements was individually converted for each of the tested airflow rates accordingly, and the output for the mean airflow rate was again found to have a polynomial curve as the best-fit curve (r=0.991, Figure 2.5).

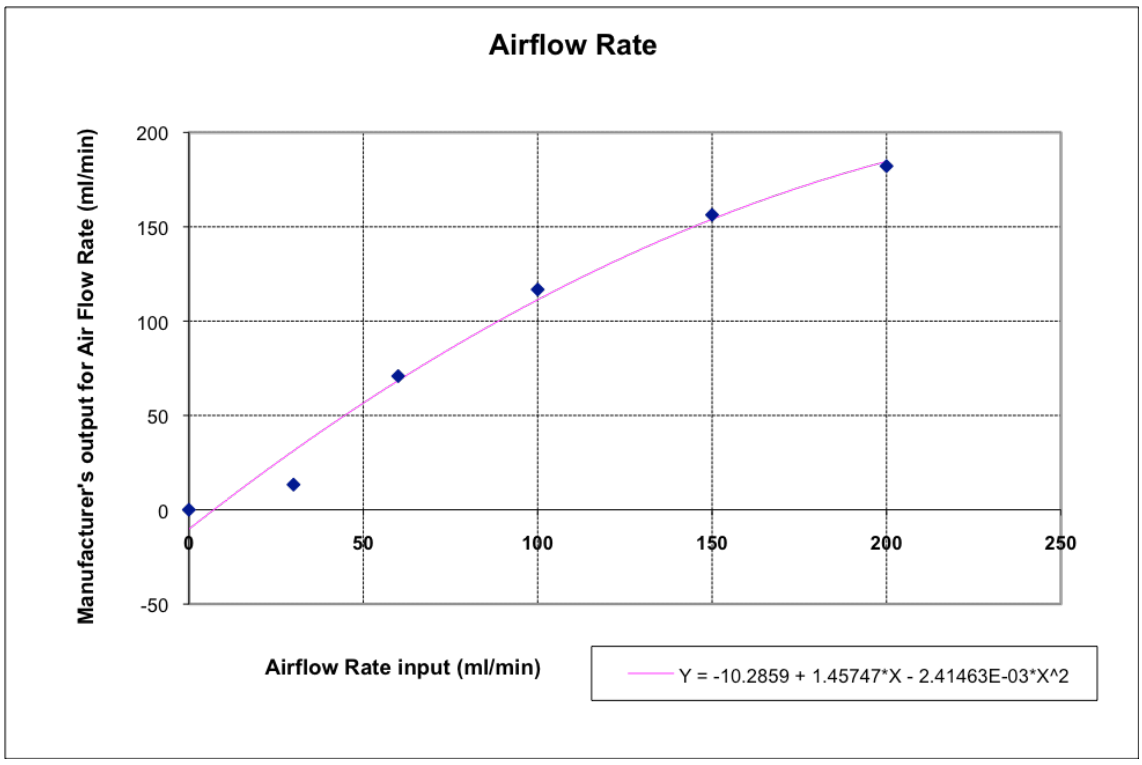

Figure 2.5: The airflow rate output generated by a regression formula: best fit curve is polynomial.

airflow (ml/min)	mean voltage (VDC) and SD	mean airflow rate output (ml/min)
0 (baseline)	0	0
30	1.761±0.021	13.35±0.16
60	2.882±0.015	70.84±0.37
100	3.778±0.039	116.74±1.20
150	4.549±0.043	156.31±1.48
200	5.054±0.056	182.16±1.02

Table 2.1: Mean values for voltage and airflow rate output.

2.1.3 Discussion

A consistent and equivalent change in airflow rate was observed, which resulted in a polynomial relationship between both the input and output of airflow rate and the airflow for a normal corneal sensitivity stimulus range. The small standard deviations indicate a consistent and repeatable rate of airflow for each airflow input/voltage output.

These results were in concordance with previous airflow rate measurements carried out by Murphy (1996) on the NCCA aesthesiometer.[287]

There seemed to be a tendency towards a plateau in the rise of airflow rate towards the 200ml/min level and there is no clear answer to this, especially in view of the high level of consistency in the results. One possible explanation may be that the airflow measured inside the instrument is under compression and that the airflow reading outside may be affected by airflow expansion. It is also important to consider that this was observed for corneal sensitivity thresholds higher than would be expected for a normal population. So, in practical terms, this effect will only slightly under-estimate corneal sensitivity in subjects who already have a considerably reduced corneal sensitivity.

Unfortunately, airflow rates lower than 30ml/min could not be verified (as they were below the airflow sensor's sensitivity range), however they would be expected to fall below a normal human corneal sensitivity threshold anyway, which has recently been reported to be 59.35±6.30ml/min using the OPM.[360] The output obtained at 30ml/min was considerably lower in comparison to those obtained from higher airflow rates, most probably due to the fact that this represents the limit from where the mass airflow sensor is able to deliver a reading. If the airflow rate of 30ml/min were to be discarded, a linear relationship between the input and output of airflow rate would result (r=0.987).

2.1.4 Conclusion

It can be concluded from this experiment that the instrument generated consistent levels of airflow rates with very little variability. However, care has to be taken when comparing corneal sensitivity thresholds obtained with this instrument to those obtained with another instrument, as the airflow characteristics may differ.

2.3 Verification of air stimulus volume

Stimulus volume is an important parameter to test, because it will have an effect on the impact of the air gas stimulus arriving on the corneal surface, the amount of corneal area covered by the air gas stimulus, and consequently it will affect the level of ocular surface sensitivity being measured. Understanding more about the consistency of the

volume provides information about the internal mechanics of the instrument, and whether it can consistently produce the same stimulus volumes. The aim of this experiment was to verify the air stimulus volume generated by the OPM Belmonte aesthesiometer.

2.3.1 Methods

A silicone rubber hose (4mm internal diameter, 102cm length) was connected to the metal exit nozzle of the OPM. The other end of the hose was submerged in a transparent vessel containing approximately 1 litre of water. An inverted glass burette (Duran, Germany) was placed in the same vessel above the opened end of the hose to collect the gas released from the nozzle. Depending on the level of stimulus airflow tested, a 100ml glass measuring cylinder or a 50ml glass burette (for titration) were used: the glass burette with 0.1ml increments was used for airflow rates up to 80ml/min (Figures 2.6 and 2.7), and the measuring cylinder with 1ml increments for airflow rates of more than 80ml/min (Figure 2.8).

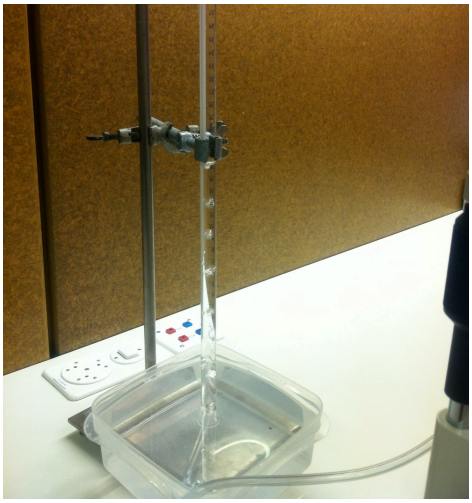

Figure 2.6 and Figure 2.7: Experiment setup with small diameter burette (0.1ml increments).

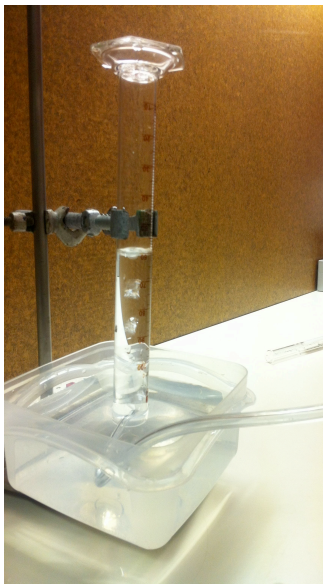

Figure 2.8: Experiment setup with larger diameter burette, during stimulus presentation (1ml increments).

The airflow volume was recorded in 5ml/min increments up to 110ml/min and in 10ml/min increments for 110 to 200ml/min. Stimulus duration was adapted to the burette size: for the airflows of 10 and 15ml/min, stimulus duration was set at 60s, for the airflows of 20 to 130ml/min it was set at 30s, and for 140ml/min it was set at 15s. These stimulus increments and durations were chosen to provide sufficient stimulus volumes that would provide a measurable displacement in the water, while not using a duration that would extend beyond the physical limitations of the burette and cylinder. For better comparison with typical stimulus airflows, the obtained air volumes were consequently converted to the equivalent of the air volume obtained per minute. All measurements were carried out five times.

2.3.2 Results

Airflow volumes obtained across all airflow rates and durations showed a linear progression with increasing levels of airflow rates (Pearson Correlation $r=0.998$, $p<0.001$, Table 2.2 and Figure 2.9). On average, there was an increase of $+7.45\pm0.03\%$ in the expected air volume obtained for each rate of airflow.

Airflow (ml/min)	Stimulus duration (s)	Mean air volume per minute (ml)	Percentage difference obtained
10	60	11.2±0.8	+10.20%
15	60	14.8±1.5	-1.33%
20	30	21.4±3.3	+7.00%
25	30	24.8±2.3	-0.80%
30	30	31.9±1.3	+6.33%
35	30	37.2±2.3	+6.29%
40	30	44.4±4.2	+12.00%
45	30	47.6±2.6	+5.78%
50	30	52.8±3.6	+5.60%
55	30	57.6±2.2	+4.73%
60	30	68.0±2.8	+13.33%
65	30	71.6±1.7	+10.15%
70	30	78.4±1.7	+12.00%
75	30	81.6±2.6	+8.80%
80	30	88.4±1.7	+10.50%
85	30	93.6±1.7	+10.12%
90	30	98.8±3.0	+9.78%
95	30	100.4±2.6	+5.68%
100	30	109.6±1.7	+9.60%
105	30	112.4±2.2	+7.05%
110	30	122.0±3.2	+10.91%
120	15	132.0±3.7	+10.00%
130	15	144.8±1.8	+11.38%
140	15	148.8±1.8	+6.29%
150	15	160.0±4.0	+6.67%
160	15	171.2±3.3	+7.00%
170	15	178.4±2.2	+4.94%
180	15	186.4±3.6	+3.56%
190	15	199.2±3.3	+4.84%
200	15	210.4±3.6	+5.20%

Table 2.2: Air volume measurements and stimulus durations.

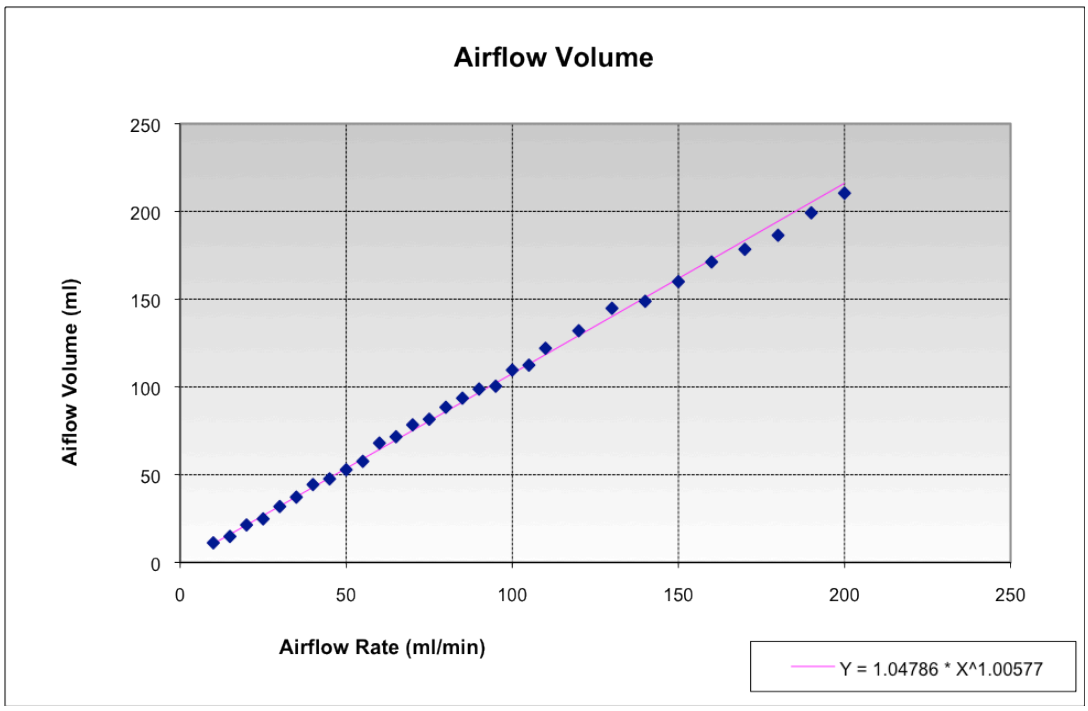

Figure 2.9: Linear progression of airflow volume (r=0.998).

2.3.3 Discussion

Again, a consistent and equivalent change in airflow volume was observed, which resulted in a linear relationship between the input and output of the level of airflow volume for a normal corneal sensitivity threshold range. Also, the small standard deviations indicate a consistent and repeatable rate of airflow for each airflow input/voltage output. These results were in concordance with previous airflow volume measurements carried out by Murphy (1996) on the NCCA aesthesiometer,[287] where a linear relationship was also obtained using a glass burette with 1ml increments.

Because of the 'dead air' in the tubing, certain latencies (a couple of seconds) for the air stimulus to arrive in the burettes were observed, due to the length of the tube connecting the aesthesiometer's exit nozzle and the burettes submerged in water. As mentioned before, it was decided to choose smaller increments of 5ml/min for the lower levels of airflow rates (up to 110ml/min) and longer durations, the lower the level of airflow rates were. The aim was to best match the capacities of the burettes used for this experiment, which would enable an evaluation beyond normal test volumes, across the breadth of the test stimulations possible in the instrument.

2.3.4 Conclusion

It can be concluded that the air stimulus volume generated by the Belmonte OPM is presented in a consistent and equivalent manner. However, the volumes were consistently higher (in a linear manner) and there was very little variability, because the standard deviations were found to be low throughout. Hence, the volume output of airflow rates can be accepted.

2.4 Verification of stimulus force

The OPM has been designed to measure mechanical ocular surface sensitivity. Hence, its air gas stimulus is required to provide a tactile element, in order to cause deformation to the ocular surface that can be sensed by the mechanically-sensitive Aδ nerve fibre endings in the ocular surface epithelia. In contrast, the Cochet-Bonnet aesthesiometer generates a tactile stimulus with use of a nylon thread, with the thread length giving an indication of the force being applied to the ocular surface. Hence it is important to verify if the OPM generates its air gas stimuli with consistent levels of force. The aim of this experiment was to measure the force exerted by the air stimulus of the BOPM at various flow rates.

2.4.1 Methods

The force exerted by the OPM was measured by directing a continuous air-jet stream vertically onto an analytical microbalance (Mettler AT261, Delta-range; precision: ±0.01mg). The unit containing the exit nozzle for the air stimulus was detached and positioned vertically above the plate of the microbalance, and all placed inside a glass box to reduce external room turbulences affecting the measurements (Figure 2.10). However, this box could not be made air-tight. The distance of the exit nozzle to the microbalance plate was chosen to be 4mm, as this was used by Stapleton et al.[21] The precise stimulus duration was set at 20 seconds. This provided sufficient time for the airflow to interact with the microbalance and provide a stable output. The airflow rate range was tested from 10 to 200ml/min, with increments of 10ml/min. Five measurements were carried out at each flow rate and were averaged for analysis.

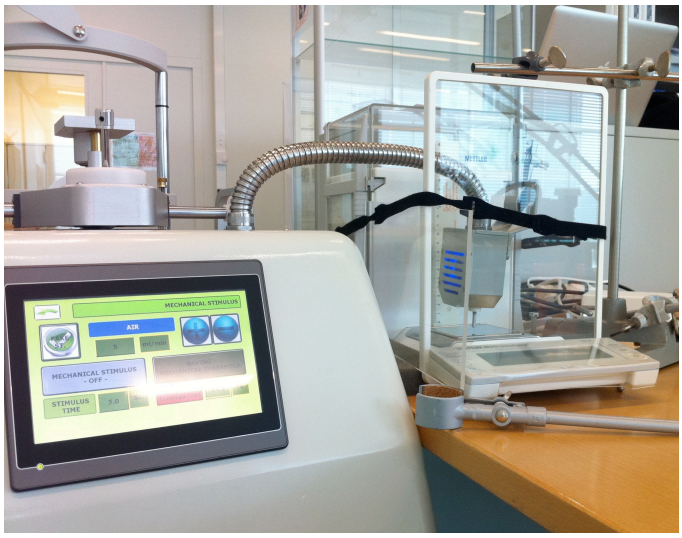

Figure 2.10: Experiment set-up for measurement of stimulus force.

2.4.2 Results

The results for the airflow force obtained showed very little variability, the standard deviations remained equally small throughout the measurements, independent of the absolute weight values recorded (Figure 2.11, Tables 2.3 and 2.4). The airflow force obtained across all airflow rates and durations was close to a linear progression with increasing airflow rates (Pearson Correlation $r=0.9845$, $p<0.001$; Figure 2.12).

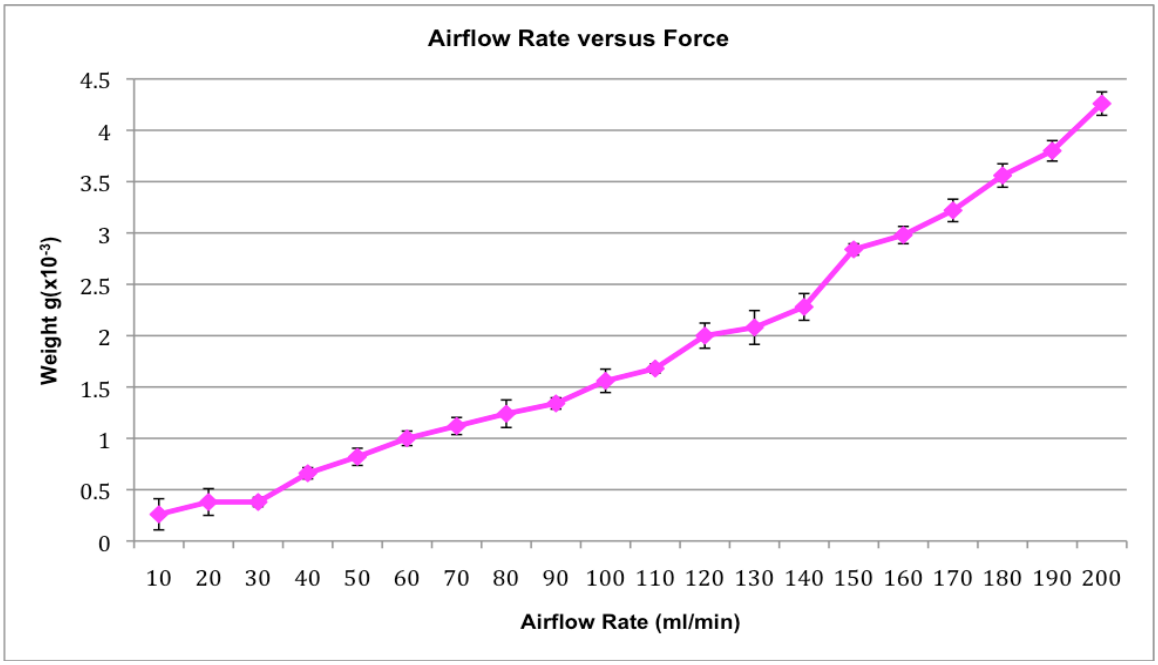

Figure 2.11: Airflow rate versus force.

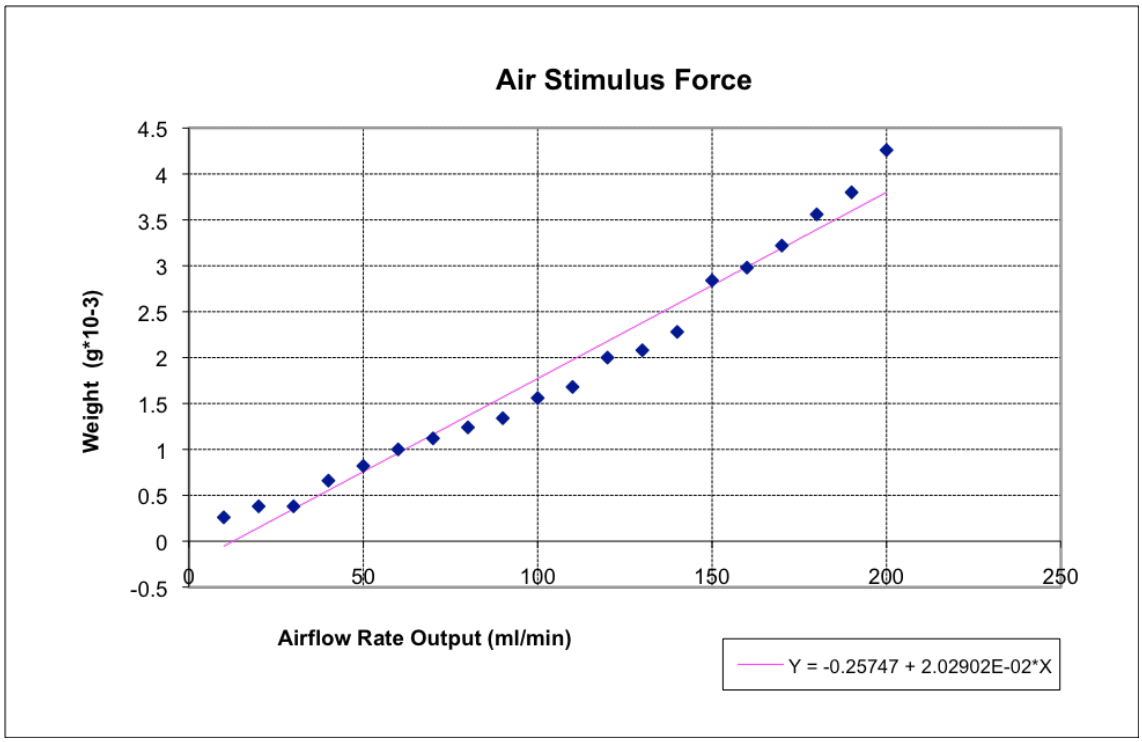

Figure 2.12: Linear progression of airflow force.

Weight ($g*10^{-3}$) versus airflow rate (ml/min)										
airflow	10	20	30	40	50	60	70	80	90	100
mean weight	0.26	0.38	0.38	0.66	0.82	1.00	1.12	1.24	1.34	1.56
SD	0.15	0.13	0.04	0.05	0.08	0.07	0.08	0.13	0.05	0.11

Table 2.3: Airflow rate versus weight for the airflow rates of 10-100ml/min.

Weight ($g*10^{-3}$) versus airflow rate (ml/min)										
airflow	110	120	130	140	150	160	170	180	190	200
mean weight	1.68	2.00	2.08	2.28	2.84	2.98	3.22	3.56	3.80	4.26
SD	0.04	0.12	0.16	0.13	0.05	0.08	0.11	0.11	0.10	0.11

Table 2.4: Airflow rate versus weight for the airflow rates of 110-200ml/min.

2.4.3 Discussion

It could be confirmed that the level of force increased in a close to linear manner in response to increasing levels of airflow rates. However, because the absolute force measurements obtained for the airflow rates less than 30ml/min were very small, they were more affected by the small fluctuations of the measurement. Possibly, the microbalance was reaching its limits of precision for these very low levels of airflow rates. Also, there could have been airflow turbulences present in the room that could have particularly affected the accuracy of the small measurements, because the chamber with the aesthesiometer nozzle above the microbalance could not be shielded completely air-tight.

Unfortunately, with the method applied for this experiment, it was not possible to assess the effect of the initial impact of the airflow on the surface, as this might be an interesting attribute of the air pulse.

2.4.4 Conclusion

It can be concluded that the force exerted by the air stimulus of the BOPM is very consistent at the various flow rates tested in this experiment.

CHAPTER 3
Stimulus temperature measurement *in vitro* and *in vivo*

3.1 Measurement of stimulus temperature with use of two thermocouples *in vitro*

A key characteristic of the Belmonte OPM aesthesiometer is that it is expected to produce thermal and mechanical stimuli. In order to do so, the OPM can heat the airflow exiting from the stimulus nozzle. The purpose of this experiment was to investigate the ability of the OPM to produce air stimuli with specific temperatures in a consistent manner. The temperature change produced within the airflow was investigated using two different types of thermocouples: a Type T wire thermocouple, and a flat Type K thermocouple. The aim was to assess stimulus temperature with different temperature settings, to verify if the recordings are consistent and if the aesthesiometer is capable of delivering a purely mechanical stimulus that does not stimulate thermal receptors.

3.1.1 Stimulus temperature measurement with use of a wired thermocouple

3.1.1.1 Methods

A Type T thermocouple (a temperature-sensitive wire with a diameter of 1.5mm; 0.025°C resolution over a temperature range of -250 to 400°C) was placed in front of the aesthesiometer nozzle (Pico Technologies, St. Neots, UK) at two distances (4mm and 8mm, Figure 3.1 showing the 4mm distance). Stapleton et al. use the shorter distance of 4mm,[21] and Gallar et al.[359] as well as Situ et al.[353] used the very similar distance of 5mm. The maximum mean air stimulus temperature and the maximum mean change in stimulus temperature were measured over three different durations of 1s, 3s and 5s. An external temperature sensor was attached to the Belmonte OPM aesthesiometer in order to record room temperature. This permitted a control of the temperature changes by which the stimulus was heated up. Humidity levels were constant at 32%. The ambient temperature was noted before each change in stimulus

characteristics (duration, distance and temperature), mean temperature throughout the study was 24.02±0.34C°.

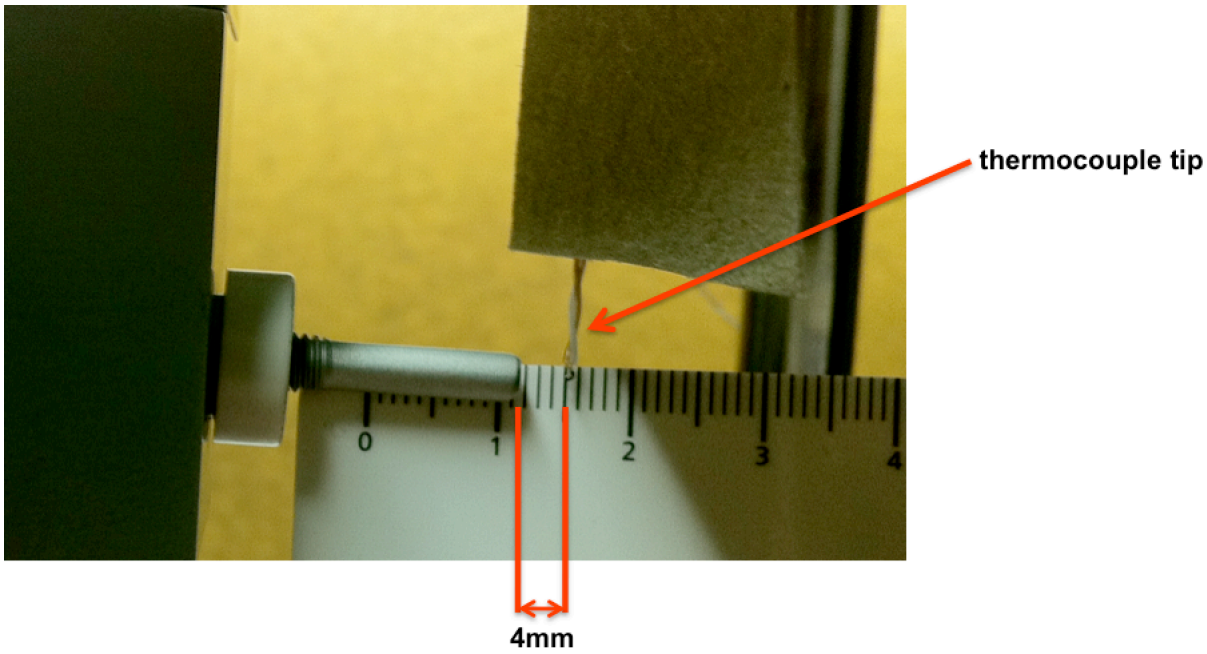

Figure 3.1: The Type T wire thermocouple placed in front of the nozzle of the Belmonte OPM aesthesiometer at 4mm distance.

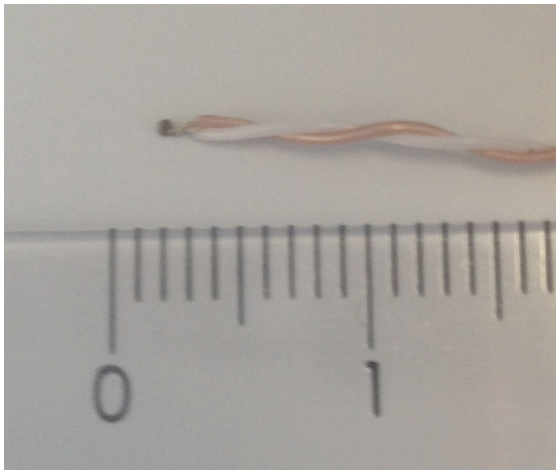

Figure 3.2: The sensor end of the wire thermocouple placed next to a mm ruler to illustrate scale.

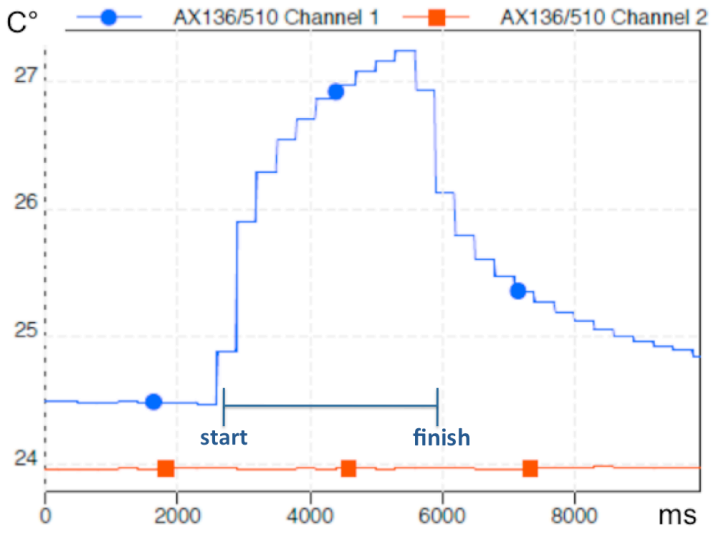

Figure 3.3: Example for a recording with the following stimulus characteristics: 'delta 20', 4mm distance, 3s duration and 60ml/min airflow rate; Channel 1 represents the stimulus temperature recording and Channel 2 represents room temperature.

Five consecutive measurements were taken of each combination of these different stimulus settings:

- The airflows were set at 30, 60 and 100ml/min: 30ml/min being likely to be just below human corneal sensitivity threshold, 60ml/min being at or just above threshold, and 100ml/min at above threshold in a normal population.[360]
- The distance to the aesthesiometer nozzle was set at 4 and 8mm: as mentioned above, 4mm was also used by Stapleton et al.[21] and is also the shortest practical distance for a measurement on a real patient, and 8mm was chosen to evaluate what happens at a longer distance away, when the air will have dispersed further.
- The standard stimulus durations were used: 1, 3 and 5s.
- Stimulus temperature with increasing increments of 5, 20, 40, 50 and 60°C, compared to ambient temperature (hereafter described as delta) was applied. This reduced range of temperature changes was chosen as an initial set-up to explore whether the wire thermocouple would work. For the mechanical stimulus setting, the delta required needed to be larger than zero, therefore 'delta 5' was chosen to be the lowest value. 'delta 60' represented the highest value that could be chosen. Even with this limited range of stimulus

temperatures, 450 individual measurements (with five repeat measurements for each test combination) were carried out.

3.1.1.2 Statistical analysis

Statistical analyses examining the difference in temperature changes for the three different airflows were carried out for the various stimulus settings tested in this study (distance and duration). For normally distributed data (Shapiro-Wilk Test), a general linear model (multifactorial ANOVA repeated measures) and subsequently post-hoc t-tests with subsequent Bonferroni corrections were applied (SPSS Version 20, Chicago, IL, USA).

3.1.1.3 Results

In the following, the maximum mean changes in stimulus temperature obtained, are displayed for each individual delta setting. The recorded mean maximum temperatures of each stimulus presentation are displayed in the appendix section 8.1.1. In addition, the mean time taken, until these maximum stimulus temperature changes were reached and the effects of the individual stimulus characteristics (such as distance, duration and airflow rate) on stimulus temperature, were evaluated.

3.1.1.3.1 Delta 5

The rise in temperature was found to be small with 'delta 5' and never exceeded 25.3°C. These results were found to be consistent, as all the standard deviations remained small (Figures 3.4 and 3.5).

When corrected for room temperature, the stimulus temperature remained close to room temperature (Figure 3.4, showing a small, but overall statistically significant temperature increase with all stimulus characteristics ($p<0.001$; $F=133.78$ for 'distance' and 'duration', $F=83.87$ for airflow rate). These recorded temperature changes were slightly more marked with the higher airflow rates, the shorter working distance and the longer stimulus durations.

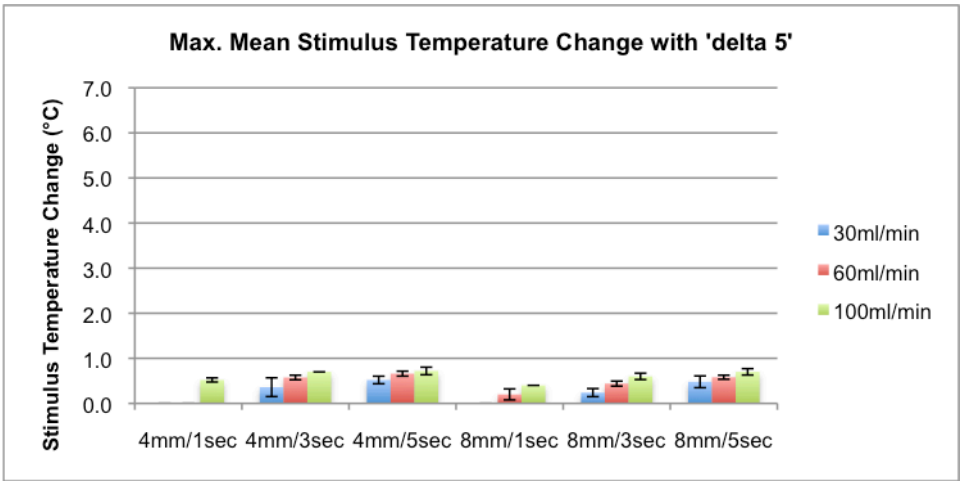

Figure 3.4: Maximum mean change in stimulus temperature with 'delta 5'

A post-hoc, pair-wise comparison confirmed that the stimulus characteristics 'distance' and 'duration' had statistically significant effects on stimulus temperature when comparing the short duration of 1s with the longer durations of 3 and 5s, independent of the distance applied (Table 3.1). However, the stimulus temperature changes did not differ to a significant degree, when only the distance was changed, as was illustrated by the pair-wise comparisons of 4mm/1s vs. 8mm/1s, giving a p-value of 1.000.

pair	4mm/1s vs. 4mm/3s	4mm/1s vs. 4mm/5s	4mm/1s vs. 8mm/1s	4mm/1s vs. 8mm/3s	4mm/1s vs. 8mm/5s	4mm/3s vs. 4mm/5s	4mm/3s vs. 8mm/1s
p-value	0.006	<0.001	1.000	0.003	0.002	0.986	0.001

pair	4mm/3s vs. 8mm/3s	4mm/3s vs. 8mm/5s	4mm/5s vs. 8mm/1s	4mm/5s vs. 8mm/3s	4mm/5s vs. 8mm/5s	8mm/1s vs. 8mm/3s	8mm/1s vs. 8mm/5s	8mm/3s vs. 8mm/5s
p-value	0.157	1.000	<0.001	0.011	1.000	0.001	0.001	0.076

Table 3.1: Pair-wise comparisons of the effects of the stimulus characteristics 'distance' and 'duration' on stimulus temperature with 'delta 5' (post-hoc t-test).

When comparing the stimulus temperature changes with different levels of airflow rates, all were statistically significant (Table 3.2).

pair	30 vs. 60ml/min	30 vs. 100ml/min	60 vs. 100ml/min
p-value	0.007	0.002	0.001

Table 3.2: Pair-wise comparisons of the effects of the stimulus characteristics 'airflow rate' on stimulus temperature with 'delta 5' (post-hoc t-test).

3.1.1.3.2 Delta 20

Not surprisingly, with 'delta 20' the stimulus temperature increases were more marked in comparison with 'delta 5', and overall were highly statistically significant, regarding all stimulus characteristics ($p<0.001$; $F=64.22$ for 'duration' and 'distance', $F=35.87$ for airflow rate). Stimulus temperatures increased by a larger amount at the 4mm distance, with the longer stimulus durations of 3 and 5s, and with higher airflow rates (Figure 3.5). These results were found to be consistent, as all the standard deviations remained small.

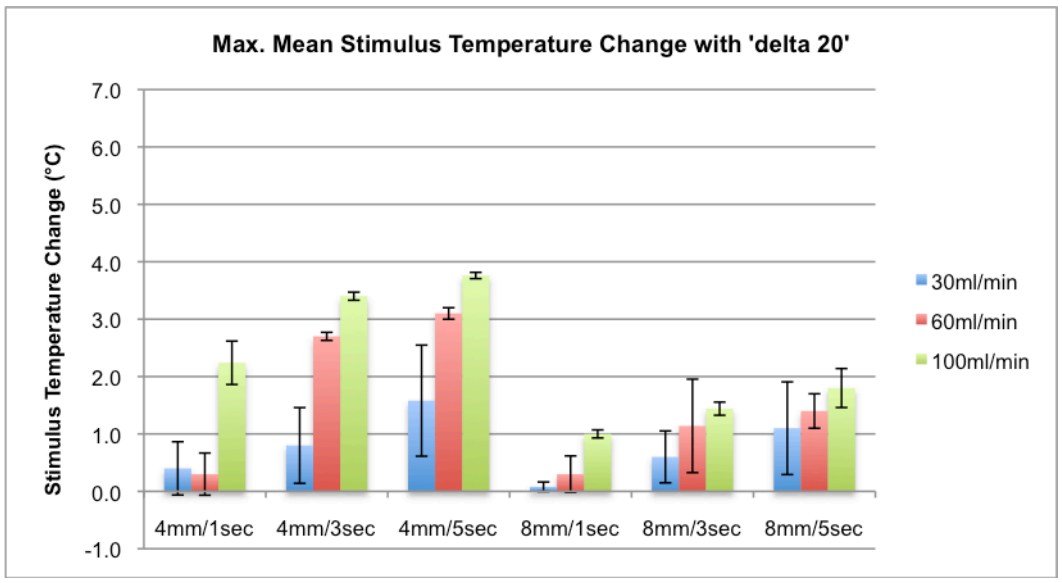

Figure 3.5: Maximum mean change in stimulus temperature with 'delta 20'.

A post-hoc pair-wise comparison revealed that the duration had a marked effect on stimulus temperature change, but in contrast to the findings with 'delta 5', the effect of distance had a greater influence on stimulus temperature change with 'delta 20' (Table 3.3).

pair	4mm/1s vs. 4mm/3s	4mm/1s vs. 4mm/5s	4mm/1s vs. 8mm/1s	4mm/1s vs. 8mm/3s	4mm/1s vs. 8mm/5s	4mm/3s vs. 4mm/5s	4mm/3s vs. 8mm/1s	4mm/3s vs. 8mm/3s
p-value	0.025	0.010	0.178	1.000	1.000	0.201	<0.001	0.015

pair	4mm/3s vs. 8mm/s	4mm/5s vs. 8mm/1s	4mm/5s vs. 8mm/3s	4mm/5s vs. 8mm/5s	8mm/1s vs. 8mm/3s	8mm/1s vs. 8mm/5s	8mm/3s vs. 8mm/5s
p-value	0.017	<0.001	0.008	0.004	0.074	0.054	1.000

Table 3.3: Pair-wise comparisons of the effects of the stimulus characteristics 'distance' and 'duration' on stimulus temperature with 'delta 20' (post-hoc t-test).

The effect of airflow rate was less marked when comparing 30 with 60ml/min than when comparing the low and medium airflow rates of 30 and 60ml/min with the higher airflow rate of 100ml/min (Table 3.4).

pair	30 vs. 60ml/min	30 vs. 100ml/min	60 vs. 100ml/min
p-value	0.109	0.003	0.003

Table 3.4: Pair-wise comparisons of the effects of the stimulus characteristics 'airflow rate' on stimulus temperature with 'delta 20' (post-hoc t-test).

3.1.1.3.3 Delta 40

As expected, the stimulus temperature increases were yet more marked and statistically significant with 'delta 40' ($p<0.001$, $F=100.44$ for 'duration' and 'distance', $F=125.14$ for airflow rate). They followed the trend of larger temperature differences with the shorter distance, the longer durations and the higher airflow rates (Figure 3.6). The variability of the measurements improved considerably with increasing levels of airflow rates.

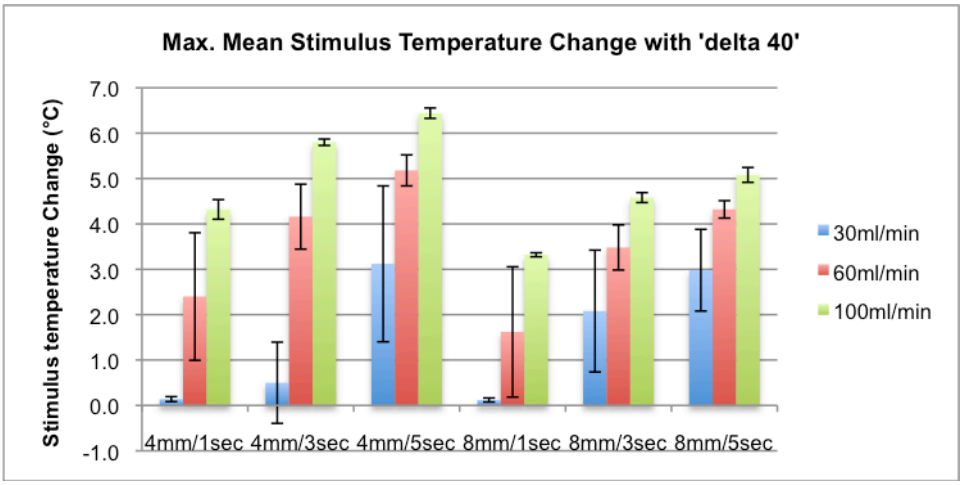

Figure 3.6: Maximum mean change in stimulus temperature with 'delta 40'

A post-hoc pair-wise comparison revealed that stimulus duration had less of an effect on stimulus temperature change: the pairs 4mm/1s vs. 8mm/1s (p=0.245), 4mm/3s vs. 8mm/3s (p=1.000) and 4mm/5s vs. 8mm/5s (p=0.090) were not statistically significant (Table 3.5).

pair	4mm/1s vs. 4mm/3s	4mm/1s vs. 4mm/5s	4mm/1s vs. 8mm/1s	4mm/1s vs. 8mm/3s	4mm/1s vs. 8mm/5s	4mm/3s vs. 4mm/5s	4mm/3s vs. 8mm/1s	4mm/3s vs. 8mm/3s
p-value	0.025	<0.001	0.245	0.024	0.003	0.006	0.011	1.000

pair	4mm/3s vs. 8mm/5s	4mm/5s vs. 8mm/1s	4mm/5s vs. 8mm/3s	4mm/5s vs. 8mm/5s	8mm/1s vs. 8mm/3s	8mm/1s vs. 8mm/5s	8mm/3s vs. 8mm/5s
p-value	0.003	0.003	0.041	0.090	0.001	0.003	0.398

Table 3.5: Pair-wise comparisons of the effects of the stimulus characteristics 'distance' and 'duration' on stimulus temperature with 'delta 40' (post-hoc t-test).

When comparing the stimulus temperature changes with different levels of airflow rates, they were all statistically significant (Table 3.6).

pair	30 vs. 60ml/min	30 vs. 100ml/min	60 vs. 100ml/min
p-value	<0.001	0.001	0.017

Table 3.6: Pair-wise comparisons of the effects of the stimulus characteristics 'airflow rate' on stimulus temperature with 'delta 40' (post-hoc t-test).

3.1.1.3.4 Delta 50

The stimulus temperature increases were yet more marked and statistically significant with 'delta 50' ($p<0.001$, $F=148.92$ for 'duration' and 'distance', $F=110.36$ for airflow rate). With the stimulus temperatures of 'delta 50', the temperature measurements obtained with the airflow rates of 60 and 100ml/min reached values close to corneal surface temperature, when the air gas stimuli were set at 4mm/3s and 4mm/5s (Figure 3.7). As before, a marked reduction in variability could be observed with the higher levels of airflow rates of 60 and 100ml/min.

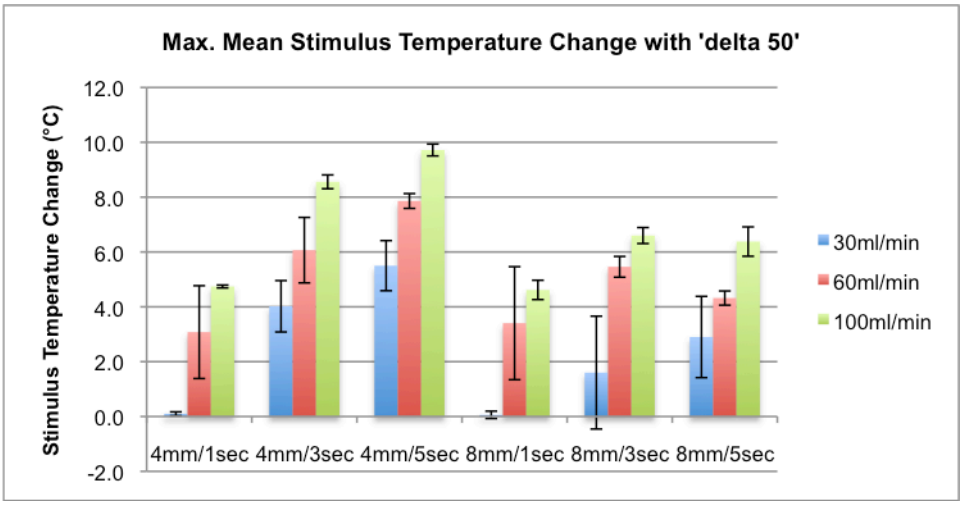

Figure 3.7: Maximum mean change in stimulus temperature with 'delta 50'.

The post-hoc pair-wise comparison indicated that the stimulus characteristics 'duration' and 'distance' had an effect on stimulus temperature, as the majority of pairs were noted to be statistically significant. The exceptions were the pair of 4mm/1s vs. 8mm/1s ($p=1.000$; probably due to the weak effect of the short stimulus duration), the pair of 8mm/1s vs. 8mm/3s ($p=0.139$), and the pair of 8mm/3s vs. 8mm/5s ($p=1.000$; probably due to the overall weaker effect from the longer working distance; Table 3.7).

pair	4mm/1s vs. 4mm/3s	4mm/1s vs. 4mm/5s	4mm/1s vs. 8mm/1s	4mm/1s vs. 8mm/3s	4mm/1s vs. 8mm/5s	4mm/3s vs. 4mm/5s	4mm/3s vs. 8mm/1s
p-value	0.001	<0.001	1.000	0.047	0.018	0.018	0.003

pair	4mm/3s vs. 8mm/3s	4mm/3s vs. 8mm/5s	4mm/5s vs. 8mm/1s	4mm/5s vs. 8mm/3s	4mm/5s vs. 8mm/5s	8mm/1s vs. 8mm/3s	8mm/1s vs. 8mm/5s	8mm/3s vs. 8mm/5s
p-value	0.006	0.013	<0.001	0.007	<0.001	0.139	0.010	1.000

Table 3.7: Pair-wise comparisons of the effects of the stimulus characteristics 'distance' and 'duration' on stimulus temperature with 'delta 50' (post-hoc t-test).

When comparing the stimulus temperature changes with different levels of airflow rates, they were all statistically significant (Table 3.8).

pair	30 vs. 60ml/min	30 vs. 100ml/min	60 vs. 100ml/min
p-value	<0.001	0.001	0.020

Table 3.8: Pair-wise comparisons of the effects of the stimulus characteristics 'airflow rate' on stimulus temperature with 'delta 50' (post-hoc t-test).

3.1.1.3.5 Delta 60

Again, the temperature increase was even more marked with 'delta 60' compared to 'delta 50' ($p<0.001$, $F=231.27$ for 'duration' and 'distance', $F=468.61$ for airflow rate). The temperature measurements obtained with the airflow rates of 60 and 100ml/min reached values comfortably matching corneal surface temperature when the air gas stimuli were set at 4mm/3s and 4mm/5s (Figure 3.8). With the short distance, the longer duration of 5s and a minimum airflow rate of 60ml/min, corneal temperature was even exceeded. Also, the air stimulus at the longer distance of 8mm came close to corneal surface temperature with the longer duration of 5s and the highest airflow rate of 100ml/min. As before, a marked reduction in variability could be observed with the higher levels of airflow rates of 60 and 100ml/min.

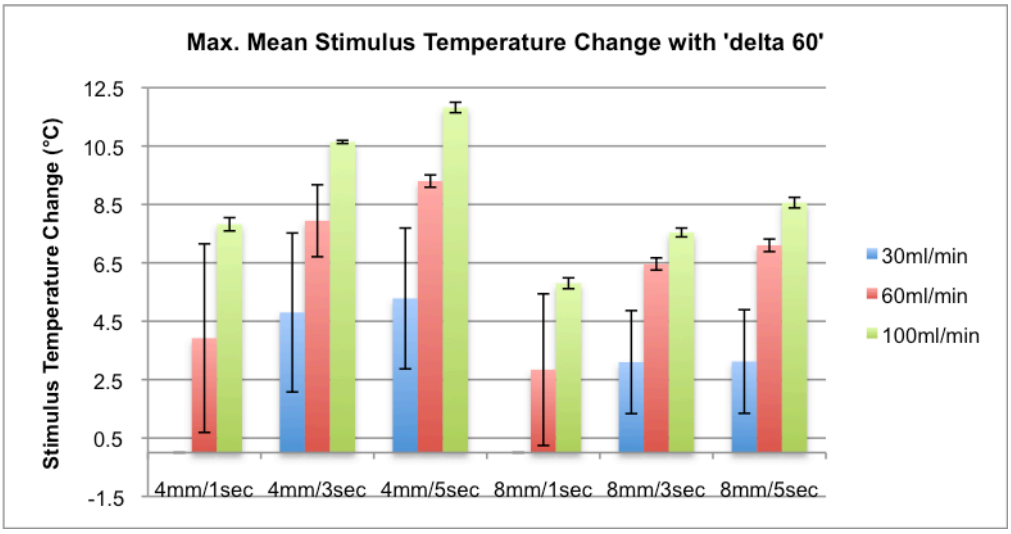

Figure 3.8: Maximum mean change in stimulus temperature with 'delta 60'.

The post-hoc pair-wise comparison showed statistical significance for all pairs, except for the pair 4mm/3s vs. 4mm/5s (p=0.145; Table 3.9).

pair	4mm/1s vs. 4mm/3s	4mm/1s vs. 4mm/5s	4mm/1s vs. 8mm/1s	4mm/1s vs. 8mm/3s	4mm/1s vs. 8mm/5s	4mm/3s vs. 4mm/5s	4mm/3s vs. 8mm/1s
p-value	<0.001	0.001	0.009	0.001	0.002	0.145	<0.001

pair	4mm/3s vs. 8mm/3s	4mm/3s vs. 8mm/5s	4mm/5s vs. 8mm/1s	4mm/5s vs. 8mm/3s	4mm/5s vs. 8mm/5s	8mm/1s vs. 8mm/3s	8mm/1s vs. 8mm/5s	8mm/3s vs. 8mm/5s
p-value	0.004	0.012	0.001	0.011	0.022	<0.001	<0.001	0.048

Table 3.9: Pair-wise comparisons of the effects of the stimulus characteristics 'distance' and 'duration' on stimulus temperature with 'delta 60' (post-hoc t-test).

When comparing the stimulus temperature changes with different levels of airflow rates, they were all statistically significant (Table 3.10).

pair	30 vs. 60ml/min	30 vs. 100ml/min	60 vs. 100ml/min
p-value	<0.001	<0.001	0.002

Table 3.10: Pair-wise comparisons of the effects of the stimulus characteristics 'airflow rate' on stimulus temperature with 'delta 60' (post-hoc t-test).

3.1.1.3.6 Mean time difference between minimum and maximum temperature

During each stimulus presentation, the mean time difference between the minimum and the maximum measured temperature was recorded in milliseconds. This gave an indication of the latency for the maximum temperature change to occur after the individual stimuli were presented. According to the thermocouple manufacturer's information (Pico Technology), a latency of 300ms was to be expected when two recording channels were used, as was the case during this experiment (one to record ambient temperature and one to record stimulus temperature).

Figures 3.9–3.13 show that the maximum stimulus temperatures were reached towards the end of the stimulus presentation, and this occurred with all other stimulus characteristics. This latency in recorded temperature changes increased with rising levels of airflow rates. Again, the degree of variability decreased considerably for the high airflow rates of 60 and 100ml/min.

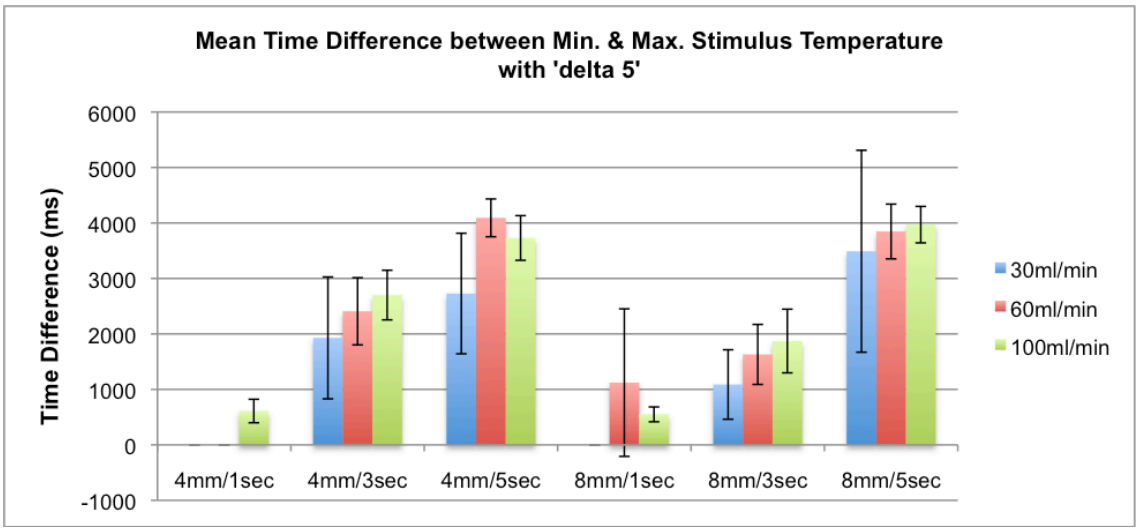

Figure 3.9: Mean time difference between min. and max. temperature with 'delta 5'.

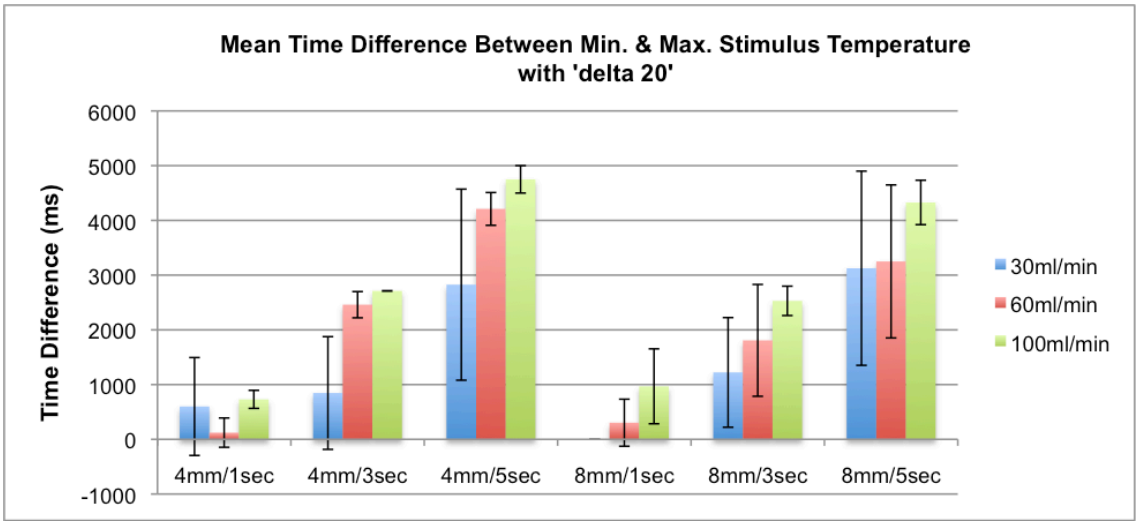

Figure 3.10: Mean time difference between min. and max. temperature with 'delta 20'.

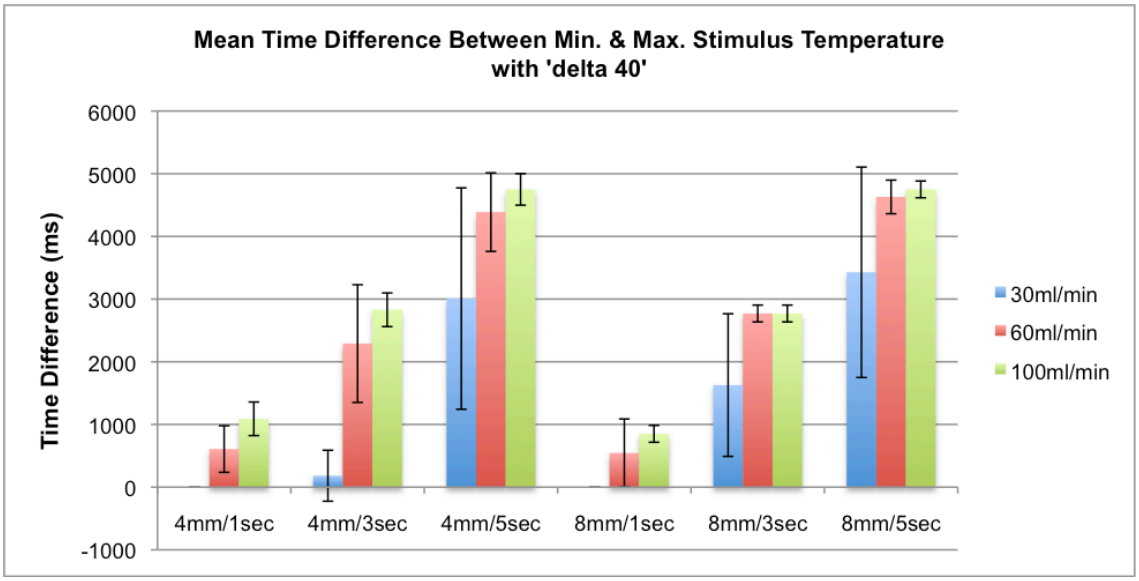

Figure 3.11: Mean time difference between min. and max. temperature with 'delta 40'.

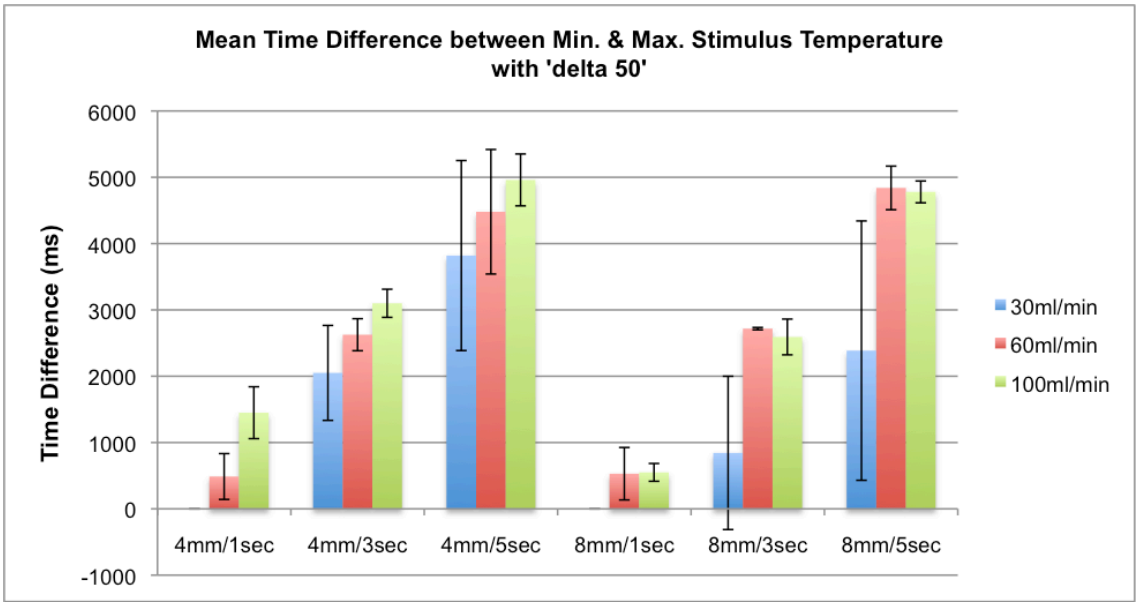

Figure 3.12: Mean time difference between min. and max. temperature with 'delta 50'.

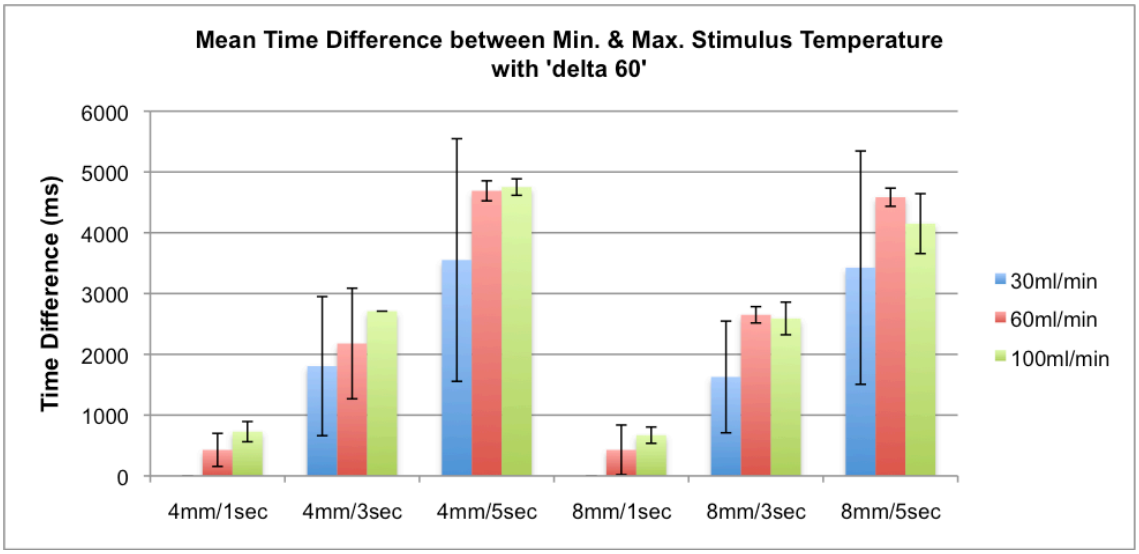

Figure 3.13: Mean time difference between min. and max. temperature with 'delta 60'.

3.1.1.3.7 The effect of stimulus characteristics (distance and duration) on the recorded stimulus temperature change with rising levels of 'delta'

As discussed previously, the stimulus characteristics 'duration' and 'distance' had a marked effect on stimulus temperature increase. This can be visually illustrated by summarising the stimulus temperature increases with the various 'deltas' tested in this study (Figures 3.14-3.16).

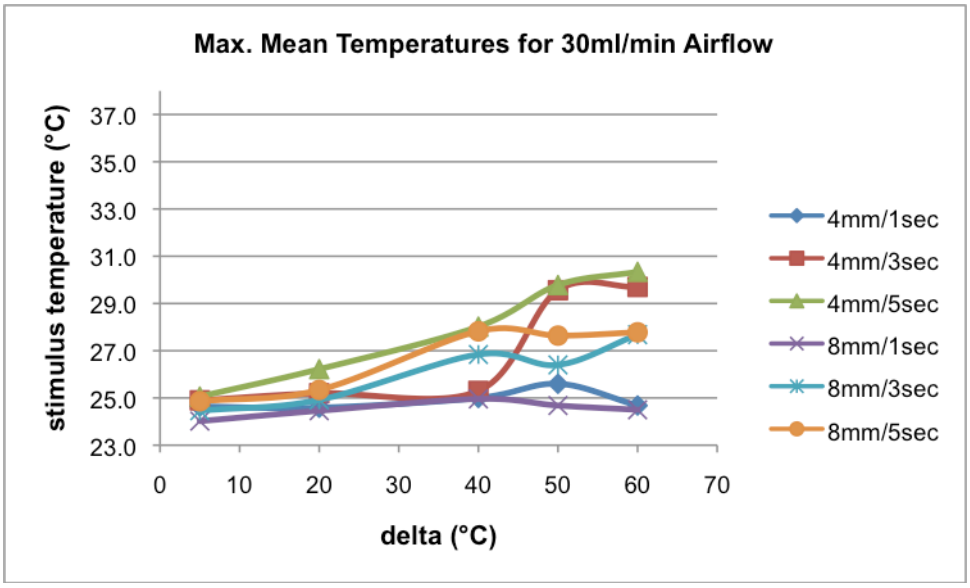

Figure 3.14: Maximum mean temperatures for airflow 30ml/min.

From Figure 3.14 it becomes clear that there was no or very little increase in temperature despite rising delta values with a low airflow rate of 30ml/min, when the short stimulus duration of 1s and/or the longer 8mm distance were chosen. However, with the longer stimulus durations of 3 and 5s, a more notable rise in temperature could be achieved at the longer working distance of 8mm with increasing delta values of ≥30. A stimulus temperature of approximately 30°C was recorded only for the stimulus at a distance of 4mm with the longer stimulus durations of 3 and 5 s, applying the highest possible levels of 'delta 50 and 60'. For delta values <30, the thermocouple was not found to be sufficiently sensitive with the low air flow rate of 30ml/min.

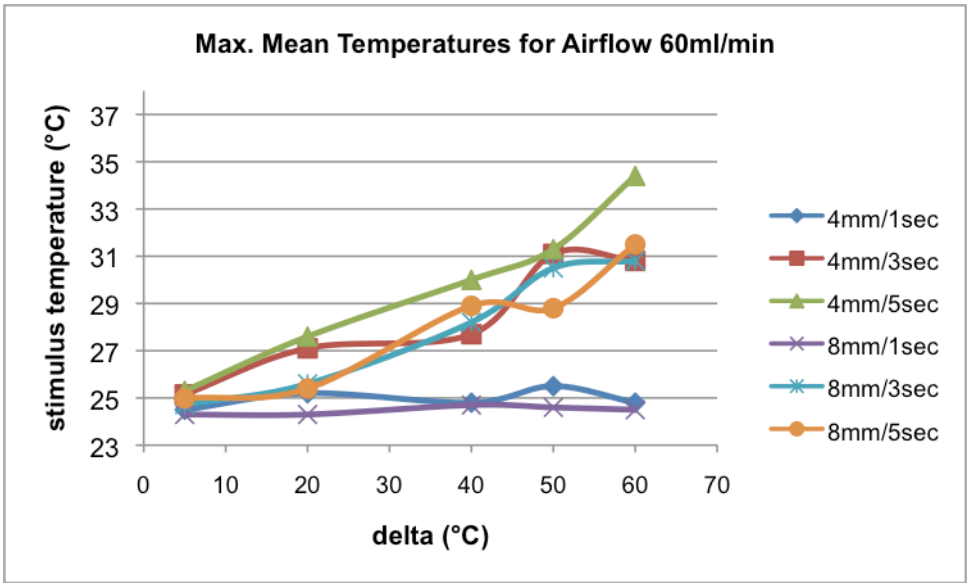

Figure 3.15: Maximum mean temperatures for airflow 60ml/min.

There was also no or very little increase in temperature despite rising delta values with a low airflow of 60ml/min, when the short stimulus duration of 1s was applied (Figure 3.15). When using the prolonged stimulus durations of 3 and 5s, rises in temperature could be achieved at both working distances and longer stimulus durations.

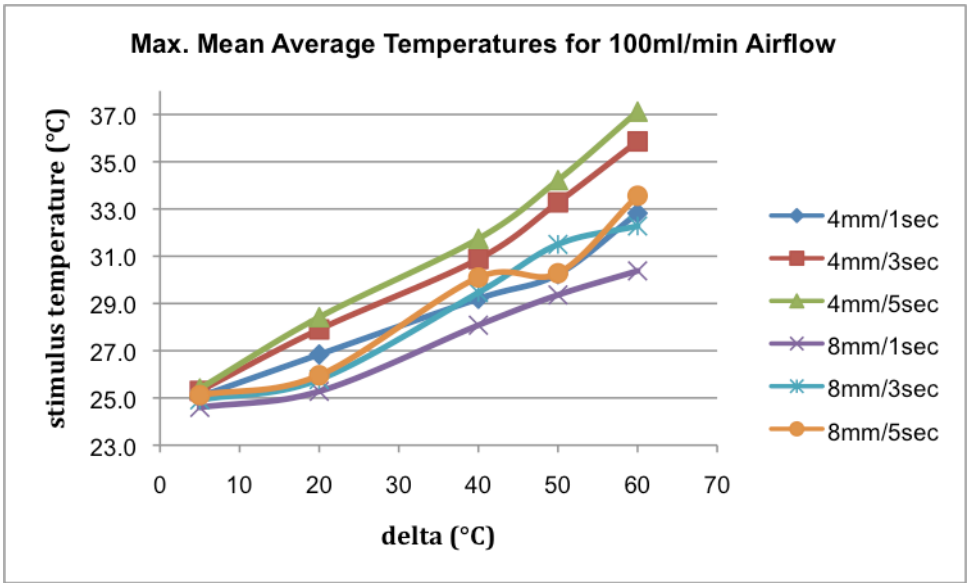

Figure 3.16: Maximum mean temperatures for airflow 100ml/min.

All stimulus settings showed an increase in temperature to a minimum of 30°C with an airflow of 100ml/min, when 'delta 60' was applied (Figure 3.16). The maximum 'delta'

change in stimulus temperature rose to 36-38°C at the 4mm distance and stimulus durations of 3 and 5s.

3.1.1.3.8 The effect of airflow rate on the recorded stimulus temperature, with rising levels of 'delta'

As was shown previously, the level of airflow rate had a marked effect on recorded stimulus temperature, it being affected by rising levels of 'delta'. By summarising the temperature increases across the various 'deltas', this effect becomes visually more apparent (Figures 3.17-3.19).

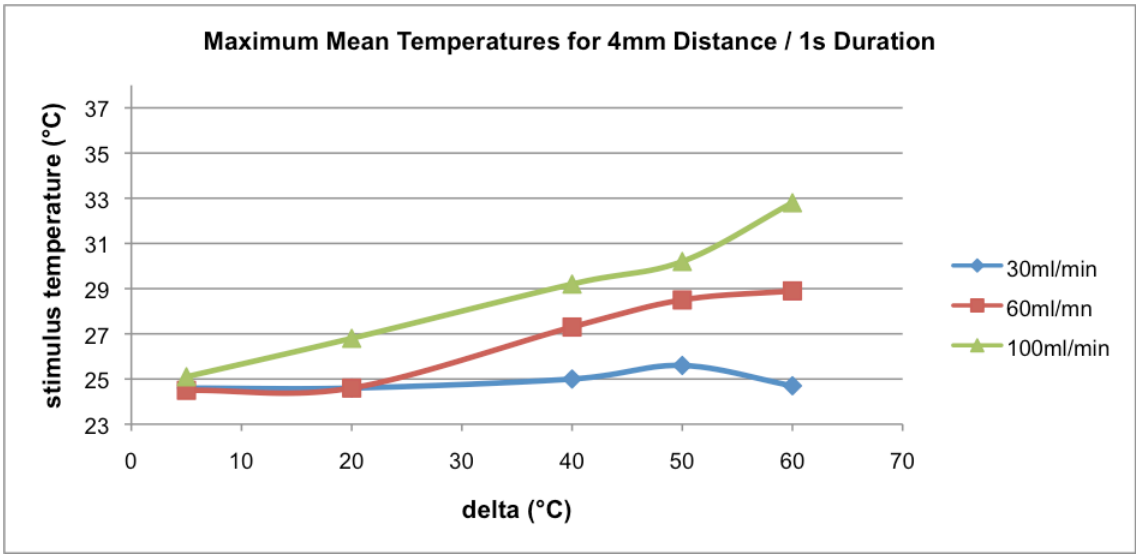

Figure 3.17: Maximum mean temperatures for 4mm distance / 1s duration.

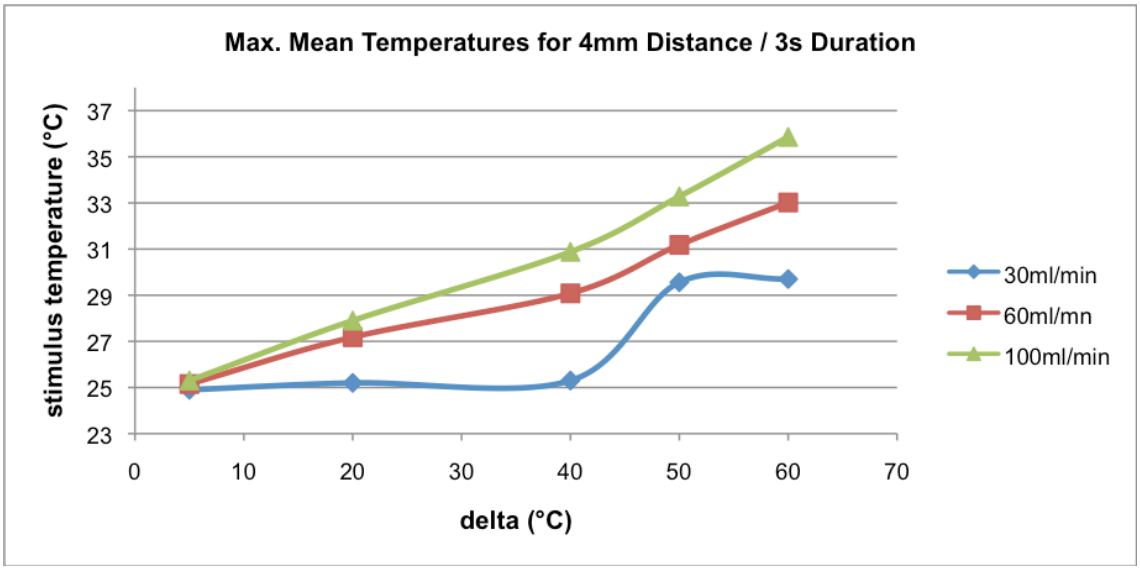

Figure 3.18: Maximum mean temperatures for 4mm distance / 3s duration.

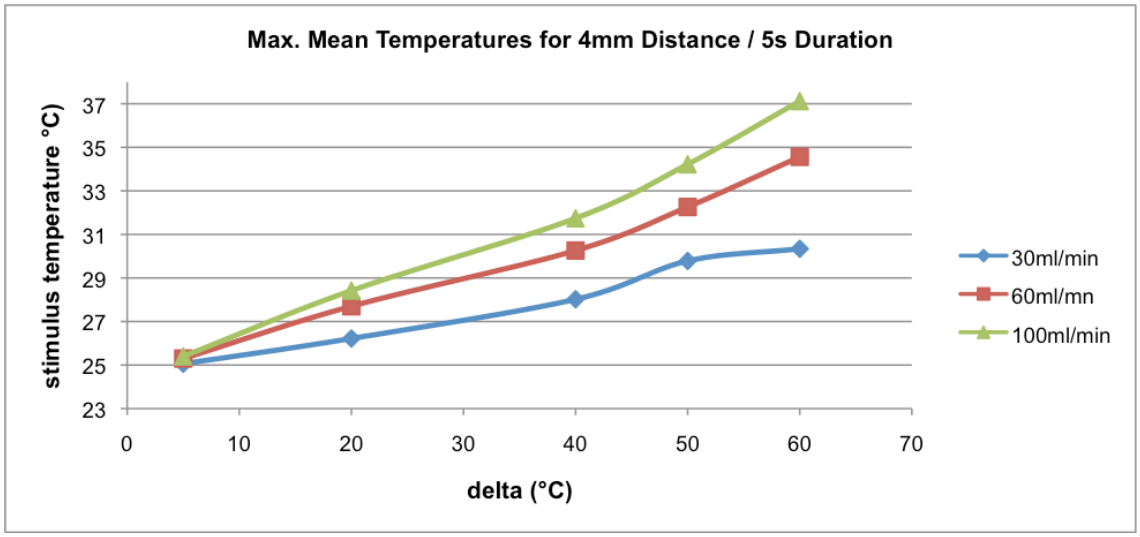

Figure 3.19: Maximum mean temperatures for 4mm distance / 5s duration.

The difference in stimulus temperatures is more pronounced for the stimulus setting at the 4mm distance and the durations of 3 and 5s (Figures 3.18 and 3.19). With 'delta 50' and the 4mm distance and the durations of 3 and 5s, the recorded stimulus temperatures came closest to the desired ocular surface temperature range of 32.9-36.0°C.

With a stimulus distance of 8mm and durations of 1 and 3s, the recorded rise in stimulus temperature was insufficient to match corneal temperature with an airflow rate of 30ml/min. (Figures 3.20 and 3.21).

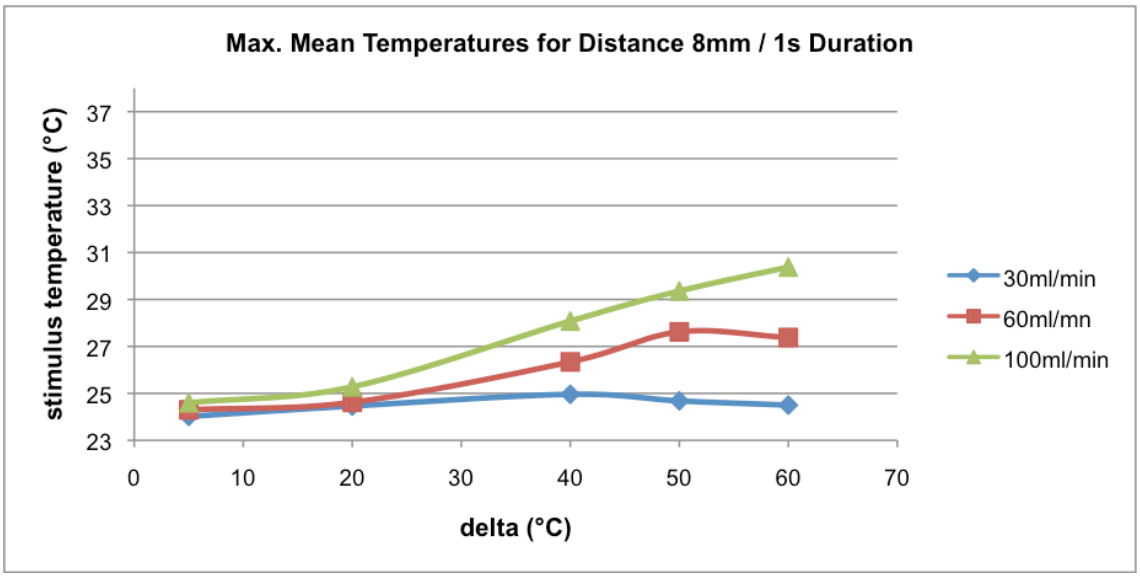

Figure 3.20: Maximum mean temperatures for 8mm distance / 1s duration.

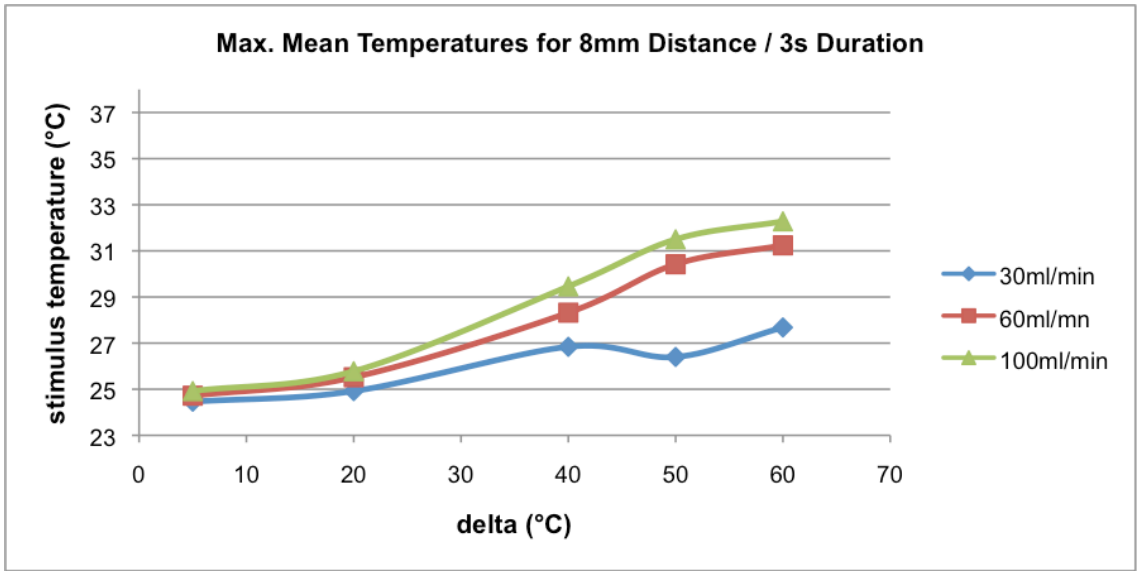

Figure 3.21: Maximum mean temperatures for 8mm distance / 3s duration.

When using a stimulus at 8mm distance, 5s duration and ‘delta 50’, the recorded rise in stimulus temperature was less than expected, while with ‘delta 60’ the jump in the recorded temperature difference between airflow 30 and 60ml/min was deemed too large (Figure 3.22).

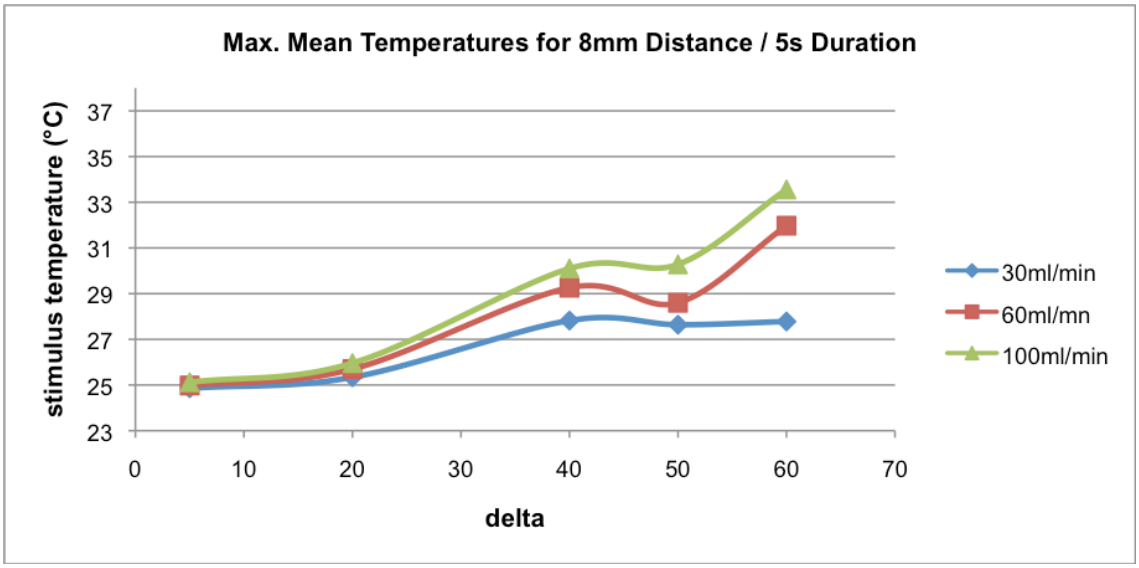

Figure 3.22: Average maximum temperatures for 8mm distance / 5s duration.

3.1.1.4 Discussion

This experiment measured the airflow temperature produced by variation in the stimulus temperature, and how this temperature was affected by the stimulus duration, airflow rate and test distance. It could be observed that all stimulus characteristics tested in this study (duration, distance and airflow rate) had statistically significant effects on the obtained stimulus temperature recordings: the longer the stimulus presentation, the shorter working distance, and the higher the level of air flow rate, the more pronounced the temperature difference was recorded by the wired thermocouple used in this experiment. The recorded temperatures rose with increasing levels of 'delta' and were statistically significant for all 'deltas' applied.

3.1.1.4.1 The effect of rising levels of delta

With 'delta 5', only small changes in stimulus temperature (not exceeding mean temperature differences of 0.7°C) could be detected by the thermocouple. This small reduction was found to be consistent, as the standard deviations were small. This finding would suggest a stimulus temperature well below normal corneal surface temperature of 32.9-36.0°C[285] and that this stimulus temperature may therefore be suitable to serve as a cooling stimulus exciting the C fibres of the corneal epithelium. Increasing stimulus duration and the airflow rate had a statistically significant effect on the recorded stimulus temperature, whereas increasing the distance did not.

As expected, 'delta 20' and 'delta 40' had a greater effect, leading to higher stimulus temperature readings. In contrast to 'delta 5', the pair-wise comparisons between the shorter and longer distance were not always statistically significant, however stimulus duration and airflow rates were noted to have stronger effects on the stimulus temperature: the longer the stimulus lasted and the higher the airflow rate was, the greater the temperature increases detected by the wire thermocouple. It was observed that the variability of repeated measurements increased substantially at the longer distance of 8mm, which was most marked at the lower air flow rate of 30 ml/min.

The stimulus temperature readings were even higher with 'delta 50' and 'delta 60', compared to the lower delta settings. With very few exceptions (the shortest stimulus duration in combination with the longer working distance), all stimulus characteristics tested in this study had a statistically significant effect on the recorded stimulus temperature. In contrast to the lower delta values, the variability of repeated measurements did not increase substantially at the longer working distance of 8mm in comparison to the shorter working distance of 4mm, it was however found to be much more marked at the lower air flow rate of 30ml/min.

The temperature recordings produced with the wire thermocouple used in this study suggested that 'delta 50' and 'delta 60' would represent the temperature settings most likely to match ocular surface temperature (OST): 'delta 50 and 60', airflow rates of 60 and 100ml/min, a working distance of 4mm and the longer stimulus durations of 3 and 5s. With 'delta 60' it reached temperatures higher than OST (36-38°C) at the shorter working distance and the longer durations of 3 and 5s.

3.1.1.4.2 The effect of the level of airflow rate

At the airflow rate of 30ml/min, the recorded temperature differences were noted to be much less marked and showed considerably more variability compared to those obtained at the air flow rates of 60 and 100ml/min. This suggests that the thermocouple may have not been sufficiently sensitive for this level of airflow. Even at the airflow rate of 60ml/min, the recorded temperature changes were small with increasing levels of

'delta', when a short stimulus duration was chosen. At 100ml/min, a considerable rise in stimulus temperature was recorded for all stimulus characteristics.

3.1.1.4.3 The effect of working distance and stimulus duration

When assessing the effect of the stimulus characteristics 'working distance' and 'stimulus duration' on the recorded stimulus temperature, greater temperature differences were noted for the shorter working distance of 4mm and the longer stimulus durations of 3 and 5s. With the shorter working distance of 4mm, a stimulus duration of 5s and 'delta' set at 50, the recorded stimulus temperatures came closest to the desired OST range of 32.9-36.0°C. The longer distance of 8mm, the short stimulus durations of 1 and 3s and the lowest level of airflow rate (30ml/min) were insufficient to generate a stimulus temperature likely to match OST.

Why was the change in stimulus temperature less marked with the longer distance of 8mm compared to the shorter distance of 4mm? This may be explained by looking at how the air stimulus disperses after it leaves the exit nozzle of the aesthesiometer. Murphy et al. showed, with the aid of Schlieren interferometry, that the airflow has a central core that is surrounded by a less prominent zone of lower pressure, a turbulent fringe.[14] This was later confirmed by Golebiowski et al., who constructed a theoretical model of the air jet of their individually designed aesthesiometer, with the use of numerical methods and algorithms, to simulate the airflow and its interaction with a solid boundary.[22] In their model, the air gas stimulus leaves the exit nozzle with a diameter of 0.50mm and reaches the corneal surface at a 4mm distance with very little dispersion. Murphy et al. observed that the central core of the airflow maintains a high level of coherence until approximately 1.5cm from the exit nozzle, when it breaks down into turbulence. This confirms that the degree of dispersion of the airflow increases, as the distance from the exit nozzle increases. It is possible that a sufficient degree of dispersion already exists at the distance of 8mm within the air gas stimulus generated by the OPM, especially when shorter stimulus durations and lower levels of airflow rates are chosen.

3.1.1.4.4 Time latency in the maximum temperature change recorded

An overall latency of the maximum temperature change towards the end of the stimulus presentation was observed. This effect was, however, partly produced by the temporal delay of 300ms for the thermocouple itself (as mentioned in Section 3.1.1.3.6), and which was been pointed out by Murphy et al., who observed the same effect when verifying the NCCA aesthesiometer.[361] Nevertheless, it appears that the air gas stimulus generated by the Belmonte OPM aesthesiometer does not generate its maximum temperature instantly, and that there is a build-up of temperature change during stimulus presentation.

3.1.1.4.5 Suitability of the wire thermocouple

The accuracy of the results gained from the wire thermocouple used in this experiment has to be questioned, as they suggest that exceedingly high stimulus temperatures would be required to match OST, namely: stimulus temperature at room temperature (23.5°C)+50°C =73°C. Feng and Simpson (2003) as well as Stapleton et al. (2004) recommended a stimulus temperature of 50°C,[20,21] and in 1999 Belmonte et al. also used 50°C,[19] however today they recommend 43°C, as suggested by the manufacturers of the OPM (equating to 'delta 19' at a room temperature of 24°C; OPM User Manual, Deriva Global S.A.). One possible explanation may be that the thermocouple has a thermal capacity greater than the thermal capacity of the mass of air trying to heat it.

Another problem is that any energy transferred to the tip of the thermocouple is continuously being conducted away along the metal of the thermocouple wires. The heat transfer to the tip from the air, compared to the conduction away from the tip by the wire, will determine the temperature obtained. This will lead to a lower reading, even if the pulse of hot air is continuous. Hence, a thin membrane would have been more suitable to record the temperature of the air stimulus.

3.1.1.5 Conclusion

This *in vitro* experiment to measure stimulus temperature with a dry, Type T wire thermocouple delivered overall consistent results with little variability (except for the airflow rate of 30ml/min). The measurements indicated that other stimulus characteristics, such as stimulus duration, working distance (between the aesthesiometer

nozzle and the thermocouple), and the level of airflow rates had a marked effect on the recorded stimulus temperature.

However, the recorded absolute stimulus temperatures obtained suggested that unrealistically high stimulus temperatures would be needed to match OST (delta 50-60). This is most likely due to the type of thermocouple generating low readings when measuring small pulses of air. Hence it was decided to repeat parts of this experiment using a moistened thermocouple with a flat surface, in order to better transmit the air stimulus temperature.

3.1.2 Stimulus temperature measurement with a flat and moistened thermocouple

A flat thermocouple surface will offer a greater surface area over which the temperature difference generated by the air gas stimulus can be detected. A moistened filter paper cover will mimic a membrane and will therefore resemble better the ocular surface that is covered by the tear-film.

3.1.2.1 Methods

A Type K, flat, and round thermocouple, with a diameter of 6.0mm (Figure 3.23), was placed in front of the aesthesiometer nozzle (Pico Technology, St. Neots, UK) and connected through the Pico data collector. A circular hole punch produced from filter paper (grade 1:11μm, Whatman, VWR International, USA), with a diameter to match that of the thermocouple, was moistened by adding 1ml of saline, which also ensured attachment by surface tension to the flat, round surface. This arrangement enhanced transmission of the temperature of the air stimulus to the thermocouple. The exit-nozzle of the aesthesiometer was placed in front of this thermocouple and aligned with the centre position (Figure 3.24). Ambient temperature was noted before each change in stimulus characteristics (duration, distance and temperature): mean temperature throughout the study was 23.82±0.08C°. Room humidity was constant and measured to be 29.0%.

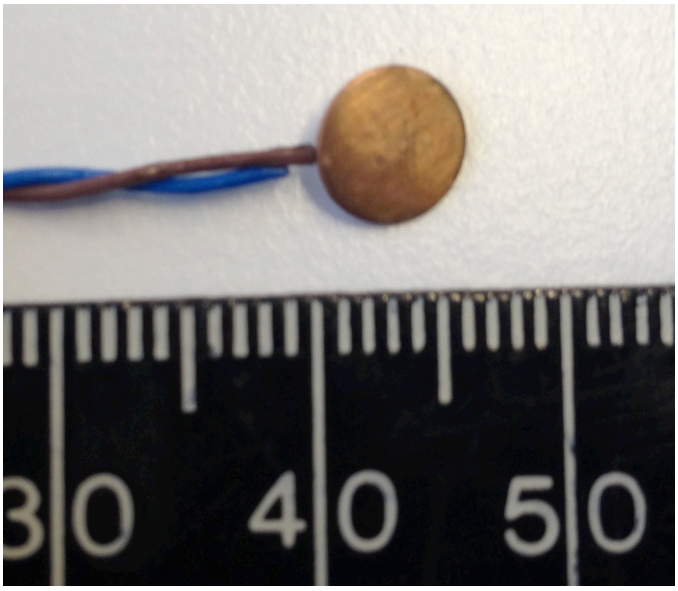

Figure 3.23: Close-up picture of the flat thermocouple (placed next to a mm scale).

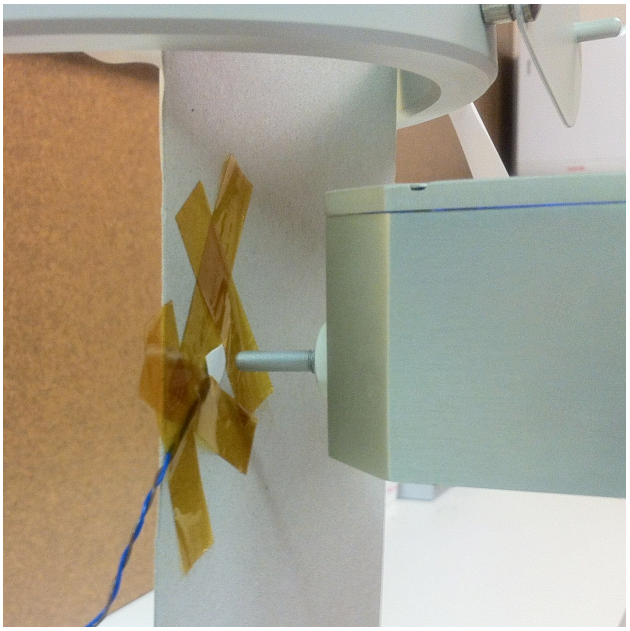

Figure 3.24: Set-up of the experiment: a moistened thermocouple covered by the filter paper was placed in front of the nozzle of the aesthesiometer.

As for the first thermocouple experiment, the air stimulus temperature produced was measured for the two distances of 4mm and 8mm, as well as the durations of 3s and 5s, but this time the 1s duration was omitted, since this time duration was found to produce only very small temperature changes and because preliminary OST measurements during stimulus presentation (with aid of a thermal camera) indicated very little change with this short duration. For each combination of stimulus characteristics, increasing

levels of airflow rate were applied (30, 60, 80 and 100ml/min). This spread of airflows extended the range from the first experiment to include the 80ml/min flowrate. Each measurement was repeated five times. For each change in distance or duration, the filter paper on the thermocouple was re-moistened with 1ml of saline, using a micro-pipette. Measurements were taken with 'delta' set at 10, 15, 20 and 30. The larger deltas of 50 and 60 were not tested since in preliminary testing with the flat thermocouple, it was found that the required temperature changes were produced with lower deltas. For 'delta 10' and 'delta 15', all stimulus characteristics (4 and 8mm distance, 3 and 5s duration) were applied, however for 'delta 20' and 'delta 30', only the stimulus setting of 4mm distance and 3s duration was tested. This refinement at 'delta 20' and 'delta 30' was chosen, because preliminary measurements of OST during stimulus presentation (with aid of a thermal camera) indicated an increase in OST with 'delta' set at ≥15 (see the following Chapter 6). It was decided to choose the distance of 4mm and the duration of 3s for 'delta 20 and 30', as they represented the stimulus settings most commonly used for corneal sensitivity measurement.

3.1.2.2 Statistical analysis

A statistical analysis examining the difference in temperature changes with different stimulus characteristics was conducted. For normally distributed data (Shapiro-Wilk Test), a general linear model (two-way ANOVA) and subsequently post-hoc t-tests (corrected with Bonferroni) were applied.

3.1.2.3 Results

3.1.2.3.1 'Delta 10'

With stimulus temperature set at 'delta 10', a decrease in temperature was noted for all stimulus settings (Figure 3.25). The temperature changes were small with low levels of airflow rates and increased consistently with higher levels of airflow rates. This resulted in statistically significant temperature changes for all stimulus distance and duration settings: p=0.020 for 4mm/3s, p=0.001 for 4mm/5s, p=0.000 for 8mm/3s and p=0.000 for 8mm/5s. All induced temperature changes were statistically significant (post-hoc t-test) – with the exception of the airflow setting at 30ml/min with 4mm/3s (Table 3.11).

In contrast to the previous experiment, this temperature change was most pronounced at the longer 8mm distance (with 5s duration). Except for the airflow rate of 100ml/min, the mean temperature changes were similar for the stimulus settings of 4mm/5s and 8mm/3s. The stimulus setting 4mm/3s induced the least temperature change. These results were found to be consistent, as the standard deviations were very low throughout, with one exception for the stimulus 8mm/5s with the highest level of airflow rate (100ml/min).

Mean temperature change with 'delta 10'				
Airflow rate (ml/min)	4mm/3s (°C)	4mm/5s (°C)	8mm/3s (°C)	8mm/5s (°C)
30	-0.03±0.05 (p=0.290)	-0.04±0.02 (p=0.009)	-0.05±0.02 (p=0.011)	-0.08±0.03 (p=0.008)
60	-0.10±0.03 (p=0.001)	-0.11±0.04 (p=0.002)	-0.15±0.03 (p=0.000)	-0.28±0.05 (p=0.000)
80	-0.13±0.03 (p=0.001)	-0.21±0.05 (p=0.001)	-0.21±0.03 (p=0.000)	-0.36±0.04 (p=0.000)
100	-0.15±0.03 (p=0.000)	-0.34±0.06 (p=0.000)	-0.23±0.04 (p=0.000)	-0.32±0.18 (p=0.017)

Table 3.11: Mean temperature change induced with stimulus temperature set at delta 10.

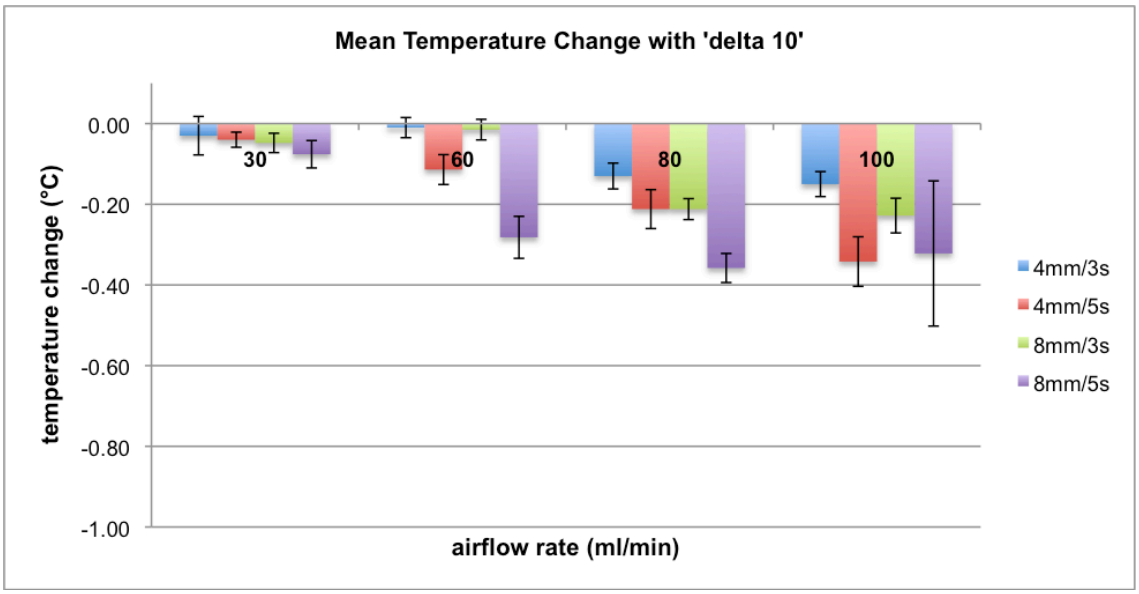

Figure 3.25: Mean temperature change with stimulus temperature set at delta 10.

A pair-wise comparison of the thermocouple temperature focused on the stimulus temperature changes with different levels of airflow rates and stimulus characteristics, with 'delta 10' (Table 3.12). There was a tendency for the rate of airflow to have a statistically more significant effect with the stimulus distance set at 4mm.

Pair-wise comparison of the thermocouple temperature changes with different levels of airflow rate				
Airflow rate (ml/min)	4mm/3s	4mm/5s	8mm/3s	8mm/5s
30 vs. 60	p=0.035	p=0.014	p=0.013	p=0.021
30 vs 80	p=0.004	p=0.003	p=0.009	p=0.002
30 vs 100	p=0.006	p=0.001	p=0.013	p=0.287
60 vs 80	p=0.173	p=0.006	p=0.120	p=0.082
60 vs 100	p=0.005	p=0.001	p=0.313	p=1.000
80 vs 100	p=1.000	p=0.005	p=1.000	p=1.000

Table 3.12: Pair-wise comparison of the thermocouple temperature changes with different levels of airflow rates and 'delta 10' (post-hoc t-test).

3.1.2.3.2 'Delta 15'

With stimulus temperature set at 'delta 15', only a marginal temperature increase was observed for the shorter distance of 4mm and the lower airflow rates of 30 and 60ml/min (Table 3.13, Figure 3.26). For all other stimulus characteristics, a small decrease in temperature was noted. As observed before, the higher the airflow rate, the more pronounced the temperature decrease was found to be. This resulted in statistically significant changes for the stimulus settings of 4mm/5s (p=0.005), 8mm/3s (p=0.000) and 8mm/5s (p=0.000), however not for 4mm/3s (p=0.640; two-way ANOVA). The change in temperature was lowest for the stimulus at 4mm/3s and greatest at 8mm/5s. As for 'delta 10', this finding was in contrast to the results gained from the previous experiment, and the stimulus gave rise to greater temperature change at the shorter distance. These results can be considered to be consistent, as the standard deviations for repeated measurements were very low for all stimulus settings.

Mean temperature change with delta 15				
airflow (ml/min)	4mm/3s (°C)	4mm/5s (°C)	8mm/3s (°C)	8mm/5s (°C)
30	0.02±0.04 (p=0.294)	0.04±0.06 (p=0.392)	-0.01±0.05 (p=0.603)	-0.06±0.02 (p=0.006)
60	0.05±0.04 (p=0.049)	0.02±0.02 (p=0.152)	-0.11±0.01 (p=0.000)	-0.15±0.01 (p=0.000)
80	-0.02±0.02 (p=0.181)	-0.07±0.02 (p=0.002)	-0.14±0.01 (p=0.000)	-0.21±0.02 (p=0.000)
100	-0.07±0.02 (p=0.002)	-0.11±0.04 (p=0.003)	-0.15±0.03 (p=0.000)	-0.24±0.04 (p=0.000)

Table 3.13: Mean temperature change induced with stimulus temperature set at 'delta 15'.

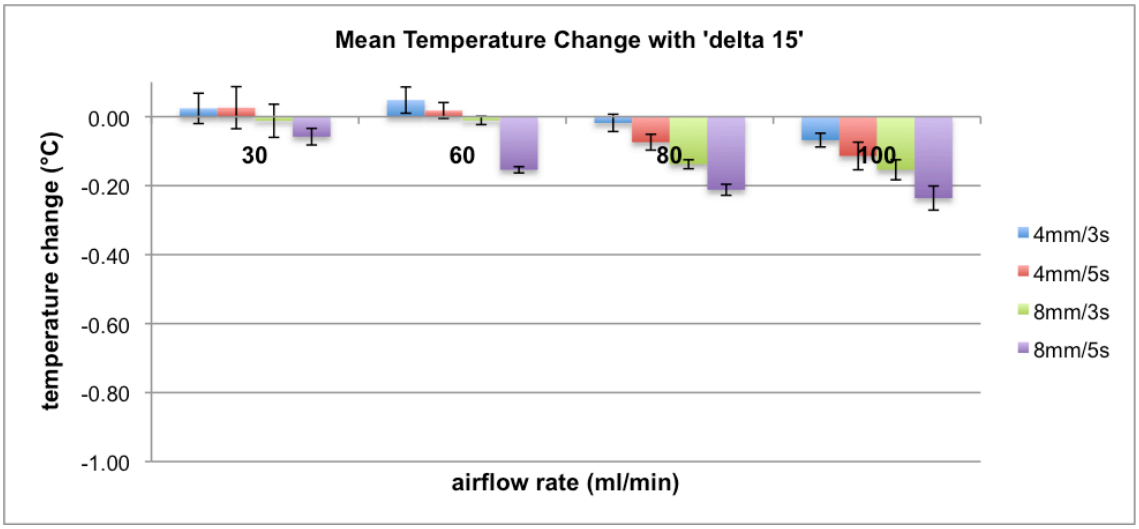

Figure 3.26: Mean temperature change with stimulus temperature set at 'delta 15'.

A pair-wise comparison of the thermocouple temperature illustrated the effects of the level of airflow rates on the stimulus characteristics 'distance' and 'duration', with 'delta 15' (Table 3.14). The effect of increasing levels of airflow rate was more often statistically significant when the longer stimulus of 5s was applied, irrespective of what distance was chosen.

Pair-wise comparison of the thermocouple temperature changes with different levels of airflow rate				
Airflow (ml/min)	4mm/3s	4mm/5s	8mm/3s	8mm/5s
30 vs. 60	p=0.007	p=0.725	p=0.295	p=0.001
30 vs 80	p=0.213	p=0.009	p=0.980	p=0.000
30 vs 100	p=1.000	p=0.003	p=0.053	p=0.001
60 vs 80	p=1.000	p=0.001	p=0.066	p=0.055
60 vs 100	p=0.702	p=0.001	p=1.000	p=0.003
80 vs 100	p=0.113	p=0.349	p=0.033	p=0.077

Table 3.14: Pair-wise comparison of the thermocouple temperature changes with different levels of airflows, at 'delta 15' (post hoc t-test).

The statistical significance of stimulus temperature changes with the air stimulus applied at rising levels of delta was calculated with fixed stimulus characteristics of 4mm distance and 3s duration (Table 3.15, Figure 3.27). Whilst the temperature difference recorded with 'deltas 10, 15 and 20' were very small (< ±0.20°C), 'delta 30' generated a temperature change of up to a mean value of +0.89°C applying the highest airflow rate. These results were considered to be consistent, as the standard deviations of repeated measurements were very low for all stimulus settings.

Mean temperature for different deltas (4mm/3s)				
airflow (ml/min)	delta 10 (°C)	delta 15 (°C)	delta 20 (°C)	delta 30 (°C)
30	-0.03±0.05 (p=0.290)	0.02±0.04 (p=0.294)	0.02±0.08 (p=0.629)	0.17±0.13 (p=0.045)
60	-0.10±0.03 (p=0.001)	0.05±0.04 (p=0.049)	0.12±0.05 (p=0.004)	0.67±0.08 (p=0.000)
80	-0.13±0.03 (p=0.001)	-0.02±0.02 (p=0.181)	0.11±0.03 (p=0.001)	0.67±0.12 (p=0.000)
100	-0.15±0.03 (p=0.000)	-0.07±0.02 (p=0.002)	0.13±0.03 (p=0.001)	0.89±0.05 (p=0.000)

Table 3.15: Mean temperature changes for rising levels of 'delta' (4mm/3s).

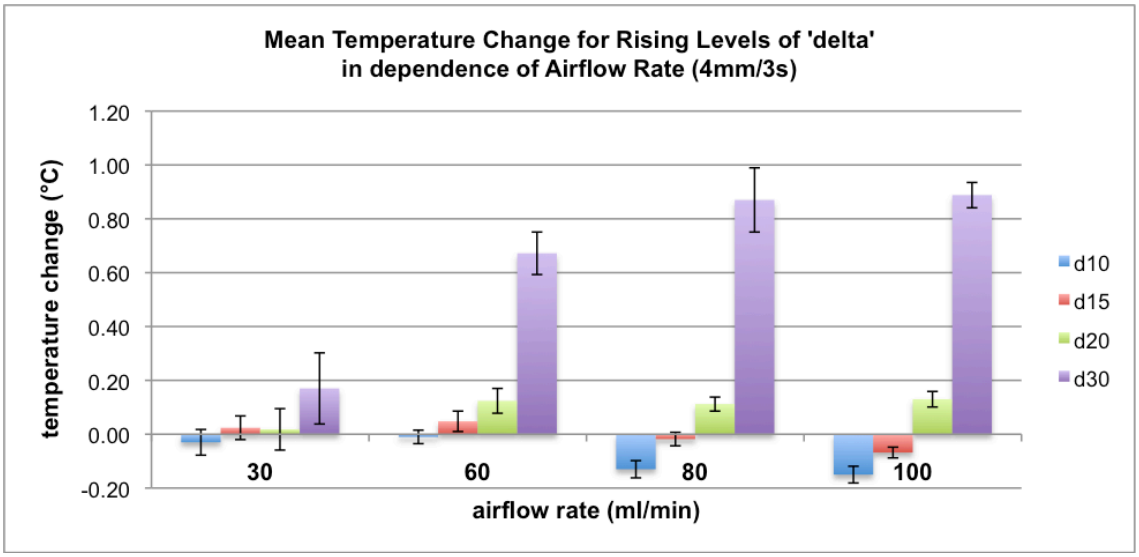

Figure 3.27: Temperature changes for rising levels of 'delta' (4mm/3s).

A pair-wise comparison of the thermocouple temperature changes with different levels of airflow rates at rising levels of delta was carried out with the stimulus characteristics set at 4mm/3s (Table 3.16). There was a trend for the different airflow rates to have a statistically significant effect on the majority of the recorded stimulus temperature differences with 'delta 10' and half of the stimulus temperature changes with 'delta 30' (when comparing the lower airflow rate of 30ml/min with the higher airflow rates of 60, 80 and 100ml/min), but less so when 'delta 15' and 'delta 20' were applied.

Pair-wise comparison of the thermocouple temperature changes with different levels of airflow at rising levels of delta (4mm/3s)				
Airflow (ml/min)	delta 10	delta 15	delta 20	delta 30
30 vs. 60	p=0.035	p=0.007	p=0.486	p=0.033
30 vs 80	p=0.004	p=0.213	p=0.564	p=0.017
30 vs 100	p=0.006	p=1.000	p=0.418	p=0.001
60 vs 80	p=0.173	p=1.000	p=1.000	p=1.000
60 vs 100	p=0.005	p=0.702	p=1.000	p=0.076
80 vs 100	p=1.000	p=0.113	p=0.128	p=0.178

Table 3.16: Pair-wise comparison of the thermocouple temperature changes with different levels of airflow rates, at rising levels of 'delta' (post-hoc t-test).

3.1.2.4 Discussion

This experiment investigated the temperature changes induced on a thermocouple by an air stimulus with different temperature settings, using the Belmonte OPM aesthesiometer. It was of particular interest to verify if recorded temperature changes could be produced in a consistent manner, as variability of repeated measurements was found to be low.

The stimulus temperatures recorded with the flat and moistened thermocouple indicated a decrease for 'delta 10' (max. mean decrease of -0.34°C) and 'delta 15' (max. mean decrease of -0.24°C), which was only statistically significant for 'delta 10'. For 'deltas 20 and 30' a temperature increase was noted, with most differences being statistically significant (max. mean temperature difference +0.13°C for 'delta 20' and +0.89°C for 'delta 30'). Although still not large, the temperature changes induced with 'delta 30' were considerably more marked than for deltas 10, 15 and 20. These absolute temperature values obtained stood in contrast to the previous thermocouple experiment, where no decrease in temperature could be observed with either of the different 'delta' settings. Also, the temperature changes measured in the previous experiment with the wired thermocouple were greater.

In concordance with the previous thermocouple experiment, temperature differences were more pronounced with increasing levels of airflow. However, at first impression, it was surprising to note more pronounced temperature decreases on the thermocouple with 'delta 10' and 'delta 15' during this experiment, when its distance to the nozzle was increased. One explanation may be that there was a greater surface area covered by the increased dispersion of the stimulus produced by a longer distance. As a result, this would have allowed the stimulus to spread over a greater surface of the thermocouple inducing a greater amount of evaporation and hence cooling. However, the cornea being covered by the tear film with lipid components may be able to resist this evaporation effect more successfully than the filter paper moistened with saline, which was used in this experiment. This would also suggest that individuals with a thin tear film (reduced lipid layer) should experience evaporative cooling sooner, compared to those with a regular and thicker lipid layer. In fact for this reason, and for the following additional

two important reasons, no direct comparison between a thermocouple and the possible effect of an air pulse on the corneal surface is possible, as was noted by Murphy et al. in 1999:[22] Firstly, there is a temporal delay in the response of the thermocouple. This latency was described during the previous wired thermocouple (Section 4.1.2.6). Secondly, neither of the two thermocouples used during these experiments were able to simulate the corneal nerve supply, as the thermocouple arrangement consists of only one large receptive field, whereas the corneal nerve supply is arranged in a series of overlapping receptive fields that increase sensitivity and amplify stimulus response.

However, these two thermocouple experiments could show that the recordings of temperature changes created by the air gas stimulation of the Belmonte OPM aesthesiometer showed a high degree of consistency of the measurements: the standard deviations of repeated recordings were always very low and the temperature changes were persistent.

3.1.2.5 Conclusion

As with the wired thermocouple, the stimulus temperatures obtained with the flat, moistened thermocouple were consistent throughout the measurements, as only small fluctuations were noted during repeated measurements. The greater stimulus temperature decrease obtained at the longer working distance of 8mm compared to 4mm suggested that there may have been a considerable degree of dispersion present at the longer working distance.

The two experiments with the different types of thermocouples recorded different absolute values in temperature changes when presented with air gas stimuli of the Belmonte OPM aesthesiometer (of different characteristics). However, because no direct comparison between these thermocouples and the corneal surface is possible, the obtained absolute temperature differences are not meant to indicate changes in OST during stimulus presentation, but to give an indication of whether the stimulus temperature generated by the OPM is consistent.

3.1.3 Conclusions of the in vitro experiments

From the measurements of the stimulus flow rate, using a microbridge mass airflow sensor, it could be concluded that the OPM delivers consistent levels of airflow rates with very little variability across the range that was tested. However, the absolute values received were deemed too high, which suggests a calibration error either for the OPM or for the test sensor. The verification of air stimulus volume with the inverted glass burette in a water bowl, connected with a silicone rubber hose to the exit nozzle of the OPM, again showed highly consistent results across the range of airflow levels being tested. While the air stimulus volume obtained was, on average, 7.45±0.03% higher than specified by the OPM manufacturer, this will have limited effect on the stimulus, but again suggests a calibration issue, this time for the OPM. Also, the stimulus force measured with an analytical microbalance delivered consistent results with very little variability. For verification of stimulus temperature, a wire thermocouple and a flat, moist thermocouple were placed at two distances (4 and 8mm) in front of the OPM exit nozzle, and different stimulus durations (1, 3 and 5s) applied. Again, the measurements obtained showed very little variability, although the absolute values differed greatly between the two different types of thermocouples: possibly reflecting that the flat and moistened thermocouple was a better simulation of the cornea by having a moist membrane. However, this was still not sufficient for accurate absolute readings, as neither of these thermocouples were found to be ideal for absolute temperature measurement of small air pulses. Nevertheless, it was found that the stimulus characteristics tested (stimulus durations, working distance and level of airflow rates) had a marked and statistically significant effect on the readings received.

It can be concluded that the Belmonte OPM aesthesiometer delivers consistent and reliable air gas stimuli, but care has to be taken when comparing absolute ocular surface sensitivity values with those of other instruments, as the absolute values of the stimulus characteristics are not calibrated with any other instrument currently used. As for stimulus temperature, *in vivo* measurements of ocular surface temperature changes during stimulus presentation with aid of a thermal camera are required to ensure that a true mechanical stimulus can be generated.

3.2 Measurement of ocular surface temperature (OST) during the presentation of the air gas stimulus

A stable and sufficient temperature range is important for the mechanical air stimulus produced by the Belmonte OPM aesthesiometer. Any cooling effect coming from the air stimulus must be excluded, by matching the stimulus temperature with the ocular surface temperature (OST). From the previous thermocouple experiments it could be concluded that the OPM generates consistent stimulus temperatures and stimulus characteristics. However, the *in vivo* variation in stimulus temperatures with these variables could not be confirmed. A normal range for OST is believed to be 32.9-36°C, with the limbus being warmer than the central part of the cornea (by 0.45 to 1.0°C, Figure 3.36)[285].

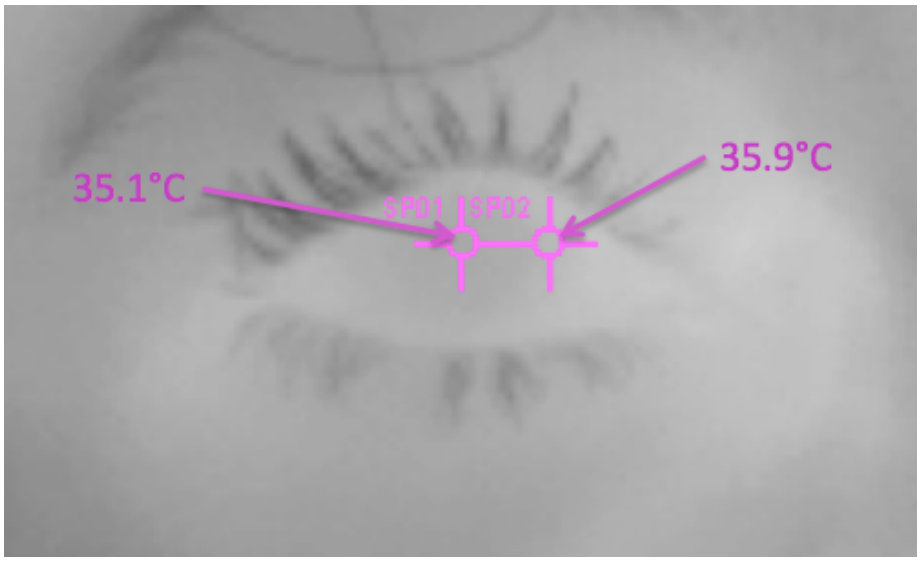

Figure 3.28: Example of the OST difference between the central cornea and the limbus.

In their review article, Purslow and Wolffsohn[285] stated that OST is influenced by the following external and internal factors: heat transfer from adjacent structures, blinking (warm tears being spread across the ocular surface during each blink) and after each blink, temperature of environment (0.15 to 0.20°C change per degree in room temperature), changing blood flow to the eye or head, and by the time of the day (it rises during the course of the day).[285] Obviously, an air gas stimulus will lead to a corneal cooling response if its temperature is set at room temperature, since this temperature

will be lower than that of the corneal surface. If, however, the stimulus temperature is chosen to match corneal temperature, it is hoped that there will be no cooling effect and that the resulting stimulus will only cause mechanical deformation and stimulate the Aδ fibres, but not the cold-sensitive C fibres. However, it is not yet clear if this is what happens with the heated mechanical stimulus or if it can still cause a cooling response resulting from tear film thinning.

The general aim of this study was to record the change of corneal surface temperature during stimulus presentation with varying stimulus temperatures, stimulus durations and distances, as well as varying levels of airflow directed toward the ocular surface. There were also two particular aims: 1) to explore if a stimulus temperature could be determined which would be equal to corneal surface temperature, and hence give rise to corneal deformation without an additional cooling effect, and 2) to measure the effect of varying levels of airflow on corneal surface temperature.

The clinical experiments took place in two parts, A and B. In part A, the effect of air gas stimuli of different temperatures on ocular surface temperature (OST) was investigated. In part B, the effects of stimulus distance, duration and levels of airflow on OST were assessed, applying the stimulus temperature most likely to match OST (as obtained from study part A).

3.2.1 General information regarding study parts A and B

Ethical approval was obtained from the human research ethics committee of the School of Optometry and Vision Sciences, Cardiff University for both study parts (project number 1368, Appendix section no. 8.1.3). The participants were volunteers from the student pool of the School of Optometry, University of Applied Sciences Northwest Switzerland in Olten. They were invited for participation via email. Prior to commencement of the study, they signed an informed consent.

Inclusion criteria for both clinical experiment periods were age younger than 40 years, no contact lens wear, absence of ocular disease including dry eye disease, and no prior use of artificial tears on the same day. The study took place in an air-conditioned room,

where the level of humidity was constant at 26%. Ambient temperature was recorded before the measurement of each stimulus type on each individual subject. It was found to be 23.06±0.34°C throughout part A, and 23.11±0.32°C for part B. Each stimulus setting was applied three times to the ocular surface of each participating subject.

3.2.1.1 Experiment set-up

OST was measured with the aid of a self-calibrating (with use of the emissivity factor of 0.95 for the cornea) thermal infrared camera (FLIR A310; thermal resolution 0.08°C, temporal resolution 30Hz; spatial resolution 320x240 pixel). The camera could not be positioned perpendicular to the cornea, but had to be offset a little to the side and therefore measured corneal temperature from an oblique position (Figure 3.30). This was necessary since the nozzle of the aesthesiometer must be positioned directly in front of the cornea, perpendicular to the ocular surface (Figure 3.31), which explains the oblique position of the thermal camera, and the long working distance of 20cm to the corneal surface.

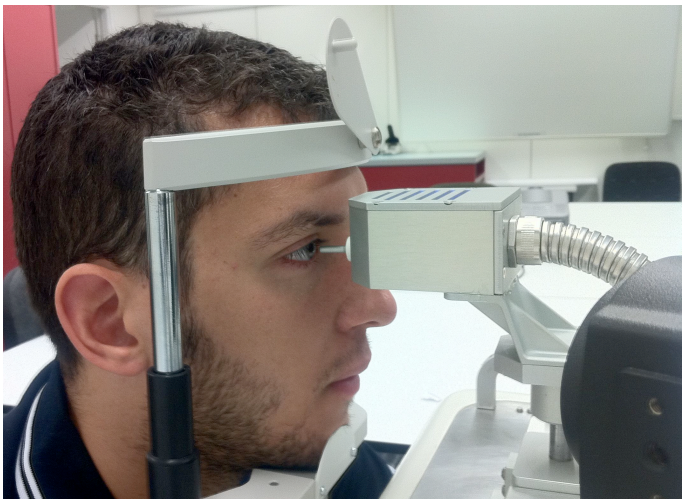

Figure 3.29: Set-up of the thermal camera during stimulus presentation: the exit nozzle aligned at 4mm in front of the centre of the cornea with the thermal camera set at an angle (in the picture to the right); a signed consent for publication was received from the subject.

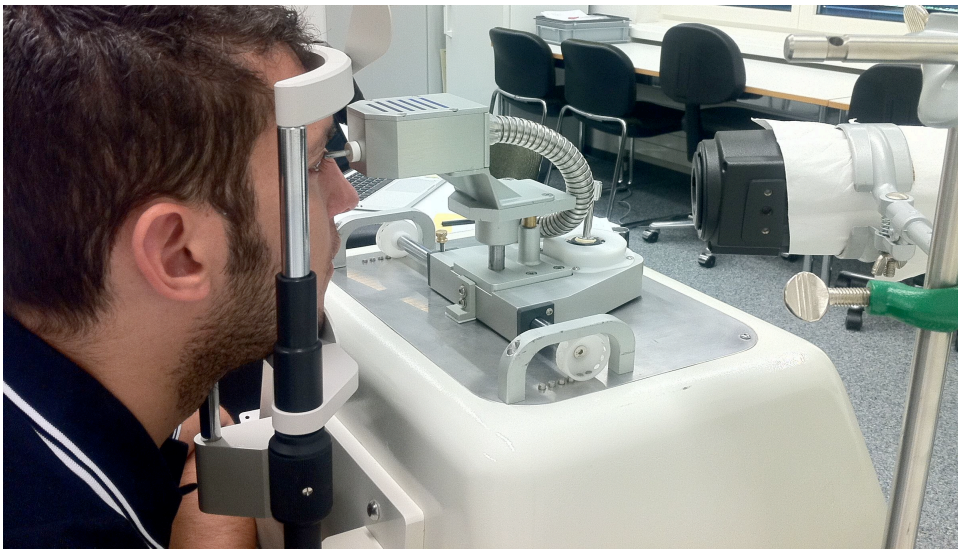

Figure 3.30: Set-up of the thermal camera during stimulus presentation – the thermal camera is set at an angle (in the picture on the right side); a signed consent for publication was received from the subject.

3.2.1.2 Air gas stimulus temperature

A range of stimuli with different temperatures was used. As mentioned before, stimulus temperature could be regulated by choosing the instrument 'delta' setting. The lowest delta setting possible was 'delta 3', i.e. the air stimulus temperature was increased within the housing of the aesthesiometer by 3°C, compared to ambient temperature. Per definition, stimulus temperature was directly dependent on room temperature, thus the 'delta 3' air stimulus had a temperature lower than the corneal surface, at a room temperature of 23-24°C, and so it was considered to be a cooling stimulus with respect to OST. During the course of this study, the effect of different deltas on OST was explored: 'delta 3, 5, 10, 15, 20, 25, 30, 40 and 50'. Hence, all levels of deltas previously tested with the thermocouples were re-examined for comparison, except for 'delta 60'. Originally it was planned to include 'delta 60' as well, however during the measurements on the first subject, it became apparent that the heating response of the cornea was much greater than anticipated with the thermocouple experiments and the aesthesiometer was not able to function properly over prolonged measurement periods with such a high stimulus temperature. As mentioned before, each 'delta' number indicated by how many degrees in Celsius the air gas stimulus temperature was increased, compared to room temperature. Since it was expected that the air stimulus would cool down to a certain degree between leaving the nozzle of the aesthesiometer

and arriving at the corneal surface,[1] and the amount of this temperature change was not known, the exact air stimulus temperature could not be calculated by simply adding room temperature and the delta of the stimulus temperature.

3.2.1.3 Analysis of OST during stimulus presentation

Approximately three thermal pictures per second could be obtained from the corneal surface during stimulus presentation. Grayscale thermal images were analysed using a purpose-designed computer programme (ThermaCAM Researcher Pro Version 2.9, FLIR Systems, 2006). The corneal area targeted by the air stimulus was marked and analysed during stimulus presentation (Figures 3.32 and 3.33).

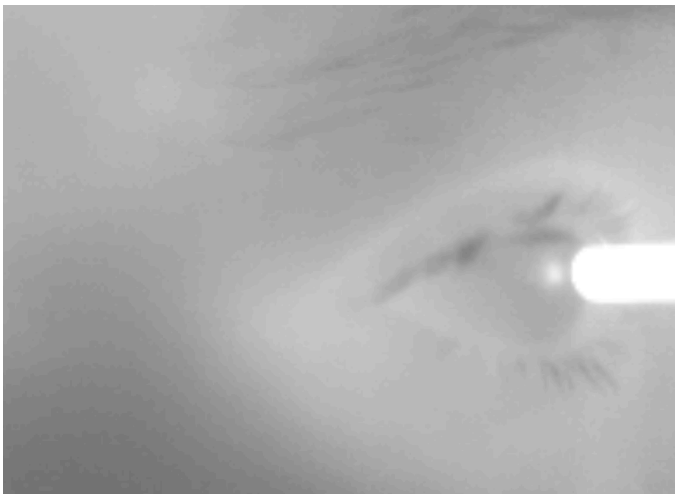

Figure 3.31: Example of localised ocular surface temperature (OST) increase during a heated air stimulus (grey scale). The white rectangular object to the right is the OPM exit nozzle.

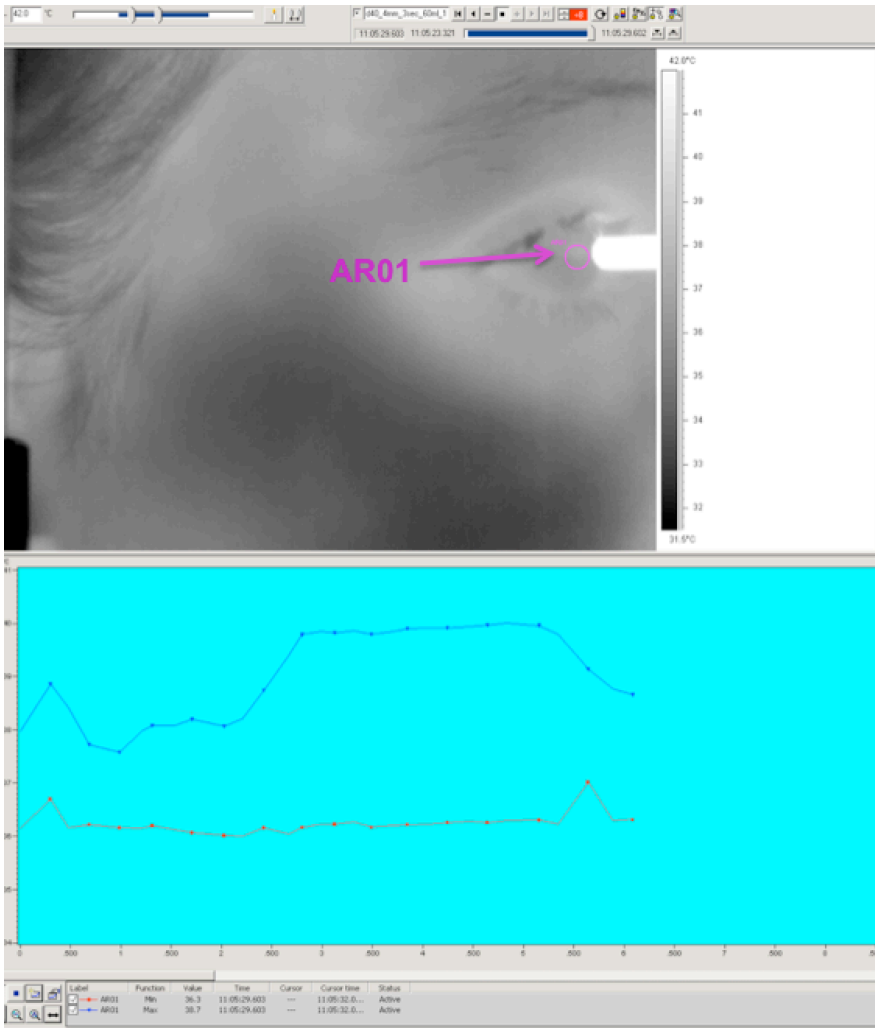

Figure 3.32: Example of a thermal image with relevant area marked for analysis of OST change, along with an example of graphical output. The upper temperature trace shows the max. OST and the lower trace shows the min. OST within ‚AR01', respectively.

OST change could be analysed with the aid of a graph positioned below the thermal image, which gave a time plot for the OST change for the full duration of the temperature recording (Figure 3.33). As mentioned above, three to four measurements were recorded per second, hence each image displays one momentary image. Towards the top-right of the figure, the minimum and maximum corneal temperatures (°C), within the marked area 'AR01' on the image, are displayed for each measurement. The area 'AR01' represented the corneal location where temperature change occurred during the duration of each stimulus. Before each stimulus presentation, the baseline minimum and maximum OST were displayed for each measurement within the area 'AR01'. For the analysis of OST change during a cooling stimulus, the baseline temperature value of

the 'minimum temperature' within area 'AR01' was noted before stimulus presentation. During a cooling stimulus presentation, the maximum OST change was noted by recording the lowest temperature value for the 'minimum temperature' within 'AR01'. The difference between the baseline and the lowest temperature represented the maximum temperature decrease. Correspondingly, during a heating stimulus, the maximum temperature change was determined by noting the difference between the lowest (baseline) and highest value of the 'maximum temperature' within area 'AR01' during stimulus presentation.

These limits ensured that the maximum effect of any temperature change occurring during stimulus presentation was detected. For stimuli giving rise to very little corneal temperature change, where it was difficult to decide whether a cooling or heating response had occurred, i.e. almost matching OST, the temperature changes for both, the 'minimum' and 'maximum temperature' during stimulus presentation were noted. If there was a decrease in temperature, the minimum temperatures were compared, and if there was an increase, the change in the 'maximum temperatures' was compared and included for analysis. Since the temperature did not always change within the entire area 'A01' during the full length of stimulus presentation, a comparison of average temperature values within 'A01' would not have represented the true maximum OST change during stimulus presentation, as some corneal locations not affected by the stimulus would have been included for analysis by error.

3.2.2 Study part A: Measurement of ocular surface temperature during stimulus presentation with rising levels of stimulus temperature

The aim of this clinical experiment was to measure the effect of air gas stimuli of different temperatures on OST, with aid of the thermal infrared camera. In particular, the cooling effect of the air stimulus with 'delta 3' across various distances, stimulus durations and levels of airflow was assessed, in order to evaluate its effect on the temperature sensitive C fibres in the corneal epithelium. Furthermore, the stimulus temperature was investigated that would induce the least change in ocular surface

temperature and would hence be most likely to be suitable for the measurement of mechanical corneal sensitivity.

3.2.2.1 Methods

This was a prospective randomised clinical study. Ten volunteers were recruited from the staff and patient pool of the Optometry Department, University of Applied Science in Olten (CH). They were invited either by email or by personal invitation in the clinic. All subjects invited to take part in the study were given a subject information sheet explaining the study prior to giving signed consent. OST was measured with the aid of a thermal infrared camera during air stimulus presentation (FLIR A310, as described above).

The cooling effect of the air stimulus with 'delta 3' on OST was assessed with the same characteristics that were applied in section 3.1:

- at the working distances of 4 and 8mm
- with the stimulus durations of 3 and 5s
- with the air flow rates of 30, 60, 80 and 100ml/min

However, in order to keep the appointment duration for individual participants on one day within an acceptable limit, not all measurements were carried out on each subject. This option was preferred to splitting up the measurements to different appointment dates, as this may have added additional variability to the results.
The following sets of measurements were carried out:

- Presentation of a cooling stimulus with the stimulus durations of 3 and 5s, the working distances of 4 and 8mm, an airflow rate of 60ml/min and 'delta 3' (three measurements per stimulus setting): ten subjects.
- Presentation of a cooling stimulus with rising levels of airflow rate (30, 60, 80 and 100ml/min) at 4mm working distance and with 3s stimulus duration (three measurements per stimulus setting): six subjects.

Furthermore, OST change was measured during stimulus presentation with rising levels of 'delta' (3, 5, 10, 15, 20, 25, 30, 40 and 50) with a fixed stimulus distance of 4mm, a

fixed stimulus duration of 3s, and a fixed level of airflow set at 60ml/min. A sub-group of six subjects participated for this part of the first study period (three measurements per stimulus setting).

OST was only measured on right eyes and the participating subjects were asked to close their eyes immediately after each measurement for 20s, in order for the tearfilm to recover after each stimulus presentation. In order to ensure a complete and stable tear film over the cornea, the subject was asked to make a full, but unforced blink, following which (within 1-2s) the stimulus was presented.[362] The correct positioning of the direction of gaze was controlled with aid of a correctly positioned fixation target at the wall.

3.2.2.2 Statistical analysis

The data were tested for normal distribution (Shapiro-Wilk Test). A general linear model (two-way ANOVA) was applied for normally distributed data and subsequently post-hoc t-tests with Bonferroni corrections were carried out (SPSS Version 20, Chicago, IL, USA).

3.2.2.3 Results

Ten subjects participated in this study, and the average subject age was 27.10±3.81 years, six subjects were female. The average ambient temperature in the testing room was 23.20±0.30°C and average ambient humidity was measured to be 38.60±2.5%.

3.2.2.3.1 Cooling stimulus with varying durations and distances to the ocular surface

During some measurements, the results were affected by excessive tearing, hence the data were analysed for outliers (boxplot analysis, SPSS Version 20, Chicago, IL, USA; Appendix section no. 8.1.1). One set of data was found to be an outlier and was consequently excluded for analysis. OST change was found to be statistically significant for the overall group ($F=326.67$; $p<0.001$) and for all the individual stimulus characteristics tested: distance 4mm and 8mm, as well as the 3 and 5s durations (Table 3.17 and Figure 3.34).

Mean temperature changes with various stimulus distances and durations applying a cooling stimulus ('delta 3', airflow rate=60ml/min)				
Stimulus type	mean temp. before stimulus (°C)	mean temp. with stimulus (°C)	mean difference (°C)	p-value
distance 4mm duration 3s	34.88±0.65	33.60±0.64	-1.28±0.31	<0.001
distance 4mm duration 5s	35.03±0.47	33.69±0.42	-1.40±0.20	<0.001
distance 8mm duration 3s	35.23±0.45	34.21±0.40	-1.05±0.17	<0.001
distance 8mm duration 5s	35.15±0.52	33.96±0.52	-1.21±0.25	<0.001

Table 3.17: Mean OST changes with different stimulus types ('delta 3').

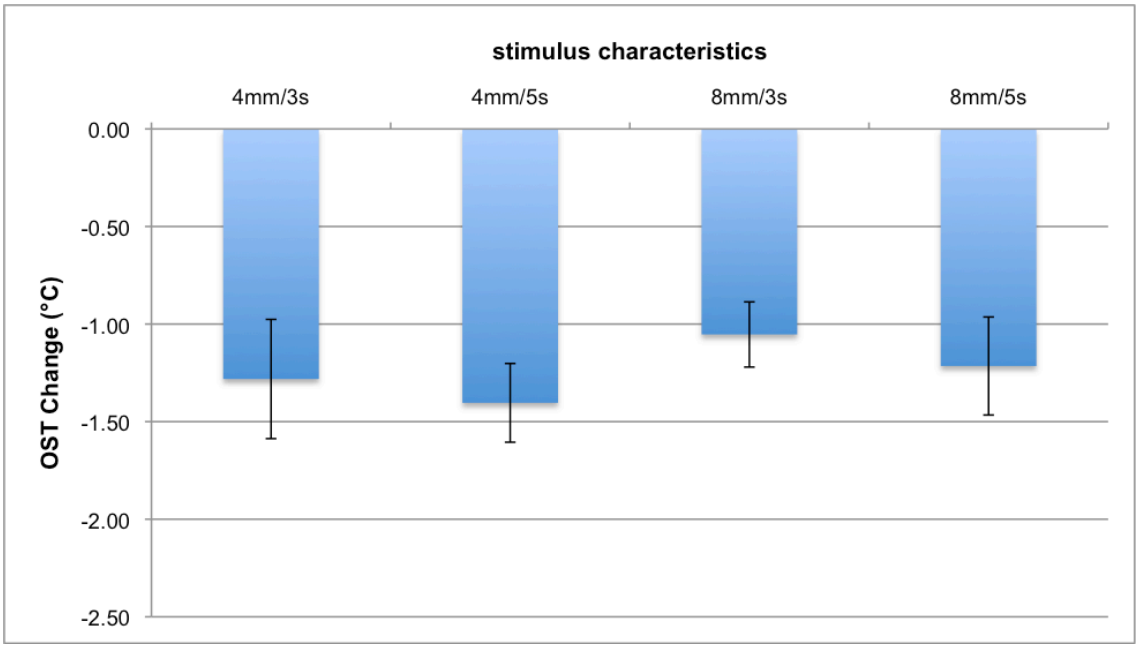

Figure 3.33: Mean OST decrease with various stimulus characteristics and airflow rate set at 60ml/min ('delta 3').

Some variation in corneal temperature change was observed between the different subjects. However, a trend in corneal temperature change was more pronounced at the shorter distance of 4mm and the longer duration of 5mm. A paired post-hoc t-test compared OST change between different stimulus characteristics, i.e. stimulus distance and duration. However, they only differed to a statistically significant degree for the

pairs 4mm/5s versus 8mm/3s, and 8mm/3s versus 8mm/5s, but not for the remaining pairs (Table 3.18).

Significance of corneal temperature change with varying stimulus characteristics ('delta 3'; airflow rate =60ml/min)	
stimulus type	p-value
4mm/3s vs. 4mm/5s	1.000
4mm/3s vs 8mm/3s	0.427
4mm/3s vs 8mm/5s	1.000
4mm/5s vs 8mm/3s	0.023
4mm/5s vs 8mm/5s	0.879
8mm/3s vs 8mm/5s	0.021

Table 3.18: Statistical analysis comparing OST change with varying stimulus characteristics ('delta 3', airflow rate 60ml/min; post-hoc t-test)

These results suggest that the shorter distance of 4mm, together with the longer duration of 5s, produce the strongest effect on OST.

3.2.2.3.2 Cooling stimulus with rising levels of airflow rates

The data were analysed for potential outliers with boxplots, however none could be identified. Stimulus distance was set at 4mm and duration was 3s for all measurements. A trend of corneal temperature changes being more pronounced with increasing levels of airflow was observed (Table 3.19 and Figure 3.35).

Mean corneal temperature change with varying levels of airflow for 4mm distance and 3s duration ('delta 3')				
airflow (ml/min)	temperature before stimulus (C°)	temperature with stimulus (C°)	temperature difference (C°)	p-value (paired t-test)
30	35.10±0.64	34.50±0.63	-0.60±0.09	0.000
60	35.09±0.41	33.79±0.62	-1.29±0.31	0.000
80	34.94±0.41	33.45±0.66	-1.49±0.50	0.001
100	34.82±0.49	33.34±0.53	-1.48±0.49	0.001

Table 3.19: Mean OST change with varying levels of airflow ('delta 3'; 4mm/3s).

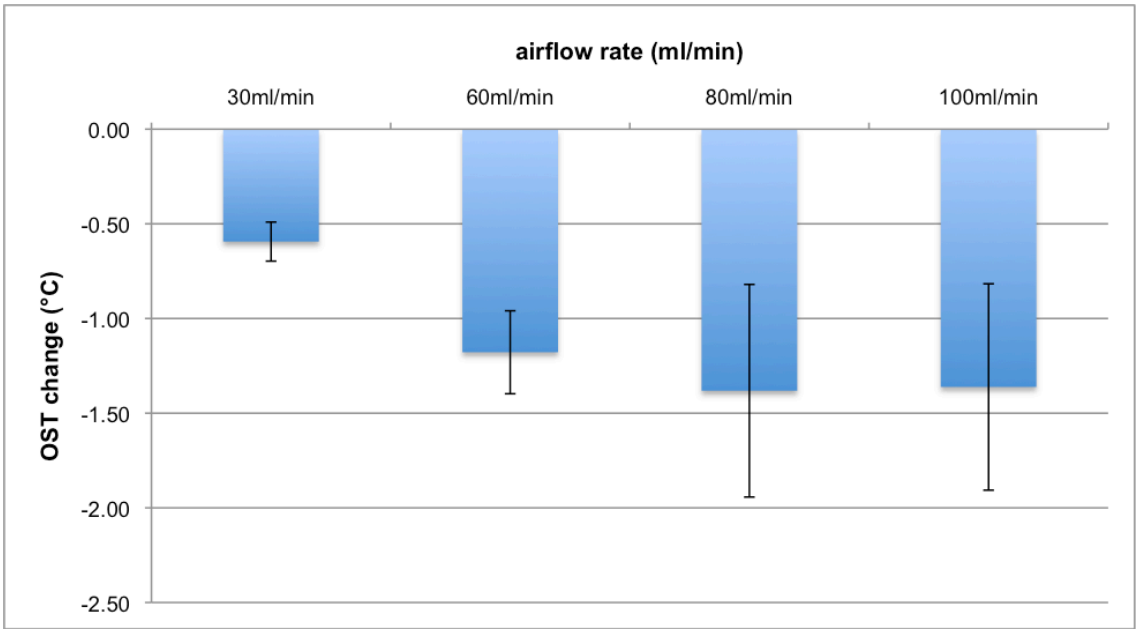

Figure 3.34: Mean OST decrease with increasing levels of airflow ('delta 3').

Although the variation in absolute OST between individuals was considerable, corneal temperature decreased in all subjects with increasing levels of airflow. The differences in corneal temperature before and during stimulus presentation were found to be statistically significant for the overall group (F=92.10; p=0.000, two-way ANOVA), as well as for the individual levels of airflow rates (Table 23). When comparing the corneal temperature differences with different levels of airflow rates, the post-hoc t-test revealed that they only differed to a statistically significant degree for the pairs 30 vs. 60ml/min, 30 vs. 80ml/min and 30 vs. 100ml/min, but not for the remaining pairs (Table 3.20). This indicated that the effect of airflow rate on stimulus temperature decreased with airflow rates higher than 60ml/min.

Statistical significance of corneal temperature change with varying levels of airflow ('delta 3'; distance 4mm, duration 3s)	
Airflow (ml/min.)	p-value
30 vs. 60	0.016
30 vs. 80	0.040
30 vs. 100	0.031
60 vs. 80	1.000
60 vs. 100	1.000
80 vs. 100	1.000

Table 3.20: Statistical significance of OST change with varying levels of airflow ('delta 3'; 4mm distance, 3s duration).

An increasing reduction in OST was observed with rising airflow rates (Figure 3.42): it was lowest at 30ml/min and highest with 80 and 100ml/min. Interestingly, the variability in OST decrease was found to be more marked with the higher levels of airflow rates, such as 80 and 100ml/min. As OST difference was also less pronounced between these two higher airflow rates, it is very possible that this may have occurred due to a greater variability in flow dispersion with increasing levels of airflow rates.

3.2.2.3.3 Heated stimulus with rising levels of 'delta'

When 'delta' was set at 3, 5 and 10, the corneal temperature decreased in all subjects. With 'delta' set at 15, it remained unchanged in subject 2 and 3, but rose very slightly in all other subjects (Table 3.21). With 'delta' set at greater than 15, corneal temperature increased in all six subjects (Table 3.21, Figure 3.36). An almost linear OST increase could be observed, proportional to the increase in stimulus temperature (Figures 3.36 and 3.37).

Corneal temperature change with increasing levels of 'delta' and a constant airflow rate set at 60ml/min, a distance of 4mm and a stimulus duration of 3 s (in °C)						
'delta'	subject 1 (C°)	subject 2 (C°)	subject 3 (C°)	subject 4 (C°)	subject 5 (C°)	subject 6 (C°)
3	-1.00	-1.57	-1.10	-1.37	-1.30	-1.03
5	-1.17	-1.37	-0.50	-0.93	-1.03	-0.83
10	-0.43	-0.20	-0.07	-0.10	-0.23	-0.13
15	0.10	0.00	0.03	0.07	0.10	0.13
20	0.90	0.73	1.43	0.93	0.37	0.23
25	-	1.37	0.78	1.97	0.80	1.13
30	2.73	1.1	3.27	2.30	2.00	1.80
40	3.90	2	3.67	3.40	3.20	2.80
50	-	1.73	5.53	4.00	-	-

Table 3.21: OST change with increasing levels of 'delta' and a constant airflow rate set at 60ml/min.

At 'delta 50', the instrument was occasionally over-heating and a stimulus presentation was therefore not possible at all times – hence, the missing values for subjects 5 and 6 (Table 3.21).

Corneal temperature changes with increasing levels of delta and a constant airflow of 60ml/min, a distance of 4mm and a stimulus duration of 3 s (in °C)			
delta	mean corneal temp. before stimulus (C°)	mean corneal temp. with stimulus (C°)	mean temp. difference (C°)
3	34.99±0.67	33.82±0.73	-1.17±0.22
5	35.23±0.68	34.26±0.49	-0.97±0.30
10	35.30±0.80	35.10±0.70	-0.20±0.13
15	36.24±0.45	36.32±0.42	+0.08±0.05
20	36.52±0.57	37.28±0.58	+0.77±0.43
30	36.98±0.53	39.09±1.17	+2.11±0.82
40	37.44±0.67	40.60±1.30	+3.16±0.68

Table 3.22: OST changes with increasing levels of 'delta'.

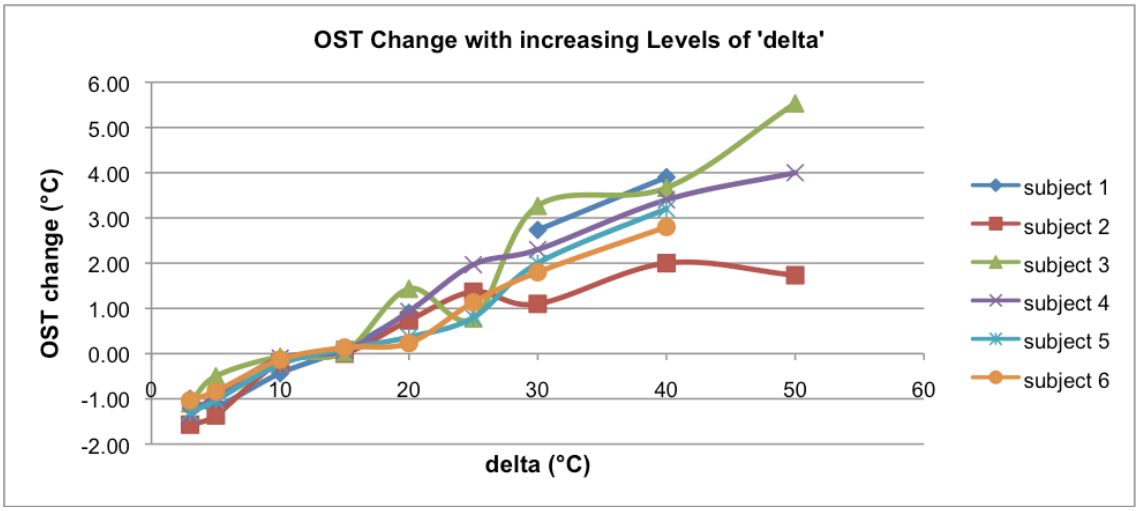

Figure 3.35: Individual OST change with increasing levels of 'delta' (°C) with constant stimulus airflow of 60ml/min, distance of 4mm and duration of 3s.

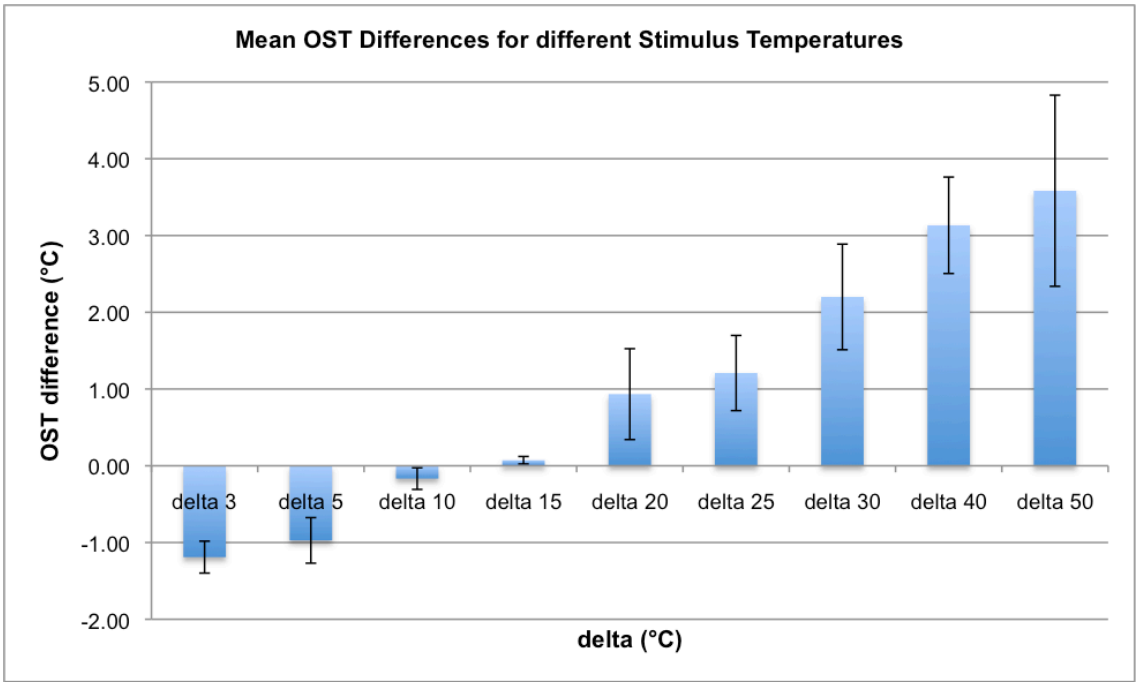

Figure 3.36: Mean OST differences for increasing stimulus temperatures with constant stimulus airflow of 60ml/min, distance of 4mm and duration of 3s.

3.2.3 Study part B: The effect of stimulus characteristics of an air gas stimulus equal to corneal temperature on OST

The effect of various stimulus characteristics (distance 4 and 8mm, duration of 3 and 5s, and various levels of airflow of 30, 60, 80 and 100ml/min) on OST was measured when using a fixed stimulus temperature most likely to match OST, as established during part A. The aim was to establish if any OST changes produced by varying airflow remained small enough to ensure a mechanical stimulus that would only excite the mechanically sensitive Aδ fibres and not the temperature sensitive C fibres in the corneal epithelium.

3.2.3.1 Methods

During part A of the study, it was noted that the corneal temperature change was smallest with 'delta 10' and 'delta 15' in all 6 subjects (Section 3.2.2.3, Table 3.21). It was therefore decided to further explore corneal temperature change with 'delta' set at 10 and 15, and with varying airflow rates in 10 additional subjects (a total of 16 subjects), who were recruited according to the same protocol as during study part A. OST was measured with the aid of a thermal infrared camera on the 10 additional subjects during air stimulus presentation (FLIR A310). The 'delta 10' and 'delta 15' air gas stimulus temperatures, which were most likely to match OST in part A, were each applied with the same various stimulus characteristics as in section 3.1 (thermocouple experiments) and section 3.2.2 (study part A at the distances of 4 and 8mm).

- with the stimulus durations of 3 and 5s
- with the airflow rates of 30, 60, 80 and 100ml/min

For the standard stimulus settings at 4mm distance and 3s duration, sixteen subjects were recruited.

For the stimulus settings at 4mm distance and 5s duration and at 8mm distance with the durations of 3s and 5s, tenj subjects were recruited.

Each measurement was carried out three times.

The results were combined and analysed for all subjects participating during parts A and B. The order of measurements was randomised for different stimulus characteristics (duration, distance and temperature), however the order of airflow rates was kept

constant, in rising order, just like the air stimuli would be presented during corneal sensitivity threshold measurements: 30, 60, 80 and 100ml/min.

3.2.3.2 Statistical analysis

The data were tested for normal distribution (Shapiro-Wilk Test). A general linear model (two-way ANOVA) was applied for normally distributed data and subsequently post-hoc t-tests with Bonferroni corrections were carried out (SPSS Version 20, Chicago, IL, USA).

3.2.3.3 Results

Average age of this second group was 25.4±2.01 years, and four subjects were female. The average ambient temperature in the testing room was 23.1±0.4°C and average ambient humidity was measured to be 37.8±2.2%.

3.2.3.3.1 Ocular surface temperature with stimulus temperature at 'delta 10'

Some of the subjects experienced tearing during stimulus presentation, therefore the data were analysed for outliers using boxplots (SPSS, Version 20; Appendix no 8.1.2). Subject numbers 9 and 10 were identified as outliers and were consequently removed from the analysis.

The changes in absolute corneal temperature for the overall group were found to be statistically significant for all stimulus characteristics ($p=0.000$, $F=50.50$ for 4mm/3s; $p=0.021$, $F=8.70$ for 4mm/5s; $p=0.000$, $F=84.65$ for 8mm/3s; $p=0.000$, $F=160.60$ for 8mm/5s, two way ANOVA).

Although the absolute OST changes during stimulus presentation were small, they were all statistically significant (post-hoc paired t-test; Tables 3.23-3.26), with the exception of the stimulus setting at 4mm/5s with airflow 30ml/min (Table 3.24). The ANOVA analysis of the temperature differences confirmed statistical significance for all stimulus characteristics ($p=0.001$, $F=8.43$ for 4mm/3s; $p=0.001$, $F=7.80$ for 4mm/5s; $p<0.001$, $F=23.28$ for 8mm/3s; $p<0.001$, $F=23.29$ for 8mm/5s).

Mean corneal temperature change with varying levels of airflow rates for 4mm distance and 3s duration ('delta 10')				
airflow rate (ml/min)	temperature before stimulus (C°)	temperature with stimulus (C°)	temperature difference (C°)	p-value (paired t-test)
30	34.80±0.85	34.60±0.86	-0.23±0.12	<0.001
60	34.61±0.81	34.22±0.87	-0.36±0.14	<0.001
80	34.73±0.91	34.17±1.03	-0.49±0.28	<0.001
100	34.67±0.90	33.96±1.14	-0.62±0.40	<0.001

Table 3.23: Mean OST changes for stimulus 4mm and 3s ('delta 10').

Mean corneal temperature change with varying levels of airflow rates for 4mm distance and 5s duration ('delta 10')				
airflow rate (ml/min)	temperature before stimulus (C°)	temperature with stimulus (C°)	temperature difference (C°)	p-value (paired t-test)
30	34.50±0.48	34.15±0.51	-0.38±0.42	0.456
60	34.57±0.54	34.07±0.42	-0.60±0.43	0.027
80	34.57±0.55	34.07±0.51	-0.64±0.26	0.006
100	34.63±0.64	33.98±0.63	-0.80±0.51	0.004

Table 3.24: Mean OST changes for stimulus 4mm and 5s ('delta 10').

Mean corneal temperature change with varying levels of airflow rates for 8mm distance and 3s duration ('delta 10')				
airflow rate (ml/min)	temperature before stimulus (C°)	temperature with stimulus (C°)	temperature difference (C°)	p-value (paired t-test
30	34.41±0.35	34.20±0.42	-0.22±0.16	0.061
60	34.41±0.33	33.97±0.40	-0.43±0.19	0.001
80	34.43±0.42	33.88±0.42	-0.54±0.13	<0.001
100	34.36±0.43	33.80±0.43	-0.54±0.07	0.001

Table 3.25: Mean OST changes for stimulus 8mm and 3s ('delta 10').

Mean corneal temperature change with varying levels of airflow rates for 8mm distance and 5s duration ('delta 10')				
airflow rate (ml/min)	temperature before stimulus (C°)	temperature with stimulus (C°)	temperature difference (C°)	p-value (paired t-test)
30	34.79±0.65	34.50±0.63	-0.28±0.14	0.017
60	34.74±0.69	34.25±0.62	-0.50±0.14	<0.001
80	34.63±0.59	33.90±0.49	-0.73±0.20	0.003
100	34.68±0.62	33.96±0.61	-0.71±0.16	0.005

Table 3.26: Mean OST changes for stimulus 8mm and 5s ('delta 10').

A pair-wise comparison of OST changes induced by the different air stimuli characteristics showed that the effect of airflow rate levelled off with the higher levels of 60, 80 and 100ml/min (Table 3.27).

Pair-wise comparison of corneal temperature changes with different levels of airflow				
Airflow (ml/min)	4mm/3s	4mm/5s	8mm/3s	8mm/5s
30 vs 60	p=0.043	p=0.061	p=0.015	p=0.059
30 vs 80	p=0.016	p=0.420	p=0.001	p=0.005
30 vs 100	p=0.010	p=0.006	p=0.002	p=0.002
60 vs 80	p=0.779	p=1.000	p=0.185	p=0.012
60 vs 100	p=0.118	p=1.000	p=0.401	p=0.021
80 vs 100	p=1.000	p=1.000	p=1.000	p=1.000

Table 3.27: Pair-wise comparison of OST changes with different levels of airflow rates (post-hoc t-test; 'delta 10').

With the exception of stimulus 4mm/5s, the decreases in OST were more pronounced for the lower airflows 30-60ml/min than for 60-100ml/min. This indicated that corneal temperature change levelled off with increasing levels of airflow rates (Figures 3.38 and 3.39).

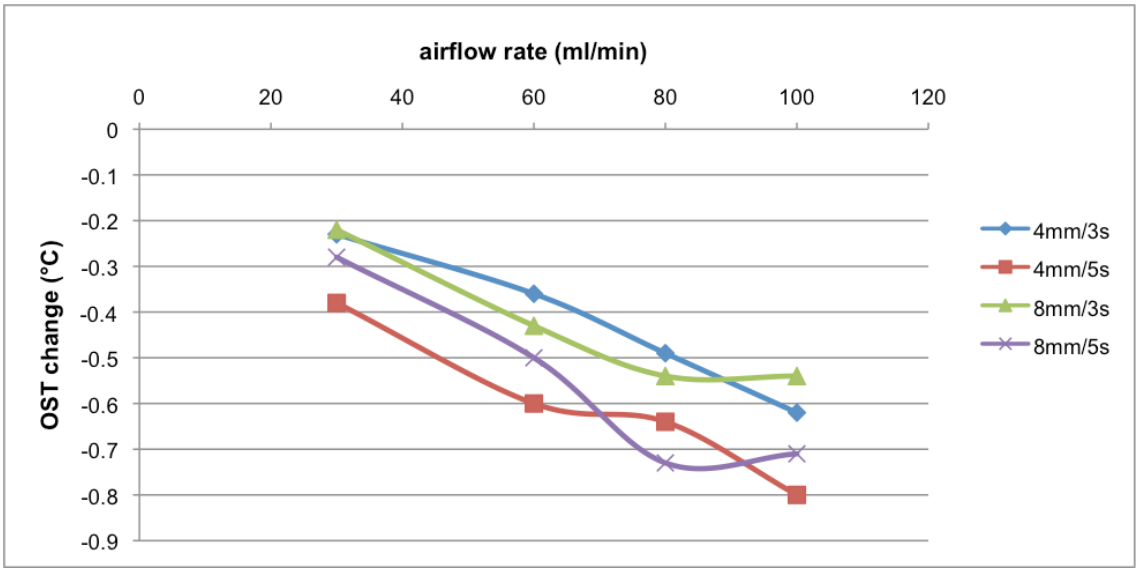

Figure 3.37: Mean corneal temperature change with varying levels of airflow ('delta 10').

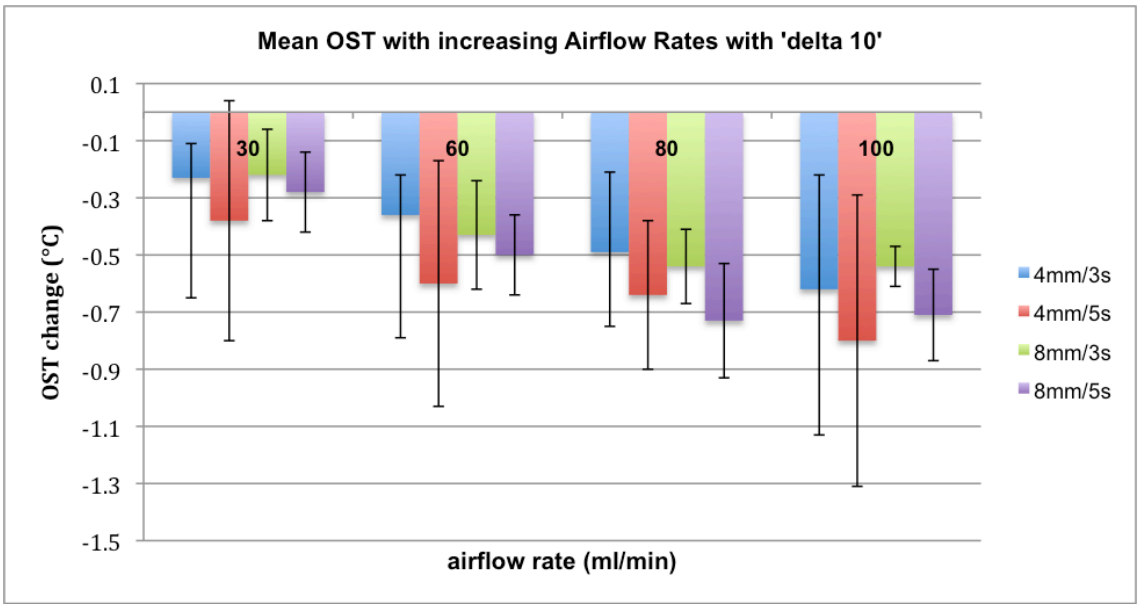

Figure 3.38: Mean corneal temperature change with varying levels of airflow ('delta 10').

3.2.3.3.2 Corneal temperature with stimulus temperature at 'delta 15'

Analogous to the results for 'delta 10', the number of subjects analysed for 'delta 15' varied between 10 and 16 subjects, depending on the stimulus characteristics applied. The analysis for outliers identified the majority of the results for 'subject 10' and 'subject 13' to be outliers, again due to excessive tearing. Consequently, these two subjects were excluded from the analysis.

The absolute OST changes for the overall group were found to be statistically significant for the stimulus characteristics 4mm/3s and 4mm/5s ($p<0.001$, $F=97.95$ for 4mm/3s; $p<0.001$, $F=63.72$ for 4mm/5s), but not for 8mm/3s and 8mm/5s ($p=0.698$, $F=0.164$ for 8mm/3s; $p=0.522$, $F=0.455$ for 8mm/5s).

Although the actual mean OST changes were small for all stimulus characteristics with 'delta 15', they reached statistical significance for almost all results at the short stimulus distance of 4mm (Tables 3.28-3.31). For the 8mm distance, they were almost never statistically significant. However, the variability for this longer working distance was found to be considerably higher (Figure 3.41). The ANOVA analysis of the temperature differences confirmed statistical significance for the stimulus characteristics of 4mm/3s and 4mm/5s for the overall group ($p<0.001$, $F=45.26$ for 4mm/3s; $p<0.001$, $F=92.00$ for 4mm/5s) and did not indicate statistical significance for the stimulus characteristics of 8mm/3s and 8mm/5s ($p=0.061$, $F=2.87$ for 8mm/3s; $p=0.417$, $F=0.99$ for 8mm/5s).

Mean corneal temperature change with varying levels of airflow rates for 4mm distance and 3s duration (delta =15)				
airflow rate (ml/min)	temperature before stimulus (C°)	temperature with stimulus (C°)	temperature difference (C°)	p-value (paired t-test)
30	35.24±0.79	35.24±0.78	0.00±0.07	1.000
60	35.09±0.75	35.27±0.75	0.18±0.17	0.002
80	35.16±0.82	35.47±0.83	0.32±0.13	<0.001
100	35.17±0.87	35.59±0.92	0.43±0.10	<0.001

Table 3.28: Mean OST changes for stimulus 4mm and 3s ('delta 15').

Mean corneal temperature change with varying levels of airflow rates for 4mm distance and 5s duration (delta =15)				
airflow rate (ml/min)	temperature before stimulus (C°)	temperature with stimulus (C°)	temperature difference (C°)	p-value (paired t-test)
30	34.74±0.56	34.81±0.56	0.07±0.06	0.012
60	34.83±0.53	34.97±0.54	0.14±0.09	0.003
80	34.91±0.49	35.19±0.47	0.28±0.11	<0.001
100	34.90±0.55	35.34±0.54	0.44±0.10	<0.001

Table 3.29: Mean OST changes for stimulus 4mm and 5s ('delta 15').

Mean corneal temperature change with varying levels of airflow rates for 8mm distance and 3s duration (delta =15)				
airflow rate (ml/min)	temperature before stimulus (C°)	temperature with stimulus (C°)	temperature difference (C°)	p-value (paired t-test)
30	34.78±0.49	34.70±0.47	-0.08±0.09	0.041
60	34.71±0.51	34.68±0.49	-0.03±0.14	0.510
80	34.63±0.45	34.64±0.41	0.00±0.14	0.936
100	34.69±0.53	34.72±0.51	0.03±0.21	0.670

Table 3.30: Mean OST changes for stimulus 8mm and 3s ('delta 15').

Mean corneal temperature change with varying levels of airflow rates for 8mm distance and 5s duration (delta =15)				
airflow rate (ml/min)	temperature before stimulus (C°)	temperature with stimulus (C°)	temperature difference (C°)	p-value (paired t-test)
30	34.65±0.65	34.58±0.57	-0.07±0.10	0.099
60	34.61±0.60	34.59±0.55	-0.02±0.09	0.537
80	34.69±0.62	34.60±0.79	-0.08±0.30	0.457
100	34.75±0.58	34.78±0.62	0.03±0.20	0.658

Table 3.31: Mean OST changes for stimulus 8mm and 5s ('delta 15').

The level of airflow rate had a statistically significant effect on OST at the shorter working distance of 4mm, but not at the longer working distance of 8mm (Table 3.32, Figures 3.47 and 3.48).

Pair-wise comparison of corneal temperature changes with different levels of airflow rates				
airflow rate (ml/min)	4mm/3s	4mm/5s	8mm/3s	8mm/5s
30 vs. 60	p=0.009	p=0.027	p=0.997	p=0.122
30 vs 80	p<0.001	p=0.001	p=0.166	p=1.000
30 vs 100	p<0.001	P<0.001	p=0.749	p=1.000
60 vs 80	p=0.027	p=0.009	p=0.153	p=1.000
60 vs 100	p<0.001	p<0.001	p=0.999	p=1.000
80 vs 100	p=0.063	p<0.001	p=1.000	p=0.613

Table 3.32: Pair-wise comparison of OST changes with different levels of airflow rates (post-hoc t-test; 'delta 15').

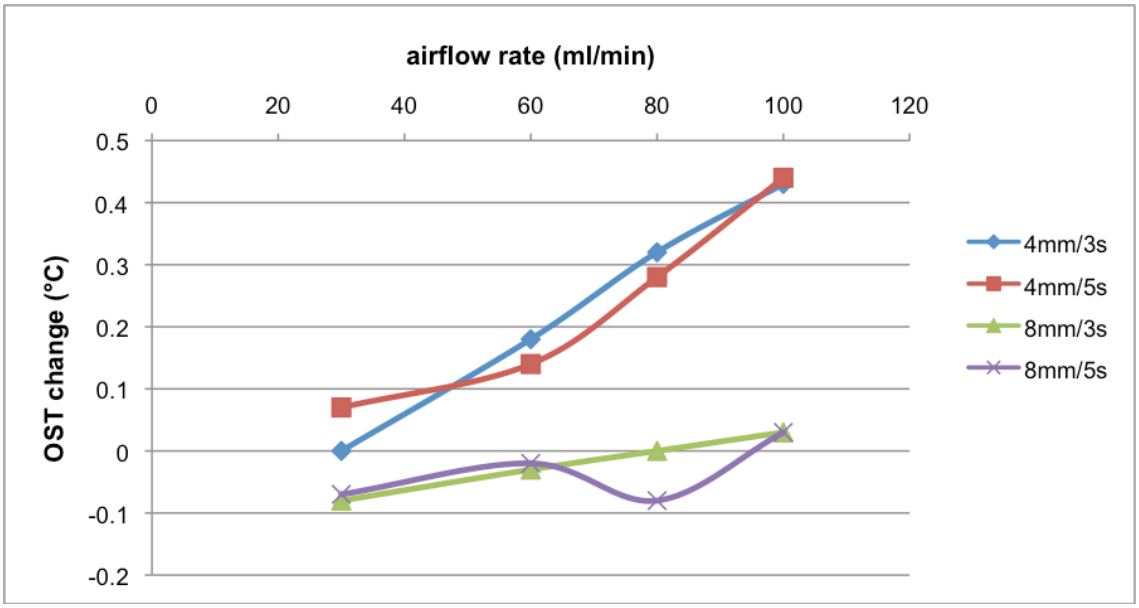

Figure 3.39: Mean OST change with varying levels of airflow rates ('delta 15')

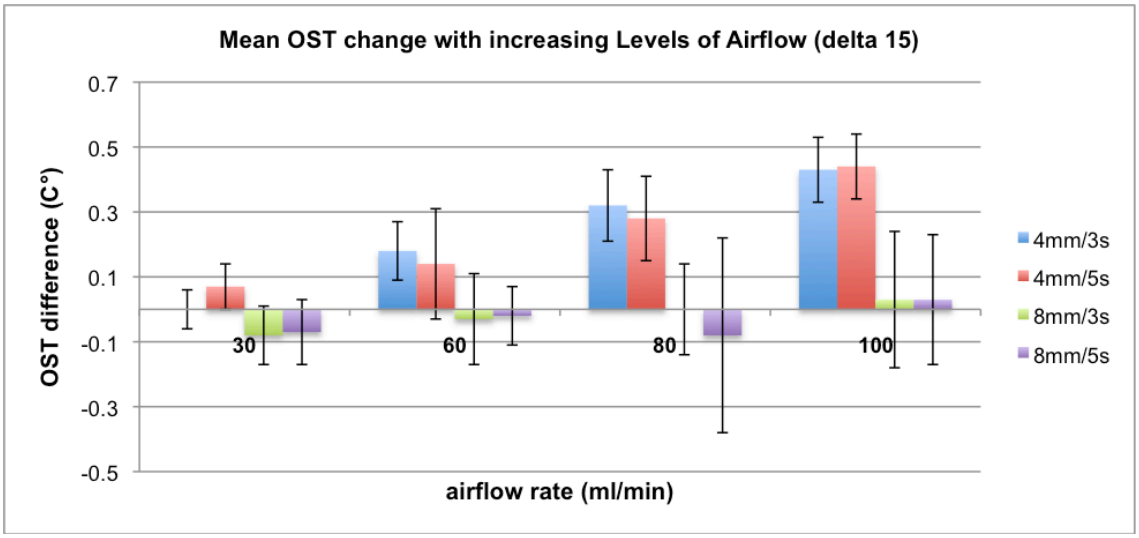

Figure 3.40: Mean OST change with varying levels of airflow (delta 15).

3.2.4 Discussion for parts A and B

This clinical study was aimed at measuring stimulus temperature of the air gas stimulus generated by the Belmonte aesthesiometer by recording changes in ocular surface temperature during stimulus duration with the use of an infrared thermal camera. Air stimuli cooler and warmer than the ocular surface were generated from two distances (4mm and 8mm) to the cornea, with two different durations (3 and 5s), as well as with different levels of airflow (30, 60, 80 and 100ml/min). The resulting changes in ocular surface temperature were analysed statistically. Additionally, it was of particular interest to establish if it was possible to generate air stimuli matching ocular surface temperature.

3.2.4.1 The study design

These OST measurements took place in two parts: during part A, the cooling effect of an air stimulus close to room temperature was investigated. Furthermore, the choice of 'delta' that would be most likely to match OST and would therefore be suitable to create a purely mechanical stimulus was evaluated. Ten subjects were enrolled to participate in part A.

Since the two investigations required 48 (cooling stimulus) and 27 (stimulus with rising levels of 'delta') measurements in full to be carried out in one day, and because there

were concerns about the reduction in tear film quality during such prolonged measurement times, it was decided to carry out the measurements with the cooling stimulus on all 10 subjects with the two distance and duration settings (one was excluded due to excessive tearing), but to additionally measure the effect of rise in airflow rates only in 6 out of the 10 subjects. Consequently, the measurements applying the air stimuli with increasing levels of 'delta' were also only carried out on 6 of the total number of 10 subjects in part A. From this experiment, it could be observed that 'delta 15' created the least change in OST, and while the air stimuli with 'delta 10' created a larger change in OST than with 'delta 15', the effect was still small enough to qualify for further investigation. Hence, part B was conducted in order to test the effect of the other stimulus characteristics such as duration, distance and airflow rate with 'delta' set at 10 and 15. For part B, ten new subjects were enrolled. Unfortunately, the measurements of two subjects had to be excluded from analysis (outliers due to excessive tearing). The results for 'delta 10' and 'delta 15' from part A were also included into the analysis. Hence, the sample size for part B varied from 8 to 14, depending on whether data were used from part A and whether an outlier needed to be excluded. However, for the stimulus characteristics most commonly used (distance 4mm and duration 3s), the sample size was n=14. A two-tailed post hoc power calculation was carried out for these standard stimulus characteristics, for each of the airflow rates applied, where a statistically significant difference was obtained (α=0.05; n=14; G*Power 3.1):

For airflow rate of 60ml/min:

- OST difference of 0.18±0.17°C; effect size = 1.059; power = 0.95

For airflow rate of 80ml/min:

- OST difference of 0.32±0.13°C; effect size = 2.46; power = 1.0

For airflow rate of 100ml/min:

- OST difference of 0.43±0.10°C; effect size = 4.3; power = 1.0

3.2.4.2 The cooling air gas stimulus

The change in OST was measured for cooling air stimuli at the two distances of 4 and 8mm, with the two durations of 3 and 5s, as well as with the increasing levels of airflow of 30, 60, 80 and 100ml/min. Although considerable individual variability in ocular surface temperature was noted, all cooling air stimuli induced a decrease in temperature. When comparing the various stimulus characteristics applied, it became apparent that the shorter distance of 4mm and the longer stimulus duration of 5s induced a greater temperature change than the longer distance of 8mm and shorter duration of 3s did. This result was not surprising, as the stimulus would be prone to disperse more markedly with the longer distance.[14] Equally, a longer duration may have a more summative effect. Correspondingly, corneal temperature change was greater with increasing levels of airflow. The pair-wise comparison indicated that this temperature change levelled off with the airflow rate exceeding 60ml/min. The influences of stimulus characteristics (distance, duration and airflow) on recorded temperature change were in concordance with the wire and flat thermocouple experiments (which found that the longer working distance reduced the effect on the recorded stimulus temperature, using the flat thermocouple).

3.2.4.3 The heated air gas stimulus

During part A, the stimulus characteristics were set at a distance of 4mm, a duration of 3s, and at an airflow rate of 60ml/min, whilst the levels of 'delta' were increased from 3 to 50. A nearly linear increase in corneal temperature was observed with increasing levels of delta. For the majority of subjects, corneal temperature change was recorded to be least with 'delta 15' and only slightly more so with 'delta 10'. Hence, during part B, the changes in OST were measured with both 'delta 10' and 'delta 15', whilst applying different stimulus characteristics: 4 and 8mm distance, 3 and 5s duration and increasing levels of airflow (30, 60, 80 and 100ml/min). With 'delta 10', small, but statistically significant decreases in corneal temperature were noted for all stimulus characteristics. As expected, these changes were more pronounced with the shorter distance of 4mm, the longer duration of 5s and increasing levels of airflow rates. With 'delta 15', corneal temperature increased with all stimulus characteristics at the shorter distance of 4mm to

a statistically significant degree, however this change was less pronounced than with 'delta 10'. At the longer distance of 8mm, corneal temperature change did not reach statistical significance for either duration or level of airflow rate with 'delta 15', except for the airflow of 30ml/min at 8mm distance and 3s duration (p=0.041). This suggests that a longer working distance would offer a greater chance to match OST, as this study showed that it was not possible to measure a true threshold for mechanical corneal sensitivity with increasing levels of airflow at 4mm with either 'delta 10' or 'delta 15', meaning that there will not exclusively be a mechanical stimulation with this type of air stimulus.

However, the variability in OST measurements was twice as marked for this longer distance of 8mm, suggesting a turbulent dispersion of the air stimulus flow on the ocular surface at this longer distance, applied across the measured air flow rate range of 30-100ml/min. Interestingly, all other research groups exclusively use the shorter working distance of 4 or 5mm with air gas aesthesiometers capable of generating an air gas stimulus similar to OST, suggesting that the experience in research practice also determined the same finding.[21,353,359]

Ideally, the OST measurements would have been repeated with additional subjects at the 8mm distance, however this particular aesthesiometer was no longer available thereafter, due to a technical fault that could not be repaired by the manufacturer. In addition, it would have been necessary to verify its clinical usefulness for the ocular surface sensitivity threshold measurements at a range of patients at this longer working distance. Assuming reliable measurements being possible, the mean ocular surface sensitivity threshold measurements would be expected to turn out higher, as the air stimulus matching OST would arrive at the ocular surface more dispersed, requiring more force for mechanical stimulation. As an increase in airflow rate has been shown to have a cooling effect on OST in this study, the resulting increased air stimulus threshold would be very likely to have an impact on OST.

In this study, the effect of cooling caused by the arrival of the air stimulus upon the ocular surface could not be completely excluded, i.e. it has to be expected that the

contribution of temperature sensitive corneal C-fibres reacting to an air-stimulus as a consequence of corneal surface temperature change cannot be eliminated, although this cooling effect of an air stimulus with 'delta 15' and a room temperature of 23-24°C must be small, with a maximum mean difference of 0.44°C. This difference has to be however considered, as the smallest temperature change likely to be sensed by the ocular surface has been proposed to be 0.3°C.[173]

3.2.5 Conclusions of the OST measurements

The most important finding from this study is that a true threshold for mechanical corneal sensitivity cannot be established with the air stimulus of the Belmonte OPM aesthesiometer with increasing levels of airflow rates, because a corneal temperature change cannot be excluded. The smallest changes in OST were observed with stimulus set at 'delta 15' and with the longer working distance of 8mm. With this setting, the corneal temperature change produced with a room temperature of 23-24°C reached a maximum mean value of 0.44°C. Yet, the variability of the OST measurements obtained at the longer working distance was found to be twice as high, compared to the 4mm working distance in this study. This particular aesthesiometer is calibrated for use at the 4mm distance, representing the preferred distance for threshold measurements of ocular surface sensitivity with this instrument. At this shorter working distance, the maximum temperature change became 0.44°C, and therefore the stimulus is more likely to have a non-mechanical, thermal component. However, further clinical studies would be very useful in order to further explore the effect of air stimulation on the ocular surface at the longer working distance of 8mm and its impact on ocular surface sensibility threshold measurement.

The 'delta 15' setting is also significantly different from the OPM recommended setting of 'delta 19'. Using the graphs, we can see that the maximum temperature change was 1.43°C (for subject 3 and delta 20, Table 3.21) at this approximate delta setting.

Stimulus intensity is controlled by airflow, but the results show that airflow itself is the prime factor in changes in OST change produced by the stimulus. So even if the stimulus is heated by a fixed delta, that delta will only be suitable for one airflow rate.

To truly remove any possible thermal stimulus from the 'mechanical' stimulus, the delta would need to adjust in synchronisation with the airflow. Moreover, in view of the physiological variation observed between subjects, some initial calibration step would be required that was able to assess the OST as the baseline for the stimulus, rather than the ambient room temperature.

3.3 Is there a mechanical element to air gas aesthesiometry?

The air stimulus generated by the NCCA aesthesiometer at room temperature is described by subjects as a cool sensation or as a breeze against the eye, partly reflecting that the temperature of the stimulus is considerably cooler than the ocular surface, and the effect of the airflow producing localised evaporation from the tear film.[22]

With the application of this type of non-invasive stimulus, the cornea is never touched directly by a stimulus probe and hence there is no direct mechanical stimulus. This would suggest that neither the mechanoreceptors nor the polymodal nociceptors respond to the air pulse, but that the cold nociceptors respond to this temperature change, that is being conveyed by the C fibres running perpendicularly to the corneal surface. Using the NCCA devised, which also uses an airflow stimulus, Murphy et al. showed that a localised temperature change on the corneal ocular surface was produced.[22] They hypothesised that the cooling of the tear film could be explained by an increased rate of evaporation as the air stimulus strikes the ocular surface, removing energy from the tear film and resulting in a temperature drop. Similarly, as in the current study, they showed that the airflow rate controls the extent of temperature change on the ocular surface: the higher the stimulus intensity, the more marked the temperature decrease would be. Furthermore, they explored if there was any accompanying mechanical deformation by observing the tear film (after instillation of sodium fluorescein) with use of a slit lamp biomicroscope during air gas stimulation, with an intensity >10x stronger (5mbars) than a normal threshold. Since they could not observe any distortion in the tear film, they concluded that any possible surface deformation would play only a minor role and that the stimulation must primarily be a temperature change.

The Belmonte OPM air gas aesthesiometer and similar models were developed by other research teams[19,21,284] to be able to apply a stimulus whose temperature can be increased with the aim to generate a mechanical stimulus, whereby stimulus temperature can be adjusted to match the OST so that the air stimulus only activates mechanical receptors.

How may mechanical stimulation affect the corneal surface? The Cochet-Bonnet aesthesiometer uses a nylon thread to stimulate directly corneal nerves.[13,18,81] This thread is pressed against the cornea, until it just bends. The stimulus pressure is controlled by varying the length of the thread: the shorter the thread, the more pressure is applied, until it bends on the corneal surface. This type of stimulus gives rise to tactile stimulation, activating mechanoreceptors and polymodal nociceptors supplying predominantly Aδ fibres running parallel to the ocular surface in the corneal epithelium. Due to the different modes of stimulation, no correlation in the measured thresholds could be established between the Cochet-Bonnet aesthesiometer and air gas aesthesiometry.[363]

High-speed photography (S-Motion High Speed Camera, AOS Technologies AG, Baden, Switzerland; 4μsec 1/frame rate) shows that the entire cornea is being indented considerably inwards upon arrival of a plastic nozzle on the corneal surface during rebound tonometry (Figure 3.42). Yet, most patients only feel a very small, short-lasting irritation, due to the high velocity of this stimulus in an electromagnetic field. Some patients are not able to feel this stimulation at all, despite this marked corneal deformation. This may be explained by the fact of temporal summation, i.e. the short stimulus duration may bring the cornea back to its original shape before the superficial nerve fibres are able to detect this brief corneal deformation in these patients.

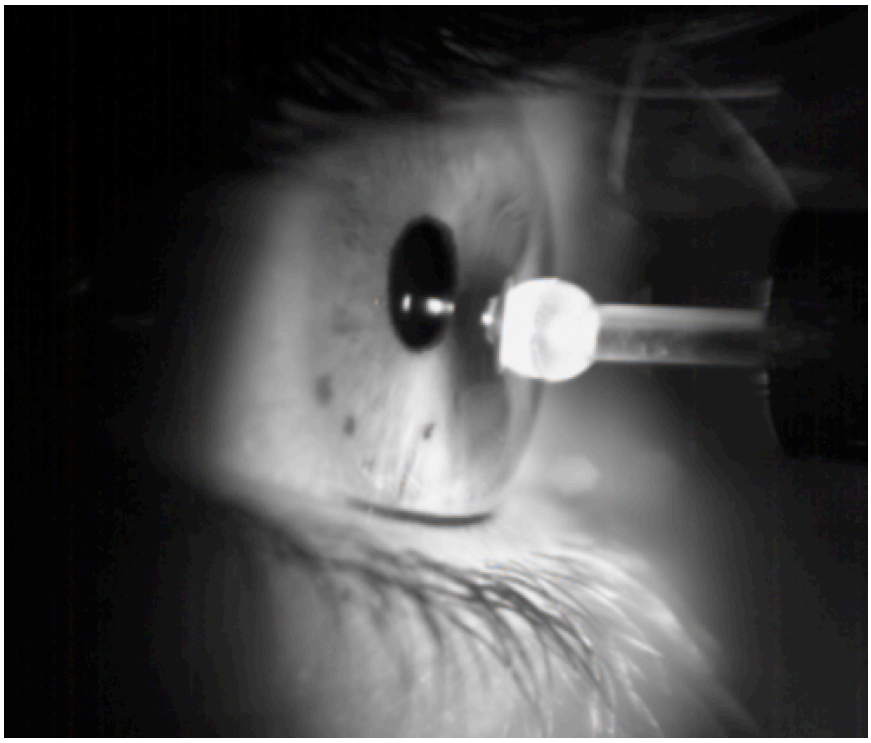

Figure 3.41: Ocular Surface deformation during rebound tonometry

Non-contact tonometry applies an air stimulus being sent to the corneal surface with gradually increasing intensity to the point where it applanates the cornea. The force required at this moment is recorded and converted into mmHg. The Ocular Response Analyzer represents a further development: it notes the moment of applanation, but the air stimulus continues to emit with increasing intensity until the cornea is indented. The force of the air column then decreases until the cornea once again reaches a point of applanation. This shows that an air gas stimulus is able to cause a change in corneal shape, if its intensity is chosen to be high enough.

In order to further explore if corneal deformation may be caused during air gas aesthesiometry, the corneal surface was recorded during the air gas stimulus presentation of the NCCA aesthesiometer by means of a high-speed camera (S-Motion High Speed) and a macro objective attached for a sufficient close-up focus. The maximum stimulus intensity of 9.20mbars at the recommended distance of 10mm and perpendicular to the ocular surface was chosen, which represented nearly 20x of a normal sensitivity threshold. A light source was placed onto the centre of the corneal surface at the point of stimulus arrival, causing a reflex at this location. If corneal

deformation were to take place during stimulus presentation, it was expected to demonstrate a distortion of this reflex. However, no such distortion was observed (Figures 3.43 and 3.44). Consequently, Murphy et al.'s conclusion that the distortion component of the stimulus must be very small, could be confirmed.[22]

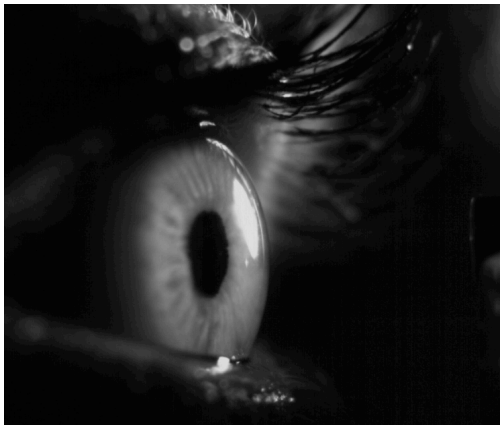

Figure 3.42 and Figure 3.43: The ocular surface during stimulus presentation with use of the NCCA (high speed photography).

3.4 Overall Conclusions

The OST measurements during stimulus presentation showed that with currently available air gas aesthesiometers it was not possible to exclude a change in OST during corneal sensitivity threshold measurement. Yet, for a truly mechanical stimulation, any possible thermal effect would have to be removed from the air gas stimulus. Even with suitable modifications (stimulus temperature synchronisation with air flow intensity and an individual calibration procedure before each corneal sensitivity threshold measurement), it is not clear if the thermal effect of an air gas stimulus can be at all avoided on the ocular surface (due to increased evaporation of the tear film). Unfortunately, no distortion of the corneal reflex could be detected either upon arrival of the strongest air gas stimulus on the ocular surface, with aid of a high-speed camera. This confirmed the hypothesis that the distortion component of the air gas stimulus must be very small.

The following chapters will therefore involve air gas aesthesiometry with a cooling stimulus to determine the relationship with tear film quality, blinking behaviour and the degree of iris pigmentation. In addition, the activity of superficial temperature sensitive corneal nerves will be investigated following cooling and heating of the ocular surface.

CHAPTER 4

An investigation of the relationship between corneal sensation, blinking, ocular surface temperature and tear film characteristics

4.1 Introduction

The blinking mechanism protects the ocular surface against any external, unwanted stimuli and allows the even spreading of the tears contained in the menisci over the surface of the eye. For a blink to occur, the antagonistic muscles of the levator palpebrae superioris and the orbicularis oculi alternately contract.[215] A normal, spontaneous eye-blink rate (SEBR) is considered to be 10-16 blinks per minute.[227] There are three types of blinks: spontaneous endogenous, reflex (both involuntary) and voluntary.[27] Reflex and spontaneous blinks represent a response to different trigeminal, visual and acoustic stimuli, whereas spontaneous blinks occur unconsciously, without any evident stimulus.[27]

Blinking plays an important role in the maintenance of the integrity of the precorneal tear film, by contributing to the maintenance of the ocular surface humidity, the drainage of tears, the secretion of lipids from meibomian glands, and the spreading of the tear lipids across the pre-corneal tear film.[243-247]

It has been hypothesised that corneal sensitivity must play an important role in triggering involuntary blinks, because it has been shown that the blink rate reduces when corneal sensation is blocked with a local anaesthetic.[10,23,24] The afferent pathway of the involuntary blink reflex runs along small unmyelinated and myelinated fibres in the long ciliary branch of the ophthalmic division of the trigeminal nerve to the pons into the medulla oblongata along the spinal trigeminal tract in the lateral medullary region and they terminate on cells of the ipsilateral spinal nucleus of the trigeminal nerve.[215] The efferent pathway is conveyed by the facial nerve.[215] The exact pathway leading from the supraorbital branch of the sensory trigeminal nerve to the ipsilateral facial nucleus in the pons is still unknown.[216] Since the reflexes arising from the cornea run through the medulla oblongata before connecting with the ipsilateral and

contralateral facial nucleus, it has been postulated that the corneal reflex and the blink reflex use similar trigeminofacial connections.[216] It has been proposed that involuntary spontaneous blinking is determined by a local corneal reflex that is dependent on corneal sensitivity, possibly triggered by ocular surface cooling when the tear film progressively evaporates.[25,217]

Yap was able to show that the blink rate increased when tear break-up time reduced.[267] Mori et al[260] suggested that evaporation-mediated cooling, which occurs during the process of tear break-up, may be detected by thermo-sensitive corneal nerves and thereby provide the signal for a blink to reform the tear film. Several studies have been unable to establish a clear relationship between blink rate, tear break-up time and corneal sensation: Doughty et al.[272] measured invasive tear break-up time with the use of fluorescein and recorded corneal sensitivity with use of the Cochet-Bonnet aesthesiometer and could not find any correlation between central corneal tactile threshold and SEBR. Unfortunately, the Cochet-Bonnet aesthesiometer measures only mechanical corneal sensitivity, as it applies a tactile stimulus to the cornea using a nylon thread. It is not, therefore, the instrument of choice for the measurement of the excitability of thermo-sensitive C fibres in the cornea. Ntola used the NCCA air gas aesthesiometer that uses a fine jet of cooling air as a stimulus, and which is designed to measure the activity of corneal C fibres, on 20 subjects.[14,271] She also measured invasive tear break-up time, applying a controlled amount and concentration of fluorescein, but limited the study by excluding subjects with a tear break-up time of less than 8 seconds.

The following study will try to overcome the shortfalls of previous studies by employing the following measures:

- Measurement of non-invasive tear break-up time (NIBUT) and evaluation of the tear lipid pattern with use of the Tearscope Plus (Keeler Ltd., Windsor, UK).
- Measurement of habitual spontaneous eye-blink rate (SEBR) / IBI, i.e. by using a more suitable task, the effect that subject gaze position and psychological state may have on blink frequency should be avoiding, or at least reduced.

- Corneal sensitivity measurement with the NCCA air gas aesthesiometer.
- No minimum NIBUT will be determined as a criterion for participation in this study.

4.1.1 Aim

The overall aim of the study was to explore the relationship between spontaneous eye-blink rate (SEBR) / inter-blink intervals (IBI), tear film quality (non-invasive tear break-up time, NIBUT, tear film lipid pattern and tear meniscus height, TMH), ocular surface temperature (OST) and central corneal sensitivity (CS) under normal conditions, in order to answer the question 'What role do corneal sensitivity and tear film quality play in triggering a blink?'

4.2 Methods

This was a prospective clinical cohort study. Forty-two volunteers were recruited from the staff and patient pool of the Optometry Department, University of Applied Science in Olten (CH). They were invited either by email or by personal invitation in the clinic. All subjects invited to take part in the study were given a subject information sheet explaining the study prior to giving signed consent. The age range was limited to between 20 and 39 years, as corneal sensitivity,[301,364,365] ocular surface temperature (OST),[366-368] and tear film stability[215,365] have been found to decrease with age. Exclusion criteria for participation in this study were: history of previous ocular surgery including refractive surgery, eyelid tattooing, eyelid surgery or corneal surgery; previous ocular trauma; Sjögren's Syndrome (absence of dry mouth), rheumatoid arthritis, diabetes or ocular infections; current or previous condition known to affect the ocular surface and/or tear film; a score ≥ 15.0 on the Ocular Surface Disease Index (OSDI) questionnaire;[369] medication or use of eye drops known to affect the ocular surface and/or tear film; pregnancy (on self-report); contact lens (CL) wear one day prior or on the day of this study.

Ethical approval was obtained from the School of Optometry and Vision Sciences Human Research Ethics Committee and the study followed the tenets of the Declaration of Helsinki (project number 1344, Appendix section no. 8.2.1).

Subjects were asked to attend the laboratory once. All measurements were made on the right eye only and not before 12:00pm (at least 4 hours after awakening; between 12:00 and 6:30pm) to avoid any possible diurnal bias in corneal sensitivity[215,305,306] or tear film stability.[215,370,371] Humidity levels and room temperature were controlled within tolerable limits, as it has been shown to influence OST,[243-247,372-374] showing a typical increase of 0.15 to 0.2°C per degree increase in room temperature.[10,11,23,24,285]

All subjects filled in the German translation of the OSDI questionnaire[375] and the following measurements were carried out: iris pigmentation grading, measurement of CS, OST, NIBUT, and tear film lipid pattern grading.

4.2.1 Procedures

4.2.1.1 Spontaneous eye-blink rate (SEBR)/Inter-blink interval (IBI)

The blinking pattern of the subjects was recorded using a digital video camera (Sony DCR-TRV27E Digital Handycam, Sony). The subject was asked to view a short German documentary (‘Brillen für Afrika’ from ‘Sachgeschichten’ from the broadcast ‘Sendung mit der Maus’ in 2012), lasting 7:55 minutes during the recording, which was presented on a computer screen (Mac Book Pro, 13 inch with retina display, Apple Computer Inc, Cupertino, CA, USA) at a distance of 2m for a natural viewing situation. The theme of the film was chosen to have a ‘neutral’ theme in order not to generate any emotions capable of affecting the subject’s blink rate frequency. For the same reason, a prolonged distance of 2m was chosen, as the short working distance of a computer workstation has been shown to negatively affect blink rate.[376] Those subjects with a refractive error wore their spectacles for distance vision. For ethical requirements, the subjects were informed of the video recording prior to commencement of the study and they signed a separate consent form for this purpose. Since the blink rate may have been affected by an awareness of being filmed (the psychological status may affect blink rate),[27] only the last five minutes of filming were considered for analysis. This duration of five minutes is considered to be an ideal duration for blink behaviour analysis.[227] The digital recording of each subject’s blink frequency was then downloaded to a computer

(Mac Book Pro, 3 GHz Intel Core i7 Processor, Apple Computer Inc, Cupertino, CA, USA) and analysed with the VLC software programme. Blink frequency was analysed in two ways: 1) Spontaneous eye-blink rate (SEBR) – the average number of blinks per minute; and, 2) Inter-blink interval (IBI) – the average time between blinks.

4.2.1.2 Ocular Surface Disease questionnaire (OSDI)

The OSDI questionnaire was developed in 1997 by the Outcomes Research Group (Allergan Inc., Irvine, CA) to grade the severity of dry eye disease (DES).[377] It is currently widely used worldwide and consists of a 12-item scale that assesses symptoms, functional limitations, and environmental factors related to dry eye. The following official score was used for the assessment of dry eye symptoms: OSDI = (sum of scores) x 25 / (number of questions answered). It has undergone psychometric testing and has been accepted by the U.S. Food and Drug Administration (FDA) for use in clinical trials.[378] Furthermore, it has been shown to acceptably fit to a Rasch measurement model, demonstrating that the OSDI is a useful instrument for discriminating between people with varying levels of ocular surface disease.[378,379] For this study, the OSDI questionnaire was applied, in order to fulfil the inclusion criterion that only subjects without DES would be able to participate, showing a OSDI score of < 15.0.

4.2.1.3 Grading of the degree of iris pigmentation

The degree of iris pigmentation of each subject was noted according to Seddon et al.:[380] They graded iris colour according to a set of photographs (named standards A-D) as follows: *grade 1* for a blue or gray iris with brown or yellow specks equal to or less than standard A, *grade 2* for a blue, gray, or green iris with brown or yellow specks equal or less than standard B but greater than standard A, *grade 3* for a green or light brown iris with brown or yellow specks equal or less than standard C, but greater than standard B, *grade 4* for a brown iris with colour equal to or less standard D, but greater than standard C and *grade 5* for a brown iris darker than standard D. They published coloured photographs together with the descriptions of the gradings and found a high inter-observer and intra-observer reliability. Currently, there is no agreement on

whether there is a correlation between iris colour and ocular surface sensitivity: Millodot used the Cochet-Bonnet aesthesiometer and found blue eyes to be considerably more sensitive as brown eyes.[308] Acosta et al. measured similar mechanical thresholds for brown and green eyes (using the Belmonte aesthesiometer), but found lower threshold values for blue eyes.[83] However, they examined a smaller sample group of blue and green eyes than that of brown eyes. Henderson et al. could not find any relationship between iris colour and tactile corneal sensitivity using the Cochet Bonnet aesthesiometer, but they did observe that the pales irises were more sensitive when using air gas aesthesiometry.[381] Lawrenson and Ruskell could not observe any difference in limbal touch sensitivity between differently coloured irises.[81] There is no conclusive explanation as to why there should be a correlation between ocular surface sensitivity, but it has been postulated that melanin in the iris might correlate directly with the amount of neuro-melanin in areas of the central nervous system.[382]

4.2.1.4 Central corneal sensitivity threshold (CCST)

Central corneal sensitivity (CS) was assessed at the central area of the cornea using the Non-Contact Corneal Aesthesiometer (NCCA). This instrument has been described previously (Chapter 1.17) and has been used to assess the effect of other external factors on corneal sensitivity.[14,328,332] It stimulates the sensory corneal nerves using a controlled pulse of air, aimed at the cornea, which produces a localised area of cooling on the anterior corneal surface.[22] The nerves respond to this stimulus, and if the temperature change produced is above threshold, the subject experiences a sensation of cooling. Using this instrument, the central corneal sensation threshold was measured using a forced-choice, double-staircase technique.[14] Alignment with the cornea is made using a customised slit-lamp attachment that allows accurate positioning of the air-jet at 1 cm away from the central corneal surface. Stimulus duration was set at 1s and the time interval between each stimulus presentation was 15s.[14,360] In order to ensure a complete and stable tear film over the cornea, the subjects were asked to make a full, but unforced blink, following which (within 1-2s) the stimulus was presented.[362]

4.2.1.5 Ocular surface temperature (OST)

Real-time measurements of OST were carried out on all subjects, each measurement lasting for the duration of five consecutive natural blinks, using a self-calibrating (with use of the emissivity factor of 0.95 for the cornea) thermal infrared camera (FLIR A310; thermal resolution 0.08°C, temporal resolution 30Hz; spatial resolution 320x240 pixel). This camera was placed directly in front of the subject's right eye, at a distance of 25cm and OST was noted in the very centre (at the same location where the CS threshold is being measured) and in the inferior part (2mm inside the limbus) of cornea. Gray-scale thermal images were analysed using a purpose-designed computer programme (ThermaCAM Researcher Pro Version 2.9, FLIR Systems, 2006). The corneal area targeted was marked within a small, circular area (as described by the area 'AR01' in section 3.2.1.3) and analysed. A mean value for OST was recorded two seconds after each of the five consecutive natural blinks, and again just before the next blink occurred. This allowed a calculation of the mean OST difference occurring between each blink.

4.2.1.6 Non-invasive break-up time (NIBUT) and tear lipid pattern

NIBUT and the tear lipid pattern were recorded using the Tearscope Plus (Keeler Ltd., Windsor, UK), which is equipped with a diffuse, cold, light-source. For NIBUT measurement, this instrument employs a grid that is projected onto the cornea, and measurements are made by observing the regularity of the image of the fine grid reflected from the tear film surface, which acts as a mirror. The image is observed until a break or distortion in the grid pattern is noted.[383] This time interval can be recorded with an integrated timer. This method of tear film break-up time measurement has been shown to be superior to the traditional invasive measurement with the use of fluorescein, which disturbs the tear film by reducing surface tension and increasing the rate of evaporation.[384,385] To improve image resolution, the fine grid was used. Subjects were instructed to blink spontaneously, as they would normally, and then to refrain from blinking after a spontaneous blink, and the grid pattern projected onto the cornea was then observed. Several forced blinks immediately before taking the measurement were avoided, as this may artificially increase the lipid layer thickness of the tear

film.[246] NIBUT was recorded as the time from the blink until the first distortion in the grid pattern, or the patient expresses a need to blink. Three consecutive measurements were taken and a median value was calculated. In addition, the tear meniscus height was measured by using the Tearscope illumination and an eyepiece graticule on the slit lamp. The tear lipid pattern was evaluated according to the classification of Guillon. (Table 4.1)[383]

Grade	Description of the lipid layer pattern
Grade 1	Open meshwork: very thin, minimal lipid layer
Grade 2	Closed meshwork: more lipid than open meshwork
Grade 3	Wave pattern: grey streak effect
Grade 4	Amorphous: thick, white even and well mixed lipid layer, showing occasional colours during the blink
Grade 5	Normal colour fringes: thicker lipid layer with a mix of brown and blue colour fringes well spread over the surface
Grade 6	Abnormal colour fringes: thicker layer with a mix of red and green colour fringes
Grade 7	Globular appearance

Table 4.1: Classification of the tear lipid pattern according to Guillon (1998).[383]

The lipid pattern was observed during two to three spontaneous blinks, each time after tear film movement, following a spontaneous blink. No grid was employed for this evaluation.

4.2.1.7 Order of procedures

1. Patient arrives in the testing room, and is asked to wait for 15 minutes to adjust to the room (this is especially important if they have just arrived inside from being outside in a hotter or colder environment).
2. Subject reads study information and signs consent forms (for participation in the study and video filming).
3. Measurement of spontaneous eye blink rate (SEBR) / IBI with video filming: the subject watches a documentary film of 7:55 minutes
4. The degree of iris pigmentation of each subject is graded and recorded.

5. One measurement of the corneal sensitivity threshold of the right eye of each subject.
6. Subject fills in the OSDI questionnaire, which takes approximately five minutes. The examiner was present in the room, in order to assist, if questions arose.
7. Real-time measurements of ocular surface temperature (OST), lasting for the duration of five consecutive natural blinks.
8. Three consecutive measurements of non-invasive tear break-up time (NIBUT); measurement of tear meniscus height (TMH); and at the same time, assessment of the lipid layer pattern without the grid, directly after each of three consecutive blinks.
9. Slit lamp examination with use of fluorescein.

Measurement
Adjustment period to room temperature (15min)
Consent forms
Blink rate (SEBR / IBI) measurement during video
Grading of iris colour
CS measurement
OSDI questionnaire
OST measurement
NIBUT / lipid layer assessment
TMH measurement
Slit lamp examination (with fluorescein)

Table 4.2: Chronological order of procedures carried out during the study.

4.2.2 Statistical analysis

The data were not found to be normally distributed (Shapiro Wilk Test, SPSS Version 20), hence the non-parametric Spearman's test was applied to test the correlations between the relevant parameters (SPSS Version 20). It was decided to not apply a Bonferroni correction, as this is not advisable in circumstances in which the variable under study are heavily inter-dependent.[386]

In addition, a backward-step, robust linear regression model was applied (R-statistics, Version 3.1.0), because the assumptions of collinearity and homoscedasticity were violated with the parametric linear regression model. IBI was chosen to be the dependent variable.

4.3 Results

Forty-two subjects participated, of which 11 were male. Average age was 27.76±5.36 years. The average ambient temperature in the testing room was 24.7±0.8°C and average ambient humidity was measured to be 41.6±4.5%.

	OSDI	Iris colour	CST (mbars)	NIBUT (secs)	Blinks per min	IBI (secs)	Lipid pattern	Tear film stability	TMH (mm)
Median / IR	8.30 / 4.20-14.60	1.00 / 1.00-3.25	0.35 / 0.30-0.40	34.55 / 12.45-53.80	11.00 / 6.95-17.05	4.57 / 3.03-7.04	3.0 / 2.75-4.25	2.00 / 1.0-3.0	0.23 / 0.20-0.30
Mean±SD	8.86±4.92	2.10±1.43	0.35±0.98	38.58±28.62	12.83±7.64	5.44±3.18	3.29±1.44	2.24±1.05	0.23±0.75

Table 4.3: Median / Interquartile Range (IR) and Mean (±Standard Deviation) of the following measurements: OSDI (ocular surface disease index), iris colour, corneal sensitivity threshold (CST), non-invasive tear break-up (NIBUT), blinks per min., inter blink interval (IBI), lipid pattern, tear film stability and tear meniscus height (TMH).

	Min OST central cornea (°C)	OST difference central cornea (°C)	Min. OST inferior cornea (°C)	OST difference inferior cornea (°C)
Median / IR	35.15 / 34.58-35.50	0.15 / 0.10-0.20	35.30 / 34.78-35.60	0.20 / 0.10-0.20
Mean± SD	34.98±0.68	0.15±0.09	35.11±0.74	0.16±0.09

Table 4.4: Median / Interquartile Range (IR) and Mean (±Standard Deviation) of min. ocular surface temperature (OST) central cornea, OST central cornea difference between blinks, min. OST inferior cornea and OST inferior cornea difference between blinks.

4.3.1 Corneal sensitivity threshold (CST)

The median / IR of CST obtained in this study on normal subjects was 0.35 / 0.30-0.40 mbars.

4.3.2 Blink frequency (SEBR and IBI)

Blink frequency was analysed in two ways: spontaneous eye-blink rate (SEBR) represents the average number of blinks per minute and the inter-blink interval (IBI) states the average time between blinks. Consequently, a subject with a high blink-rate will have a low inter-blink interval. Blink frequency for this study was analysed in both formats. Incomplete vs. complete blinks could not be differentiated with the video recording applied in this study.

The median / interquartile range (IR) for the SEBR was 11/ 6.95-17.05 blinks/min, and for the IBI was 4.57/ 3.03-7.04 secs. While the SEBR may appear a more intuitive measure, it is affected by the time taken to collect the data. For this study, the SEBR was measured over five minutes, which effectively reduces the number of measurements, for calculating the average SEBR, to five. In contrast, the IBI measurement has an average of 13 measurements per minute, or 65 minutes in total (for the full 5 minute measurement time). This sampling error difference was demonstrated in the size of the IR, where the SEBR IR was 6.95-17.05 blinks/min and the IBI interquartile range was 3.03-7.04 secs.

The mean spontaneous eye blink rate (SEBR) of 12.83±7.64 found in this study was very similar to the average SEBR of 14.5±3.3 as reported by Doughty in his review paper.[227]

4.3.3 Tear film quality (NIBUT, TMH and lipid pattern evaluation)

The median / IR for NIBUT obtained in this study on normal subjects was 34.55 / 12.45-53.80 seconds, and was hence found to be higher than in some other published clinical studies.[387-389] This may be explained by the inclusion criterion of a low OSDI value of <15 for participation in this study and the young age group, with a mean of

27.76±5.36 years. In an age group <45 years, Maissa and Guillon obtained a mean NIBUT of 20±13.9s;[389] 39% of the participants in this group study had NIBUT values of >20s. The prevalence of different lipid patterns observed in the current study compared fairly well with those estimated in the Tearscope Plus manual[390] (Table 4.5).

Lipid pattern observed	Mean NIBUT ± standard deviation (seconds)	Distribution in current study (%)	Distribution published by the Tearscope Plus manual (%)[390]
open meshwork	11.50±6.82	16.7	15
closed meshwork	11.37±2.91	7.1	14
wave / flow	32.37±14.69	35.7	29
amorphous	72.09±29.63	16.7	19
normal colour	56.01±30.85	21.4	17
abnormal colour	33.8±8.34	4.8	not stated
globular	-	-	6

Table 4.5: NIBUT measurements for different lipid patterns and distribution compared to the Tearscope Plus manual.

Tear film stability has been shown to be most stable with the flow, amorphous and normal colour lipid patterns, whereas open meshwork and the abnormal colour fringes have the poorest quality: a four-fold increase in tear evaporation could be shown when the lipid layer was absent or when abnormally coloured fringes were observed.[387] According to Guillon, the amorphous lipid layer indicates a stable lipid layer, whereas open and closed meshwork, flow and normal colours describe an average lipid layer, and the globular and abnormal colour fringes describe an unstable tear film.[383] The reduced tear film stability with a thicker lipid layer may be explained by a reduced aqueous tear volume underlying the lipid layer.[391] In order to better reflect tear film stability, the lipid patterns were divided into the following four grades, with grade 1 representing poor and grade 4 representing the most stable tear film quality, whereby the obtained NIBUT measurements were taken into account:

Grade 1 – open and closed meshwork, abnormal colour fringes, globular appearance

Grade 2 – wave / flow

Grade 3 – normal colours

Grade 4 – amorphous

Isreb et al. observed a positive correlation between lipid layer thickness and tear break-up time (with the use of fluorescein) on 44 eyes with dry eye disease symptoms ($r=0.653$, $p<0.01$),[392] confirming that a thicker lipid layer is desirable and is correlated with an optimal tear film stability and tear film characteristics. This may suggest a better tear film stability, and hence a longer break-up time with a tear film showing normal colour fringes, rather than showing an amorphous lipid pattern. In the current study, however, eyes showing an amorphous lipid pattern exhibited, on average, a longer NIBUT and were therefore graded as having a superior tear film stability (Table 4.5). According to the Tearscope Plus instruction manual, a lipid layer was graded as 'amorphous', when it appeared as 'thick, white, even and well-mixed that may have shown colours during the blink'.[390] In other words, there may have already been some colours present during the blink that were not visible after the blink. In the current study, this type of lipid layer was found to be more stable (i.e. showing a longer NIBUT rate) than a tear film with a further increase in lipid layer thickness, which continued to exhibit a normal colour pattern after the blink. This finding was in accordance with the results published by Craig et al.[393]

4.3.4 Dry eye symptoms (OSDI)

The median / IR score for the OSDI questionnaire obtained in this study was 8.30 / 4.20-14.60, which represents a normal range for a normal population.

4.3.5 Ocular surface temperature (minimum central and inferior OST and OST difference between blinks)

The median / IR of minimum central OST between blinks obtained in this study was 35.15°C / 34.58-35.50, and its mean value was found to be 34.98±0.68°C. These results are within a normal range for OST of 32.9-36°C,[285] and showed very little variability between the healthy participants at an average ambient temperature of 24.7±0.8°C in the

testing room. On average, the central OST decreased by 0.15±0.09°C between each blink. The minimum inferior OST was found to be slightly higher with a median /IR of 35.30°C / 34.78-35.60 and a mean of 35.11±0.74°C. The inferior OST difference between blinks was slightly higher than in the central part of cornea, with a median of 0.20°C / 0.10-0.20 and a mean of 0.16±0.09°C.

4.3.6 Degree of iris pigmentation

The median / IR of grading the degree of iris pigmentation was found to be 1.0 / 1.00-3.25 and the mean grade was 2.10±1.43 in this study, which shows a tendency to less strongly pigmented irides in the Caucasian participants: Twenty-four subjects had grade 1 (blue or grey iris with brown or yellow specks equal to or less than standard A) with a median CS threshold of 0.325, three had grade 2 with a median CS threshold of 0.350 (blue, grey, or green iris with brown or yellow specks equal to or less than standard B), five were found to have grade 3 with a median CS threshold of 0.350 (a green or light brown iris with brown or yellow specks equal to or less than standard C but greater than standard B), seven had grade 4 with a median CS threshold of 0.350 (brown iris with the colour equal to or less than standard D), and only three subjects were graded with 5 with a median CS threshold of 0.250 (brown iris darker than standard D; Figure 4.1).

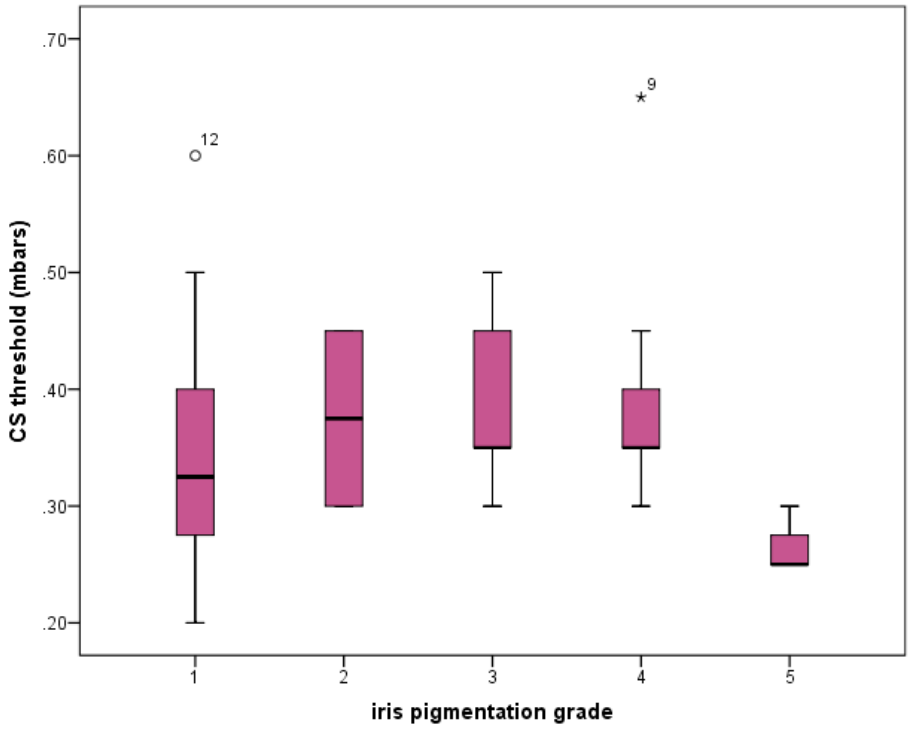

Figure 4.1: Boxplots of corneal sensitivitiy thresholds (mbars) for each iris grade.

4.3.7 Correlations between corneal sensitivity, iris colour, dry eye symptoms, blink rate / inter-blink interval, ocular surface temperature, non-invasive tear break-up time / lipid pattern and tear meniscus height

The correlations between CST, OSDI score, blink rate / IBI, OST and tear film characteristics are summarised in Table 4.6, and presented in scatterplots (Figures 4.2-4.9).

Moderate but statistically significant correlations between CST and NIBUT ($r=0.535$; $p<0.001$), between CST and blink rate / IBI ($r=-0.398$; $p<0.001$ / $r=0.360$; $p=0.010$), between lipid pattern and OST ($r=0.556$; $p<0.001$) and between CST and OST ($r=0.371$; $p=0.008$) were observed. More significant correlations were noted between NIBUT and blink rate / IBI ($r=-0.696$, $p<0.001$; Figure 3 / $r=0.672$; $p<0.001$), between OST and NIBUT ($r=0.639$; $p<0.001$, between tear film stability and NIBUT ($r=0.744$; $p<0.001$), and between tear film stability and blink rate ($r=-0.571$; $p<0.001$).

No correlation could be found between iris colour and any of the variables examined in this study.

	CST	OSDI	Iris pigmen-tation	NIBUT	SEBR	IBI	Lipid pattern	Tear film stability	TMH	Min. OST central cornea	OST difference central cornea	Min. OST inferior cornea	OST difference inferior cornea
CST	--												
OSDI	-0.306 (p=0.024)	--											
Iris pigmentation	0.074 (p=0.320)	0.208 (p=0.093)	--										
NIBUT	0.535 (p<0.001)	-0.194 (p=0.110)	0.145 (p=0.180)	--									
SEBR	-0.398 (p=0.005)	0.122 (p=0.220)	-0.159 (p=0.157)	-0.696 (p<0.001)	--								
IBI	0.360 (p=0.010)	-0.112 (p=0.239)	0.118 (p=0.228)	0.672 (p<0.001)	-0.964 (p<0.001)	--							
Lipid pattern	0.325 (p=0.018)	-0.049 (p=0.380)	-0.153 (p=0.166)	0.675 (p<0.001)	-0.561 (p<0.001)	0.532 (p<0.001)	--						
Tear film stability	0.534 (p<0.001)	-0.291 (p=0.031)	0.063 (p=0.346)	0.744 (p<0.001)	-0.571 (p<0.001)	0.519 (p<0.001)	0.697 (p<0.001)	--					
TMH	0.049 (p=0.380)	0.022 (p=0.444)	-0.045 (p=0.389)	0.028 (p=0.429)	-0.163 (p=0.151)	0.125 (p=0.216)	0.354 (p=0.011)	-0.040 (p=0.401)	--				
Min. OST central cornea	0.371 (p=0.008)	-0.039 (p=0.466)	-0.020 (p=0.451)	0.639 (p<0.001)	-0.478 (p=0.001)	0.474 (p=0.001)	0.556 (p<0.001)	0.518 (p<0.001)	0.116 (p=0.232)	--			
OST difference central cornea	0.252 (p=0.053)	-0.238 (p=0.064)	-0.071 (p=0.328)	0.362 (p=0.009)	-0.217 (p=0.084)	0.181 (p=0.126)	0.289 (p=0.032)	0.390 (p=0.005)	0.144 (p=0.182)	0.298 (p=0.028)	--		
Min. OST inferior cornea	0.330 (p=0.017)	0.015 (p=0.406)	0.087 (p=0.289)	0.620 (p<0.001)	-0.545 (p<0.001)	0.552 (p<0.001)	0.500 (p=0.001)	0.488 (p=0.001)	0.069 (p=0.286)	0.937 (p<0.001)	0.249 (p=0.122)	--	
OST difference inferior cornea	0.192 (p=0.112)	-0.039 (p=0.403)	0.175 (p=0.133)	0.392 (p=0.005)	-0.204 (p=0.097)	0.167 (p=0.145)	0.381 (p=0.006)	0.333 (p=0.015)	0.064 (p=0.344)	0.427 (p=0.012)	0.414 (p=0.003)	0.426 (p=0.002)	--

Table 4.6: Correlation coefficients (r) between corneal sensitivity threshold (CST), dry eye symptoms (OSDI), iris pigmentation, non-invasive tear break-up time (NIBUT), Spontaneous Eye Blink-Rate (SEBR) / inter-blink interval (IBI), lipid pattern, tear meniscus height (TMH), minimum ocular surface temperature (OST) in the central cornea, OST difference between blinks in the central cornea, minimum OST in the inferior cornea and OST difference in the inferior cornea (Spearman's test, SPSS Version 20).

4.3.7.1 Scatterplots of the correlations

The scatterplots illustrate a moderate and statistically significant correlation between CST and NIBUT, as well as with IBI (Figures 4.2 and 4.3). A good correlation could be observed between blink frequency and NIBUT (Figures 4.4 and 4.5). In comparison, tear film quality shows a weaker correlation with NIBUT and blink frequency (Figures 4.6-4.8). The scatterplot for iris colour and corneal sensitivity threshold shows a poor correlation between the two parameters (Figure 4.9).

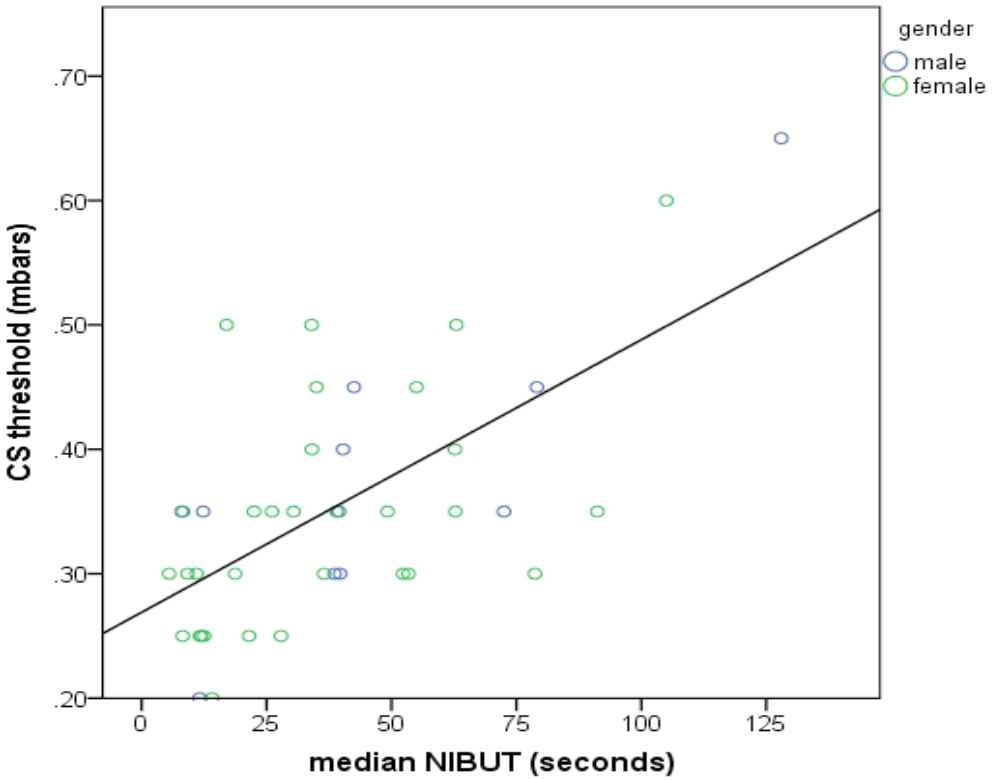

Figure 4.2: Scatterplot for median non-invasive tear break-up time (NIBUT, in seconds) and corneal sensitivity threshold (mbars); r = 0.535, p<0.001.

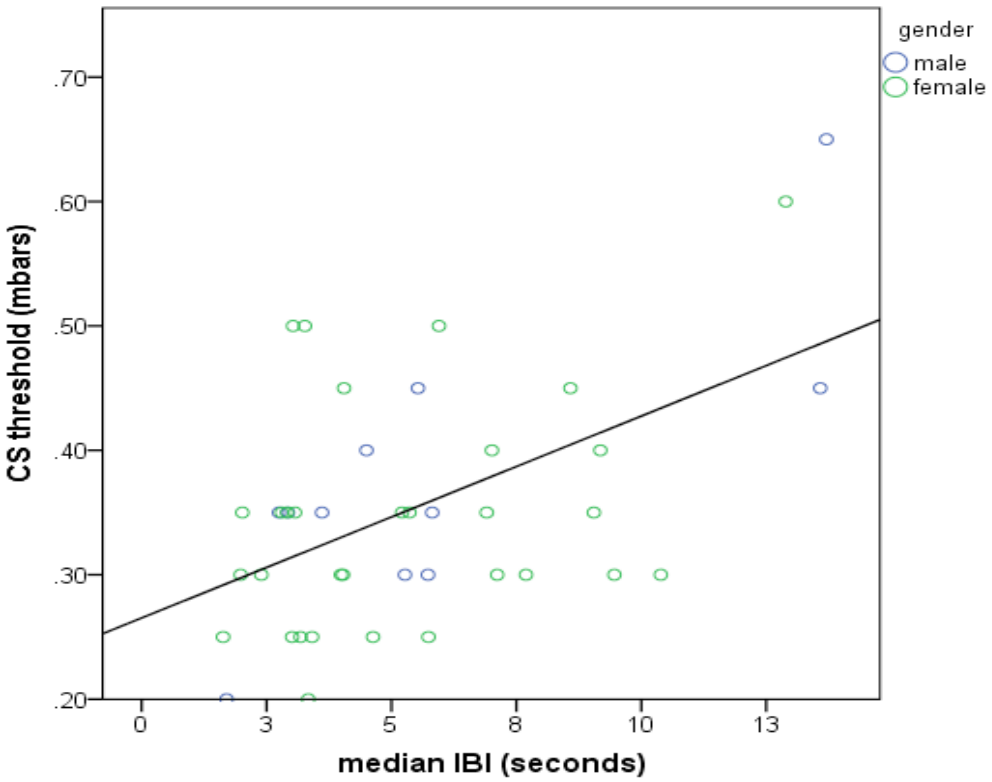

Figure 4.3: Scatterplot for median inter-blink interval (IBI, in seconds) and corneal sensitivity threshold (mbars); r = 0.360, p = 0.010.

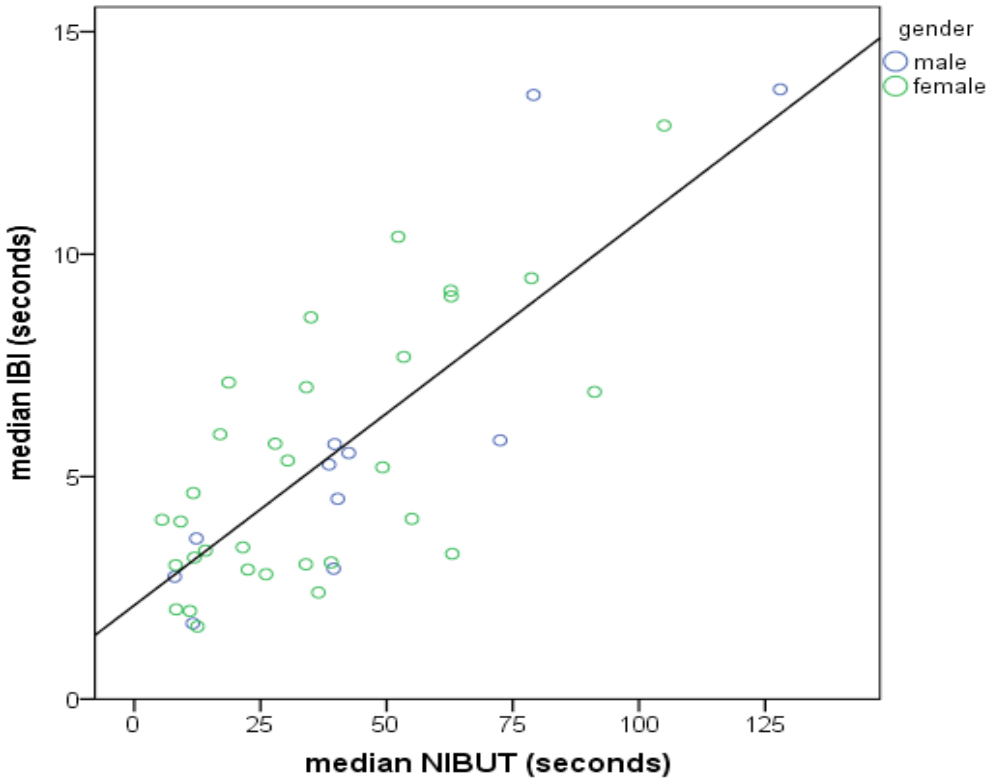

Figure 4.4: Scatterplot for median non-invasive tear break-up time (NIBUT in seconds) and median inter-blink interval (IBI, in seconds); r = 0.672, p < 0.001.

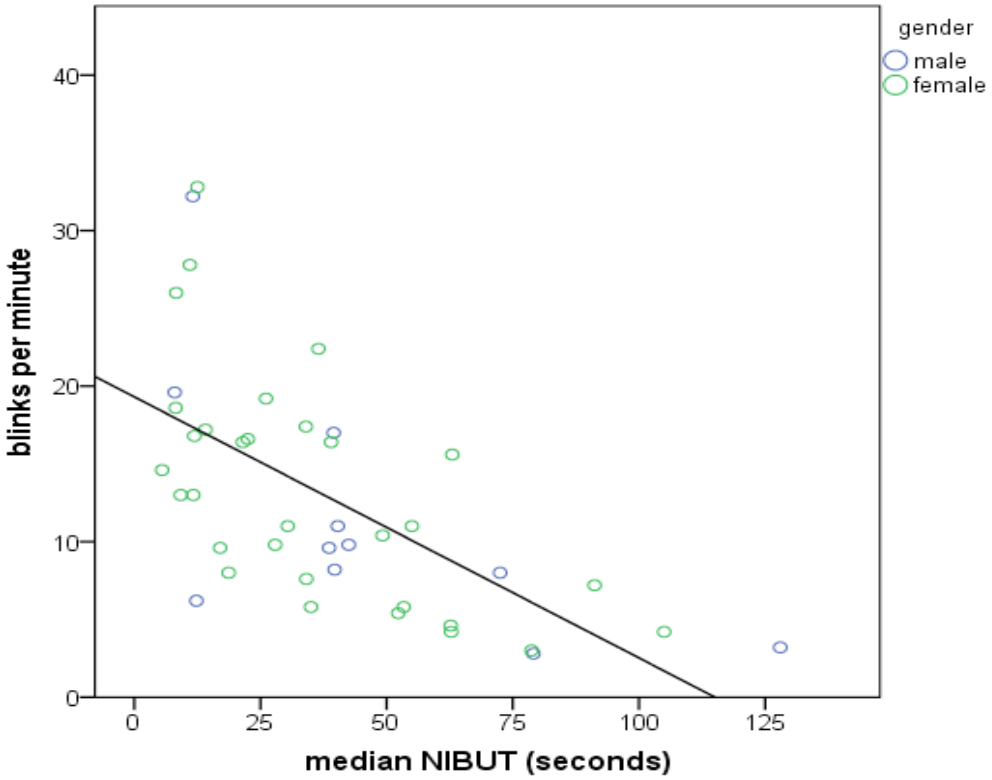

Figure 4.5: Scatterplot for median non-invasive tear break-up time (NIBUT, in seconds) and blinks per minute (SEBR); r = -0.696, p < 0.001.

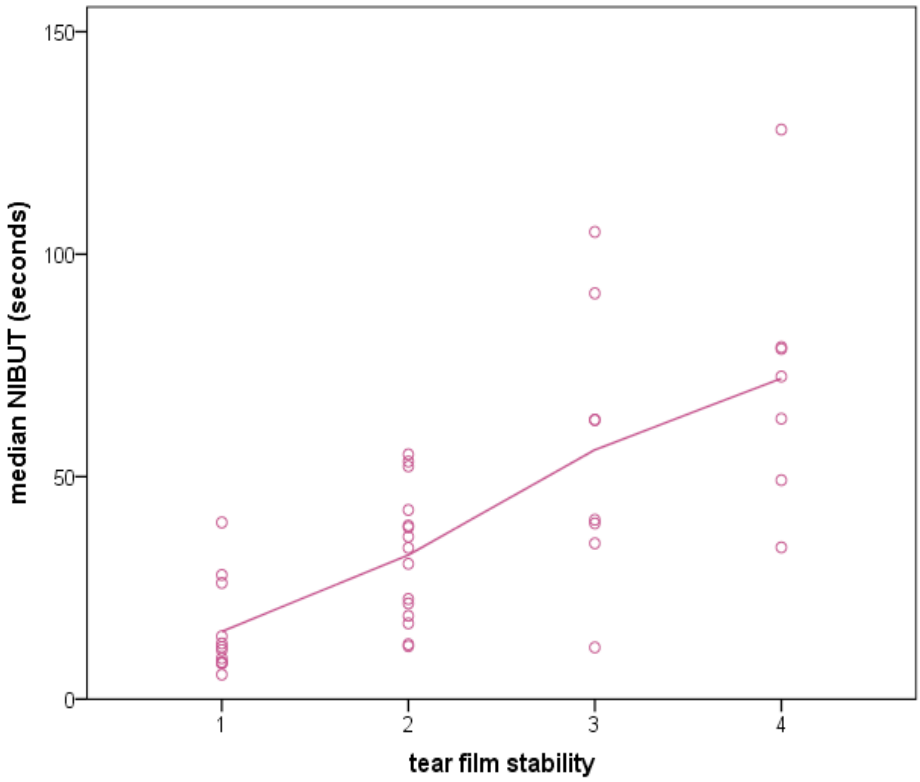

Figure 4.6: Scatterplot for tear film stability and median non-invasive tear break-up time (NIBUT); r = 0.744, p < 0.001

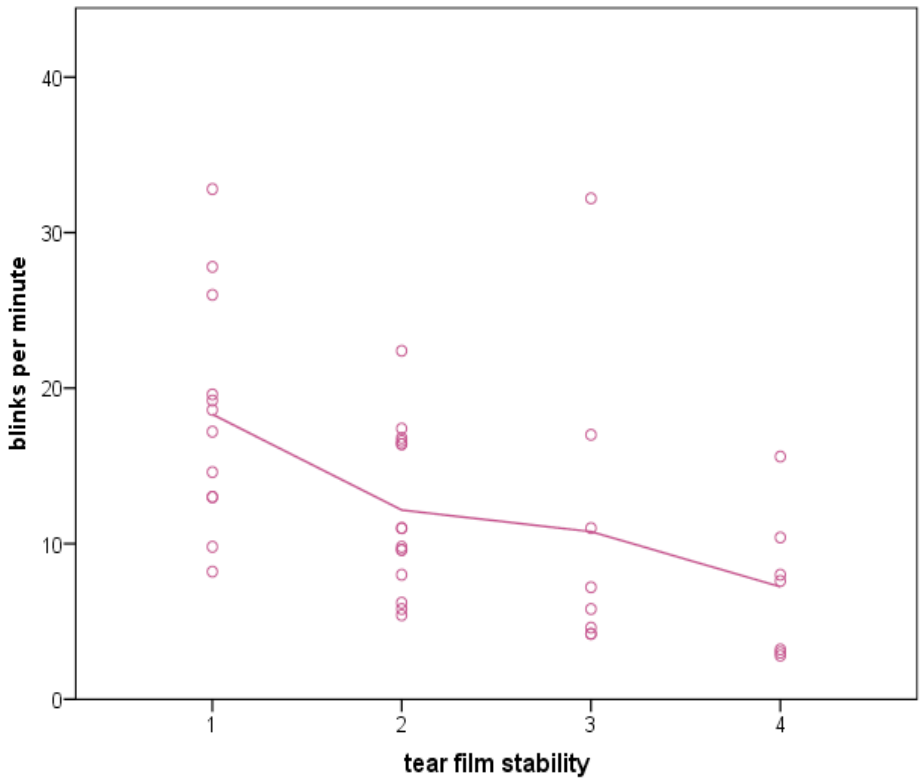

Figure 4.7: Scatterplot for tear film stability and blinks per minute (SEBR); r = -0.571, p < 0.001.

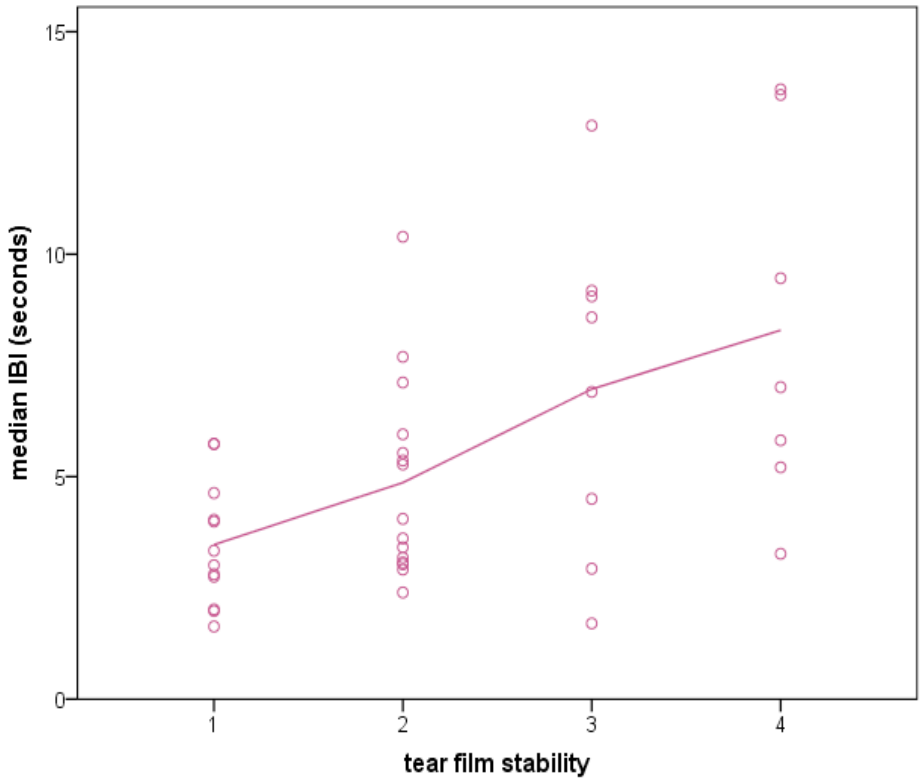

Figure 4.8: Scatterplot for tear film stability and median inter-blink interval (IBI, in seconds); r = 0.519, p <0.001

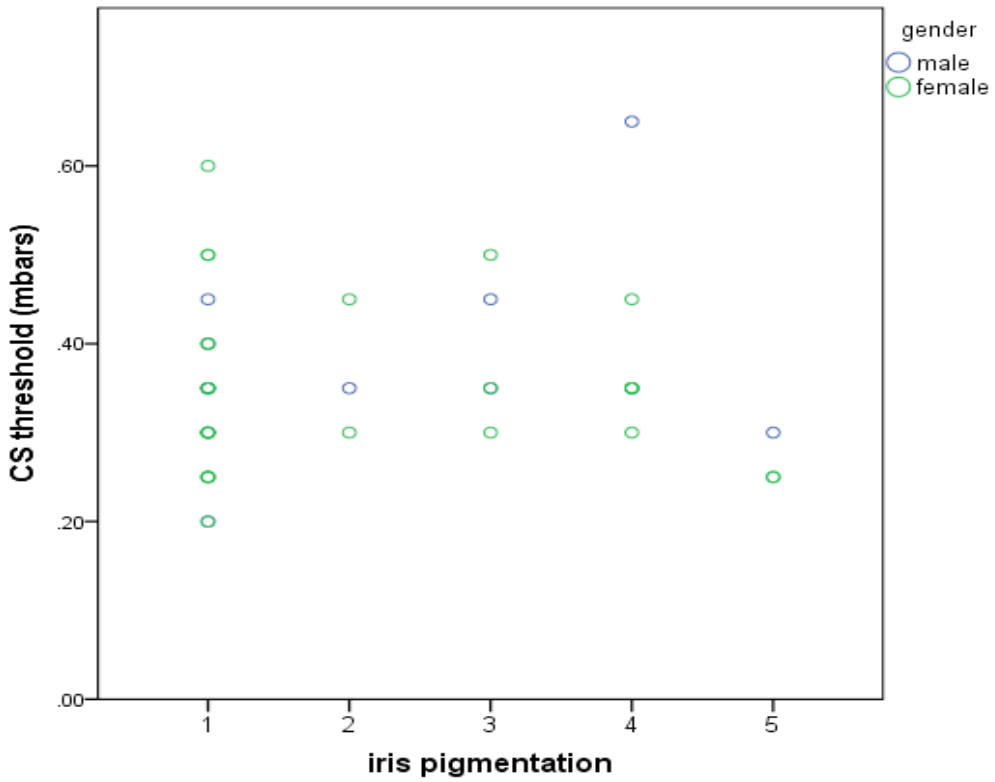

Figure 4.9: Scatterplot for iris colour grade and corneal sensitivity threshold (mbars); r = 0.071, p = 0.320.

4.3.7.2 Robust linear regression model

A robust linear regression model for non-parametric data was applied (R-statistics, Version 3.1.0), whereby IBI was chosen to be the dependent variable and NIBUT, lipid pattern, tear film stability (NIBUT), CS, minimum central OST and minimum inferior OST as predictor variables. The back-step model was applied and not found to be sufficiently significant for the variables: lipid pattern, tear film stability and CS. Consequently, the final model was carried out only for NIBUT, minimum central OST and minimum inferior OST as predictor variables. It was found to be significant ($p<0.001$) and explained 65.0% of the variance ($R^2=0.650$, adjusted $R^2=0.6224$).

The model was described as the following:

Dependent Variable = Intercept + A *(IV_1) + B*(IV_2) + C*(IV_3) ; IV=independent variable.

IBI = -1.56358+ 0.07705*NIBUT – 3.72759*min. central OST + 3.82674*min. inferior OST

The beta coefficient for NIBUT was t=7.275 ($p<0.01$), for min. central OST it was t=-1.906 (p=0.0643) and for min. inferior OST it was t=1.987 (p=0.0542).

4.3.7.3 Post-hoc power calculation

A post-hoc power calculation was carried out for the correlations between the parameters CST, NIBUT, SEBR, IBI, tearfilm stability and min. OST in the central cornea and the results are summarised in Table 4.7 (G*Power 3.1): the powers between these parameters ranged between 0.69 and 1.0.

	CST	NIBUT	SEBR	IBI	Tear film stability	Min. OST central cornea
CST	--					
NIBUT	0.98	--				
SEBR	0.77	1.0	--			
IBI	0.69	1.0	1.0	--		
Tear film stability	0.98	1.0	0.99	0.98	--	
Min. OST central cornea	0.70	1.0	0.95	0.95	0.98	--

Table 4.7: Post hoc power calculation (G*Power 3.1).

4.4 Discussion

This study explored the relationship between corneal sensitivity, tear film quality (NIBUT, lipid pattern, TMH and OST), dry eye symptoms (OSDI) and blink frequency (SEBR / IBI) in normal subjects. A non-invasive measurement of tear film break-up was chosen (NIBUT), the habitual SEBR was recorded, and corneal sensitivity was measured with a non-invasive method (NCCA air gas aesthesiometer).

The NIBUT measurements in this study exceeded the median IBI of 4.57 seconds by far – even the lower value of the interquartile range of 12.45 seconds for NIBUT was found to be considerably higher than the higher value of the interquartile range of 7.04 for IBI. It can hence be concluded that NIBUT exceeded IBI for the subjects participating in this study, as it would be required for normal eyes without dry eye disease, as defined by the ocular surface protection index.[394] Median TMH was found to be normal at 0.23mm / 0.20-0.30 (IR), as well as the median value for grading of the lipid pattern of 3.0 / 2.75-4.25 (IR), which corresponds to a wave pattern of appearance and is most commonly found in a normal population. Yokoi et al. could show a good correlation between TMH and the initial velocity of the tear film lipid layer spread after a blink:[395] a shorter spreading time of the tear film after a blink indicates a more stable tear film, and a longer spreading time is characteristic of a aqueous tear-deficient dry eye.

Blink frequency was found to moderately correlate with corneal sensitivity in this study. A better, but still moderate, correlation could be found between blink frequency and OST, an even better, but still moderate, correlation was observed for blink frequency and lipid pattern, and a high, statistically significant correlation was found for blink frequency and NIBUT. This suggests that the thinning of the tear film before break-up contributes to triggering a spontaneous involuntary eye-blink. However, no statistically significant correlation could be found between either blink frequency and TMH, or between iris colour and corneal sensitivity.

4.4.1 Blinking, corneal sensitivity and tear film characteristics

It has been proposed that involuntary spontaneous blinking is partially determined by a local corneal reflex that is dependent on corneal sensitivity, possibly triggered by ocular surface cooling when the tear film progressively evaporates.[25,217] The eye-blink spreads tears over the cornea and the conjunctiva, promoting stability to the tear film. Blinking is hence vital in maintaining optical performance, ocular surface health and tear film drainage.[28,248]

However, blink rate is greatly variable and under cortical control.[27] It is strongly influenced by external factors, psychologic and physiologic influences, and activity-

related factors.[27] SEBR increases during anxiety,[250] visual fatigue,[252,253] sleep deprivation,[254-257] driving,[258] or flying,[259] and tasks that require speech.[233,260,261] It is reduced during reading[261,262] or when concentrating on a text on video display:[9,263-265] the more difficult the task, the greater the resulting blink inhibition will be. Conversation, anger and excitement markedly increase the blink rate. Furthermore, neurological and psychiatric diseases have an influence, as Cruz et al. reviewed:[28] SEBR is recognised as a clinical marker of central dopaminergic activity: a low SEBR could be recorded in conditions with hypodopamine activity (e.g. Parkinson disease, progressive supranuclear palsy and attention deficit/hyperactivity disorder). SEBR was found to be high in conditions with hyperdominergic activity (e.g. Huntington disease, schizophrenia, or focal dystonia and neuro-developmental conditions).

Despite the cortical control, ocular surface conditions have been associated with SEBR: blink rate may be influenced by tear film quality,[23,267] as SEBR was shown to be higher in dry eye patients than that of the normal population,[9,23,249] and which can be influenced by use of artificial tears and protective eyeglasses.[249] Nakamori et al. recorded a blink rate in patients with dry eye disease of 34.1±2.4 per min as supposed to normals with to 20.1±1.6 per min.[23] Also, the maximum time during which a person can keep their eyes open was shown to be decreased among dry eye patients.[23] Ocular surface damage has been shown to increase the blink rate.[268]

Topical anaesthesia has been shown to reduce, but not to abolish SEBR.[10,23,24,269] Situ et al. established a weak to moderate correlation between NIBUT and ocular surface sensation in patients with dry eyes ($r=0.31$ for cornea, $r=0.40$ for conjunctiva; air gas aesthesiometry).[270] No previous study could establish a correlation between corneal sensitivity and blink rate (Table 4.8): Ntola observed a correlation of $r=0.236$ without statistical significance ($p=0.315$), however this was after having excluded subjects with a TBUT <8 seconds.[271] Collins et al. could show that infrequent blinking can result from diminished corneal sensitivity, however they could only establish a moderate correlation without statistical significance ($r=0.56$, $p>0.10$).[10] The SEBR rate was also recorded whilst the subjects were involved in conversation, which may have artificially increased SEBR. Lastly, their sample group comprised of only 9 subjects. Doughty et

al. also investigated the correlation between tactile ocular surface sensitivity (Cochet Bonnet aesthesiometer) and SEBR, whereby they recorded SEBR during 5 mins. in silence, without any visual stimulation for the participating subjects.[272] They could not establish any correlation between central corneal tactile threshold and SEBR, however for the conjunctival tactile threshold, they found an inverse moderate relationship: the lower the conjunctival sensitivity, the higher SEBR was found to be ($r=0.588$, $p<0.001$). These surprising results can be questioned, as the Cochet Bonnet aesthesiometer has been shown to have many limitations, most importantly a truncated stimulus range and imprecise stimulus application.[14] It may therefore not be sensitive enough for subtle sensitivity differences in normal subjects. Furthermore, a SEBR without any visual stimulation at all may not necessarily be natural. Other research also showed a strong relationship between corneal sensation and tear film drying dynamics.[273]

Several investigations found significant negative correlations between TBUT (with use of flourescein) and SEBR:[267,274,275] Yap et al. found a strong and statistically significant correlation of $r=0.69$ ($p<0.01$), when the subjects were filmed with a hidden camera during a period of 5 minutes whilst waiting in the exam room.[267] Al-Abdulmunem also observed a strong correlation in 159 healthy students when they recorded their blink rate by observation in a lecture theatre ($r=0.74$, $p<0.05$).[274] Collins et al. established a moderate correlation between TBUT and blink frequency, however without statistical significance ($r=0.38$, $p>0.10$). Prause and Norn found a weak to moderate correlation between TBUT and blink frequency ($r=0.33$; $p<0.05$) for normals and a stronger, moderate effect for patients with Sjögrens syndrome ($r=0.58$; $p<0.05$).[275] However, they measured SEBR during reading, which may have had an inhibitory effect. Tsubota and Nakamori observed an influence of ocular surface area on blink rate,[276] however these results were disputed by Zaman et al., who could not find any correlation between ocular surface area and spontaneous eyeblink activity in elderly Caucasians.[230] The ocular surface area was unfortunately not measured for the subjects participating in this study.

Acosta et al., as well as Nakamori et al., were able to decrease SEBR during computer work with the use of artificial tears,[23,277] which supports the hypothesis that sensory

input from the corneal and conjunctival sensory fibres modulates the neural circuits involved in spontaneous blinking. They concluded that SEBR at rest may be partially influenced by extrinsic factors, such as ocular surface conditions, whereas a low SEBR induced by the performance of an attentive task may be mainly governed by intrinsic neural mechanisms. The resulting strong inhibition of neural blinking mechanisms during the computer task is stronger than the sensory input from the cornea and conjunctiva. It has been suggested that spontaneous blinking originates in the central nervous system and is modulated by internal factors, such as fine motor controls, speech centres, emotional and psychological states, cognition and attention.[24] Thus, both central and neural control and local ocular sensory input may jointly act to stimulate blinks.

One reason for the less strong correlation between CS and blink frequency than between NIBUT and blink frequency in this study may be that the good feedback loop between NIBUT and the initiation of a blink in healthy eyes hinders the activation of superficial corneal nerves. As discussed above, the median NIBUT of 34.55s obtained for the subjects in this study indicated a very good tear film quality. A more significant correlation between CS and blink frequency would be expected in eyes during the beginning stages of the dry eye disease process, where a sensitisation of the superficial corneal nerves and an increased blink frequency have been reported.[326,396]

Clinical studies investigating the correlation between blink frequency and corneal sensitivity		
Author / year	**Sample size / subject description**	**Correlation between Blink frequency and corneal sensitivity**
Doughty et al. (2009)[272]	60 normal males	No correlation (r=0.082; p≥0.50)
Ntola (2006)[271]	9 normal males; 11 normal females	Weak, statistically not significant (r=0.236; p=0.315)
Collins et al. (1989)[10]	9 normal subjects	Moderate, statistically not significant (r=0.56; p>0.10)

Table 4.8: Summary of previous studies investigating the correlation between blink frequency and corneal sensitivity.

4.4.2 Ocular surface temperature (OST)

Several studies have suggested that the measured temperature on the surface of the cornea is essentially that of the tears,[397-399] and that radiation detected directly from the cornea itself is only possible where the tears are absent. Assuming a tear film thickness of 3μm,[195] the infrared radiation from the cornea is completely absorbed by the tear film. Hence, OST measurement and its correlation with tear film quality gained considerable interest. Each blink spreads warm tears over the ocular surface, after which an immediate heat transfer from the tear film to the environment takes place, leading to a decrease in OST over time after each blink.[400,401] The tear film destabilises after a blink, most probably due to evaporation, leading to a cooling response due to the positive latent heat of vaporisation as the liquid changes into gas and heat is transferred to the atmosphere.[393] In dry eye disease, the rate of evaporation has been shown to increase, due to a poor lipid layer quantity or quality.[402,403] Several studies have shown OST to be increased in eyes with a poor tear film quality immediately after the blink, compared to controls.[25,26,404,405] The resulting larger difference in temperature between the eye and the atmosphere may further accelerate the subsequent cooling rate.[404] As mentioned above and shown in the current study, subjects with a short NIBUT tend to

blink more frequently, which would increase the measured OST immediately after a blink. Purslow et al. showed that eyes with a longer NIBUT tended to be cooler initially and to exhibit smaller temperature changes in between blinks.[405]

In the current study, central OST was measured to be slightly lower than in the inferior cornea (in proximity to the inferior limbus), which may be explained by the fact that the vascularised limbal area has been shown to be warmer than the avascular corneal centre.[397,401] The rate of cooling between blinks was similar for the central and inferior cornea in this study. The minimum central and inferior OST temperatures (immediately before a blink) were highly correlated with NIBUT in this study ($r=0.639$, $p<0.01$ for central OST, and $r=0.620$, $p<0.01$ for inferior OST), suggesting a lower cooling rate with better NIBUT measurements. The correlations between OST and lipid pattern/tear film stability were consequently good as well. Also, higher OST measurements correlated well with longer inter-blink intervals, supporting the hypothesis that evaporation contributes to the initiation of a blink. The direct correlation between OST and CS, however, was not observed to be strong in this study.

4.4.3 Iris colour and corneal sensitivity

Lightly-pigmented eyes tend to be more sensitive to light, as light irises transmit more light than eyes with dark irises.[406] Intuitively, one may be tempted to believe that lighter coloured eyes may possess a denser corneal innervation and may be therefore be more sensitive than darker eyes. Acosta et al. reasoned as follows:[83] because peripheral branching of sensory nerve axons depends on growth factors, such as NGF, and some of the axons of polymodal sensory neurons supplying the cornea also branch into the iris, they speculated that melanocytes of the iris that possess trk receptors for NGF[407] may compete with the sensory nerve fibres for this neurotrophin. This may decrease the number of peripheral nerve terminals, including branches directed to the cornea, in a degree proportional to the iris pigmentation.[408] Indeed, Acosta et al. measured similar mechanical thresholds for brown and green eyes (using the Belmonte aesthesiometer), but lower threshold values for blue eyes.[83] However, they examined a smaller sample group of blue and green eyes than that of brown eyes. Millodot used the Cochet-Bonnet aesthesiometer and found blue eyes to be considerably more sensitive than brown

eyes.[308] However, Lawrenson and Ruskell could not observe any difference in limbal touch sensitivity between differently coloured irises either.[81] In this study, no statistically significant relationship could be observed between the degree of iris pigmentation and corneal sensitivity ($r=0.074$, $p>0.05$), hence a trend towards lower corneal sensitivity (higher CS threshold) for more pigmented irises could not be observed. In fact, the three subjects with the darkest iris grade even had lower sensitivity thresholds than those with lighter pigmented irises. More studies with larger sample groups are required.

4.5 Conclusion

This is the first study to show a moderate and statistically significant correlation between corneal sensitivity and blink frequency. However, the mechanisms involved in the initiation of an eye-blink are complex, as the local ocular sensory input only represents one trigger, next to other external influences and internal factors that are under cortical control. A stronger correlation between NIBUT, blink frequency and OST could be confirmed in this study, emphasising the fact that ocular surface condition represents one important trigger for the initiation of an eye-blink. A relationship between the degree of iris pigmentation and corneal sensitivity could not be established in this study.

CHAPTER 5

An investigation of the relationship between heating and cooling of the ocular surface on the corneal sensitivity threshold

5.1 Introduction

Electrophysiological recordings from the cat and guinea pig cornea have shown that cold thermoreceptors exhibit a spontaneous firing rate of nerve impulses at a normal ocular surface temperature (34-35°C), and that they increase the frequency and amplitude of their impulse activity when temperature decreases.[29,30] Within 1-2 minutes, the receptors adapt to a new baseline with a higher level of impulse frequency, proportional to the new temperature level.[409] The speed and magnitude of temperature reduction at the ocular surface, as well as the final static temperature, are encoded by the firing frequency of these cold thermoreceptors.[30,410] The receptors have been shown to discriminate a temperature difference of 0.1°C or less.[29,30,411] Psychophysical experiments with use of air gas aesthesiometry concluded that a temperature decrease of 1-2°C below the normal basal level of corneal temperature could be differentiated.[32,174] Murphy et al. proposed the smallest temperature change likely to be sensed by the ocular surface to be 0.3°C.[173] However, upon warming of the ocular surface, cold thermoreceptors are silenced.[29,31] A fraction of polymodal fibres have been shown to also increase their firing rate when corneal temperature is reduced to less than 29°C.[32,33] So, reducing the ocular surface temperature will change the resting electrical activity level of cold-sensitive nerves, possibly making them more or less responsive.[412] It can be hypothesised that since reducing ambient corneal temperature to at least 33°C will increase the resting neural activity of the cold receptors,[29,30] and since increasing neural activity is used to show temperature decrease, consequently the remaining range of increase in neural activity might be reduced, resulting in a reduction in sensitivity to subsequent temperature reductions in the cornea. Or it could be hypothesised that while neural activity increases, the adaptation to the new baseline allows the system to 're-set' and sensitivity is preserved. Finally, it can be hypothesised that these two responses may be combined, assuming that there is a finite range of neural activity, in which case the system can re-set only to a limited extent, after which sensitivity is reduced or lost.

What might happen to this neural adaptation and response if the cornea is warmed above the normal surface temperature?

Increasing ambient corneal temperature has been shown to silence the cold receptors[29-31] and to activate polymodal nociceptors at temperatures over 39-40°C. This can either lead to an enhanced neural response of all the previously silenced cold receptors to the cooling air stimulus of the NCCA aesthesiometer, resulting in an increase in sensitivity. Or, there could be a decrease in sensitivity, due to a delay caused by the initial silencing of the activated polymodal nociceptors and / or due to the adaptation to the new baseline ambient corneal temperature. Alternatively, there might be a combined response, analogous to the hypothesis for the nervous activity change after reducing ambient corneal temperature as mentioned above.

Besides the changes in neural activity resulting from temperature change in the cornea, an altered corneal temperature may also have indirect effects on an air-pulse stimulus sensation perception as a result of changes in the tear film. A warmer eye may show an improved lipid layer quality and tear stability, which may decrease the rate of evaporation, and therefore temperature change, during the air stimulus and result in an apparently lower sensitivity in the subject. Alternatively, it is possible that corneal nerve fibres will show increased activity, and therefore sensitivity, when the cooling stimulus reaches the ocular surface, as there will be a greater difference between the stimulus temperature and ocular surface temperature. Another hypothesis is that, at normal corneal temperatures, cold nociceptors exhibit a low on-going activity, which should be silenced when the corneal surface is warmed above a threshold. Subsequent cooling of this warmer corneal surface may therefore lead to a more vigorous response, as the difference in neural activity between a heated corneal surface and a cooling stimulus could be greater than the difference between a corneal surface at resting level and a cooling stimulus, resulting in a higher sensitivity to a cooling stimulus.

The opposite effects on corneal sensitivity may be expected when the ocular surface is cooled: a cooler eye may reduce nerve activity producing an apparent reduction in sensitivity, because there will be less of a difference between the stimulus and the ocular surface temperature. On the other hand, the cooling may lead to a less stable tear

film, increasing the rate of evaporation, thereby encouraging temperature change, and leading to an increased corneal sensitivity measurement.

Finally, all of these ocular surface effects may happen in combination with the underlying neural effects of temperature change.

5.1.2 Aim

The overall aim of this study is to take one first step to explore these hypotheses by investigating the effect of heating and cooling of the ocular surface, combined with the resulting changes in tear film quality, on ocular surface sensation. In particular, the course of recovery, after the heating / cooling procedure, for the ocular surface temperature (OST) and any potential corneal sensitivity threshold (CST) change will be observed.

5.2 Methods

This was a prospective, clinical cohort study. The same 42 volunteers as in the previous study (Chapter 4) were recruited from the staff and patient pool of the Optometry Department, University of Applied Science in Olten (CH). They were invited either by email or by personal invitation in the clinic. All subjects invited to take part in the study were given a subject information sheet, explaining the study, prior to giving signed consent. The age range was limited to between 20 and 39 years, as corneal sensitivity (CS),[301,364,365] OST,[366-368] and tear film stability[365] have been found to decrease with age. Exclusion criteria for participation in this study were: history of previous ocular surgery including refractive surgery, eyelid tattooing, eyelid surgery or corneal surgery; previous ocular trauma; Sjögren's Syndrome (absence of dry mouth), rheumatoid arthritis, diabetes or ocular infections; current or previous condition known to affect the ocular surface and/or tear film; a score ≥ 15.0 on the Ocular Surface Disease Index (OSDI) questionnaire; medication or use of eye drops known to affect the ocular surface and/or tear film; pregnancy (on self-report); contact lens (CL) wear one day prior or on the day of this study. Ethical approval was obtained from the Cardiff School of Optometry and Vision Sciences Human Research Ethics Committee, and the study followed the tenets of the Declaration of Helsinki (project number 1344, Appendix section no. 8.2.1).

Subjects were asked to attend the laboratory on two different days. All measurements were made on the right eye only and not before 12:00pm (between 12:00 and 6:30pm) to avoid any possible diurnal bias in corneal sensitivity[305,306] or tear film stability.[370] Humidity levels and room temperature were controlled within tolerable limits, as it has been shown to influence OST,[372-374] showing a typical increase of 0.15 to 0.2°C per degree increase in room temperature.[11,285]

All subjects filled in the German translation off the OSDI questionnaire[375] and the following measurements were carried out on each subject during both visits: baseline CST, OST, non-invasive tear break-up time (NIBUT) and tear film lipid pattern evaluation. Subsequently, the eyes were heated during one visit and cooled during the other visit (in randomised order). After completion of the heating/cooling period, OST and CST were measured in turn, until baseline measurements were reached again. Finally, the NIBUT measurement was repeated.

5.2.1 Procedures

5.2.1.1 Ocular Surface Disease questionnaire (OSDI)

The OSDI questionnaire was described in detail in the previous Chapter 4.2.1.2.
As in Chapter 4, the OSDI questionnaire was applied, in order to fulfil the inclusion criterion that only subjects without DES would be able to participate, showing an OSDI score of < 15.0.

5.2.1.2 Central corneal sensitivity threshold (CST)

CST was assessed at the central area of the cornea using the Non-Contact Corneal Aesthesiometer (NCCA). This instrument has been described previously (Chapter 1.17 and 4.2.1.4) and has been used to assess the effect of other external factors on corneal sensitivity.[14,328,332] As in the previous study (Chapter 4), stimulus duration was set at 1s and the time interval between each stimulus presentation was 15s. In order to ensure a complete and stable tear film over the cornea, the subjects were asked to make a full, but unforced blink, following which (within 1-2s) the stimulus was presented.[362]

5.2.1.3 Ocular surface temperature (OST)

Real time measurements of OST were carried out on all subjects, over a period of five consecutive natural blinks, using the same self-calibrating (with use of the emissivity factor of 0.95 for the cornea) thermal infrared camera (FLIR A310; thermal resolution 0.08°C, temporal resolution 30Hz; spatial resolution 320x240 pixel) as in the previous studies and analysed in the same way as in Chapters 3 and 4 (sections 3.2.1.3 and 4.2.1.5), using grey-scale thermal images using a purpose-designed computer programme (ThermaCAM Researcher Pro Version 2.9, FLIR Systems, 2006). A mean value for OST in the region of the central cornea was recorded two seconds after each of the five consecutive natural blinks at baseline, with the infrared camera placed in a perpendicular position to the central cornea. After the heating or cooling period, CST and a mean value for OST in the region of the central cornea were recorded alternately, with short time intervals in between, until the OST reached baseline level again. For the OST measurements immediately after the cooling/heating period, the camera was repositioned at a slight angle from the normal, alongside the NCCA installed which needed to be aligned normal to the cornea for correct stimulus presentation. This allowed measurement of both the CS threshold and OST in quick succession.

5.2.1.4 Non-invasive break-up time (NIBUT) and tear lipid pattern

NIBUT and the tear lipid pattern were recorded with use of the Tearscope Plus (Keeler Ltd., Windsor, UK) equipped with a diffuse cold light source. The same method of measurement was chosen as described in Chapter 4.2.1.6.

In the previous Chapter 4, an additional grading scale for tear film stability was adopted, in order to account for the decrease in tear film stability with tear lipid layers thicker than the amorphous lipid pattern:[383]

Grade 1 – open and closed meshwork, abnormal colour fringes, globular appearance

Grade 2 – wave / flow

Grade 3 – normal colours

Grade 4 – amorphous

This grading scale was also applied for this current study.

5.2.1.5 Heating of the ocular surface

Each subject wore a lid-warming device (Blephasteam, Thea Pharma, Germany) for 10 mins, as recommended by the manufacturer. These devices consist of a pair of goggles with eyepieces that create a wet chamber combining heat and moisture. Two disposable rings, which were moistened with sterile and preservative free saline (Avizor Saline Monodose, Avizor, Madrid, Spain), were inserted inside each eyepiece to produce humidity. The subject's eyes did not come into contact with the rings. The goggles have been shown to provide more effective warming than warm and moist compresses.[413] Within two minutes, the mean temperature within the heated chamber was measured to be 40.55±0.98°C in a clinical study.[413] OST has been show to increase by a mean value of 2.77°C by application of the Blephasteam heat goggles.[414] The subjects were asked to keep their eyes open whilst wearing the heat goggles in this study.

Immediately after removal of the heat goggles, CST and OST were recorded alternately, with minimal time intervals in between, until the OST had reached baseline level again.

5.2.1.6 Cooling of the ocular surface

Thirty minutes prior to the appointment, a BlephaCura gel mask (Optima Pharmazeutische GmbH, Wang, Germany) was placed in the freezer (temperature measured inside the freezer: -14.80°C). The subjects were then instructed to wear this cool gel mask for a 10 minute period. For protection of the skin from the cold mask, a thick cotton cloth was placed between the gel mask and the facial skin around the eyes, where the mask would touch, however sparing out the eyes. The subjects were instructed to keep their eyes closed whilst wearing the cold mask. Care was taken, to place the mask onto the face, such that the closed eyes would not experience any pressure from the mask, as this might have had an influence on the CST. To ensure this, the subject held the mask in the correct position on their temples.

Immediately after removal of the cold gel mask, CST and OST were recorded alternately, with minimal time intervals in between, until OST had reached baseline level again.

5.2.1.7 Order of procedures

- Patient arrived in the testing room, and was asked to wait for 15 minutes to adjust to the room (this was especially important if they had just arrived inside from being outside in the cold).
- During the first appointment: Subject filled in the consent forms and the OSDI questionnaire. The examiner was present in the room, in order to assist, if questions arose.
- One measurement of baseline ocular surface sensation (as described in Chapter 4).
- Five consecutive measurements of ocular surface temperature (as described in Chapter 4).
- Three consecutive measurements of NIBUT and assessment lipid layer pattern (as described in Chapter 4).
- Heating treatment with heat goggles or cooling treatment with cold gel mask during second or third visit. The order of treatments was randomised: one half of subjects received heating during the first visit, the other half received cooling during the first visit.
- Immediately after removal of the heat goggles/cool gel mask, alternate measurements of ocular surface sensation and corneal temperature were taken.
- Three consecutive measurements of NIBUT and assessment of the lipid layer pattern without the grid (as described in Chapter 4).

Measurement	Visit 1 or 2
Adjustment period to room temperature (15min)	**1 and 2**
Consent forms	**1**
OSDI questionnaire	**1**
CST measurement	**1 and 2**
Slit lamp examination	**1 and 2**
OST measurement	**1 and 2**
NIBUT/lipid layer assessment	**1 and 2**
Heating/cooling period	**1 or 2**
Alternate CS/OST measurements	**1 and 2**
NIBUT/lipid layer assessment	**1 and 2**

Table 5.1: Chronological order of procedures

5.2.2 Statistical analysis

The data were not found to be normally distributed (Shapiro-Wilk Test, Programme Ri386 3.1.0), hence the non-parametric Wilcoxon signed-rank Test was applied to test the difference between baseline and after the corneal heating/cooling procedure (Programme Ri386 3.1.0).

Due to the variable time required for the data collection for individual OST and CS-threshold measurements after the heating and cooling periods, these measurements could not be obtained at the exact same time intervals for all participating subjects. Hence, a non-linear, asymptotic regression model was applied for the period immediately after each, the heating and cooling period of the cornea. The 'Akaike information criterion (AIC)' was used in order to test the goodness of the model and in order to evaluate for the best model under consideration of the initial OST/CS difference (F1), time constant (F2) and the asymptotic temperature difference (F3). Model 1 considered all three coefficients F1, F2 and F3. Model 2 only considered F1 and F2, model 3 only considered F1 and model 4 only considered F2. An additional F test (ANOVA) was carried out, in order to assure the choice of the most simple model, according to the law of parsimony. A bootstrap method was used to calculate the 95% confidence interval for the individual measurements and the Monte Carlo method was used to calculate the 95% confidence interval for the model fit (Programme Ri386 3.1.0).

5.3 Results

Forty-two subjects participated, of which 11 were male. Average age was 27.76±5.36 years.

5.3.1 Heating of the ocular surface

The average ambient temperature in the testing room was 24.9±1.17°C and the average ambient humidity was 45.13±5.73%. After completion of the heating procedure, the first OST measurement was carried out immediately after removal of the heating goggles. The corneal sensitivity measurement thereafter varied individually (depending on the subjects' responses) and took, on average, 98.0±33.2 seconds. The fastest

measurement was completed after 45 seconds and the longest measurement took 3 minutes.

Mean OST change in this group of subjects was +3.96°C, which was statistically significant ($p<0.001$). This increase in corneal temperature correlated well with previously published levels.[413,414] The decrease in median CST (increase in sensitivity) after the heating period was found to be 0.10 mbars. Although this change represents only two sensitivity increments (2*0.05mbars), this was also found to be statistically significant ($p=0.002$). However, the heating procedure did not have any statistically significant effect on tear film quality ($p=0.970$ for NIBUT, $p=0.713$ for lipid pattern grading, $p=0.584$ for tear film stability grading). The median/interquartile range and mean±standard deviation values are summarised in Table 5.2, and the results for the statistical analysis are displayed in Table 5.3.

	Median / IR	**Mean±SD**
OSDI	8.30 / 4.20-14.60	8.86±4.92
Baseline CST (mbars)	0.35 / 0.30-0.40	0.35±0.09
CS after heating procedure (mbars)	0.25 / 0.20-0.35	0.30±0.13
Baseline OST (°C) at the central cornea	35.20 / 34.45-35.52	35.00±0.72
OST at the central cornea after heating procedure (°C)	39.10 / 38.60-39.50	38.96±0.74
Baseline NIBUT (secs)	32.40 / 13.97-53.62	39.48±30.03
NIBUT after heating procedure (secs)	28.30 / 10.95-63.65	40.37±37.12
Baseline lipid pattern	3.00 / 2.25-4.00	3.19±1.23
Lipid pattern after heating procedure	3.00 / 2.25-4.00	3.24±1.34
Baseline tear film stability	2.00 / 1.00-4.00	2.43±1.21
Tear film stability after heating procedure	2.00 / 1.13-3.00	2.33±1.05

Table 5.2: Median/Interquartile Range (IR) and Mean ±Standard Deviation for: OSDI (Ocular Surface Disease Index), central corneal sensitivity threshold (CST) at baseline and after the heating procedure, central ocular surface temperature (OST) at baseline and after the heating procedure, non-invasive tear break-up time (NIBUT) at baseline and after the heating procedure, lipid pattern grading at baseline and after the heating procedure, tear film stability grading at baseline and after the heating procedure.

	p-value	V value
CST	0.002	582
OST	< 0.001	0
NIBUT	0.970	448
Lipid pattern	0.713	95
Tear film stability	0.584	98

Table 5.3: Wilcoxon signed-rank test for the effect of the heating procedure on CST, OST, NIBUT and tear film quality.

5.3.1.1 Post-hoc power calculation

A post-hoc power calculation was carried out for the two variables CS threshold and OST, for which a statistically significant change was obtained (α=0.05; n=42; G*Power 3.1):

For CS threshold:

- Difference = -0.054±0.120mbars; effect size = 0.450; power = 1.0

For OST:

- Difference = +3.96±0.81°C; effect size = 4.883; power = 1.0

5.3.1.2 Mean OST change and recovery time after the heating procedure

After 20 mins, OST had reached baseline level for the entire sample group. For analysis, Model 2 (considering the coefficients 'OST difference' and 'time constant') was the best one, having the lowest AIC value (132.0252). The additional F test (ANOVA) did not show any statistically significant advantage for Model 1 over Model 2 (p=0.998), and so Model 2 was chosen as being the simpler one, according to the law of parsimony. The decrease in OST dropped at a faster rate immediately after the heating procedure before levelling out at a slower rate to reach the baseline temperature (Figure 5.1). Inter-subject variability was greater immediately after heating the ocular surface, but reduced to a low amount when baseline OST was reached. For each subject, the time-point was noted, at which baseline OST was reached again. These data were found to be normally distributed (Shapiro-Wilk, p=0.068; Programme Ri386 3.1.0), and this mean time point was 518.5±108.5 secs.

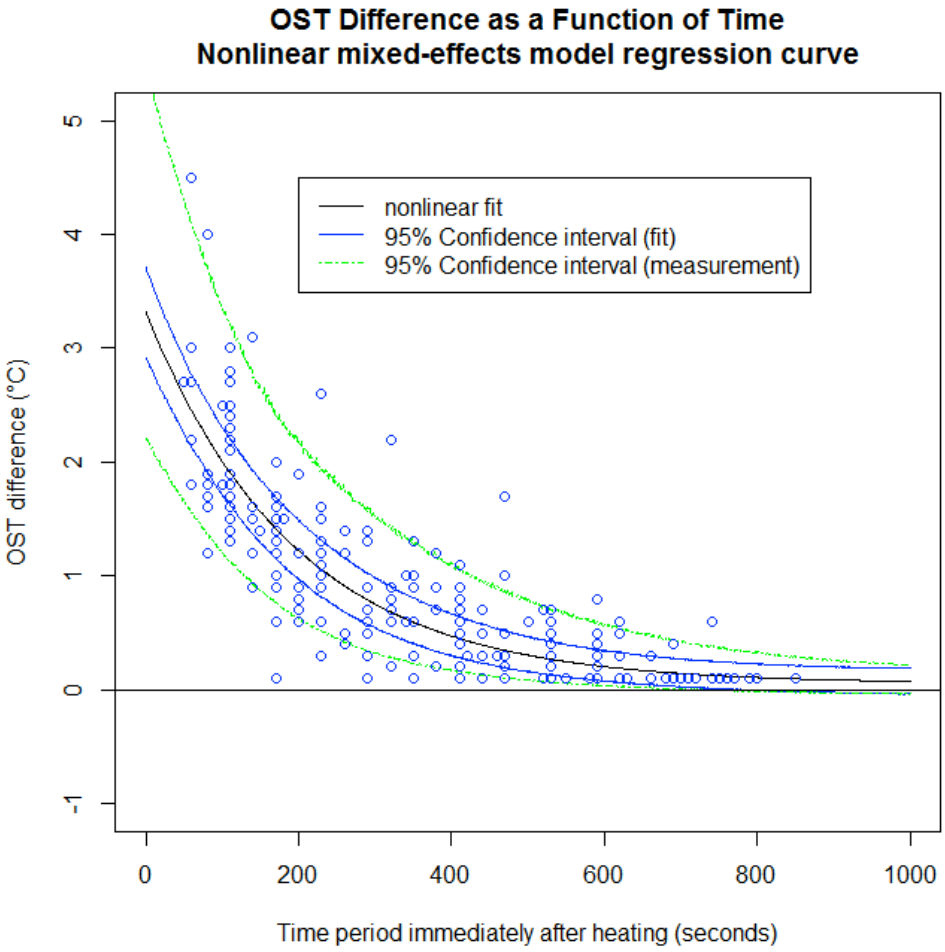

Figure 5.1: OST difference as a function of time: a non-linear mixed effects model regression curve for the time period immediately after the heating period.

5.3.1.3 Central CST measurements after heating the ocular surface

A statistically significant increase in central CST was noted immediately after the heating procedure (mean difference=-0.05 mbars, median difference=-0.10 mbars; p=0.002) for the overall group for most subjects (Figure 5.2). For analysis, Model 2 (considering the coefficients 'OST difference' and 'time constant') was the best one, having the lowest AIC value (-630.5793). Model 1 could not be successfully applied for this set of data. The additional F test (ANOVA) showed a statistically significant difference between Model 3 and Model 2 ($p<0.001$), hence Model 2 was applied. Considerable fluctuation was observed, before baseline CS threshold was reached again. Baseline CST was reached after approximately seven minutes post-heating, which was earlier than the time taken for OST to reach baseline values again.

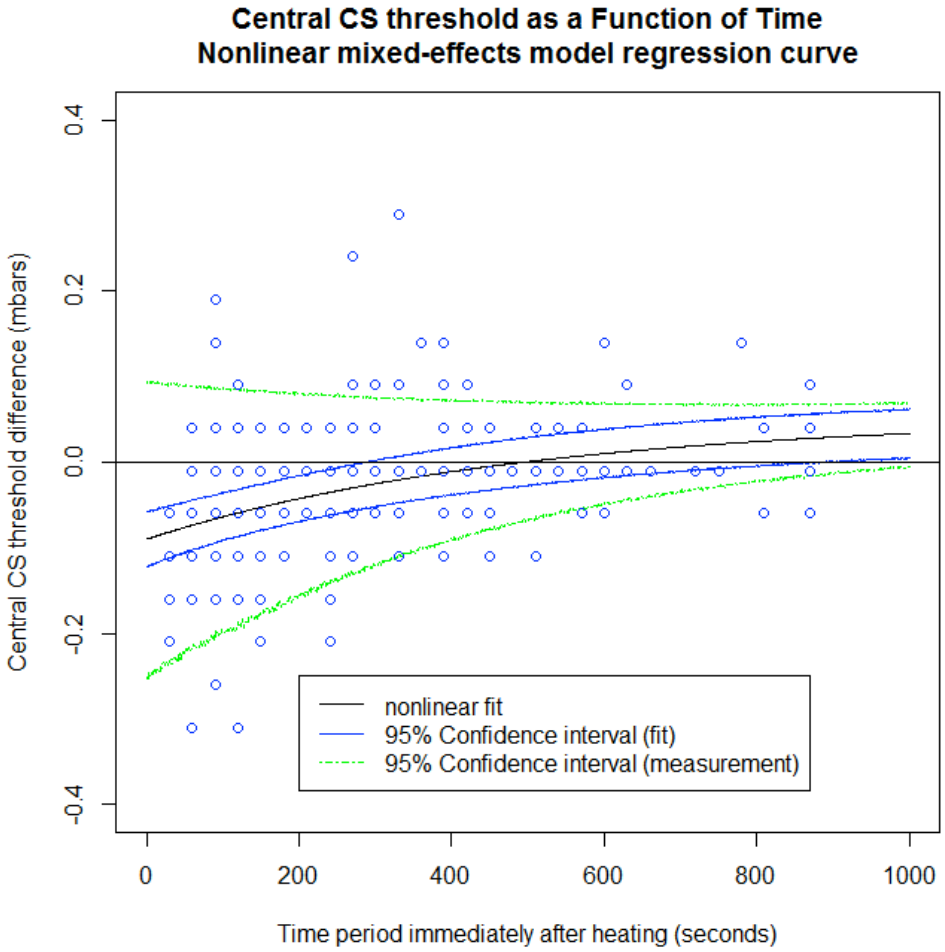

Figure 5.2: Central CST as a function of time: a non-linear mixed effects model regression curve for the time period immediately after the heating period.

For each subject, the time point was noted, at which baseline OST was reached again. These data were not found to be normally distributed (Shapiro-Wilk, p=0.015; Programme Ri386 3.1.0) and the median time point was 420.2 secs (IR 210.0 – 660.0.secs).

5.3.2 Cooling of the ocular surface

The average ambient temperature in the testing room was 24.76±1.29°C and average ambient humidity was 46.00±5.40%. After completion of the cooling procedure, the first OST measurement was carried out immediately after removal of the cooling mask. The corneal sensitivity measurement thereafter varied individually (depending on the subject's responses) and took, on average, 112.0±35.78 seconds. The fastest

measurement was completed after 40 seconds and the longest measurement took 3 minutes and 15 seconds.

Mean central OST temperature change was -4.51°C, which was statistically significant ($p<0.001$). The increase in median CST (decrease in sensitivity) after the cooling period was found to be 0.10 mbars. Although this change only represents two sensitivity increments, this was also found to be statistically significant ($p<0.001$). However, the cooling of the ocular surface did not have any statistically significant effect on tear film quality ($p=0.094$ for NIBUT, $p=0.100$ for lipid pattern grading, $p=0.084$ for tear film stability grading). There was, however, some tendency towards a less stable tear film, as NIBUT and the lipid pattern gradings decreased.

The median/interquartile range and mean ±standard deviation values are summarised in the Table 5.4, and the results for the statistical analysis are displayed in Table 5.5.

	Median / IR	**Mean±SD**
OSDI	8.30 / 4.20-14.60	8.86±4.92
Baseline CST (mbars)	0.30 / 0.30-0.35	0.34±0.09
CST after cooling procedure (mbars)	0.40 / 0.30-0.59	0.46±0.21
Baseline OST (°C) at the central cornea	35.00 / 34.50-35.40	34.87±0.68
OST at the central cornea after cooling procedure (°C)	30.60 / 29.80-31.25	30.36±1.36
Baseline NIBUT (secs)	25.90 / 16.65-40.77	36.78±30.75
NIBUT after cooling procedure (secs)	17.40 / 12.38-43.92	32.17±31.45
Baseline lipid pattern	3.00 / 2.00-4.00	3.05±1.38
Lipid pattern after cooling procedure	3.00 / 2.00-3.00	2.81±1.25
Baseline tear film stability	2.00 / 1.00-3.00	2.24±1.05
Tear film stability after cooling procedure	2.00 / 1.00-2.00	2.02±0.98

Table 5.4: Median / Interquartile Range (IR) and Mean (±Standard Deviation) for: OSDI (Ocular Surface Disease Index), central corneal sensitivity threshold (CST) at baseline and after the cooling procedure, central ocular surface temperature (OST) at baseline and after the cooling procedure, non-invasive tear break-up time (NIBUT) at baseline and after the cooling procedure, lipid pattern grading at baseline and after the cooling procedure, tear film stability grading at baseline and after the cooling procedure.

	p-value	V value
CST	< 0.001	32
OST	< 0.001	903
NIBUT	0.094	448
Lipid pattern	0.100	69
Tear film stability	0.084	44.5

Table 5.5: Wilcoxon signed-rank test for the effect of the cooling procedure on CST, OST, NIBUT and tear film quality.

5.3.2.1 Post-hoc power calculation

A post-hoc power calculation was carried out for the two variables CST and OST, for which a statistically significant change was obtained (α=0.05; n=42; G*Power 3.1):

For CST:

- Difference = +0.117±0.162mbars; effect size =0.722 ; power = 0.99

For OST:

- Difference = -4.51±1.32°C; effect size = 3.417; power = 0.99

5.3.2.2 Mean OST change and recovery time after the cooling procedure

Similarly to the heating procedure, baseline OST was reached again for the overall group after approximately 20 mins. For analysis, Model 1 (considering the three coefficients CST difference, time constant and the asymptotic temperature difference) and Model 2 (considering the coefficients 'CST difference' and 'time constant') were best, having the lowest AIC value (184.6849 for model 1 and 184.5136 for model 2). The additional F test (ANOVA) did not show any statistically significant advantage with Model 1 over Model 2 (p=0.1763), hence Model 2 was chosen as being the simpler, according to the law of parsimony.

For each subject, the time point was noted, at which baseline OST was reached again. These data were found to be normally distributed (Shapiro-Wilk, p=0.1994; Programme Ri386 3.1.0), and the mean time point was 915.7±190.5 secs.

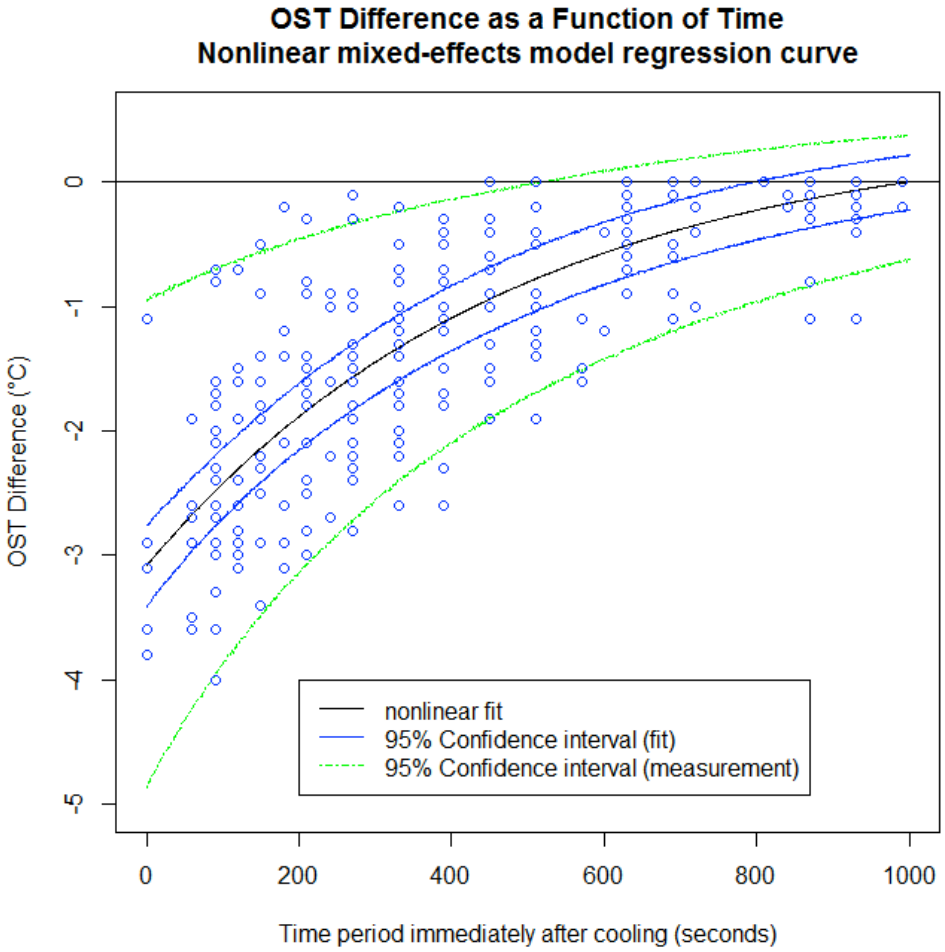

Figure 5.3: OST difference as a function of time: a non-linear mixed effects model regression curve for the time period immediately after the cooling period.

5.3.2.3 Central CST measurements after cooling the ocular surface

A statistically significant decrease in central CST was noted immediately after the heating procedure (mean difference=0.12 mbars, median difference=0.10 mbars; $p<0.001$) for the overall group. Subject variability was observed to be more marked immediately after the heating period, and stabilised towards the end of the recovery period. Baseline CST was reached again after approximately 7 minutes post heating, which was earlier than when OST had reached baseline values again. For analysis, Model 3 (considering the coefficient 'initial OST/CST difference') was best, having the lowest AIC value (-662.6391). The Models 1 and 2 could not be successfully applied for this set of data.

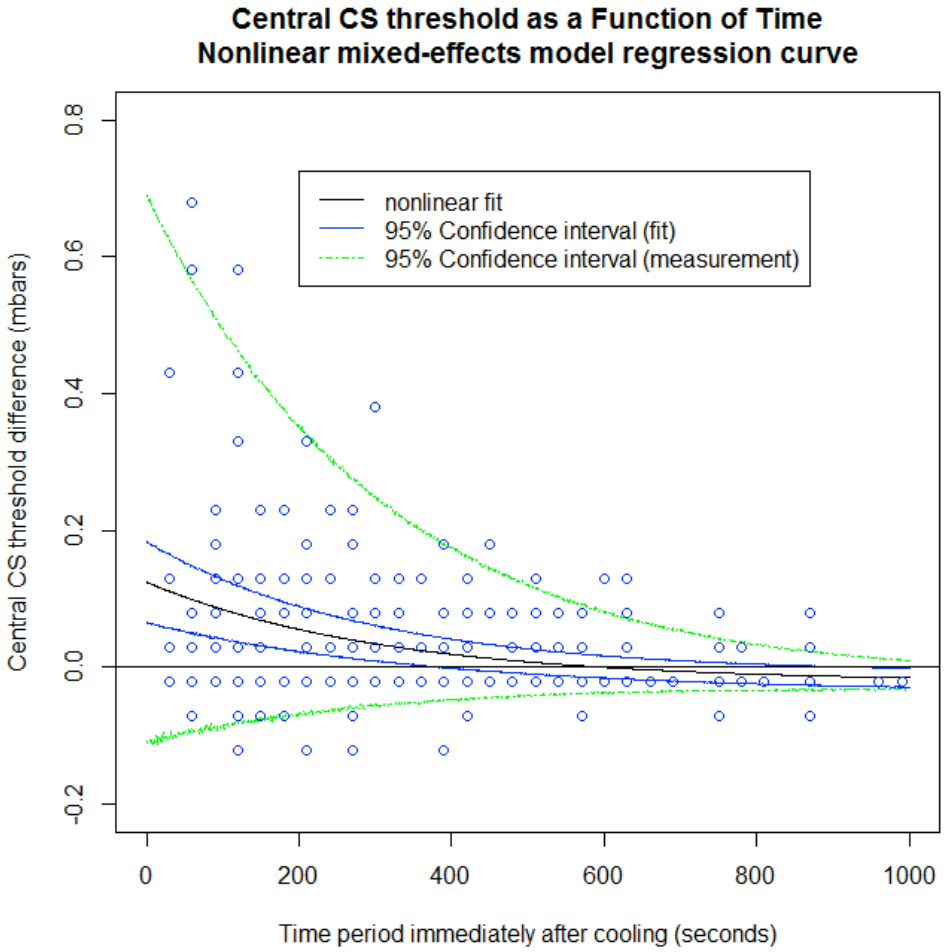

Figure 5.4: Central CST as a function of time: a non-linear mixed effects model regression curve for the time period immediately after the cooling period.

For each subject, the time point was noted, at which baseline OST was reached again. These data were not found to be normally distributed (Shapiro-Wilk, p=0.002; Programme Ri386 3.1.0) and this median time point was 420.0 secs (IR 165.0 – 780.0.secs).

5.4 Discussion

This study explored the immediate effect of heating and cooling of the ocular surface (by means of a lid-warming device and a cooling mask) on OST and the CST of the corneal nerves to a cooling stimulus (with use of the NCCA air gas aesthesiometer). During the recovery period, OST and CST were continuously recorded until baseline recordings were reached again, and this allowed an evaluation on how in nature this recovery period took place. At the end of the recovery period, tear film characteristics

(NIBUT and lipid pattern evaluation) were additionally noted, in order to estimate if they might have had an influence on the obtained OST and CST during the recovery period.

Looking first at the course of decrease / increase in OST after the heating / cooling period, the study found that it followed an exponential slope as displayed by the nonlinear mixed-effects model regression curves (Figures 5.1 and 5.3). CST reached baseline values before OST did, after both the heating and cooling period. After both the heating and cooling procedure, the variability in CST changes during the recovery period was much more marked than the recorded increases / decreases in OST for the subject group in this study. This can in part be explained by the difference in nature of measurements: OST measurement is an objective measurement with aid of a thermal camera, whereas CST measurement represents a psychophysical test that is dependent on the subjective subject perception, which is affected by the subject's alertness. In addition, at CST a stimulus is perceived only 50% of the time, affecting precision of this measurement.

Focussing on the time course of OST change after the heating / cooling period, the study found that the time period after heating until baseline OST was reached again, was much shorter than the time period after cooling, and the amount of variability was less marked during this cooling down period (a mean period of 518.5±108.5s compared to 915.7±190.5s). This may in part be explained by the fact that the change in OST was more marked after the cooling than after the heating procedure (a mean change of -4.51°C in OST immediately after cooling compared to +3.96°C immediately after heating). An additional explanation may be that the cornea is avascular and that it may therefore take longer to warm up this tissue, as this has to occur with the repeated spreading of warm tears over the ocular surface, while heat loss can occur through many more vectors provided by radiation, conduction and evaporation.[401]

These heat loss vectors may have additionally slowed down the process of ocular warming for the same reasons. For example, tear film quality was impaired by the cooling procedure, which could have accelerated the rate of evaporation from the tear film,[393] counteracting the process of warming up the ocular surface during the recovery

period. At the end of the recovery period after the cooling procedure, a trend for a tear film with reduced NIBUT rate and a slightly thinner lipid layer was observed in the current study, although this was not statistically significant. Hence, it can be speculated that the tear film quality may have been affected even more, immediately after the cooling period, which may have increased the evaporation rate and hence may have prolonged the OST recovery period. After recovery from the heating procedure, no statistically significant change in tear film characteristics could be observed: NIBUT measurements were slightly lower, but no change in tear lipid layer thickness was noted. However, it is possible that there may have been a notable change immediately after the heating procedure, a time point at which the tear film was not assessed during this study.

Turning to changes in corneal sensitivity, the study found that the median CST decreased by 0.10mbars (two sensitivity increments) immediately after the heating procedure (to a statistically significant degree) and that the median CST increased by the same amount after the cooling procedure (also to a statistically significant degree). The temperature of the air-pulse stimulus used in this study remained stable at ambient temperature, which was measured to be 24.9±1.17°C during the heating appointments, and 24.76±1.29°C during the cooling appointments, respectively. This resulted in a greater mean temperature difference between the stimulus and the heated ocular surface of 14.06°C, and a much smaller mean temperature difference between the stimulus and the cooled ocular surface of 5.6°C. However, the change in central CST was found to be small after both, heating and cooling of the ocular surface, although this difference was found to be statistically significant. This makes a sensitisation of the cold thermoreceptors after the cooling or heating procedure to appear unlikely. In fact, nerve terminal impulses in the guinea-pig corneal cold-sensitive receptors have been shown to be similar to those found in mammalian cutaneous cold-sensitive receptors (in the skin),[415,416] and direct sensitisation of cutaneous cold receptors could not be shown to occur merely by means of a heating or cooling procedure.[417] Several authors reported no effect of local skin temperature on cutaneous thermal detection threshold.[418,419] Assuming then a static nervous activity at a higher level of impulse frequency on the superficial ocular surface after either, the heating or cooling procedure, one would expect lower CST after heating the ocular surface, compared to after cooling it, purely

because of the greater temperature difference between the air-pulse stimulus and the heated ocular surface, than between the stimulus and the cooled ocular surface. This was observed in the current study. However, one could have expected an even larger difference in CST, considering the large temperature difference between the heated ocular surface, the constant air gas stimulus temperature and the small temperature difference between the cooled ocular surface and the air gas stimulus temperature.

The less stable tear film observed after the cooling period may suggest that there may have been a marked reduction in tear film quality immediately after the cooling procedure, which may have counteracted the initial decrease in the obtained CST.

This study concentrated on observation of the continuous increase / increase of OST and the CST throughout the recovery period after the heating / cooling procedure and did not additionally explore how much localised change in OST occurs at CST immediately after cooling / heating, and this is a weakness of the study. In order to explore if corneal thermoreceptors are affected in their sensitivity immediately after heating / cooling them, it would be necessary to either adapt stimulus temperature to achieve the same difference between air gas stimulus temperature and OST after the heating/cooling procedure as at baseline, or to measure OST change during stimulus presentation at CST. Successfully adapting stimulus temperature, however, would be difficult, as the previous experiment has shown that OST change is affected by stimulus intensity (Measurement of OST during the presentation of an air gas stimulus, Chapter 3).

5.5 Conclusion

This study described an exponential change in OST after the heating / cooling procedure to reach baseline again, with a longer time course required after the cooling response. Recordings of tear film characteristics after completion of the recovery period suggest that tear film quality might have been affected especially by the cooling procedure.

Only a small decrease in CST immediately after the heating procedure, and a small increase in CST immediately after the cooling procedure were noted, despite the fact that there was a much larger temperature difference between the ocular surface and the air gas stimulus following the heating procedure and a much smaller temperature

difference between the ocular surface and the air gas stimulus following the cooling procedure. This may suggest that the heating / cooling procedures did not affect the sensitivity of thermoreceptors on the ocular surface. However, for clarification of this matter, the experiment in the following Chapter 6 will investigate OST during stimulus presentation at CST, immediately after the heating / cooling procedure. Additionally, the tear film characteristics will be assessed again at an earlier time point after the heating / cooling period.

CHAPTER 6

An investigation of ocular surface temperature change occurring at corneal sensitivity threshold after heating and cooling of the ocular surface

6.1 Introduction

The previous clinical study (Chapter 5) explored the effect of heating and cooling of the ocular surface on the corneal sensitivity threshold (CST) to a cooling stimulus provided by the NCCA air gas aesthesiometer, by means of a lid warming device and a cooling mask. However, a conclusion on the effect of heating or cooling of the ocular surface on nervous activity was not possible, because there was a stronger cooling effect on the warmer ocular surface induced by the air-pulse stimulus of constant temperature (similar to ambient room temperature) after the heating procedure, than on the cooler ocular surface after the cooling procedure. Due to the study design, where CST and ocular surface temperature (OST) were measured *alternately* and not *simultaneously* during the recovery period after the heating / cooling procedure, the localised actual temperature change at the central cornea necessary at CST could not be measured. However, this would be necessary in order to establish whether the apparently higher corneal sensitivity after the heating procedure was due to the stronger cooling effect from the air gas stimulus, and thus that a stronger nervous activity in the temperature sensitive cold nociceptors accounted for it, or that there was a previously undetected effect occurring at the local level of air-pulse stimulus. For further exploration of this matter, it is necessary to record the localised OST change simultaneously during the air gas stimulus presentation on the central cornea.

During the previous clinical study (Chapter 5), tear film characteristics were determined at baseline and again 20mins later, after the recovery period following the heating / cooling procedure was completed. At that point of time, a trend for a small decrease in both, non-invasive tear break-up time (NIBUT) and in tear film stability were noted, especially after the cooling treatment, which may have been more marked immediately after the cooling procedure. As tear film quality could be shown to correlate with CST

during the study in Chapter 4, this may have also influenced the CSTs obtained in the previous study in Chapter 5.

6.1.1 Aim

The aim of the study was to explore the immediate effect of heating and cooling of the ocular surface on ocular surface sensation, by recording localised OST change simultaneously during the air gas stimulus presentation for CST measurement. Additionally, the effect of the heating / cooling procedure on tear film characteristics was determined.

6.2 Methods

This was a prospective clinical cohort study. Forty-two volunteers, who had already participated in the clinical studies of Chapters 4 and 5 were invited. The subjects were from the staff and patient pool of the Optometry Department, University of Applied Science in Olten (CH) and were invited either by email or by personal invitation in the clinic. All subjects invited to take part in the study were given a subject information sheet, explaining the study, prior to giving signed consent. As for the clinical studies in Chapters 4 and 5, the age range was limited to between 20 and 39 years, as corneal sensitivity,[301,364,365] ocular surface temperature (OST),[366-368] and tear film stability[365] have been found to decrease with age. Exclusion criteria for participation in this study were: history of previous ocular surgery including refractive surgery, eyelid tattooing, eyelid surgery or corneal surgery; previous ocular trauma; Sjögren's Syndrome (absence of dry mouth), rheumatoid arthritis, diabetes or ocular infections; current or previous condition known to affect the ocular surface and/or tear film; a score ≥15.0 on the Ocular Surface Disease Index (OSDI) questionnaire; medication or use of eye drops known to affect the ocular surface and/or tear film; pregnancy (on self-report); contact lens (CL) wear one day prior or on the day of this study. Ethical approval was obtained from the School of Optometry and Vision Sciences Human Research Ethics Committee and the study followed the tenets of the Declaration of Helsinki (project number 1344, Appendix section numbers 8.2.1 and 8.2.2).

Subjects were asked to attend the laboratory on two different days. All measurements were made on the right eye only and not before 12:00pm (between 12:00 and 6:30pm) to avoid any possible diurnal bias in corneal sensitivity[305,306] or tear film stability.[370] Humidity levels and room temperature were controlled within tolerable limits, as it has been shown to influence OST,[372-374] showing a typical increase of 0.15 to 0.2°C per degree increase in room temperature.[11,285]

All subjects filled in the German translation off the OSDI questionnaire[375] and the following measurements were carried out on the same subjects during both visits: measurement of baseline corneal surface sensitivity, OST, non-invasive tear break-up time (NIBUT) and tear film lipid pattern evaluation. Subsequently, the eyes were heated up during one visit and cooled down during the other visit (in randomised order). After completion of the heating/cooling period, OST and CST were simultaneously. NIBUT was recorded immediately thereafter.

6.2.1 Procedures

6.2.1.1 Ocular Surface Disease questionnaire (OSDI)

The OSDI questionnaire was described in detail in the previous Chapter 4.2.1.2.
As during the clinical studies in Chapters 4 and 5, the German translation of the OSDI questionnaire was applied,[375] in order to fulfil the inclusion criterion that only subjects without dry eye disease (DES) would be able to participate, showing a OSDI score of <15.0.

6.2.1.2 Corneal sensitivity threshold (CST)

CST was assessed at the central area of the cornea using the NCCA. This instrument has been described previously (Chapter 1.17 and 4.2.1.4) and has been used to assess the effect of other external factors on corneal sensitivity.[14,328,332] As in the previous studies (Chapters 4 and 5), the double staircase method for CST determination was applied. Stimulus duration was set at 1s and the time interval between each stimulus presentation was 15s. In order to ensure a complete and stable tear film over the cornea,

the subjects were asked to make a full, but unforced blink, following which (within 1-2s) the stimulus was presented.[362]

6.2.1.3 Ocular surface temperature (OST)

Real time measurements of ocular surface temperature (OST) were carried out on all subjects, over a period of five consecutive natural blinks, using the same self-calibrating (with use of the emissivity factor of 0.95 for the cornea) thermal infrared camera (FLIR A310; thermal resolution 0.08°C, temporal resolution 30Hz; spatial resolution 320x240 pixel) as in the previous studies and analysed in the same way as in Chapters 3, 4 and 5 (sections 3.2.1.3, 4.2.1.5 and 5.2.1.2), using grey-scale thermal images created by a purpose-designed computer programme (ThermaCAM Researcher Pro Version 2.9, FLIR Systems, 2006). A mean value for OST in the region of the central cornea was recorded two seconds after each of the five consecutive natural blinks at baseline, with the infrared camera placed in a perpendicular position to the central cornea. Immediately after the heating or cooling period, OST was recorded once in the central region of the cornea 2s after a blink and - in contrast to the previous experiment in Chapter 5 - again *simultaneously* during air gas stimulus presentation onto the cornea (with means of the NCCA) for CST measurement. The maximum change in localised OST during air gas stimulus presentation was noted and will be referred to in the following. As in the previous clinical studies, the angle of the thermal camera was set at a slight angle next to the slit lamp with the NCCA installed perpendicularly to the central cornea, for all OST measurements immediately after the heating / cooling period. OST was recorded continuously during CST measurement. With use of a stopwatch, each time point of air gas stimulus presentation and the corresponding air gas stimulus intensity employed were noted. This enabled the analysis of localised OST change at CS threshold during air gas stimulus presentation after completion of the experiment had been completed.

6.2.1.4 Non-invasive-break up time (NIBUT) and tear lipid pattern

Non-invasive tear break-up time (NIBUT) and the tear lipid pattern were recorded with use of the Tearscope Plus (Keeler Ltd., Windsor, UK) equipped with a diffuse cold light source. The same method of measurement was chosen as described in Chapter 4.2.1.6.
In the previous Chapters 4 and 5, an additional grading scale for tear film stability was adopted, in order to account for the decrease in tear film stability with tear lipid layers thicker than the amourphous lipid pattern:[383]
Grade 1 – open and closed meshwork, abnormal colour fringes, globular appearance
Grade 2 – wave / flow
Grade 3 – normal colours
Grade 4 – amorphous
This grading scale was also applied for this current study.

In the previous study (Chapter 5), this measurement was carried out after completion of the recovery period from heating / cooling the ocular surface (approx. 20mins later). In this experiment, this measurement was carried out immediately after one single simultaneous CST / OST measurement (only max. 5mins. after the heating / cooling procedure).

6.2.1.5 Heating of the ocular surface

Each subject wore a lid-warming device (Blephasteam, Thea Pharma, Germany) for 10 minutes, as recommended by the manufacturer. These goggles and their use were described in Chapter 5. Immediately after removal of the lid warming device, OST was determined and subsequently the CST measurement and OST were determined simultaneously (during air-pulse stimulus presentation).

6.2.1.6 Cooling of the ocular surface

Thirty minutes prior to the appointment, a BlephaCura gel mask (Optima Pharamazeutische GmbH, Wang, Germany) was placed in the freezer. The subjects were then instructed to wear this cool gel mask for the duration of 10 minutes according to the same instructions as stated in Chapter 5. Immediately after removal of the cool

gel mask, OST was determined and subsequently the CST measurement and OST were determined simultaneously (during air-pulse stimulus presentation).

6.2.1.7 Order of procedures

- Patient arrived in the testing room, and was asked to wait for 15 minutes to adjust to the room (this was especially important if they had just arrived inside from being outside in the cold).
- During the first appointment: subject filled in the consent forms and the OSDI questionnaire. The examiner was present in the room, in order to assist, if questions arised.
- One measurement of baseline ocular surface sensation (as described in Chapters 4 and 5) and OST measurement during stimulus presentation at CST.
- Five consecutive measurements of ocular surface temperature (as described in Chapters 4 and 5).
- Three consecutive measurements of NIBUT and assessment lipid layer pattern (as described in Chapters 4 and 5).
- Heating treatment with heat goggles or cooling treatment with cold gel mask during second or third visit. The order of treatments was randomised: one half of subjects received heating during the first visit, the other half received cooling during the first visit.
- Immediately after removal of the heat goggles / cool gel mask, OST was determined and subsequently the CST and OST were determined simultaneously (during air gas stimulus presentation), i.e. OST was recorded during stimulus presentation on the corneal surface.
- Three consecutive measurements of NIBUT with the fine grid and assessment of the lipid layer pattern without the grid (as described in Chapters 4 and 5).

Measurement	Visit 1/2
Adjustment period to room temperature (15min)	1/2
Consent forms	1
OSDI questionnaire	1
CST measurement	1/2
Slit lamp examination	1/2
OST measurement	1/2
NIBUT /lipid layer assessment	1/2
Heating / cooling period	1 or 2
CST and simultaneous OST measurement	1/2
NIBUT / lipid layer assessment	1/2

Table 6.1: Chronological order of procedures

6.2.2 Statistical analysis

The data were not found to be normally distributed (Shapiro-Wilk Test, SPSS. Version 20), hence the non-parametric Wilcoxon signed-rank Test was applied, in order to test a difference between baseline and after the corneal heating/cooling procedure, as well as the difference in OST difference at CST after the heating/cooling period (SPSS, Version 20). Additionally, the effect size r was calculated [r = Z / √number of observations (56)]. Furthermore, the correlation between stimulus intensity and localised OST change was explored and displayed with the non-parametric Spearman's test and as scatterplots (SPSS, Version 20).

6.3 Results

Twenty-eight subjects participated, of which 10 were male. The average age was 28.75±5.99 years.

6.3.1 Heating of the ocular surface

The average ambient temperature in the testing room was 23.72±0.69°C, and average ambient humidity was measured to be 45.71±12.90%. After completion of the heating procedure, the first OST and CST measurements were carried out immediately after

removal of the lid-warming device. Mean OST temperature increase at the central cornea in this group of subjects was +3.01°C and turned out to be statistically significant (Tables 6.2 and 6.3), compared to baseline OST ($p<0.001$). This was less marked than during the previous heating experiment, where a mean OST difference of 3.96°C was observed (Chapter 5). The decrease in median CST (increase in sensitivity) after the heating period was found to be 0.05 mbars ($p=0.018$), which was also less pronounced than the median difference of 0.10 mbars in the previous experiment. As in the clinical study in Chapter 5, the heating procedure did not have any statistically significant effect on tear film quality ($p=0.186$ for NIBUT and $p=0.167$ for tear film stability grading). However, this time, where this measurement was carried out much sooner after the heating procedure, a statistically significant increase in tear lipid layer thickness could be observed ($p<0.001$). The median/interquartile range and mean (±standard deviation) values are summarised in the Table 6.2, and the results for the statistical analysis are displayed in Table 6.3.

	Median / IR	Mean±SD
OSDI	10.40 / 4.20-14.60	9.35±5.10
Baseline CST (mbars)	0.30 / 0.25-0.31	0.29±0.07
CST after heating procedure (mbars)	0.25 / 0.20-0.30	0.25±0.05
Baseline OST (°C) at the central cornea	34.75 / 34.50-35.00	34.73±0.52
OST at the central cornea after heating procedure (°C)	38.10 / 37.51-38.40	37.95±0.69
Baseline NIBUT (s)	18.60 / 10.85-26.77	26.66±26.49
NIBUT after heating procedure (s)	20.80 / 16.00-33.67	26.16±13.94
Baseline lipid pattern	3.00 / 2.00-4.25	3.07±1.51
Lipid pattern after heating procedure	5.00 / 3.00-5.00	4.07±1.44
Baseline tear film stability	2.00 / 1.00-3.00	2.00±1.05
Tear film stability after heating procedure	3.00 / 1.00-3.00	2.29±0.94
Aperture (mm)	10.50 / 9.50-11.00	10.25±0.96
TMH (mm)	0.20 / 0.15-0.30	0.22±0.09

Table 6.2: Median/Interquartile Range (IR) and Mean ±Standard Deviation for: OSDI (Ocular Surface Disease Index), central corneal sensitivity threshold (CST) at baseline and after the heating procedure, central ocular surface temperature (OST) at baseline and after the heating procedure, non-invasive tear break-up time (NIBUT) at baseline and after the heating procedure, lipid pattern grading at baseline and after the heating procedure, tear film stability grading at baseline and after the heating procedure, eye aperture and tear meniscus height (TMH).

	p-value	Z value / effect size r
CST	0.018	-2.537 / -0.34
OST	< 0.001	-4.543 / -0.61
NIBUT	0.1355	-1.355 / -0.18
Lipid pattern	<0.001	-3.570 / -0.48
Tear film stability	0.156	-1.417 / -0.19

Table 6.3: Wilcoxon signed-rank test for the effect of the heating procedure on CST, OST, NIBUT and tear film quality.

6.3.1.1 OST change at CST during stimulus presentation

The median OST temperature difference during stimulus presentation at CST at baseline before heating the ocular surface was found to be -0.60°C, and after the heating procedure it was greater at a median of OST change of -0.80°C. This means that a larger OST change was required after the heating procedure (compared to baseline), in order for the subjects to sense the stimulus (p=0.027; Table 6.4). The effect size r was -0.30, which - according to Cohen's criteria,[420] represents a medium effect.

	OST difference at CST at baseline	OST difference at CST after heating	Difference in OST change at baseline and after heating	Statistical significance (Wilcoxon)
Median / IR	-0.60 / -0.8 – (-0.50)	-0.80 / -0.95 – (-0.60)	-0.10 / -0.30 – 0.05	p=0.027 (Z=-2.232; effect size: r=-0.417)
Mean±SD	-0.63±0.20	-0.84±0.44	-0.20±0.48	

Table 6.4: OST difference during stimulus presentation at CST before and after heating the ocular surface and statistical analysis (Wilcoxon signed rank test).

A two-tailed post hoc power calculation was carried out for the difference in OST at CS threshold and was found to be 0.545 (α=0.05; n=28; G*Power 3.1).

6.3.1.2 Correlations between OST difference and CST during stimulus presentation

The central CST at baseline (before heating) was significantly correlated with central OST difference (r=0.654, p<0.01, Spearman's test). However, this relationship was no longer significant after completion of the heating procedure (r=0.450, p>0.05, Spearman's test). The scatterplots illustrate the better correlation before, and the poor correlation after, the heating procedure (Figures 6.1 and 6.2).

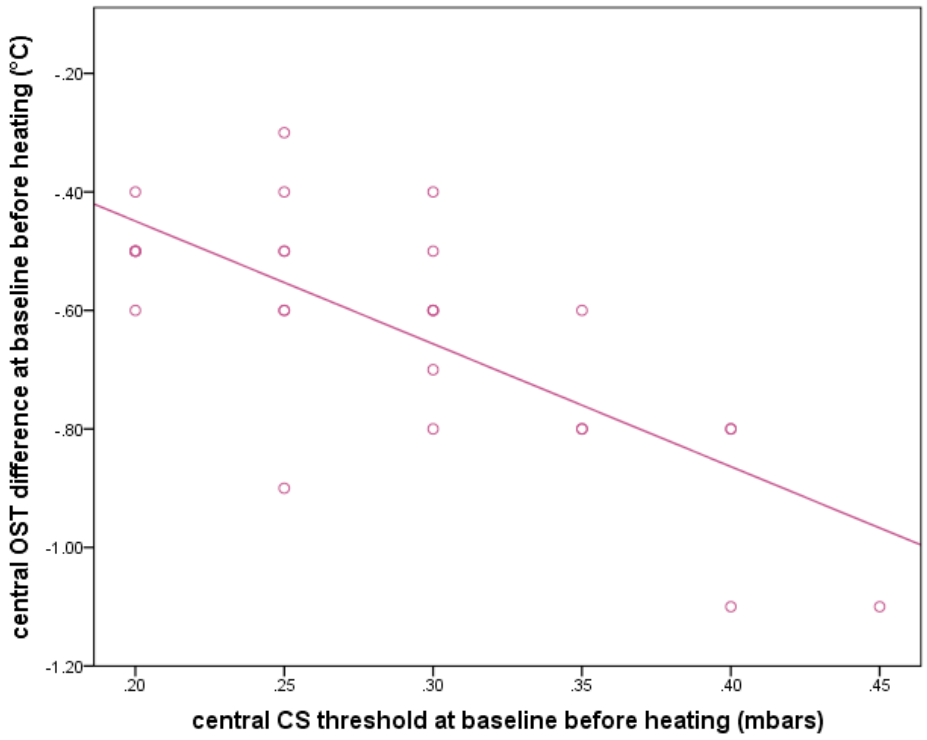

Figure 6.1: Scatterplot showing the correlation between the central CST (mbars) at baseline and central OST difference (°C) at baseline (before heating the ocular surface).

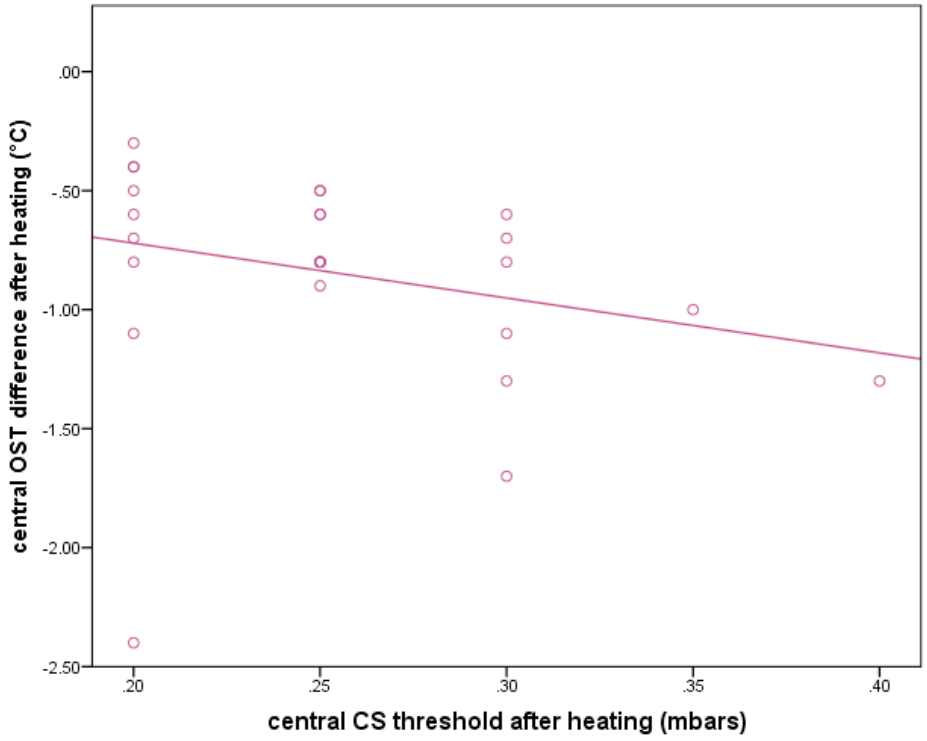

Figure 6.2: Scatterplot showing the correlation between central CST (mbars) and central OST difference (°C) after heating the ocular surface.

6.3.1.3 OST change during stimulus presentation with varying stimulus intensities

The median OST during stimulus presentation showed a linear relationship to stimulus intensity (r^2=0.985; Figure 6.3): with increasing stimulus intensity, a proportional median OST decrease could be observed. With higher stimulus intensities (0.80-1.20 mbars), the inter-subject fluctuations were considerably larger (Table 6.5 and Figure 6.4), compared to the lower stimulus intensities.

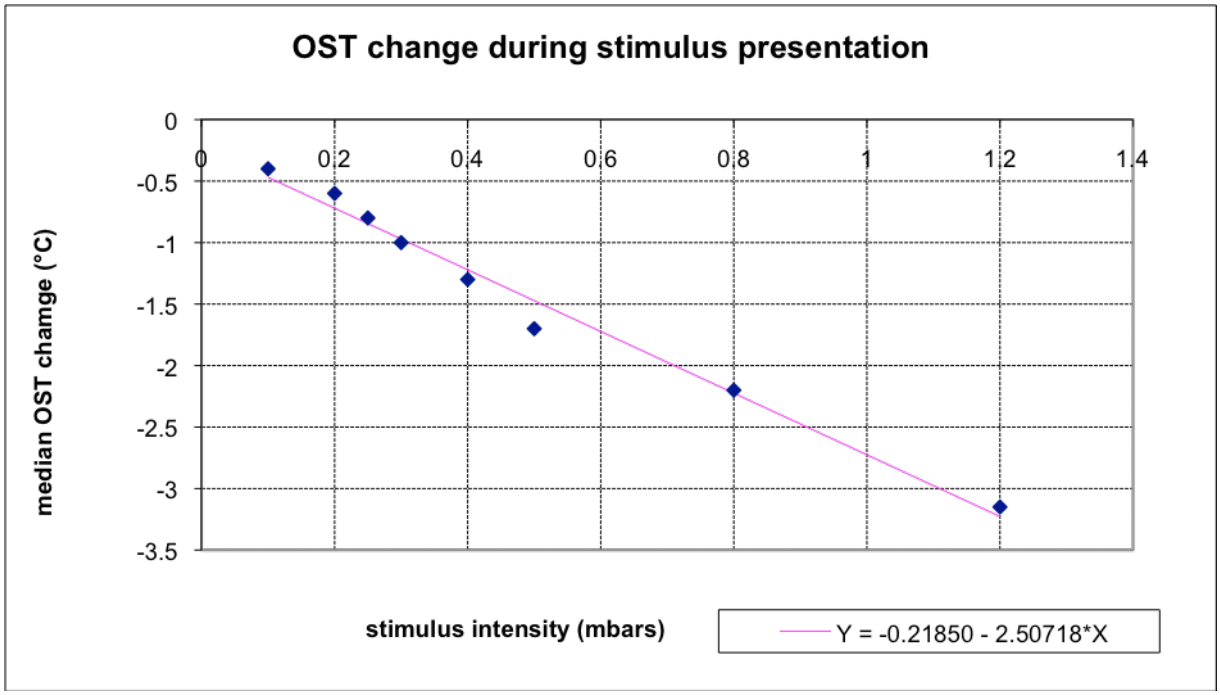

Figure 6.0.3: Median OST change during stimulus presentation with rising stimulus intensity after heating the ocular surface.

OST change during stimulus presentation								
Stimulus intensity (mbars)	0.1	0.2	0.25	0.30	0.40	0.50	0.80	1.20
Median OST change (°C)	-0.40	-0.60	-0.80	-1.00	-1.30	-1.70	-2.20	-3.15
Mean OST change ±standard deviation (°C)	-0.38 ±0.13	-0.70 ±0.44	-0.84 ±0.33	-1.00 ±0.39	-1.35 ±0.38	-1.62 ±0.58	-2.30 ±0.84	-4.73 ±1.03

Table 6.5: OST change during stimulus presentation with rising stimulus intensity after heating the ocular surface.

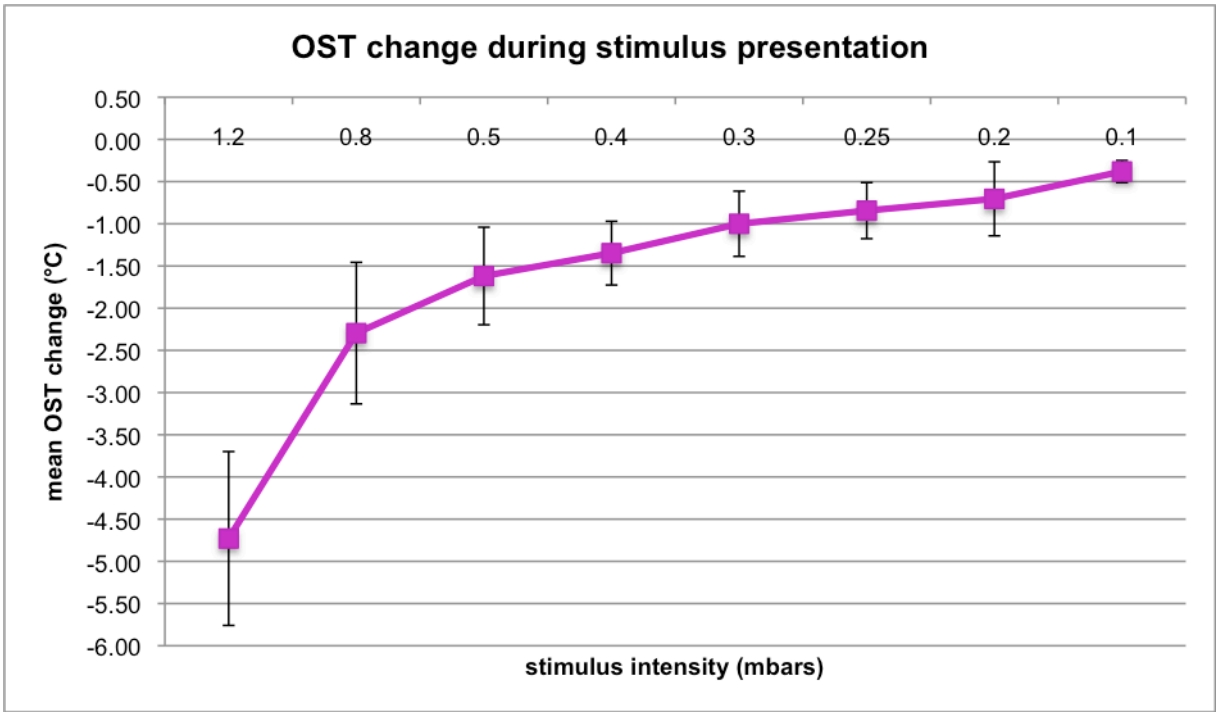

Figure 6.4: Mean OST change during stimulus presentation with rising stimulus intensity after heating the ocular surface.

6.3.2 Cooling of the ocular surface

The average ambient temperature in the testing room was 23.64±0.86°C and average ambient humidity was measured to be 46.02±13.10%. After completion of the cooling procedure, the first OST and CS measurements were carried out immediately after removal of the cooling mask. Mean central OST temperature change was -4.78°C and turned out to be statistically significant, compared to baseline OST ($p<0.001$). This decrease in OST was comparable to how it was recorded during the clinical study in Chapter 5 (-4.51°C). The increase in median CST (decrease in sensitivity) after the cooling period was found to be 0.05 mbars ($p=0.002$), which was less marked than the median difference of 0.10 mbars in the previous experiment, however it was the same median amount of change as after the heating procedure in this experiment.

A significant effect could be observed regarding tear film stability in this study ($p=0.012$ for NIBUT and $p=0.007$ for tear film stability grading), in contrast to the previous experiment (Chapter 5), where this measurement had been carried out much

later after the cooling procedure. However, no significant change in lipid layer could be recorded (p=0.264).

This finding, in contrast to the previous experiment can be explained by the fact that the tear film was assessed after the first OST and CST measurement immediately after the cooling period, whereas previously it was assessed after completion of the recovery period, at which time most of any possible tear film changes induced by the cooling period would have most probably disappeared. The median/interquartile range and mean (±standard deviation) values are summarised in Table 6.6, and the results for the statistical analysis are displayed in Table 6.7.

	Median / IR	**Mean±SD**
OSDI	10.40 / 4.20-14.60	9.35±5.10
Baseline CST (mbars)	0.30 / 0.20-0.35	0.29±0.08
CST after cooling procedure (mbars)	0.35 / 0.29-0.40	0.35±0.09
Baseline OST (°C) at the central cornea	34.60 / 34.38-34.90	34.56±0.64
OST at the central cornea after cooling procedure (°C)	29.80 / 28.80-30.50	29.78±1.78
Baseline NIBUT (secs)	20.70 / 10.05-41.08	30.73±27.95
NIBUT after cooling procedure (secs)	12.60 / 10.40-26.88	21.14±19.54
Baseline lipid pattern	3.00 / 2.00-4.00	3.07±1.44
Lipid pattern after cooling procedure	3.00 / 2.25-4.00	2.68±1.47
Baseline tear film stability	2.00 / 1.00-3.25	2.18±1.19
Tear film stability after cooling procedure	1.50 / 1.00-2.00	1.82±1.02
Aperture (mm)	10.50 / 9.50-11.00	10.25±1.06
TMH (mm)	0.20 / 0.15-0.30	0.22±0.07

Table 6.6: Median / Interquartile Range (IR) and Mean (±Standard Deviation) of the following measurements: OSDI (Ocular Surface Disease Index), central corneal sensitivity threshold (CST) at baseline and after the cooling procedure, central ocular surface temperature (OST) at baseline and after the cooling procedure, non-invasive tear break up time (NIBUT) at baseline and after the cooling procedure, lipid pattern grading at baseline and after the cooling procedure, tear film stability grading at baseline and after the cooling procedure, eye aperture and tear meniscus height (TMH).

	p-value	Z value / effect size r
CST	0.002	-3.026 / -0.40
OST	< 0.001	-4.542 / -0.61
NIBUT	0.012	-2.528 / -0.34
Lipid pattern	0.264	-1.147 / -0.15
Tear film stability	0.007	-1.852 / 0.25

Table 6.7: Wilcoxon signed-rank test for the effect of the cooling procedure on CST, OST, NIBUT and tear film quality.

6.3.2.1 OST change at CST during stimulus presentation

The median OST temperature difference during stimulus presentation at CS threshold before heating the ocular surface was found to be -0.60°C, and after the heating procedure it was greater with a median of OST change of -0.95°C. This means that a larger OST change was required, in order for the subjects to sense the stimulus after the cooling procedure, compared to what was required at baseline (p=0.003; Table 6.8). The effect size r was -0.39, which, according to Cohen's criteria represents a medium effect.

	OST difference at CS threshold at baseline	OST difference at CS threshold after cooling	Difference in OST change at baseline and after cooling	Statistical significance (Wilcoxon)
Median /IR	-0.60/ -0.83 – (-0.50)	-0.95 / -1.10 – (-0.60)	-0.10 / -0.40 – 0.00	p=0.003 (z=-2.930; effect size: r=-0.50)
Mean±SD	-0.68±0.26	-0.95±0.47	-0.21±0.42	

Table 6.8: OST difference during stimulus presentation at CS threshold before and after cooling the ocular surface (Wilcoxon signed rank test).

A two-tailed post hoc power calculation was carried out for the difference in OST at CS threshold and was found to be 0.70 (α=0.05; n=28; G*Power 3.1).

6.3.2.1 Correlations between OST difference and CST during stimulus presentation

The central CST at baseline (before cooling) showed a good and significant correlation with the median central OST difference ($r=0.722$, $p<0.01$, Spearman's test). However, this relationship was no longer significantly correlated, immediately after completion of the cooling procedure ($r=0.061$, $p>0.05$, Spearman's test). The scatterplots illustrate this better correlation before, and a poor correlation after, the cooling procedure (Figures 6.5 and 6.6).

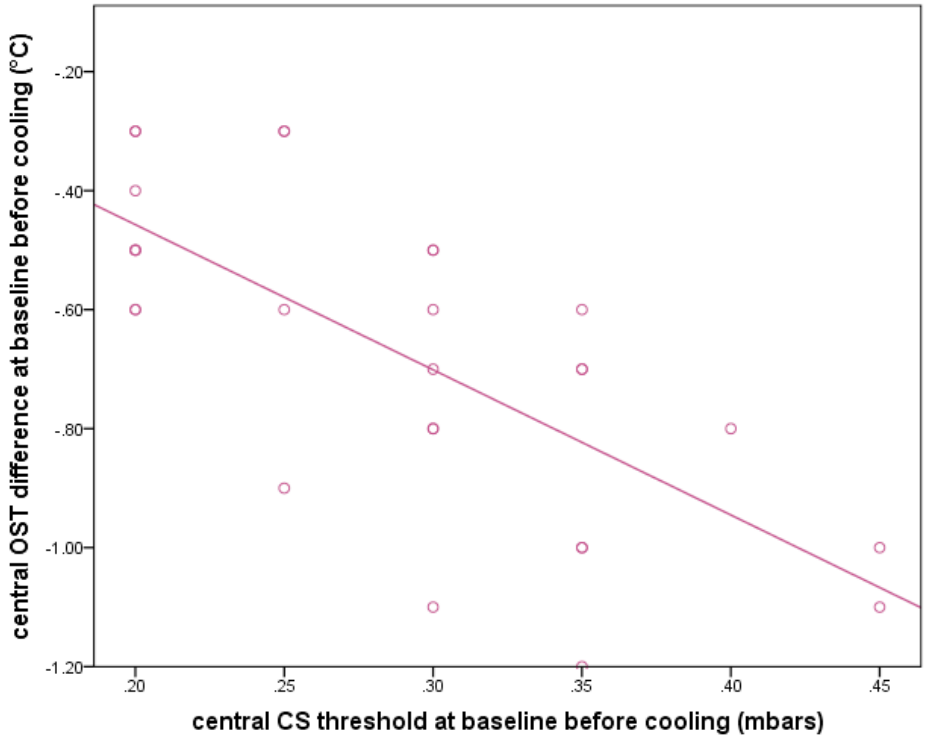

Figure 6.5: Scatterplot showing the correlation between the central CST (mbars) at baseline and central OST difference (°C) at baseline (before cooling the ocular surface).

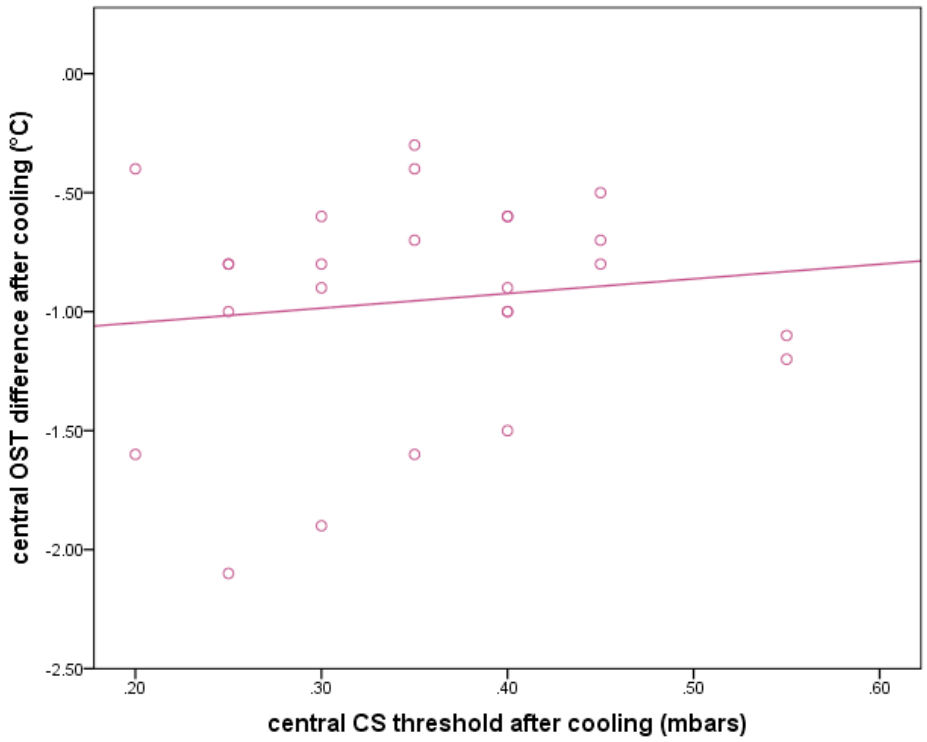

Figure 6.6: Scatterplot showing the correlation between central CST (mbars) and central OST difference (°C) after cooling the ocular surface.

6.3.2.2 OST change during stimulus presentation with varying stimulus intensities

The median OST during stimulus presentation showed a linear relationship to stimulus intensity (r^2=0.9604; Figure 6.7): with increasing stimulus intensity, a proportional median OST decrease could be observed. Compared to after the heating period, the inter-subject fluctuations were less marked at the higher stimulus intensities (0.80-1.20 mbars; Table 6.9 and Figure 6.8).

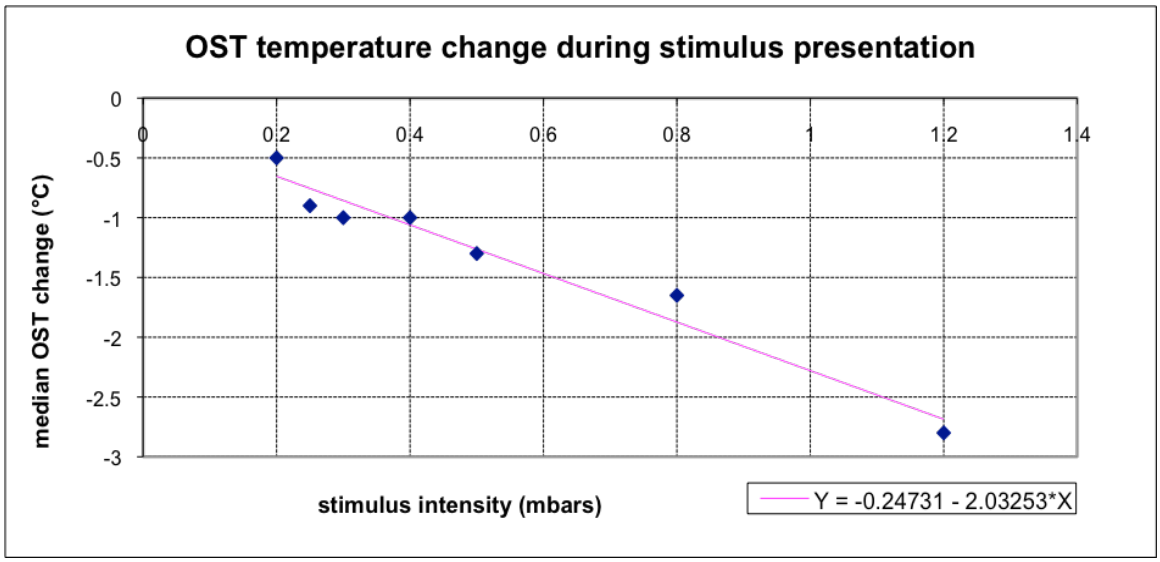

Figure 6.7: Median OST change during stimulus presentation with rising stimulus intensity after cooling the ocular surface.

Ocular Surface Temperature change during stimulus presentation							
Stimulus intensity (mbars)	0.20	0.25	0.30	0.40	0.50	0.80	1.20
Median OST change (°C)	-0.50	-0.90	-1.00	-1.00	-1.30	-1.65	-2.80
Mean OST change ± standard deviation (°C)	-0.80 ±0.58	-1.25 ±0.71	-1.29 ±0.81	-1.36 ±0.89	-1.47 ±0.78	-2.14 ±1.19	-2.97 ±1.20

Table 6.9: OST change during stimulus presentation with rising stimulus intensity after cooling the ocular surface.

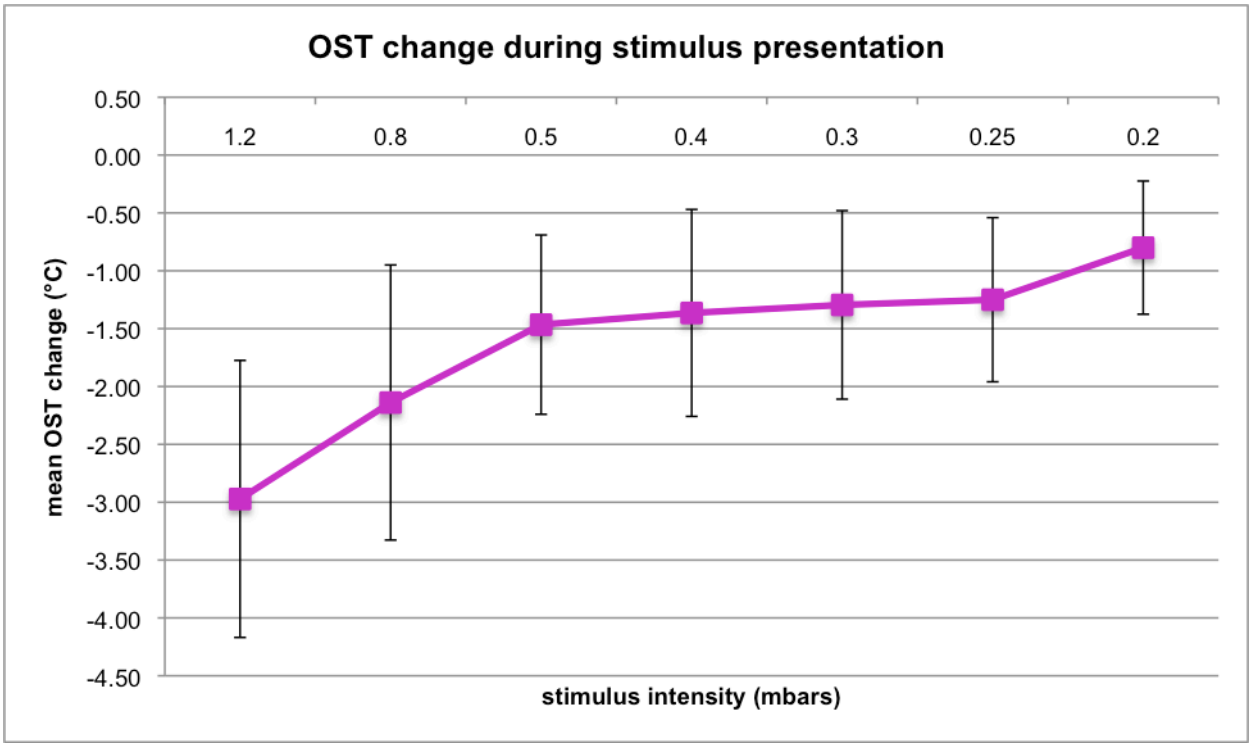

Figure 6.8: Mean OST change during stimulus presentation with rising stimulus intensity after cooling the ocular surface.

6.4 Discussion

This study explored the effect of heating and cooling of the ocular surface (with means of a lid warming device and a cooling mask) on its sensitivity to a cooling stimulus provided by the NCCA, as well as on tear film quality. In order to determine if this heating and/or cooling procedure affected the nervous activity of the superficial thermoreceptors, OST change was recorded during the presentation of the air-pulse stimulus to the ocular surface. The heating effect on the ocular surface in the current study was more marked on the larger sample size in the clinical study in Chapter 5 (mean difference of 0.95°C), however the cooling effect was slightly more marked in the current study than in the clinical study in Chapter 5 (mean difference of 0.27°C). These differences can be attributed to the subject variability and to a slightly lower ambient temperature during the current study, compared to the study in Chapter 5 (a mean difference of 1.18°C during the heating appointments and a mean difference of 1.12°C during the cooling appointments).

As in the previous study in Chapter 5, the ocular surface sensitivity threshold decreased after the heating procedure (suggesting an increased corneal sensitivity; Table 6.2), and it increased after the cooling procedure in the current study (suggesting a decrease in corneal sensitivity; Table 6.6).

However, the difference in median CST after both the heating and cooling procedures was only 0.05 mbars in the current study (representing the smallest measurable increment with the NCCA; Tables 6.2 and 6.6), compared to 0.10 mbars during the previous study in Chapter 5.

As a consequence of heating the ocular surface, the lipid pattern thickness increased significantly (Tables 6.2 and 6.3), which is in agreement with a study conducted by Bilkhu et al.[421] This finding, in contrast to the previous experiment (Chapter 5), can be explained by the fact that in the current study the tear film was assessed after the first OST and CST measurement, immediately after the heating period, whereas previously it was assessed after completion of the recovery period, at which time most of any possible tear film changes induced by the heating period would have most probably disappeared. Following the cooling period of the ocular surface during the current study, a statistically significant reduction in tear film stability and in NIBUT was noted (Tables 6.6 and 6.7).

When considering the OST change at CST after the heating, as well as the cooling period, no difference was noted at baseline (Tables 6.2 and 6.6), which suggests good repeatability for the CS measurement. Following heating or cooling of the ocular surface, a larger OST change was noted at CST compared to baseline, which was more marked after the cooling procedure (a median difference of -0.95°C OST change after cooling, and a median difference of -0.80°C after heating). This would suggest a lower ocular surface sensation immediately after both the heating and cooling procedure, as a greater OST decrease was required, before the subjects were able to sense the air-pulse stimulus. In view of the opposite effect of the heating/cooling procedure on tear film characteristics, this suggests that the tear film was not responsible for this apparent decrease in temperature sensitivity on the ocular surface. A good correlation between

stimulus intensity at CST and localised OST decrease could be observed at baseline, before the heating and cooling procedure respectively (Figures 6.1 and 6.5). Interestingly however, immediately after the heating/cooling procedure, this correlation was found to be poor (Figures 6.2 and 6.6). This appears to stand in direct contrast to the obtained linear relationship between stimulus intensity and the median OST change (Figures 6.3 and 6.7). One possible explanation may be the considerable inter-subject variability in OST change measurement after the heating/cooling procedure compared to baseline: the standard deviations for OST change at the CST doubled from 0.20°C to 0.44°C after the heating procedure, and from 0.26°C to 0.47°C after the cooling procedure (Tables 6.4 and 6.8).

The apparent decrease in temperature sensitivity on the ocular surface in the current study suggests that both heating and cooling of the ocular surface affected the ability of the thermoreceptors on the ocular surface to react to temperature change at their changed level of impulse frequency in a similar manner. After the heating procedure, these thermoreceptors may have been less reactive, maybe due to the temperature increase having reduced or even silenced their static nervous activity, as has been shown in electrophysiological studies.[29,30] Following the cooling procedure, the static nervous activity may have adapted to a higher level of impulse frequency,[29,30] rendering them possibly less reactive towards an additional cooling effect by the air gas stimulus. This finding does not confirm the hypothesis that these superficial corneal thermoreceptors should react similarly to cutaneous cold-sensitive receptors,[415,416] whose thermal detection threshold has not been observed to change after adaptation to an increased or decreased level of impulse frequency induced by temperature change.[417-419]

6.5 Conclusion

The findings of this study suggest that heating or cooling of the ocular surface affects the sensitivity of cold thermoreceptors in the superficial cornea. After both, an increase and a decrease of OST, a greater localised OST decrease induced by the air gas stimulus was necessary in order for it to be perceived by the subjects participating in this study.

This occurred despite the fact that the tear film lipid layer was increased after the heating procedure and decreased after the cooling procedure. If the tear film characteristics affected the CST measurements, the resulting real reduction in corneal temperature sensitivity would be likely to turn out lower after the heating procedure and equally higher after the cooling procedure. Indeed, a good correlation could be found between the CST measured with air gas aesthesiometry and tear film stability in Chapter 4.

CHAPTER 7

Summary and recommendations for future work

7.1 Verification of the stimulus characteristics of the Belmonte OPM aesthesiometer *in vitro* and *in vivo*

The aims were to evaluate if the Belmonte OPM pneumatic aesthesiometer provides a reliable stimulus to obtain accurate and repeatable corneal sensitivity measurements and to record stimulus temperature measurement of the Belmonte air gas aesthesiometer ‚Ocular pain meter' *in vitro* and *in vivo.*

The stimulus characteristics of the Belmonte OPM pneumatic aesthesiometer were investigated *in vitro* and *in vivo* in this project. Stimulus flow rate, air stimulus volume and force were recorded *in vitro*. Stimulus temperature was measured *in vitro* (using thermocouples) and *in vivo* (via a thermal infrared camera). The stimulus characteristics measured *in vitro* showed little variability and may therefore be considered as reliable. Stimulus temperature recorded *in vivo* showed that a change in stimulus flow rate produced a small, but statistically significant effect on ocular surface temperature (OST). Consequently, this air stimulus may not be described as being exclusively 'mechanical', since it provokes an additional response from the temperature sensitive C fibres. To truly remove any possible thermal effect from this 'mechanical' stimulus, stimulus temperature would need to be adjusted in synchronisation with the airflow. Moreover, in view of the physiological variation observed between subjects, some initial calibration step would be required that was able to assess the OST as the baseline for the stimulus, rather than the ambient room temperature. Previously, Murphy et al. hypothesised that the cooling of the tear film could be explained by an increased rate of evaporation as the air stimulus strikes the ocular surface, removing energy from the tear film and resulting in a temperature drop.[22] They explored if there was any accompanying mechanical deformation, by observing the tear film (after instillation of sodium fluorescein) with use of a slit lamp biomicroscope during air-pulse stimulation with an intensity of >10x stronger (5 mbars) than a normal threshold. Since no distortion in the tear film was observed, it was concluded that any possible surface deformation would play only a minor role and that the stimulation must primarily be a temperature change. In order to further explore if corneal deformation may be caused

during air gas aesthesiometry, the corneal surface was recorded during the air-pulse stimulus presentation of the non-contact corneal aesthesiomter (NCCA) by means of a high-speed camera (S-Motion High Speed) and a macro objective lens attached to provide a sufficient focus close-up, as part of this project. The maximum stimulus intensity of 9.20 mbars at the recommended distance of 10mm and perpendicular to the ocular surface was chosen, which represented nearly 20x the normal sensitivity threshold. A light source was placed onto the centre of the corneal surface at the point of stimulus arrival, causing a reflex at this location. If corneal deformation were to take place during stimulus presentation, it was expected to demonstrate a distortion of this reflex. However, no such distortion was observed. Consequently, Murphy et al.'s conclusion that the distortion component of the stimulus must be very small could be confirmed. Hence, future work should focus on the development of new aesthesiometer that is able to generate a true tactile stimulus – not generated by air - for mechanical ocular surface sensitivity measurement.

7.2 The relationship between corneal sensation, blinking, ocular surface temperature, tear film quality and degree of iris pigmentation

The aim was to explore the relationship between corneal sensation (using the cooling stimulus of the NCCA), blinking (spontaneous eye blink rate and inter-blink interval), ocular surface temperature (OST), tear film quality (non-invasive tear break up time and lipid pattern) and degree of iris pigmentation.

The relationship between corneal sensitivity threshold (CST), spontaneous eye blink-rate (SEBR), OST and tear film characteristics, (non invasive tear film break-up time (NIBUT) and tear film lipid pattern), were explored in this project. A moderate correlation between corneal sensitivity and blink frequency was established and a strong correlation between tear film quality, SEBR and OST was obtained, emphasising that ocular surface condition represents an important trigger for the initiation of a blink. One reason for the less strong correlation between CST and blink frequency than between NIBUT and SEBR in this study may be that the good feedback loop between NIBUT and the initiation of a blink in healthy eyes hinders the activation of superficial corneal

nerves. A more significant correlation between CST and blink frequency would be expected in eyes during the early stages of the dry eye disease process, where a sensitisation of the superficial corneal nerves and an increased SEBR have been reported.[326,396] However, the mechanisms involved in the initiation of an eye-blink are complex, as the local ocular sensory input only represents one trigger, next to other external influences and internal factors that are under cortical control. It would be interesting to further explore this matter in future work.

Additionally, the relationship between the degree of iris pigmentation and corneal sensitivity was explored. Since peripheral branching of sensory nerve axons depends on growth factors, such as NGF, and since some of the axons of polymodal sensory neurons supplying the cornea also branch into the iris, it has been speculated that melanocytes of the iris that possess trk receptors for NGF[407] may compete with the sensory nerve fibres for this neurotrophin. This may decrease the number of peripheral nerve terminals, including branches directed to the cornea, in a degree proportional to the iris pigmentation.[408] However, no relationship between the degree of iris pigmentation and corneal sensitivity could be established in this study.

7.3 The relationship between heating and cooling of the ocular surface on corneal sensitivity threshold

The aim was to investigate the relationship between heating and cooling of the ocular surface on ocular surface sensation, using the cooling stimulus of the NCCA.

The relationship between heating and cooling of the ocular surface on CST were investigated in this project. CST (attained using the NCCA), OST and tear film quality were obtained at baseline, and after increasing and decreasing OST (using a lid warming device or a cooling gel mask, respectively), until OST baseline level was reached again. Additionally, OST was recorded simultaneously during stimulus presentation at CST, immediately after heating and cooling of the ocular surface. After both, an increase and a decrease of OST, a greater localised OST decrease was required at CST. This means that heating or cooling of the ocular surface may affect the nervous activity (i.e. sensitivity) of the thermoreceptors in the superficial cornea. After the heating procedure, these thermoreceptors may have been less reactive, due to the

temperature increase having reduced or even silenced their static nervous activity, as has been shown in electrophysiological studies.[29,30] Following the cooling procedure, the static nervous activity may have adapted to a higher level of impulse frequency,[29,30] rendering them possibly less reactive towards an additional cooling effect by the air-pulse stimulus. This finding does not confirm the hypothesis that these superficial corneal thermoreceptors should react similarly to cutaneous cold-sensitive receptors,[415,416] whose thermal detection threshold has not been observed to change after adaptation to an increased or decreased level of impulse frequency induced by temperature change.[417-419] Future work could further explore the changes in nervous activity following a cooling and / or heating procedure on the ocular surface of eyes with ocular surface pathology, such as dry eye disease or with peripheral neurological degenerative disorders such as diabetes. Once a new aesthesiometer with a true tactile stimulus becomes available, it also would be very interesting to investigate sensory adaptation to mechanical stress such as during contact lens wear: what are the inter-individual differences and is there a correlation between contact lens discomfort and the degree of sensory adaptation?

7.4 Evaluation of the agreement in measurements between clinical studies in Chapters 4, 5 and 6

The aim was to evaluate baseline measurements obtained in Chapters 4-6, in view of the agreement in the results obtained.

The following baseline measurements were compared: CST measurement (with use of the NCCA) at baseline; NIBUT and tear film stability grading based on lipid pattern assessment at baseline; and OST measurement.

No statistical significance was observed regarding any of the repeated measurements carried out during the studies in Chapters 4 and 5. The measurements carried out during the study in Chapter 6 took place one year later and the sample size was considerably smaller. During the study in Chapter 6, the CST-, NIBUT-, and OST-measurements turned out to be statistically lower, and a non-statistically significant trend towards a lower tear film quality grading was observed. During this later study period, the ambient temperature was slightly lower (a mean difference of 1.18°C during the heating

appointments and a mean difference of 1.12°C during the cooling appointments), which may have most probably lead to a lower OST in this cohort of subjects. The time difference between the studies in Chapter 4 and 5, and the one in Chapter 6, as well as the smaller sample size in the study in Chapter 6 may contribute to the lower NIBUT measurements and tear film stability gradings. In study part A, a moderate to good correlation could be shown between NIBUT and both tear film quality and CS measurement, which may explain for the trend to a lower CST (i.e. higher corneal sensitivity) in the sample group of the study in Chapter 6.

These findings highlight the influence of environmental factors, such as room temperature, which should be considered for future studies during tear film and air gas aesthesiometry measurements.

CHAPTER 8

Appendices

8.1 Appendices for Chapter 3

8.1.1 Appendices for chapter 3.1.1.3

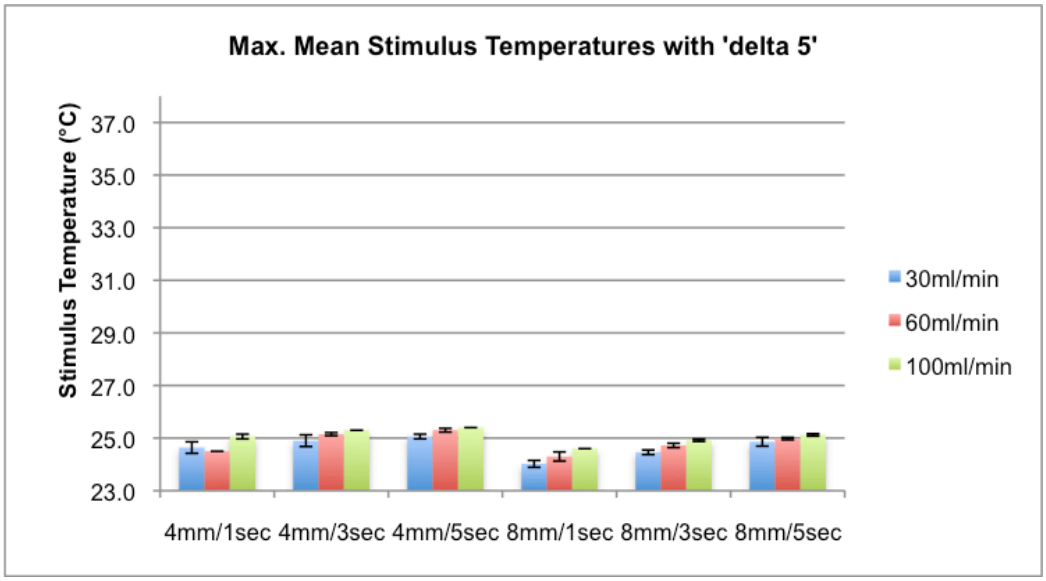

Figure 8.1: Maximum mean temperatures measured with 'delta 5'.

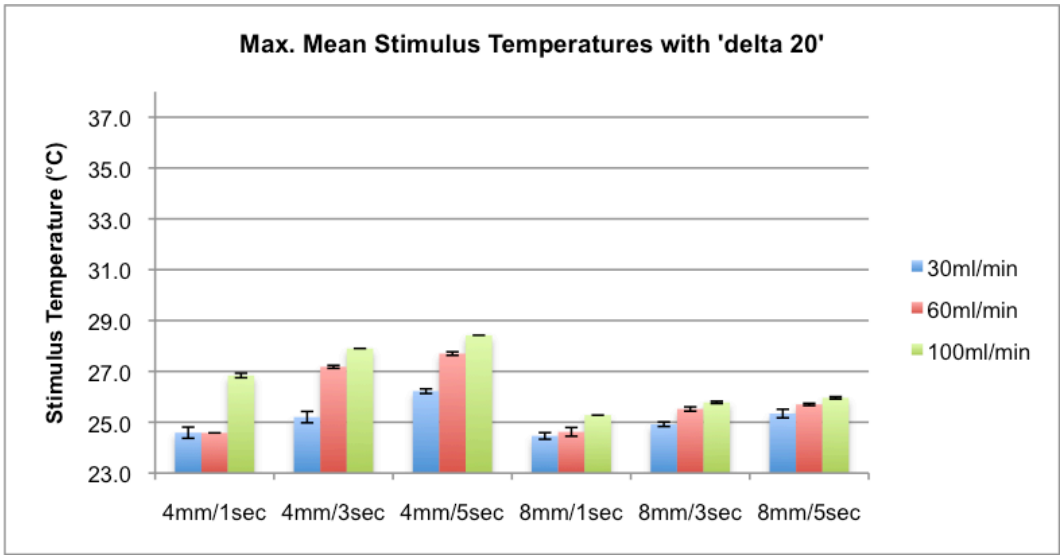

Figure 8.2: Maximum mean temperatures measured with 'delta 20'.

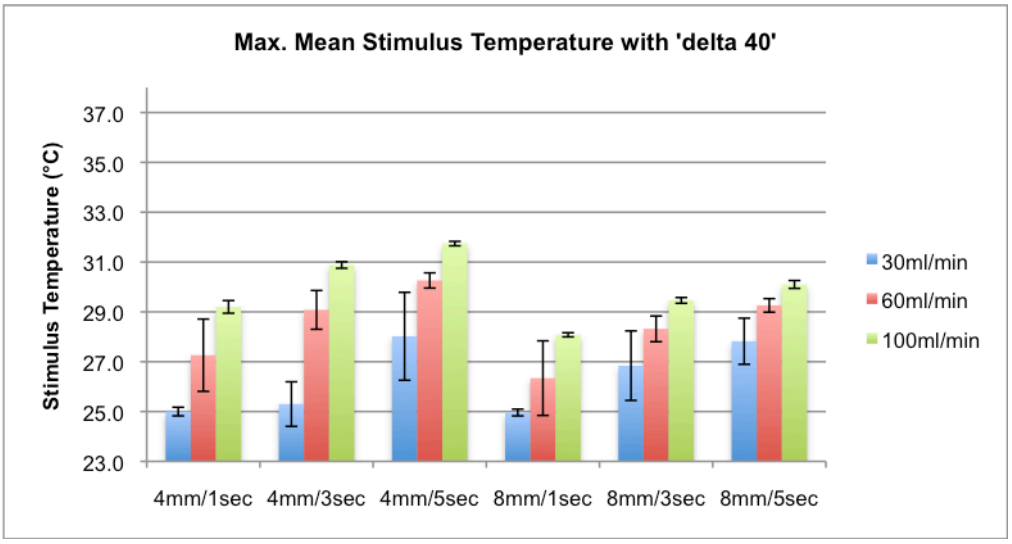

Figure 8.3: Maximum mean temperatures measured with 'delta 40'.

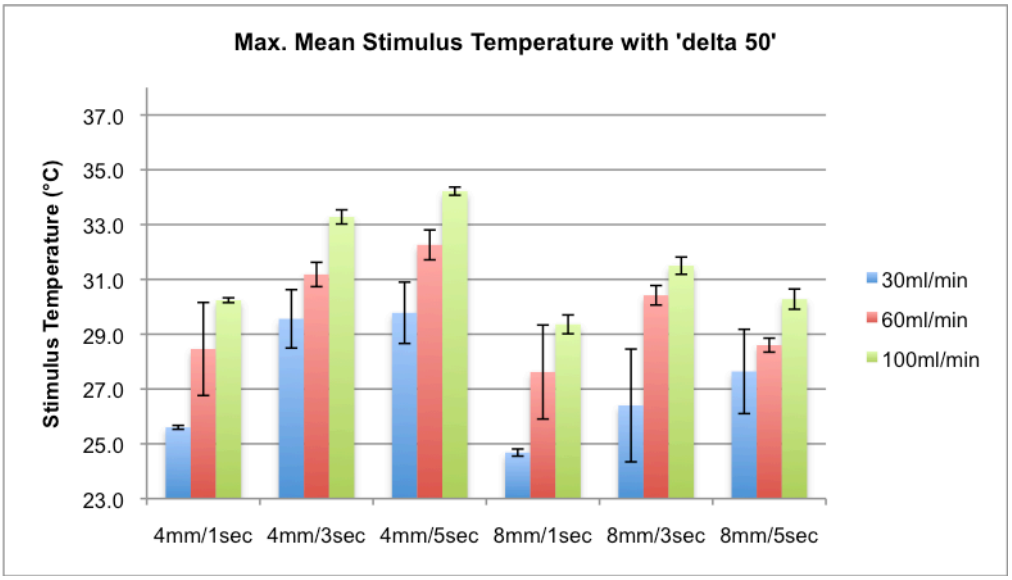

Figure 8.4: Maximum mean temperatures measured with 'delta 50'.

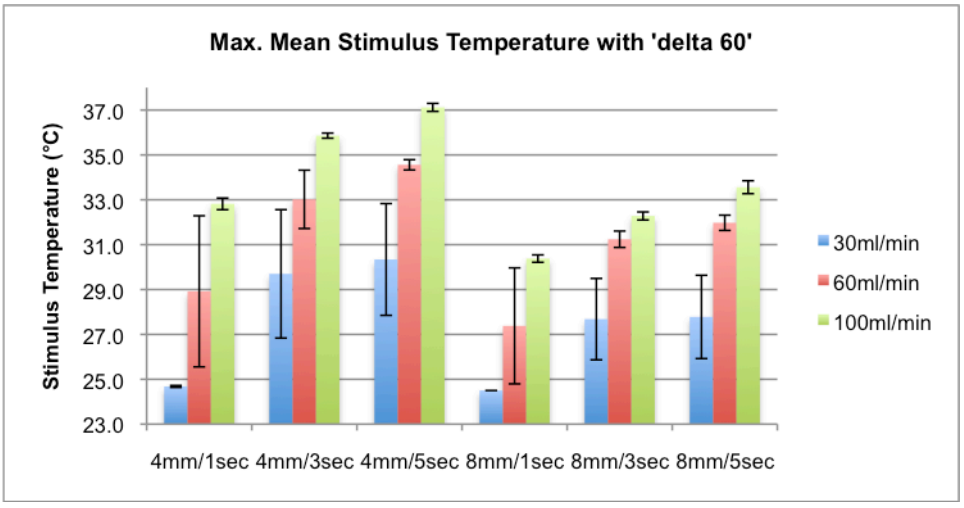

Figure 8.5: Maximum mean temperatures measured with 'delta 60'.

8.1.2 Appendix for chapter 3.2.2.3.1

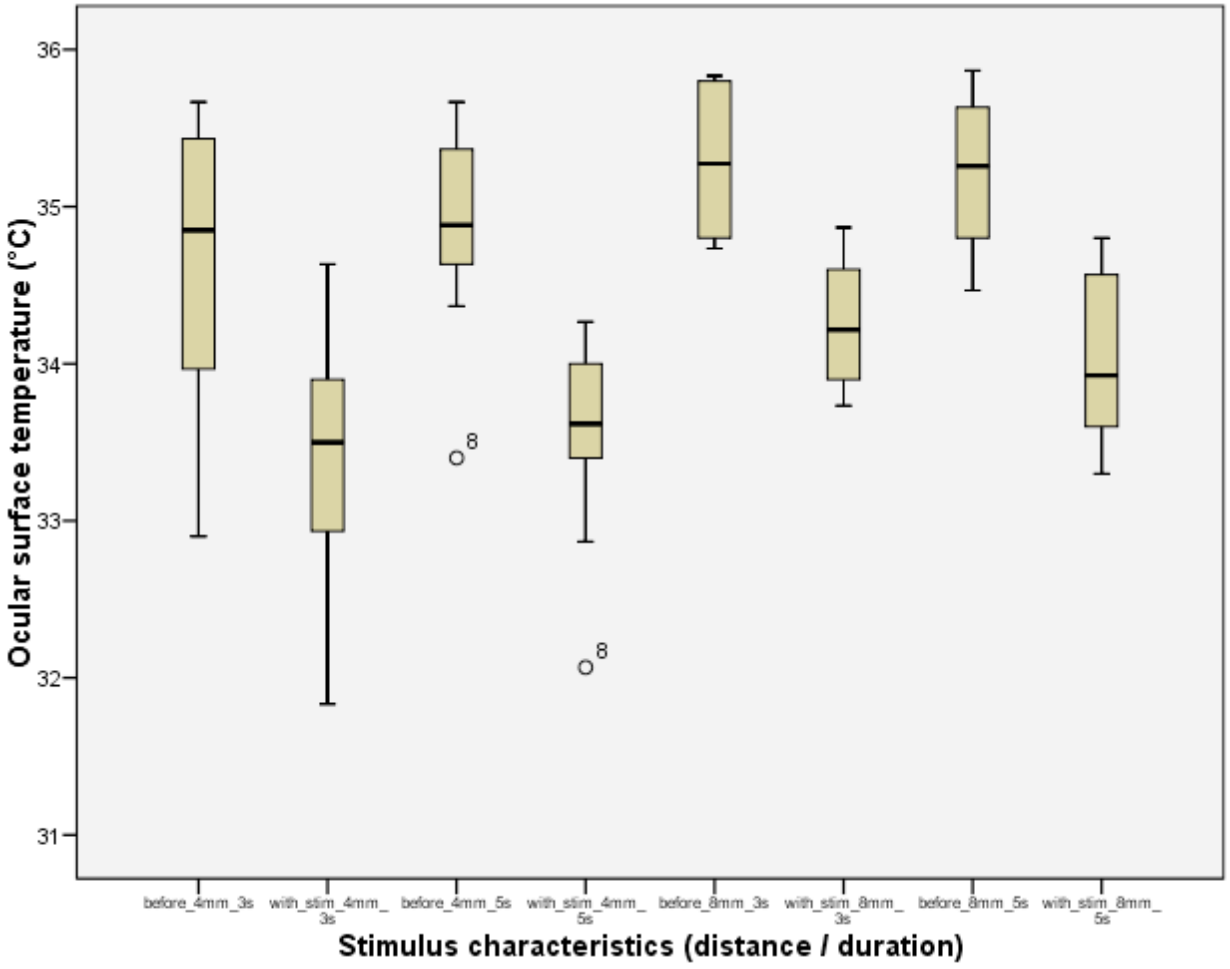

Figure 8.6: Boxplot analysis for OST with varying durations and distances to the ocular surface at baseline and during the presentation of a cooling stimulus.

8.1.3 Appendix for chapter 3.2.3.3.1

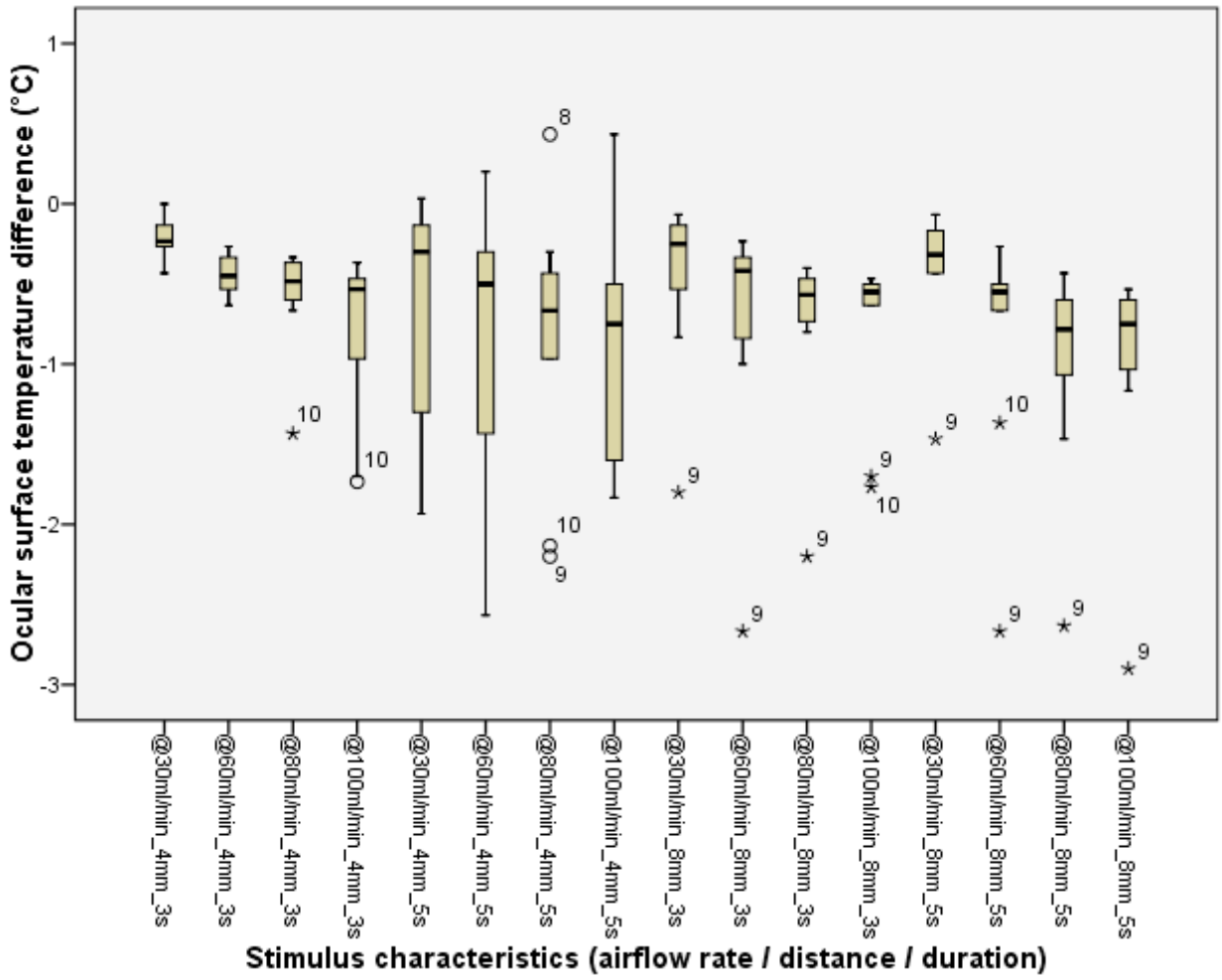

Figure 8.7: Boxplot analysis for OST difference with different durations and distances to the ocular surface during the presentation of a cooling stimulus at ‚delta 10'.

8.1.4 Ethics approval No. 1368

SCHOOL OF OPTOMETRY AND VISION SCIENCES

HUMAN SCIENCE ETHICAL COMMITTEE

CARDIFF UNIVERSITY
PRIFYSGOL CAERDYDD

Project Number: 1344

Project title: An investigation of the relationship between corneal sensation and blinking, non-invasive tear break up time, heating and cooling of the ocular surface.

Audit

Lead Investigators: Daniela Nosch
Investigators: Dr Paul Murphy, Prof Chris Purslow, Dr Heiko Pult, Dr Julie Albon

Date: 8th March 2013

With reference to the above application, I am pleased to confirm that approval has been granted. This ethical approval is granted subject to appropriate roles and responsibilities being identified and a signed agreement being put in place prior to the research commencing.

Please inform the Research Ethics Committee immediately of any changes to the protocol, changes to personnel involved, or of any unforeseen circumstances arising from the study.

Please note the data retention periods specified by the University

- For non-funded non-clinical research, data shall be retained for no less than 5 years, or 2 years post-publication
- Undergraduate project data shall be retained at least until the end of the University appeals process.

Signed:

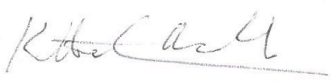

Dr Julie Albon
Chairperson

Approval form

8.1.4 Poster BCLA 2013

Is there a true Mechanical Stimulus with the Belmonte OPM Aesthesiometer?

Daniela S Nosch[1,2], Heiko Pult[1,3], Paul J Murphy[4], Christine Purslow[5]

[1]Contact Lens Anterior Eye Research Unit (CLEAR),School of Optometry and Vision Sciences, Cardiff University, Cardiff, UK; [2]Institute of Optometry, University of Applied Sciences Nordwestschweiz, Olten, Switzerland; [3]Dr. Heiko Pult –Optometry & Vision Research, Germany; [4]Optometry and Vision Sciences, University of Waterloo, Waterloo, Canada; [5]Optometry Department, Plymouth University, Plymouth, UK

Introduction

Air gas aesthesiometry overcomes some of the limitations of the 'gold standard', the Cochet-Bonnet aesthesiometer.[1, 2] However, for true mechanical corneal sensitivity measurement, the airflow stimulus temperature of the aesthesiometer must equal corneal temperature at the corneal surface, to avoid additional response from temperature-sensitive nerves.

Aim

The aim of this study was to record corneal surface temperature changes during the presentation of the air-stimulus with varying temperatures and pressures, using the Belmonte aesthesiometer (OPM).

Methods

Ocular surface temperature change was measured during air stimulus presentation of the OPM in 14 subjects (7 females, mean age 25.14±2.18 years), using a thermal infrared camera (FLIR A310; **Figures 1 and 2**).
Inclusion criteria were age younger than 40 years, no contact lens wear, absence of ocular disease including dry eye and no use of artificial tears on the day.
Room temperature was kept constant at 23.0-23.5°C. Each stimulus setting was applied to the ocular surface three times.

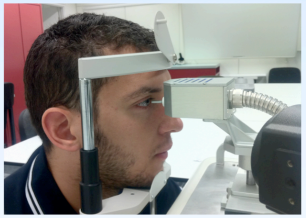

Figure 1: set-up of the thermal camera and aesthesiometer

First study period

6 subjects (2 males, age 25±2.37 years); ocular surface temperature change was recorded during stimulus presentation with rising levels of stimulus temperature, 4mm distance (nozzle to eye), 3s duration and the airflow rate set at 60ml/min.

Second study period

8 subjects (6 males, age 25.4±2.01 years); ocular surface temperature was recorded with stimulus temperatures most likely to match corneal surface temperature: room temperature +10 and +15°C (delta 10 and 15), with various stimulus characteristics (4 and 8mm distance; 3 and 5s duration; increasing airflow rates: 30, 60, 80 and 100ml/min).

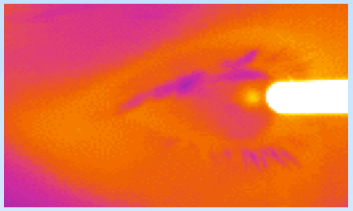

Figure 2: Localised Corneal Temperature during a heated air stimulus

Results

First study period

Ocular surface temperature changed with increasing stimulus temperatures / 'deltas' (**Figure 3 and Table 1**):

- a marked decrease with 'delta 3 and 5'
- a marginal decrease with 'delta 10'
- a marginal increase with 'delta 15'
- a marked increase with 'delta >15'.

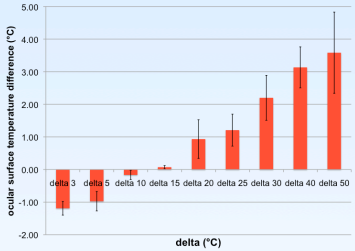

Figure 3: Results for ocular surface temperature changes with increasing levels of 'delta' and an airflow rate of 60ml/min

delta	n	temperature before stimulus (C°)	temperature with stimulus (C°)	temperature difference (C°)
3	6	34.99±0.67	33.82±0.73	-1.17±0.22
5	6	35.23±0.68	34.26±0.49	-0.97±0.30
10	6	35.30±0.80	35.10±0.70	-0.20±0.13
15	6	36.24±0.45	36.32±0.42	+0.08±0.05
20	6	36.52±0.57	37.28±0.58	+0.77±0.43
30	6	36.98±0.53	39.09±1.17	+2.11±0.82
40	6	37.44±0.67	40.60±1.30	+3.16±0.68

Table 1: Ocular surface temperature changes with increasing levels of 'delta' and a fixed airflow rate of 60ml/min

Second Study Period

'Delta' set at 10 (room temperature +10°C)

A small but statistically significant decrease in ocular surface temperature was noted for all stimulus characteristics (**Figure 4**; two-way ANOVA: p=0.000, F=50.50 for 4mm/3s; p=0.021, F=8.70 for 4mm/5s; p=0.000, F=84.65 for 8mm/3s; p=0.000, F=160.60 for 8mm/5s).

Ocular surface temperature changes were more pronounced with the shorter distance of 4mm, the longer duration of 5s and increasing airflow rates.

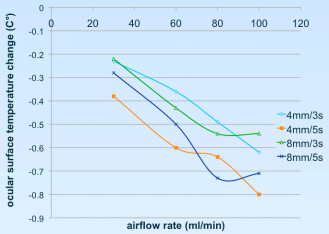

Figure 4: Mean ocular surface temperature change with 'delta 10'

'Delta' set at 15 (room temperature +15°C)

Ocular surface temperature increased with all stimulus characteristics (but less than with 'delta 10', **Figure 5**).
This difference was statistically significant for the overall group at the shorter distance of 4mm (two-way ANOVA: p=0.000, F=97.95 for 4mm/3s; p=0.000, F=63.72 for 4mm/5s), but not for the longer distance of 8mm (two-way ANOVA: p=0.698, F=0.164 for 8mm/3s; p=0.522, F=0.455 for 8mm/5s).

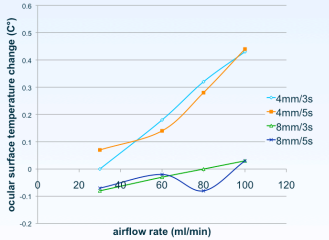

Figure 5: Mean ocular surface temperature change with 'delta 15'

At the shorter distance of 4mm, the ocular surface temperature changes were statistically significant for all levels of airflow rates during the shorter (3s) and the longer (5s) stimulus durations with increasing levels of airflow rates, except for the airflow rate of 30 ml/min with the 3s stimulus duration (**Tables 1 and 2**).

airflow (ml/min)	n	temperature before stimulus (C°)	temperature with stimulus (C°)	temperature difference (C°)	p-value (paired t-test)
30	14	35.24±0.79	35.24±0.78	0.00±0.07	1.000
60	14	35.09±0.75	35.27±0.75	0.18±0.17	0.002
80	14	35.16±0.82	35.47±0.83	0.32±0.13	0.000
100	14	35.17±0.87	35.59±0.92	0.43±0.10	0.000

Table 1: Mean ocular surface temperature change for **4mm / 3s**.

airflow (ml/min)	n	temperature before stimulus (C°)	temperature with stimulus (C°)	temperature difference (C°)	p-value (paired t-test)
30	8	34.74±0.56	34.81±0.56	+0.07±0.06	0.012
60	8	34.83±0.53	34.97±0.54	+0.14±0.09	0.003
80	8	34.91±0.49	35.19±0.47	+0.28±0.11	0.000
100	8	34.90±0.55	35.34±0.54	+0.44±0.10	0.000

Table 2: Mean ocular surface temperature change for **4mm / 5s**.

Conclusion

Although stimulus temperature was set to produce no temperature change on the corneal surface, the need to vary stimulus-airflow to change stimulus intensity, produced a small, but statistically significant effect on corneal surface temperature. Consequently, this air stimulus may not be exclusively 'mechanical', exciting only A-δ fibres sensitive to deformation, but may also have an additional response from the temperature-sensitive C fibres.

References

1. Murphy PJ, Patel S, Marshall J. A new non-contact corneal aesthesiometer (NCCA). Ophthalmic Physiol Opt. 1996 Mar 16(2):101-7.
2. Belmonte C, Acosta MC, Schmelz M, Gallar J. Measurement of corneal sensitivity to mechanical and chemical stimulation with a CO2 esthesiometer. Invest Ophthalmol Vis Sci. 1999 Feb;40(2): 513-9.

Contact / Poster Download

daniela.nosch@fhnw.ch

8.2 Appendices for Chapter 4-6

8.2.1 Ethics approval number 1344

SCHOOL OF OPTOMETRY AND VISION SCIENCES

HUMAN SCIENCE ETHICAL COMMITTEE

CARDIFF UNIVERSITY
PRIFYSGOL CAERDYDD

Project Number: 1344

Project title: An investigation of the relationship between corneal sensation and blinking, non-invasive tear break up time, heating and cooling of the ocular surface.

Audit

Lead Investigators: Daniela Nosch
Investigators: Dr Paul Murphy, Prof Chris Purslow, Dr Heiko Pult, Dr Julie Albon

Date: 8th March 2013

With reference to the above application, I am pleased to confirm that approval has been granted. This ethical approval is granted subject to appropriate roles and responsibilities being identified and a signed agreement being put in place prior to the research commencing.

Please inform the Research Ethics Committee immediately of any changes to the protocol, changes to personnel involved, or of any unforeseen circumstances arising from the study.

Please note the data retention periods specified by the University

- For non-funded non-clinical research, data shall be retained for no less than 5 years, or 2 years post-publication
- Undergraduate project data shall be retained at least until the end of the University appeals process.

Signed:

Dr Julie Albon
Chairperson

Approval form

8.2.2 Approval of amendments to ethics approval number 1344

School of Optometry and Vision Sciences
Ysgol Optometreg a Gwyddorau'r Golwg

Head of School *Pennaeth Yr Ysgol* Professor *Yr Athro* Marcela Votruba

College of Biomedical and Life Science
Cardiff University
Maindy Road
Cardiff
CF24 4HQ
Wales UK

Tel *Ffôn* +44(0)29 2087 4374
Fax *Ffacs* +44(0)29 2087 4859
http://www.cardiff.ac.uk/optom/

Prifysgol Caerdydd
Heol Maindy
Caerdydd
CF24 4HQ
Cymru, Y Deyrnas Gyfunol

SCHOOL RESEARCH ETHICS AUDIT COMMITTEE

Project Number: 1344

Project title: An investigation of the relationship between corneal sensation and blinking, non-invasive tear break up time, heating and cooling of the ocular surface.

Lead Investigator(s): Daniella Nosch

Date: 27th April 2014 **Project expiry date:** 31.12.14

With reference to the above application, I am pleased to confirm that the request to amend the above ethics application has been granted.

The amendments are:

i) Extension of the study expiry to 31st Dec 2014
ii) recall of some patients of study 1344 to attend on 2 further occasions
iii)repeat some measures e.g. NIBUT and simultaneously measure OST at CS threshold
iv) an additional procedure: measurement of apical aperture with the aid of a slit lamp.

Please remember that the ethical approval for this project was granted subject to appropriate roles and responsibilities being identified and a signed agreement being put in place prior to the research commencing. These will also apply to the current amendment(s).

Please inform the School Research Ethics Audit Committee immediately of any further changes to the protocol, personnel involved, or of any unforeseen circumstances arising from the study.

Please note the data retention periods specified by the University

- For non-funded non-clinical research, data shall be retained for no less than 5 years, or 2 years post-publication
- Undergraduate project data shall be retained at least until the end of the University appeals process

Signed:

Dr Ashley Wood
On behalf of SREAC

Approval form 2014_1905

8.3 Evaluation of the agreement in measurements between the clinical studies in Chapters 4, 5 and 6

The following baseline measurements were evaluated in view of the agreement in the results obtained: corneal sensitivity threshold (CST) measurement with use of the NCCA air gas aesthesiometer; non-invasive tear break up time (NIBUT) and tear film stability grading based on the lipid pattern assessment, both with the use of the Keeler Tearscope Plus; ocular surface temperature (OST) measurement with use of a thermal camera (FLIR A310).

8.3.1 Statistical analysis

CST, NIBUT, lipid pattern and OST measurements were carried out at baseline during the clinical studies in Chapters 4, 5 and 6. Because the data were not normally distributed, the non-parametric Friedman test with multiple comparisons was applied (BIAS Version 9.11, 2011). For comparison of the data of the studies in chapter 4 and 5 with the data of the study in chapter 6, only the 28 subjects participating in all three study parts were considered, i.e. the 14 subjects participating in the studies of the Chapters 4 and 5 but not in the study in Chapter 6, were not considered for the comparison of the data of the study of Chapter 6 with the data of the studies in Chapters 4 and 5. This ensured the comparison of data with equal sample sizes. In cases of statistical significance obtained with the Friedman test, post hoc comparisons were carried out, whereby the p-values were corrected with the Bonferroni-Holm test. Additionally, boxplots were generated, in order to graphically show the differences in CS, NIBUT, OST and tear film stability grading at baseline of the study in Chapter 4 and at baseline before the heating and cooling periods in Chapters 5 and 6 (SPSS, Version 20).

8.3.2 Agreement in corneal sensitivity measurement

No statistically significant difference in measurements were noted between the studies in Chapters 4 and 5, and between the two CST baseline measurements within the study period of Chapter 5 ($p=0.184$; Friedman's $Chi^2=3.389$). When including the measurements carried out in the study of Chapter 6 (with the reduced sample size of n=28), a statistically significant difference was noted between the results for the studies

in Chapter 4 and 5 and the study in Chapter 6 (p=0.001; Friedman's Chi^2=17.937), confirming a trend to a decrease in CSTs in the study in Chapter 6 compared to the studies in Chapters 4 and 5 (Table 8.2). Regarding the differences between the individual measurement periods, statistical significance was reached between the CST measurement during the study in Chapter 4 and the baseline CST measurement in the study in Chapter 6 before the heating procedure (p=0.015; Table 8.1). Furthermore, the pair comparisons between the CST measurement of the study in Chapter 5 at baseline before heating and the CST measurement of the study in Chapter 6 at baseline before heating and between the CST measurement of the study in Chapter 5 at baseline before cooling and the CST measurement of the study in Chapter 6 at baseline before heating were statistically significant (p=0.007 and p=0.014, respectively). However, the baseline CST measurements before the heating/cooling procedure during the study in Chapter 6 did not differ statistically from each other. The results of the statistical analysis for the pair comparisons are summarised in Table 8.1.

CST measurement	t-value	df	p-value (corrected with Bonferroni-Holm)
study of Ch.4 vs. study of Ch.6 before heating	3.1934	96	0.015
study of Ch. 4 vs. study of Ch.6 before cooling	2.3806	96	0.099
study of Ch. 5 before heating vs. study of Ch. 6 before heating	3.4838	96	0.007
study of Ch. 5 before heating vs. study of Ch. 6 before cooling	2.6709	96	0.062
study of Ch.5 before cooling vs. study of Ch.6 before heating	3.2515	96	0.014
study of Ch. 5 before cooling vs. study of Ch.6 before cooling	2.4386	96	0.994
study of Ch.5 before heating vs. study of Ch.6 before cooling	0.8129	96	1.000

Table 8.1: Multiple Friedman test with post-hoc Bonferroni-Holm correction for the CST measurements during the studies in Chapters 4,5 and 6.

	CST (mbars) study of Ch.4	CST (mbars) study of Ch.5 before heating	CST (mbars) study of Ch.5 before cooling	CST (mbars) study of Ch.6 before heating	CST (mbars) study of Ch.6 before cooling
Median / IR	0.35 / 0.30-0.40	0.35 / 0.30-0.40	0.30 / 0.30-0.35	0.275 / 0.25-0.31	0.30 / 0.20-0.35
Mean± SD	0.35±0.98	0.35±0.09	0.34±0.09	0.29±0.07	0.29±0.08

Table 8.2: Overview of the CST measurements during the studies in Chapters 4,5 and 6 at baseline.

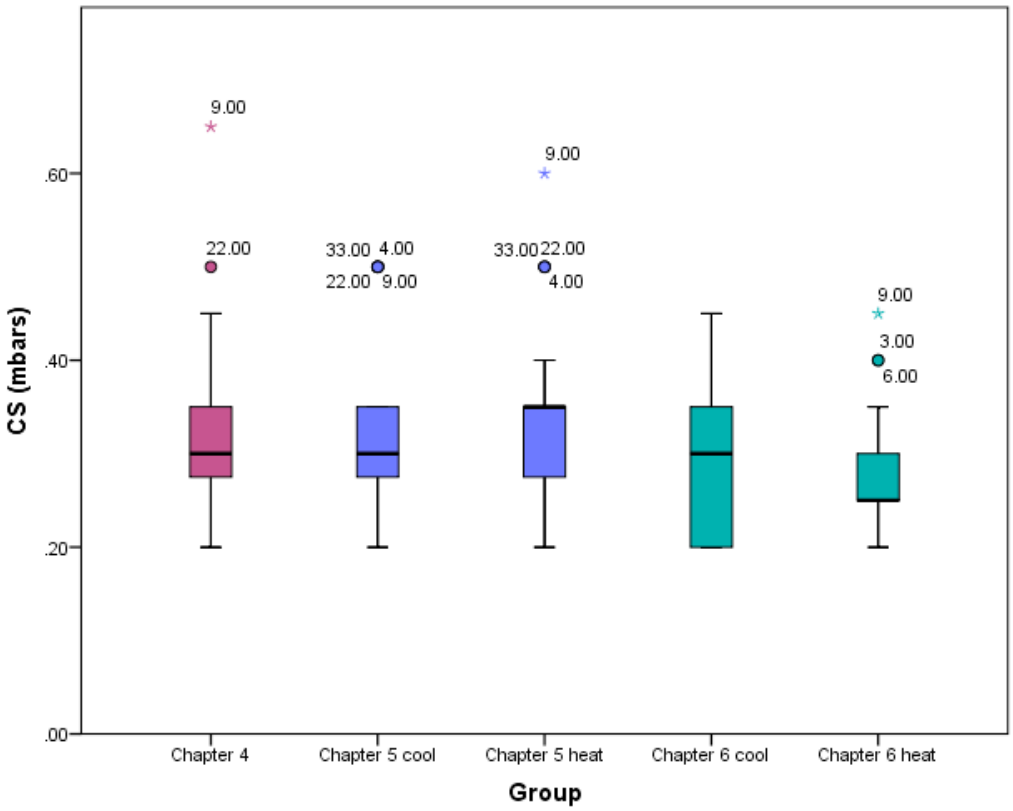

Figure 8.8: Boxplots for the CST measurements at baseline during the studies in Chapters 4, 5 and 6.

8.3.3 Agreement in NIBUT measurements

On overall comparison between the NIBUT measurements in study part A and the baseline NIBUT measurements in the study of Chapter 5 just about reached statistical significance ($p=0.046$; Friedman's $Chi^2=6.143$). However, individual comparisons between these NIBUT measurements did not reach statistical significane, applying the post hoc Bonferroni-Holm correction (Table 8.3).

NIBUT measurement	t-value	df	p-value (corrected with Bonferroni-Holm)
study of Ch.4 vs. study of Ch.5 before heating	0.3359	82	0.738
study of Ch.4 vs. study of Ch.5 before cooling	2.3515	82	0.063
study of Ch.5 before heating vs. study of Ch.5 before cooling	2.0155	82	0.094

Table 8.3: Post-hoc comparisons of NIBUT measurements during the studies in Chapters 4 and 5, with Bonferroni-Holm correction.

When including the measurements carried out during the study in Chapter 6, a statistically significant difference was noted between the results for the studies in the Chapters 4 and 5 and the study in Chapter 6 ($p<0.001$; Friedman's $Chi^2=19.986$), confirming a trend to a decrease in NIBUT measurements in the study of Chapter 6 compared to the studies in Chapter 4 and 5 (Table 8.5). Regarding the differences between the individual measurement periods, statistical significance was reached between the NIBUT measurement during the study in Chapter 4 and the two baseline NIBUT measurement in the study of Chapter 6 ($p=0.001$ for the study in Chapter 6 before the heating procedure and $p=0.041$ for the study in Chapter 6 before the cooling procedure). Furthermore, the pair comparison between the NIBUT measurement in the study of Chapter 5 at baseline before heating and the NIBUT measurement in the study of Chapter 6 at baseline before heating was statistically significant ($p=0.003$). However, the baseline NIBUT measurements before the heating/cooling procedure during the study of Chapter 6 did not differ statistically from each other. The results of the statistical analysis for the pair comparisons are summarised in Table 8.4.

NIBUT measurement	t-value	df	p-value (corrected with Bonferroni-Holm)
study in Ch.4 vs. study in Ch.6 before heating	4.0505	108	0.001
study in Ch.4 vs. study in Ch.6 before cooling	2.8538	108	0.041
study in Ch.5 before heating vs. study in Ch.6 before heating	3.7283	108	0.003
study in Ch.5 before heating vs.. study in Ch.6 before cooling	2.5316	108	0.090
study in Ch.5 before cooling vs.. study in Ch.6 before heating	1.8411	108	0.309
study in CH.5 before cooling vs.. study in Ch.6 before cooling	0.6444	108	1.000
study in CH.6 before heating vs.. study in Ch.6 before cooling	1.1967	108	0.702

Table 8.4: Multiple Friedman test with post-hoc Bonferroni-Hom correction for the NIBUT measurements during the studies in Chapters 4, 5 and 6.

	NIBUT (secs) study in Ch.4	NIBUT (secs) study in Ch.5 before heating	NIBUT (secs) study in Ch.5 before cooling	NIBUT (secs) study in Ch.6 before heating	NIBUT (secs) study in Ch.6 before cooling
Median / IR	34.55 / 12.45-53.80	32.40 / 13.97-53.62	25.90 / 16.65-40.77	18.60 / 10.85-26.77	20.70 / 10.05-41.08
Mean± SD	38.58±28.62	39.48±30.03	36.78±30.75	26.66±26.49	30.73±27.95

Table 8.5: Overview of the NIBUT measurements during the studies in Chapters 4, 5 and 6 at baseline.

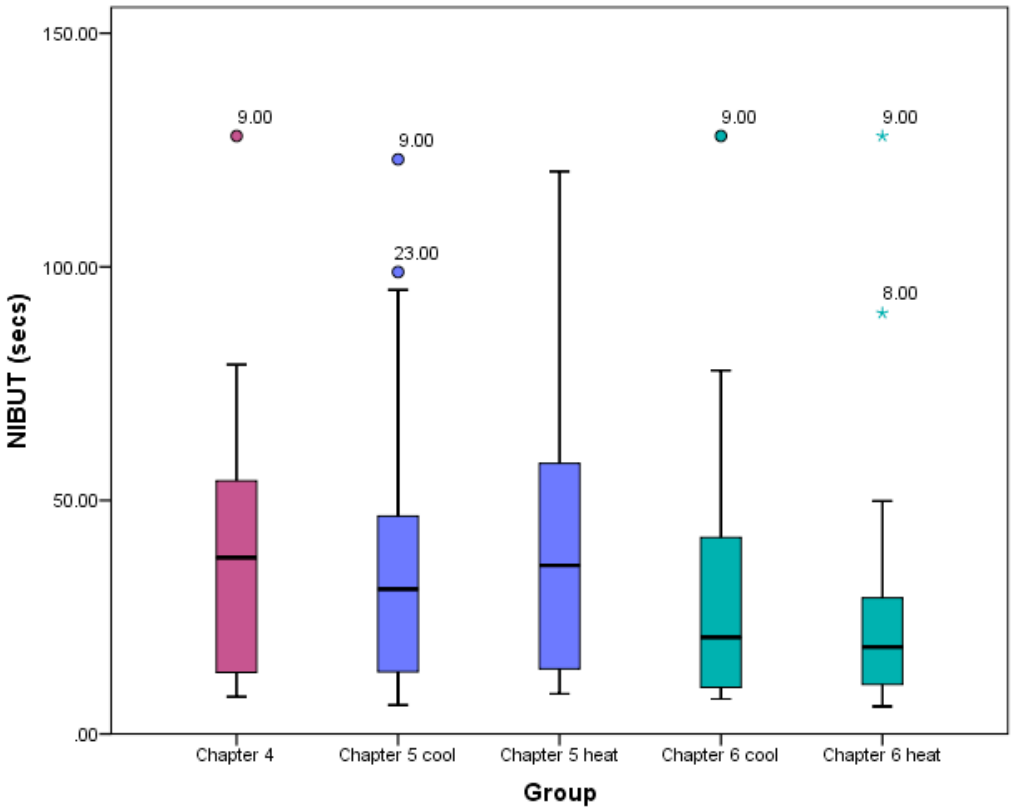

Figure 8.9: Boxplots for the NIBUT measurements at baseline during the studies in Chapters 4, 5 and 6.

8.3.4 Agreement in OST measurements

No statistically significant difference in measurements were noted between the studies in Chapters 4 and 5, and between the two OST baseline measurements within the study in Chapter 5 ($p=0.054$; Friedman's $Chi^2=5.851$). When including the measurements carried out in the study in Chapter 6, a statistically significant difference was noted between the results for the studies in Chapters 4 and 5, and the study in Chapter 6 ($p<0.001$; Friedman's $Chi^2=29.521$), confirming a trend to a decrease in OST thresholds in the study in Chapter 6 compared to the studies in Chapters 4 and 5 (Table 8.7). Regarding the differences between the individual measurement periods, statistical significance was reached between the OST measurement during the study in Chapter 4 and the two baseline OST measurement in the study in Chapter 6 ($p=0.002$ for the study in Chapter 6 before the heating procedure and $p<0.001$ for the study in Chapter 6 before the cooling procedure). Furthermore, the pair comparison between the OST measurement in the study in Chapter 5 at baseline before heating and the OST measurement in the study in Chapter 6 at baseline before heating and before cooling

were statistically significant ($p<0.001$ for baseline OST in study period before heating and $p<0.001$ before cooling, respectively). However, the baseline OST measurements before the heating/cooling procedure during the study in Chapter 6 did not differ statistically from each other. The results of the statistical analysis for the pair comparisons are summarised in Table 8.6.

OST measurement	t-value	df	p-value (corrected with Bonferroni-Holm)
study in Ch.4 vs. study in Ch.6 before heating	3.8163	108	0.002
study in Ch.4 vs. study in Ch.6 before cooling	4.5991	108	<0.001
study in Ch.5 before heating vs. study in Ch.6 before heating	4.0609	108	<0.001
study in Ch.5 before heating vs.. study in Ch.6 before cooling	4.8438	108	<0.001
study in Ch.5 before cooling vs.. study in Ch.6 before heating	1.2232	108	0.672
study in Ch.5 before cooling vs.. study in Ch.6 before cooling	2.0060	108	0.189
study in Ch.6 before heating vs.. study in Ch.6 before cooling	0.7828	108	0.871

Table 8.6: Multiple Friedman test with post-hoc Bonferroni-Holm correction for the OST measurements during studies in Chapters 4,5 and 6.

	OST (°C) study in Ch.4	OST (°C) study in Ch.5 before heating	OST (°C) study in Ch.5 before cooling	OST (°C) study in ch.6 before heating	OST (°C) study in Ch.6 before cooling
Median / IR	35.15 / 34.58-35.50	35.20 / 34.45-35.52	35.00 / 34.50-35.40	34.75 / 34.50-35.00	34.60 / 34.38-34.90
Mean± SD	34.98±0.68	35.00±0.72	34.87±0.68	34.73±0.52	34.56±0.64

Table 8.7: Overview of the OST measurements during the studies in Chapters 4,5 and 6 at baseline.

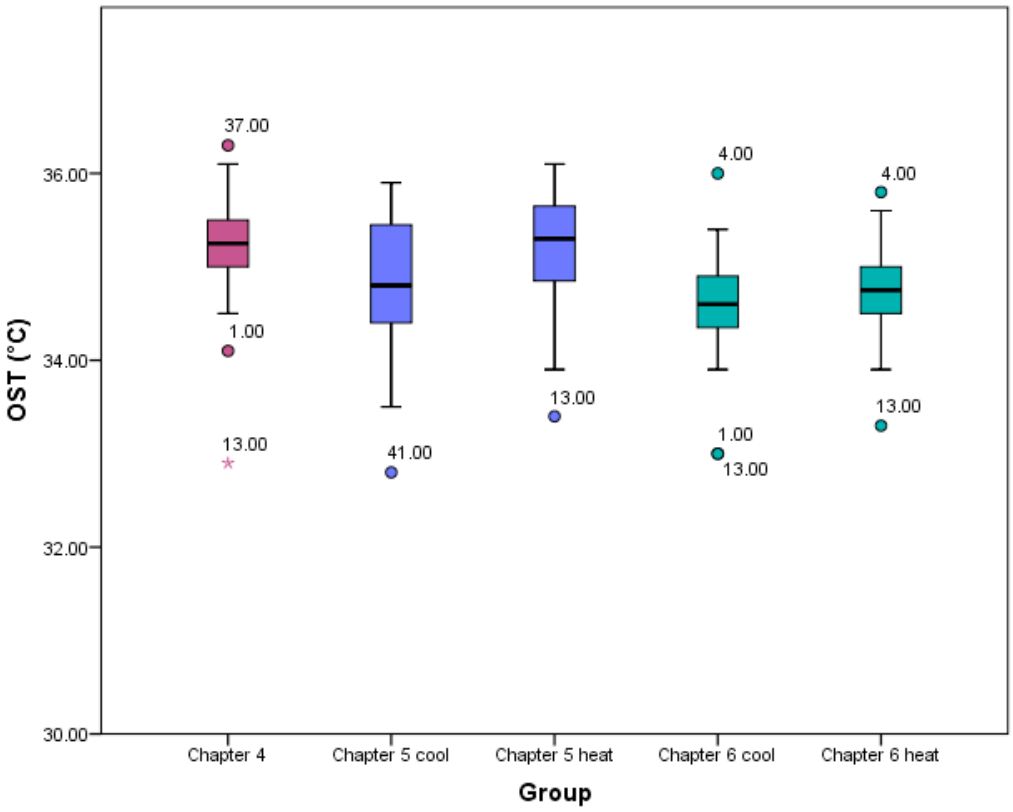

Figure 8.10: Boxplots for the OST measurements at baseline during the studies in Chapters 4, 5 and 6.

8.3.5 Agreement in tear film stability gradings

No statistically significant difference in measurements were noted between study period A and B, and between the two tear film quality gradings within study period B ($p=0.759$; Friedman's $Chi^2=0.551$). When including the measurements carried out in study part C, no statistically significant difference was noted between the results for study period A&B and study period C either ($p=0.265$; Friedman's $Chi^2=5.225$), although a trend to a lower tear film stability grading was observed in the mean values (Table 8.8).

	Tear film stability study in Ch.4	Tear film stability study in Ch.5 before heating	Tear film stability Study in Ch.5 before cooling	Tear film stability study in Ch.6 before heating	Tear film stability study in Ch.6 before cooling
Median / IR	2.00 / 1.0-3.0	2.00 / 1.00-4.00	2.00 / 1.00-3.00	2.00/ 1.00-3.00	2.00 / 1.00-3.25
Mean± SD	2.24±1.05	2.43±1.21	2.24±1.05	2.00±1.05	2.18±1.19

Table 8.8: Overview of the tear film stability gradings during the studies in Chapters 4,5 and 6 at baseline.

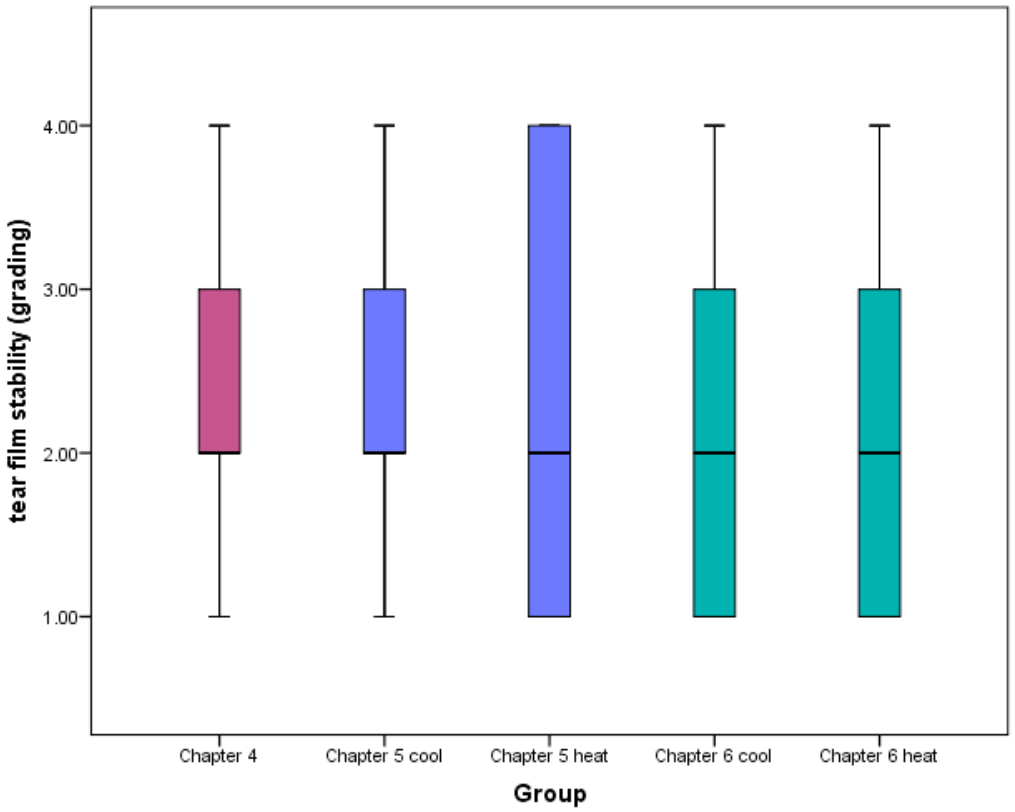

Figure 8.11: Boxplots for the tear film stability gradings at baseline during the studies in Chapters 4, 5 and 6.

8.3.6 Discussion and Conclusion

No statistical significance was observed regarding any of the repeated measurements carried out during the studies in Chapters 4 and 5. The measurements carried out during the study in Chapter 6 took place one year later and the sample size was considerably smaller. During the study in Chapter 6, the CST-, NIBUT-, and OST-measurements

turned out to be statistically lower, and a non-statistically significant trend towards a lower tear film quality grading was observed. During this later study period, the ambient temperature was slightly lower (a mean difference of 1.18°C during the heating appointments and a mean difference of 1.12°C during the cooling appointments), which may have most probably lead to a lower OST in this cohort of subjects. The time difference between the studies in Chapter 4 and 5, and the one in Chapter 6, as well as the smaller sample size in the study in Chapter 6 may be contribute to the lower NIBUT measurements and tear film stability gradings. In study part A, a moderate to good correlation could be shown between NIBUT & tear film quality and CST measurement, which may explain for the trend to a lower CST (i.e. higher corneal sensitivity) in the sample group of the study in Chapter 6.

CHAPTER 9

References

1. Müller L. Corneal nerves: structure, contents and function. *Exp Eye Res*. 2003;76(5):521–542.

2. Belmonte C, Acosta MC, Gallar J. Neural basis of sensation in intact and injured corneas. *Exp Eye Res*. 2004;78(3):513–525.

3. Nakamura M, Nishida T, Ofuji K, Reid TW, Mannis MJ, Murphy CJ. Synergistic effect of substance P with epidermal growth factor on epithelial migration in rabbit cornea. *Exp Eye Res*. 1997;65(3):321–329.

4. Nishida T, Nakamura M, Ofuji K, Reid TW, Mannis MJ, Murphy CJ. Synergistic effects of substance P with insulin-like growth factor-1 on epithelial migration of the cornea. *J Cell Physiol*. 1996;169(1):159–166.

5. Brown SM. Neurotrophic and Anhidrotic Keratopathy Treated With Substance P and Insulinlike Growth Factor 1. *Arch Ophthalmol*. 1997;115(7):926-927.

6. Murphy CJ, Marfurt CF, McDermott A, et al. Spontaneous chronic corneal epithelial defects(SCCED) in dogs: Clinical features, innervation, and effect of topical SP, with or without IGF-1. *Invest Ophthalmol Vis Sci*. 2001;42(10):2252–2261.

7. Baker KS, Anderson SC, Romanowski EG, Thoft RA, SundarRaj N. Trigeminal ganglion neurons affect corneal epithelial phenotype. Influence on type VII collagen expression in vitro. *Invest Ophthalmol Vis Sci*. 1993;34(1):137–144.

8. Araki K, Ohashi Y, Kinoshita S, Hayashi K, Kuwayama Y, Tano Y. Epithelial wound healing in the denervated cornea. *Current Eye Research*. 1994;13(3):203–211.

9. Tsubota K. Tear dynamics and dry eye. *Prog Retin Eye Res*. 1998;17(4):565–596.

10. Collins M, Seeto R, Campbell L, Ross M. Blinking and corneal sensitivity. *Acta Ophthalmologica*. 1989;67(5):525–531.

11. Mapstone R. Determinants of corneal temperature. *British Journal of Ophthalmology*. 1968;52(10):729–741.

12. Murphy PJ, Armstrong E, Woods LA. A comparison of corneal and conjunctival sensitivity to a thermally cooling stimulus. *Adv Exp Med Biol*. 2002;506(Pt A):719–722.

13. Cochet P, Bonnet R. L'esthésiométrie Cornéenne. Réalisation Et Intérêt Pratique. *Bulletin Societes d'Ophtalmologie de France;* 1961:541–550.

14. Murphy PJ, Patel S, Marshall J. A new non-contact corneal aesthesiometer

(NCCA). *Ophthalmic Physiol Opt*. 1996;16(2):101–107.

15. Bonnet R, Millodot M. Corneal aesthesiometry: its measurement in the dark. *American Journal of Optometry and archives of American Academy of Optometry*. 1966;43(4):238–243.

16. Millodot M, O'Leary DJ. Corneal fragility and its relationship to sensitivity. *Acta Ophthalmologica*. 1981;59(6):820–826.

17. Golebiowski B, Papas E, Stapleton F. Assessing the sensory function of the ocular surface: implications of use of a non-contact air jet aesthesiometer versus the Cochet-Bonnet aesthesiometer. *Exp Eye Res*. 2011;92(5):408–413.

18. Millodot M, Larson W. Effect of bending of the nylon thread of the Cochet-Bonnet aesthesiometer Upon the Recorded Pressure. *The Contact Lens;* 1967:5–6.

19. Belmonte C, Acosta MC, Schmelz M, Gallar J. Measurement of corneal sensitivity to mechanical and chemical stimulation with a CO2 esthesiometer. *Invest Ophthalmol Vis Sci*. 1999;40(2):513–519.

20. Feng Y, Simpson TL. Nociceptive sensation and sensitivity evoked from human cornea and conjunctiva stimulated by CO2. *Invest Ophthalmol Vis Sci*. 2003;44(2):529–532.

21. Stapleton F, Tan ME, Papas EB, et al. Corneal and conjunctival sensitivity to air stimuli. *British Journal of Ophthalmology*. 2004;88(12):1547–1551.

22. Murphy PJ, Morgan PB, Patel S, Marshall J. Corneal surface temperature change as the mode of stimulation of the non-contact corneal aesthesiometer. *Cornea*. 1999;18(3):333–342.

23. Nakamori K, Odawara M, Nakajima T, Mizutani T, Tsubota K. Blinking is controlled primarily by ocular surface conditions. *Am J Ophthalmol*. 1997;124(1):24–30.

24. Naase T, Doughty MJ, Button NF. An assessment of the pattern of spontaneous eyeblink activity under the influence of topical ocular anaesthesia. *Graefes Arch Clin Exp Ophthalmol*. 2005;243(4):306–312.

25. Fujishima H, Toda I, Yamada M, Sato N, Tsubota K. Corneal temperature in patients with dry eye evaluated by infrared radiation thermometry. *British Journal of Ophthalmology*. 1996;80(1):29–32.

26. Mori A, Oguchi Y, Okusawa Y, Ono M, Fujishima H, Tsubota K. Use of high-speed, high-resolution thermography to evaluate the tear film layer. *Am J Ophthalmol*. 1997;124(6):729–735.

27. Stern JA, Walrath LC, Goldstein R. The endogenous eyeblink. *Psychophysiology*. 1984;21(1):22–33.

28. Cruz AAV, Garcia DM, Pinto CT, Cechetti SP. Spontaneous eyeblink activity. *Ocul Surf*. 2011;9(1):29–41.

29. Gallar J, Pozo MA, Tuckett RP, Belmonte C. Response of sensory units with unmyelinated fibres to mechanical, thermal and chemical stimulation of the cat's cornea. *J Physiol (Lond)*. 1993;468:609–622.

30. Carr RW, Pianova S, Fernandez J, Fallon JB, Belmonte C, Brock JA. Effects of heating and cooling on nerve terminal impulses recorded from cold-sensitive receptors in the guinea-pig cornea. *J Gen Physiol*. 2003;121(5):427–439.

31. Tanelian DL, Beuerman R. Responses of rabbit corneal nociceptors to mechanical and thermal stimulation. *Exp Neurol*. 1984;84(1):165–178.

32. Acosta MC, Belmonte C, Gallar J. Sensory experiences in humans and single-unit activity in cats evoked by polymodal stimulation of the cornea. *J Physiol (Lond)*. 2001;534(Pt. 2):511–525.

33. Belmonte C, Giraldez F. Responses of cat corneal sensory receptors to mechanical and thermal stimulation. *J Physiol (Lond)*. 1981;321:355–368.

34. Burton H. Somatic Sensations From the Eye. *Adler's Physiology of the Eye*. 9 ed. Mosby Inc; 1992:71–100.

35. Oduntan O, Ruskell G. The source of sensory fibres of the inferior conjunctiva of monkeys. *Graefes Arch Clin Exp Ophthalmol*. 1992;230(3):258–263.

36. Dawson DG, Ubels JL, Edelhauser HF. Cornea and Sclera. *Adler's Physiology of the Eye,* Elsevier Saunders. 2011.

37. Doughty MJ, Zaman ML. Human corneal thickness and its impact on intraocular pressure measures: a review and meta-analysis approach. *Surv Ophthalmol*. 2000;44(5):367–408.

38. Edelhauser HF, Ubels JL. The cornea and the sclera. *Adler's Physiology of the Eye*. 2003.

39. Ehlers N. Some comparative studies on the mammalian corneal epithelium. *Acta Ophthalmologica*. 1970;48(4):821–828.

40. Klyce SD, Beuerman R. Structure and function of the cornea. *The cornea*. 1988:3–54.

41. Hanna C, Bicknell DS, O'Brien C. Cell turnover in the adult human eye. *Arch Ophthalmol*. 1961;65:695–698.

42. McLaughlin BJ, Caldwell RB, Sasaki Y, Wood TO. Freeze-fracture quantitative comparison of rabbit corneal epithelial and endothelial membranes. *Current Eye Research*. 1985;4(9):951–962.

43. Beuerman R, Pedroza L. Ultrastructure of the human cornea. *Microsc Res Tech*.

1996;33(4):320–335.

44. Anderson RA. Actin filaments in normal and migrating corneal epithelial cells. *Invest Ophthalmol Vis Sci*. 1977;16(2):161–166.

45. Gipson IK, Spurr-Michaud SJ, Tisdale AS. Anchoring fibrils form a complex network in human and rabbit cornea. *Invest Ophthalmol Vis Sci*. 1987;28(2):212–220.

46. Kruse FE. Stem cells and corneal epithelial regeneration. *Eye (Lond)*. 1994;8 (Pt 2):170–183.

47. Thoft RA, Friend J. The X, Y, Z hypothesis of corneal epithelial maintenance. *Invest Ophthalmol Vis Sci*. 1983;24(10):1442–1443.

48. Tseng SC. Concept and application of limbal stem cells. *Eye (Lond)*. 1989;3 (Pt 2):141–157.

49. Hanna C, O'Brien C. Cell production and migration in the epithelial layer of the cornea. *Arch Ophthalmol*. 1960;64:536–539.

50. Gipson IK, Spurr-Michaud S, Tisdale A, Keough M. Reassembly of the anchoring structures of the corneal epithelium during wound repair in the rabbit. *Invest Ophthalmol Vis Sci*. 1989;30(3):425–434.

51. Gipson IK, Spurr-Michaud SJ, Tisdale AS. Hemidesmosomes and anchoring fibril collagen appear synchronously during development and wound healing. *Dev Biol*. 1988;126(2):253–262.

52. Vracko R, Benditt EP. Basal lamina: the scaffold for orderly cell replacement. Observations on regeneration of injured skeletal muscle fibers and capillaries. *J Cell Biol*. 1972;55(2):406–419.

53. Scott JE, Haigh M. 'Small'-proteoglycan:collagen interactions: keratan sulphate proteoglycan associates with rabbit corneal collagen fibrils at the 'a' and “c” bands. *Biosci Rep*. 1985;5(9):765–774.

54. Kamma-Lorger CS, Boote C, Hayes S, et al. Collagen and mature elastic fibre organisation as a function of depth in the human cornea and limbus. *Journal of structural biology*. 2010;169(3):424–430.

55. Johnson DH, Bourne WM, Campbell RJ. The ultrastructure of Descemet's membrane. I. Changes with age in normal corneas. *Arch Ophthalmol*. 1982;100(12):1942–1947.

56. Binder PS, Rock ME, Schmidt KC, Anderson JA. High-voltage electron microscopy of normal human cornea. *Invest Ophthalmol Vis Sci*. 1991;32(8):2234–2243.

57. Gipson IK, Grill SM, Spurr SJ, Brennan SJ. Hemidesmosome formation in vitro. *J Cell Biol*. 1983;97(3):849–857.

58. Joyce NC. Proliferative capacity of the corneal endothelium. *Prog Retin Eye Res*. 2003;22(3):359–389.

59. Maurice DM. The location of the fluid pump in the cornea. *J Physiol (Lond)*. 1972;221(1):43–54.

60. Trenberth SM, Mishima S. The effect of ouabain on the rabbit corneal endothelium. *Investigative ophthalmology*. 1968;7(1):44–52.

61. Zhihov A, Stachs O, Kraak R, Stave J, Guthoff RF. In vivo confocal microscopy of the ocular surface. *Ocul Surf*. 2006;4(2):81–93.

62. Patel DV, McGhee CNJ. Mapping of the normal human corneal sub-basal nerve plexus by in vivo laser scanning confocal microscopy. *Invest Ophthalmol Vis Sci*. 2005;46(12):4485–4488.

63. He J, Bazan NG, Bazan HEP. Mapping the entire human corneal nerve architecture. *Exp Eye Res*. 2010;91(4):513–523.

64. Lum E, Golebiowski B, Swarbrick HA. Mapping the corneal sub-basal nerve plexus in orthokeratology lens wear using in vivo laser scanning confocal microscopy. *Invest Ophthalmol Vis Sci*. 2012:1–33.

65. Müller LJ, Vrensen GF, Pels L, Cardozo BN, Willekens B. Architecture of human corneal nerves. *Invest Ophthalmol Vis Sci*. 1997;38(5):985–994.

66. Müller LJ, Pels L, Vrensen GF. Ultrastructural organization of human corneal nerves. *Invest Ophthalmol Vis Sci*. 1996;37(4):476–488.

67. Schimmelpfennig B. Nerve structures in human central corneal epithelium. *Graefes Arch Clin Exp Ophthalmol*. 1982;218(1):14–20.

68. MacIver MB, Tanelian DL. Free nerve ending terminal morphology is fiber type specific for A delta and C fibers innervating rabbit corneal epithelium. *J Neurophysiol*. 1993;69(5):1779–1783.

69. MacIver MB, Tanelian DL. Structural and functional specialization of A delta and C fiber free nerve endings innervating rabbit corneal epithelium. *J Neurosci*. 1993;13(10):4511–4524.

70. Belmonte C, Gallar J, Pozo MA, Rebollo I. Excitation by irritant chemical substances of sensory afferent units in the cat's cornea. *J Physiol (Lond)*. 1991;437:709–725.

71. Aracil A, Gallar J. [Actualization on the neurobiology of the corneal sensitivity: a need]. *Arch Soc Esp Oftalmol*. 2004;79(8):371-372.

72. Ruskell GL. Innervation of the conjunctiva. *Trans Ophthalmol Soc U K*. 1985;104 (Pt 4):390–395.

73. Krause W. *Über Nervenendigungen.* Zeitschrift rationelle Medizin; 1859:28–

43.

74. Lawrenson JG, Ruskell GL. The structure of corpuscular nerve endings in the limbal conjunctiva of the human eye. *J Anat*. 1991;177:75–84.

75. Petroll WM, Cavanagh HD, Jester JV. Clinical confocal microscopy. *Curr Opin Ophthalmol*. 1998;9(4):59–65.

76. Cavanagh H, Jester JV, Essepian J, Shields W, Lemp MA. Confocal microscopy of the living eye. *CLAO J*. 1990;16(1):65–73.

77. Jester JV, Petroll WM, Cavanagh HD. Corneal stromal wound healing in refractive surgery: the role of myofibroblasts. *Prog Retin Eye Res*. 1999;18(3):311–356.

78. Tervo T, Moilanen J. In vivo confocal microscopy for evaluation of wound healing following corneal refractive surgery. *Prog Retin Eye Res*. 2003;22(3):339–358.

79. Rozsa AJ, Beuerman RW. Density and organization of free nerve endings in the corneal epithelium of the rabbit. *Pain*. 1982;14(2):105–120.

80. Boberg-Ans J. Experience in Clinical Examination of Corneal Sensitivity: Corneal Sensitivity and the Naso-Lacrimal Reflex after Retrobulbar Anaesthesia. *British Journal of Ophthalmology*. 1955;39(12):705–726.

81. Lawrenson JG, Ruskell GL. Investigation of limbal touch sensitivity using a Cochet-Bonnet aesthesiometer. *British Journal of Ophthalmology*. 1993;77(6):339–343.

82. Norn M. Conjunctival sensitivity in normal eyes. *Acta Ophthalmol (Copenh)*. 1973;51:58–66.

83. Acosta MC, Alfaro ML, Borrás F, Belmonte C, Gallar J. Influence of age, gender and iris color on mechanical and chemical sensitivity of the cornea and conjunctiva. *Exp Eye Res*. 2006;83(4):932–938.

84. McGowan DP, Lawrenson JG, Ruskell GL. Touch sensitivity of the eyelid margin and palpebral conjunctiva. *Acta Ophthalmologica*. 1994;72(1):57–60.

85. Paton L. The trigeminal and its ocular lesions. *The British Journal of Ophthalmology*. 1926:305–342.

86. Heigle TJ, Pflugfelder SC. Aqueous tear production in patients with neurotrophic keratitis. *Cornea*. 1996;15(2):135–138.

87. Wilson SE, Ambrósio R. Laser in situ keratomileusis-induced neurotrophic epitheliopathy. *Am J Ophthalmol*. 2001;132(3):405–406.

88. Beuerman R, Schimmelpfennig B. Sensory denervation of the rabbit cornea affects epithelial properties. *Exp Neurol*. 1980;69(1):196–201.

89. Gilbard JP, Rossi SR. Tear film and ocular surface changes in a rabbit model of neurotrophic keratitis. *Ophthalmology*. 1990;97(3):308–312.

90. Knyazev GG, Knyazeva GB, Tolochko ZS. Trophic functions of primary sensory neurons: are they really local? *Neuroscience*. 1991;42(2):555–560.

91. Sugiura S, Matsuda H. [Electron microscopic observations on the corneal epithelium after sensory denervation]. *Nippon Ganka Gakkai Zasshi*. 1967;71(8):1123–1137.

92. Lim CH. Innervation of the cornea of monkeys and the effects of denervation. *Br J Physiol Opt*. 1976;31(4):38–42.

93. Sigelman S, Dohlman CH, Friedenwald JS. Mitotic and wound healing activities in the rat corneal epithelium; influence of various hormones and endocrine glands. *AMA Arch Ophthalmol*. 1954;52(5):751–757.

94. Alper MG. The anesthetic eye: an investigation of changes in the anterior ocular segment of the monkey caused by interrupting the trigeminal nerve at various levels along its course. *Trans Am Ophthalmol Soc*. 1975;73:323–365.

95. Mackie IA. Role of the corneal nerves in destructive disease of the cornea. *Trans Ophthalmol Soc U K*. 1978;98(3):343–347.

96. Holden BA, Polse KA, Fonn D, Mertz GW. Effects of cataract surgery on corneal function. *Invest Ophthalmol Vis Sci*. 1982;22(3):343–350.

97. Vannas A, Holden BA, Sweeney DF, Polse KA. Surgical incision alters the swelling response of the human cornea. *Invest Ophthalmol Vis Sci*. 1985;26(6):864–868.

98. Schimmelpfennig B, Beuerman R. A technique for controlled sensory denervation of the rabbit cornea. *Graefes Arch Clin Exp Ophthalmol*. 1982;218(6):287–293.

99. Garcia-Hirschfeld J, Lopez-Briones LG, Belmonte C. Neurotrophic influences on corneal epithelial cells. *Exp Eye Res*. 1994;59(5):597–605.

100. Chan KY, Haschke RH. Actions of a trophic factor(s) from rabbit corneal culture on dissociated trigeminal neurons. *J Neurosci*. 1981;1(10):1155–1162.

101. Chan KY, Haschke RH. Isolation and culture of corneal cells and their interactions with dissociated trigeminal neurons. *Exp Eye Res*. 1982;35(2):137–156.

102. Emoto I, Beuerman R. Stimulation of neurite growth by epithelial implants into corneal stroma. *Neurosci Lett*. 1987;82(2):140–144.

103. Lambiase A, Manni L, Bonini S, Rama P, Micera A, Aloe L. Nerve growth factor promotes corneal healing: structural, biochemical, and molecular analyses of rat and human corneas. *Invest Ophthalmol Vis Sci*.

2000;41(5):1063–1069.

104. You L, Kruse FE, Völcker HE. Neurotrophic factors in the human cornea. *Invest Ophthalmol Vis Sci*. 2000;41(3):692–702.

105. Mathers WD, Nelson SE, Lane JL, Wilson ME, Allen RC, Folberg R. Confirmation of confocal microscopy diagnosis of Acanthamoeba keratitis using polymerase chain reaction analysis. *Arch Ophthalmol*. 2000;118(2):178–183.

106. Yamada M, Ogata M, Kawai M, Mashima Y. Decreased substance P concentrations in tears from patients with corneal hypesthesia. *Am J Ophthalmol*. 2000;129(5):671–672.

107. Jordan A, Baum J. Basic tear flow. Does it exist? *Ophthalmology*. 1980;87(9):920–930.

108. Miller A, Costa M, Furness JB, Chubb IW. Substance P immunoreactive sensory nerves supply the rat iris and cornea. *Neurosci Lett*. 1981;23(3):243–249.

109. Tervo K, Tervo T, Eränkö L, Eränkö O. Substance P immunoreactive nerves in the rodent cornea. *Neurosci Lett*. 1981;25(1):95–97.

110. Reid TW, Murphy CJ, Iwahashi CK, Foster BA, Mannis MJ. Stimulation of epithelial cell growth by the neuropeptide substance P. *J Cell Biochem*. 1993;52(4):476–485.

111. Nakamura M, Nagano T, Chikama T, Nishida T. Up-regulation of phosphorylation of focal adhesion kinase and paxillin by combination of substance P and IGF-1 in SV-40 transformed human corneal epithelial cells. *Biochem Biophys Res Commun*. 1998;242(1):16–20.

112. Chikama T, Nakamura M, Nishida T. Up-regulation of integrin alpha5 by a C-terminus four-amino-acid sequence of substance P (phenylalanine-glycine-leucine-methionine- amide) synergistically with insulin-like growth factor-1 in SV-40 transformed human corneal epithelial cells. *Biochem Biophys Res Commun*. 1999;255(3):692–697.

113. Araki-Sasaki K, Aizawa S, Hiramoto M, et al. Substance P-induced cadherin expression and its signal transduction in a cloned human corneal epithelial cell line. *J Cell Physiol*. 2000;182(2):189–195.

114. Kieselbach GF, Ragaut R, Knaus HG, König P, Wiedermann CJ. Autoradiographic analysis of binding sites for 125I-Bolton-Hunter-substance P in the human eye. *Peptides*. 1990;11(4):655–659.

115. Denis P, Fardin V, Nordmann JP, et al. Localization and characterization of substance P binding sites in rat and rabbit eyes. *Invest Ophthalmol Vis Sci*. 1991;32(6):1894–1902.

116. Nakamura M, Ofuji K, Chikama T, Nishida T. The NK1 receptor and its participation in the synergistic enhancement of corneal epithelial migration by substance P and insulin-like growth factor-1. *Br J Pharmacol*. 1997;120(4):547–552.

117. Yamada M, Ogata M, Kawai M, Mashima Y, Nishida T. Substance P and its metabolites in normal human tears. *Invest Ophthalmol Vis Sci*. 2002;43(8):2622–2625.

118. Kingsley RE, Marfurt CF. Topical substance P and corneal epithelial wound closure in the rabbit. *Invest Ophthalmol Vis Sci*. 1997;38(2):388–395.

119. Nakamura M, Ofuji K, Chikama T, Nishida T. Combined effects of substance P and insulin-like growth factor-1 on corneal epithelial wound closure of rabbit in vivo. *Current Eye Research*. 1997;16(3):275–278.

120. Nakamura M, Chikama T, Nishida T. Up-regulation of integrin alpha 5 expression by combination of substance P and insulin-like growth factor-1 in rabbit corneal epithelial cells. *Biochem Biophys Res Commun*. 1998;246(3):777–782.

121. Chikama T, Fukuda K, Morishige N, Nishida T. Treatment of neurotrophic keratopathy with substance-P-derived peptide (FGLM) and insulin-like growth factor I. *Lancet*. 1998;351(9118):1783–1784.

122. Lee R. Regulation of cell survival by secreted proneurotrophins. *Science*. 2001;294(5548):1945–1948.

123. Morishige N, Komatsubara T, Chikama T, Nishida T. Direct observation of corneal nerve fibres in neurotrophic keratopathy by confocal biomicroscopy. *Lancet*. 1999;354(9190):1613–1614.

124. Jones MA, Marfurt CF. Calcitonin gene-related peptide and corneal innervation: a developmental study in the rat. *J Comp Neurol*. 1991;313(1):132–150.

125. Mertaniem P, Ylätupa S, Partanen P, Tervo T. Increased release of immunoreactive calcitonin gene-related peptide (CGRP) in tears after excimer laser keratectomy. *Exp Eye Res*. 1995;60(6):659–665.

126. Heino P, Oksala O, Luhtala J, Uusitalo H. Localization of calcitonin gene-related peptide binding sites in the eye of different species. *Current Eye Research*. 1995;14(9):783–790.

127. Tran MT, Ritchie MH, Lausch RN, Oakes JE. Calcitonin gene-related peptide induces IL-8 synthesis in human corneal epithelial cells. *J Immunol*. 2000;164(8):4307–4312.

128. Mikulec AA, Tanelian DL. CGRP increases the rate of corneal re-epithelialization in an in vitro whole mount preparation. *J Ocul Pharmacol Ther*. 1996;12(4):417–423.

129. Marfurt CF, Murphy CJ, Florczak JL. Morphology and neurochemistry of canine corneal innervation. *Invest Ophthalmol Vis Sci*. 2001;42(10):2242–2251.

130. Candia OA, Neufeld AH. Topical epinephrine causes a decrease in density of beta-adrenergic receptors and cathecholamine-stimulated chloride transport in the rabbit cornea. *Biochim Biophys Acta*. 1978;543(3):403–408.

131. Cavanagh HD, Colley AM. Cholinergic, adrenergic, and PGE1 effects on cyclic nucleotides and growth in cultured corneal epithelium. *Metab Pediatr Syst Ophthalmol*. 1982;6(2):63–74.

132. Elena PP, Denis P, Kosina-Boix M, Saraux H, Lapalus P. Beta adrenergic binding sites in the human eye: an autoradiographic study. *J Ocul Pharmacol*. 1990;6(2):143–149.

133. Walkenbach RJ, Ye GS, Reinach PS, Boney F. Alpha 1-adrenoceptors in human corneal epithelium. *Invest Ophthalmol Vis Sci*. 1991;32(12):3067–3072.

134. Grayson TH, Ellis JM, Chen S, Graham RM, Brown RD, Hill CE. Immunohistochemical localisation of alpha1B-adrenergic receptors in the rat iris. *Cell and Tissue Research*. 1998;293(3):435–444.

135. Voaden MJ. The effects of superior cervical ganglionectomy and-or bilateral adrenalectomy on the mitotic activity of the adult rat cornea. *Exp Eye Res*. 1971;12(3):337–341.

136. Jones MA, Marfurt CF. Sympathetic stimulation of corneal epithelial proliferation in wounded and nonwounded rat eyes. *Invest Ophthalmol Vis Sci*. 1996;37(13):2535–2547.

137. Murphy CJ, Campbell S, Araki-Sasaki K, Marfurt CF. Effect of norepinephrine on proliferation, migration, and adhesion of SV-40 transformed human corneal epithelial cells. *Cornea*. 1998;17(5):529–536.

138. Liu GS, Trope GE, Basu PK. Beta adrenoceptors and regenerating corneal epithelium. *J Ocul Pharmacol*. 1990;6(2):101–112.

139. Ehinger B. Connections between adrenergic nerves and other tissue components in the eye. *Acta Physiol Scand*. 1966;67(1):57–64.

140. Sugiura S, Yamaga C. [Studies on the adrenergic nerve of the cornea]. *Nippon Ganka Gakkai Zasshi*. 1968;72(7):872–879.

141. Ehinger B. A comparative study of the adrenergic nerves to the anterior eye segment of some primates. *Z Zellforsch Mikrosk Anat*. 1971;116(2):157–177.

142. Toivanen M, Tervo T, Parranen TM, Vannas A, t, Hervonen A. Histochemical demonstration of adrenergic nerves in the stroma of human cornea. *Invest Ophthalmol Vis Sci*. 1987;28(2):398–400.

143. Colley AM, Cavanagh HD, Drake LA, Law ML. Cyclic nucleotides in

muscarinic regulation of DNA and RNA polymerase activity in cultured corneal epithelial cells of the rabbit. *Current Eye Research*. 1985;4(9):941–950.

144. Grando SA, Horton RM, Pereira EF, et al. A nicotinic acetylcholine receptor regulating cell adhesion and motility is expressed in human keratinocytes. *J Invest Dermatol*. 1995;105(6):774–781.

145. Zia S, Ndoye A, Nguyen VT, Grando SA. Nicotine enhances expression of the alpha 3, alpha 4, alpha 5, and alpha 7 nicotinic receptors modulating calcium metabolism and regulating adhesion and motility of respiratory epithelial cells. *Res Commun Mol Pathol Pharmacol*. 1997;97(3):243–262.

146. Bourcier T, Rondeau N, Paquet S, et al. Expression of neurotensin receptors in human corneal keratocytes. *Invest Ophthalmol Vis Sci*. 2002;43(6):1765–1771.

147. Patapoutian A, Reichardt LF. Trk receptors: mediators of neurotrophin action. *Curr Opin Neurobiol*. 2001;11(3):272–280.

148. Dechant G, Barde Y-A. The neurotrophin receptor p75(NTR): novel functions and implications for diseases of the nervous system. *Nat Neurosci*. 2002;5(11):1131–1136.

149. de Castro F, Silos-Santiago I, López de Armentia M, Barbacid M, Belmonte C. Corneal innervation and sensitivity to noxious stimuli in trkA knockout mice. *Eur J Neurosci*. 1998;10(1):146–152.

150. Lambiase A, Bonini S, Micera A, Rama P, Bonini S, Aloe L. Expression of nerve growth factor receptors on the ocular surface in healthy subjects and during manifestation of inflammatory diseases. *Invest Ophthalmol Vis Sci*. 1998;39(7):1272–1275.

151. Bonini S, Lambiase A, Rama P, Caprioglio G, Aloe L. Topical treatment with nerve growth factor for neurotrophic keratitis. *Ophthalmology*. 2000;107(7):1347–1351.

152. Kruse FE, Tseng SC. Growth factors modulate clonal growth and differentiation of cultured rabbit limbal and corneal epithelium. *Invest Ophthalmol Vis Sci*. 1993;34(6):1963–1976.

153. Madduri S, Papaloïzos M, Gander B. Synergistic effect of GDNF and NGF on axonal branching and elongation in vitro. *Neurosci Res*. 2009;65(1):88–97.

154. Koh SW. Ciliary neurotrophic factor released by corneal endothelium surviving oxidative stress ex vivo. *Invest Ophthalmol Vis Sci*. 2002;43(9):2887–2896.

155. Koh SW, Waschek JA. Corneal endothelial cell survival in organ cultures under acute oxidative stress: effect of VIP. *Invest Ophthalmol Vis Sci*. 2000;41(13):4085–4092.

156. You L, Ebner S, Kruse FE. Glial cell-derived neurotrophic factor (GDNF)-induced migration and signal transduction in corneal epithelial cells. *Invest*

Ophthalmol Vis Sci. 2001;42(11):2496–2504.

157. Lele PP, Weddell G. The relationship between neurohistology and corneal sensibility. *Brain*. 1956;79(1):119–154.

158. Lele PP, Weddell G. Sensory nerves of the cornea and cutaneous sensibility. *Exp Neurol*. 1959;1:334–359.

159. Giraldez F, Geijo E, Belmonte C. Response characteristics of corneal sensory fibers to mechanical and thermal stimulation. *Brain Res*. 1979;177(3):571–576.

160. Brock JA, McLachlan EM, Belmonte C. Tetrodotoxin-resistant impulses in single nociceptor nerve terminals in guinea-pig cornea. *J Physiol (Lond)*. 1998;512 (Pt 1):211–217.

161. Brock JA, Pianova S, Belmonte C. Differences between nerve terminal impulses of polymodal nociceptors and cold sensory receptors of the guinea-pig cornea. *J Physiol (Lond)*. 2001;533(Pt 2):493–501.

162. Bessou P, Perl ER. Response of cutaneous sensory units with unmyelinated fibers to noxious stimuli. *J Neurophysiol*. 1969;32(6):1025–1043.

163. Chen X, Gallar J, Pozo MA, Baeza M, Belmonte C. CO2 stimulation of the cornea: a comparison between human sensation and nerve activity in polymodal nociceptive afferents of the cat. *Eur J Neurosci*. 1995;7(6):1154–1163.

164. Tanelian DL, MacIver MB. Simultaneous visualization and electrophysiology of corneal A-delta and C fiber afferents. *J Neurosci Methods*. 1990;32(3):213–222.

165. Aracil A, Belmonte C, Gallar J. Functional Types of Conjunctival Primary Sensory Neurons. *Invest Ophthalmol Vis Sci.*; 2001.

166. Belmonte C, Garcia-Hirschfeld J, Gallar J. Neurobiology of ocular pain. *Prog Retin Eye Res*. 1997;16(1):117–156.

167. Bonanno JA, Polse KA. Corneal acidosis during contact lens wear: effects of hypoxia and CO2. *Invest Ophthalmol Vis Sci*. 1987;28(9):1514–1520.

168. Kenshalo DR. Comparison of thermal sensitivity of the forehead, lip, conjunctiva and cornea. *Journal of applied physiology*. 1960;15:987–991.

169. Beuerman R, Tanelian D. Corneal pain evoked by thermal stimulation. *Pain*. 1979;7(1):1–14.

170. Robinson CJ, Torebjörk HE, LaMotte RH. Psychophysical detection and pain ratings of incremental thermal stimuli: a comparison with nociceptor responses in humans. *Brain Res*. 1983;274(1):87–106.

171. Adriaensen H, Gybels J, Handwerker HO, Van Hees J. Suppression of C-fibre discharges upon repeated heat stimulation may explain characteristics of

concomitant pain sensations. *Brain Res*. 1984;302(2):203–211.

172. Ochoa J, Torebjörk E. Sensations evoked by intraneural microstimulation of C nociceptor fibres in human skin nerves. *Journal of Physiology*. 1989;415:583–599.

173. Murphy PJ, Patel S, Morgan PB, Marshall J. The minimum stimulus energy required to produce a cooling sensation in the human cornea. *Ophthalmic Physiol Opt*. 2001;21(5):407–410.

174. Acosta MC, Tan ME, Belmonte C, Gallar J. Sensations evoked by selective mechanical, chemical, and thermal stimulation of the conjunctiva and cornea. *Invest Ophthalmol Vis Sci*. 2001;42(9):2063–2067.

175. Feng Y, Simpson TL. Characteristics of human corneal psychophysical channels. *Invest Ophthalmol Vis Sci*. 2004;45(9):3005–3010.

176. Caterina M, Schumacher M, Tominaga M, Rosen T, Levine J, Julius D. The capsaicin receptor: a heat-activated ion channel in the pain pathway. *Nature*. 1997;389(6653):816–824.

177. Waldmann R, Champigny G, Bassilana F, Heurteaux C, Lazdunski M. A proton-gated cation channel involved in acid-sensing. *Nature*. 1997;386(6621):173–177.

178. McKemy D, Neuhausser W, Julius D. Identification of a cold receptor reveals a general role for TRP channels in thermosensation. *Nature*. 2002;416(6876):52–58.

179. Peier AM, Moqrich A, Hergarden AC, et al. A TRP channel that senses cold stimuli and menthol. *Cell*. 2002;108(5):705–715.

180. Viana F, la Peña de E, Belmonte C. Specificity of cold thermotransduction is determined by differential ionic channel expression. *Nat Neurosci*. 2002;5(3):254–260.

181. LaMotte RH, Campbell JN. Comparison of responses of warm and nociceptive C-fiber afferents in monkey with human judgments of thermal pain. *J Neurophysiol*. 1978;41(2):509–528.

182. Dalton P. Psychophysical and behavioral characteristics of olfactory adaptation. *Chem Senses*. 2000;24:487–492.

183. Öhman A, Lader M. Selective attention and “habituation” of the auditory averaged evoked response in humans. *Physiol Behav*. 1972;8(1):79–85.

184. Ernst M, Lee M, Dworkin B, Zaretsky HH. Pain perception decrement produced through repeated stimulation. *Pain*. 1986;26:221–231.

185. Chen J, Feng Y, Simpson TL. Human corneal adaptation to mechanical, cooling, and chemical stimuli. *Invest Ophthalmol Vis Sci*. 2010;51(2):876–881.

186. Beuerman R, Maitchouk DY, Varnell RJ, Pedroza-Schmidt. Interactions between lacrimal function and the ocular surface. *Curr Opin Kyoto.* 1998;2:1–10.

187. Stern ME, Beuerman R, Fox RI, Gao J, Mircheff AK, Pflugfelder SC. The pathology of dry eye: the interaction between the ocular surface and lacrimal glands. *Cornea*. 1998;17(6):584–589.

188. Stern ME, Beuerman R, Fox RI, Gao J, Mircheff AK, Pflugfelder SC. A unified theory of the role of the ocular surface in dry eye. *Adv Exp Med Biol*. 1998;438:643–651.

189. Lemp MA, Baudouin MCC, MD, et al. The definition and classification of dry eye disease: report of the Definition and Classification Subcommittee of the International Dry Eye WorkShop (2007). *Ocul Surf*. 2007;5(2):75–92.

190. Stern ME, Gao J, Siemasko KF, Beuerman RW, Pflugfelder SC. The role of the lacrimal functional unit in the pathophysiology of dry eye. *Exp Eye Res*. 2004;78(3):409–416. doi:10.1016/j.exer.2003.09.003.

191. Stern ME, Schaumburg CS, Pflugfelder SC. Dry eye as a mucosal autoimmune disease. *Int Rev Immunol*. 2013;32(1):19–41.

192. Wolff E. The mucocutaneous junction of the lidmargin and the distribution of the tear fluid. *Trans Am Ophthalmol Soc*. 1946;66:291–308.

193. Miller KL, Polse KA, Radke CJ. Black-line formation and the “perched” human tear film. *Current Eye Research*. 2002;25(3):155–162.

194. Gaffney EA, Tiffany JM, Yokoi N, Bron AJ. A mass and solute balance model for tear volume and osmolarity in the normal and the dry eye. *Prog Retin Eye Res*. 2010;29(1):59–78.

195. King-Smith PE, Fink BA, Hill RM, Koelling KW, Tiffany JM. The thickness of the tear film. *Current Eye Research*. 2004;29(4-5):357–368.

196. Wang J, Fonn D, Simpson TL, Jones L. Precorneal and pre- and postlens tear film thickness measured indirectly with optical coherence zomography. *Invest Ophthalmol Vis Sci*. 2003;44(6):2524–2528.

197. Norn MS. Semiquantitative interference study of fatty layer of precorneal film. *Acta Ophthalmologica*. 1979;57(5):766–774.

198. Olsen T. Reflectometry of the precorneal film. *Acta Ophthalmologica*. 1985;63(4):432–438.

199. Mishima S, Maurice DM. The oily layer of the tear film and evaporation from the corneal surface. *Exp Eye Res*. 1961;1:39–45.

200. Craig JP, Tomlinson A. Importance of the lipid layer in human tear film stability and evaporation. *Optom Vis Sci*. 1997;74(1):8–13.

201. Bron AJ, Tiffany JM, Gouveia SM, Yokoi N, Voon LW. Functional aspects of the tear film lipid layer. *Exp Eye Res*. 2004;78(3):347–360.

202. Foulks GN. The correlation between the tear film lipid layer and dry eye disease. *Surv Ophthalmol*. 2007;52(4):369–374.

203. Dartt DA. Dysfunctional neural regulation of lacrimal gland secretion and its role in the pathogenesis of dry eye syndromes. *Ocul Surf*. 2004;2(2):76–91.

204. Rolando M, Zierhut M. The ocular surface and tear film and their dysfunction in dry eye disease. *Surv Ophthalmol*. 2001;45 Suppl 2:S203–10.

205. Smolin G. The defence mechanism of the outer eye. *Trans Ophthalmol Soc U K*. 1985;104 (Pt 4):363–366.

206. Chen Y, Mehta G, Vasiliou V. Antioxidant defenses in the ocular surface. *Ocul Surf*. 2009;7(4):176–185.

207. Argueso P. Glycobiology of the ocular surface: mucins and lectins. *Jpn J Ophthalmol*. 2013;57(2):150–155.

208. Dartt DA. Regulation of mucin and fluid secretion by conjunctival epithelial cells. *Prog Retin Eye Res*. 2002;21(6):555–576.

209. Evinger C, Manning KA, Sibony PA. Eyelid movements. Mechanisms and normal data. *Invest Ophthalmol Vis Sci*. 1991;32(2):387–400.

210. Gordon G. Observations upon the movements of the eyelids. *British Journal of Ophthalmology*. 1951;35(6):339–351.

211. Bjork A, Kugelberk E. The electrical activity of the muscles of the eye and eyelids in various positions and during movement. *Electroencephalogr Clin Neurophysiol*. 1953;5(4):595–602.

212. van Allen MW, Blodi FC. Electromyographic study of reciprocal innervation in blinking. *Neurology*. 1962;12:371–377.

213. Holder DS, Scott A, Hannaford B, Stark L. High resolution electromyogram of the human eyeblink. *Electromyogr Clin Neurophysiol*. 1987;27(6-7):481–488.

214. Esteban A, Salinero E. Reciprocal reflex activity in ocular muscles: implications in spontaneous blinking and Bell's phenomenon. *Eur Neurol*. 1979;18(3):157–165.

215. Asbell PA, Lemp MA. *Dry Eye Disease*. Thieme; 2006.

216. Ongerboer de Visser BW. Anatomical and functional organization of reflexes involving the trigeminal system in man: jaw reflex, blink reflex, corneal reflex, and exteroceptive suppression. *Adv Neurol*. 1983;39:727–738.

217. Mori A, Oguchi Y, Goto E, et al. Efficacy and safety of infrared warming of the

eyelids. *Cornea*. 1999;18(2):188–193.

218. Abelson MB, Holly FJ. A tentative mechanism for inferior punctate keratopathy. *Am J Ophthalmol*. 1977;83(6):866–869.

219. Doane MG. Interactions of eyelids and tears in corneal wetting and the dynamics of the normal human eyeblink. *Am J Ophthalmol*. 1980;89(4):507–516.

220. Collins MJ, Iskander DR, Saunders A, Hook S, Anthony E, Gillon R. Blinking patterns and corneal staining. *Eye Contact Lens*. 2006;32(6):287–293.

221. Pult H, Riede-Pult BH, Murphy PJ. The relation between blinking and conjunctival folds and dry eye symptoms. *Optometry & Vision Science*. 2013;90(10):1-7.

222. McMonnies CW. Incomplete blinking: exposure keratopathy, lid wiper epitheliopathy, dry eye, refractive surgery, and dry contact lenses. *Cont Lens Anterior Eye*. 2007;30(1):37–51.

223. Vold SD, Carroll RP, Nelson JD. Dermatochalasis and dry eye. *Am J Ophthalmol*. 1993;115(2):216–220.

224. Murube J, Murube E. Near vision accommodation in horizontality with VDT: why low blinking and dry eye? *Adv Exp Med Biol*. 2002;506(Pt B):1205–1211.

225. Korb DR, Blackie CA, McNally EN. Evidence suggesting that the keratinized portions of the upper and lower lid margins do not make complete contact during deliberate blinking. *Cornea*. 2013;32(4):491–495.

226. Pult H, Riede-Pult BH, Murphy PJ. A new perspective on spontaneous blinks. *Ophthalmology*. 2013;120(5):1086–1091.

227. Doughty MJ. Consideration of three types of spontaneous eyeblink activity in normal humans: during reading and video display terminal use, in primary gaze, and while in conversation. *Optometry & Vision Science*. 2001;78(10):712–725.

228. King DC, Michels KM. Muscular tension and the human blink rate. *J Exp Psychol*. 1957;53(2):113–116.

229. Carney LG, Hill RM. The nature of normal blinking patterns. *Acta Ophthalmologica*. 1982;60(3):427–433.

230. Zaman ML, Doughty MJ, Button NF. The exposed ocular surface and its relationship to spontaneous eyeblink rate in elderly caucasians. *Exp Eye Res*. 1998;67(6):681–686.

231. Sun WS, Baker RS, Chuke JC, et al. Age-related changes in human blinks. Passive and active changes in eyelid kinematics. *Invest Ophthalmol Vis Sci*. 1997;38(1):92–99.

232. Zametkin AJ, Stevens JR, Pittman R. Ontogeny of spontaneous blinking and of habituation of the blink reflex. *Ann Neurol*. 1979;5(5):453–457.

233. Bentivoglio AR, Bressman SB, Cassetta E, Carretta D, Tonali P, Albanese A. Analysis of blink rate patterns in normal subjects. *Mov Disord*. 1997;12(6):1028–1034.

234. Peshori KR, Schicatano EJ, Gopalaswamy R, Sahay E, Evinger C. Aging of the trigeminal blink system. *Experimental brain research Experimentelle Hirnforschung Expérimentation cérébrale*. 2001;136(3):351–363.

235. Ponder E, Kennedy WP. On the Act of Blinking. *Quart J Exp Physiol;* 1928:89–110.

236. Zaman ML, Doughty MJ. Some methodological issues in the assessment of the spontaneous eyeblink frequency in man. *Ophthalmic Physiol Opt*. 1997;17(5):421–432.

237. Sibony PA, Evinger C, Manning KA. Eyelid movements in facial paralysis. *Arch Ophthalmol*. 1991;109(11):1555–1561.

238. Garcia DM, Messias A, Costa LO, Pinto CT, Barbosa JC, Cruz AAV. Spontaneous blinking in patients with Graves' upper eyelid retraction. *Current Eye Research*. 2010;35(6):459–465.

239. Bristow D, Haynes J-D, Sylvester R, Frith CD, Rees G. Blinking suppresses the neural response to unchanging retinal stimulation. *Curr Biol*. 2005;15(14):1296–1300.

240. Ridder WH, Tomlinson A. Spectral characteristics of blink suppression in normal observers. *Vision Res*. 1995;35(18):2569–2578.

241. Ridder WH, Tomlinson A. A comparison of saccadic and blink suppression in normal observers. *Vision Res*. 1997;37(22):3171–3179.

242. Thomas LE, Irwin DE. Voluntary eyeblinks disrupt iconic memory. *Percept Psychophys*. 2006;68(3):475–488.

243. Holly FJ. Tear film physiology. *Am J Optom Physiol Opt*. 1980;57(4):252–257.

244. Holly FJ. Physical chemistry of the normal and disordered tear film. *Trans Ophthalmol Soc U K*. 1985;104 (Pt 4):374–380.

245. Doane MG. Blinking and the mechanics of the lacrimal drainage system. *Ophthalmology*. 1981;88(8):844–851.

246. Korb DR, Baron DF, Herman JP, et al. Tear film lipid layer thickness as a function of blinking. *Cornea*. 1994;13(4):354–359.

247. Tiffany JM. The role of meibomian secretion in the tears. *Trans Ophthalmol Soc U K*. 1985;104 (Pt 4):396–401.

248. Linton RG, Curnow DH, Riley WJ. The meibomian glands: an investigation into the secretion and some aspects of the physiology. *British Journal of Ophthalmology*. 1961;45(11):718–723.

249. Tsubota K, Hata S, Okusawa Y, Egami F, Ohtsuki T, Nakamori K. Quantitative videographic analysis of blinking in normal subjects and patients with dry eye. *Arch Ophthalmol*. 1996;114(6):715–720.

250. Kojima M, Shioiri T, Hosoki T, Sakai M, Bando T, Someya T. Blink rate variability in patients with panic disorder: new trial using audiovisual stimulation. *Psychiatry Clin Neurosci*. 2002;56(5):545–549.

251. Mackintosh JH, Kumar R, Kitamura T. Blink rate in psychiatric illness. *The British Journal of Psychiatry*. 1983;143(1):55–57.

252. Kaneko K, Sakamoto K. Spontaneous blinks as a criterion of visual fatigue during prolonged work on visual display terminals. *Percept Mot Skills*. 2001;92(1):234–250.

253. Stern JA, Boyer D, Schroeder D. Blink rate: a possible measure of fatigue. *Hum Factors*. 1994;36(2):285–297.

254. Barbato G, De Padova V, Paolillo AR, Arpaia L, Russo E, Ficca G. Increased spontaneous eye blink rate following prolonged wakefulness. *Physiol Behav*. 2007;90(1):151–154.

255. Barbato G, Ficca G, Muscettola G, Fichele M, Beatrice M, Rinaldi F. Diurnal variation in spontaneous eye-blink rate. *Psychiatry Res*. 2000;93(2):145–151.

256. Crevits L, Simons B, Wildenbeest J. Effect of sleep deprivation on saccades and eyelid blinking. *Eur Neurol*. 2003;50(3):176–180.

257. Barbato G, Ficca G, Beatrice M, Casiello M, Muscettola G, Rinaldi F. Effects of sleep deprivation on spontaneous eye blink rate and alpha EEG power. *Biol Psychiatry*. 1995;38(5):340–341.

258. Lal SKL, Craig A. Driver fatigue: electroencephalography and psychological assessment. *Psychophysiology*. 2002;39(3):313–321.

259. Morris TL, Miller JC. Electrooculographic and performance indices of fatigue during simulated flight. *Biological Psychology*. 1996;42(3):343–360.

260. Mori A, Egami F, Nakamori K, et al. Quantitative videographic analysis of blink patterns of newscasters. *Graefes Arch Clin Exp Ophthalmol*. 2008;246(10):1449–1453.

261. Karson CN, Berman KF, Donnelly EF, Mendelson WB, Kleinman JE, Wyatt RJ. Speaking, thinking, and blinking. *Psychiatry Res*. 1981;5(3):243–246.

262. Cho P, Sheng C, Chan C, Lee R, Tam J. Baseline blink rates and the effect of visual task difficulty and position of gaze. *Current Eye Research*.

2000;20(1):64–70.

263. Freudenthaler N, Neuf H, Kadner G, Schlote T. Characteristics of spontaneous eyeblink activity during video display terminal use in healthy volunteers. *Graefes Arch Clin Exp Ophthalmol*. 2003;241(11):914–920.

264. Tsubota K, Nakamori K. Dry eyes and video display terminals. *N Engl J Med*. 1993;328(8):584.

265. Schlote T, Kadner G, Freudenthaler N. Marked reduction and distinct patterns of eye blinking in patients with moderately dry eyes during video display terminal use. *Graefes Arch Clin Exp Ophthalmol*. 2004; 242(4):306–312.

266. Colzato LS, van den Wildenberg WPM, Hommel B. Reduced spontaneous eye blink rates in recreational cocaine users: evidence for dopaminergic hypoactivity. *PLoS ONE*. 2008;3(10):e3461.

267. Yap M. Tear break-up time is related to blink frequency. *Acta Ophthalmologica*. 1991;69(1):92–94.

268. Gilbard JP, Farris RL. Ocular surface drying and tear film osmolarity in thyroid eye disease. *Acta Ophthalmologica*. 1983;61(1):108–116.

269. Borges FP, Garcia DM, Cruz AAVE. Distribution of spontaneous inter-blink interval in repeated measurements with and without topical ocular anesthesia. *Arq Bras Oftalmol*. 2010;73(4):329–332.

270. Situ P, Simpson TL, Jones LW, Fonn D. Conjunctival and corneal hyperesthesia in subjects with dryness symptoms. *Optom Vis Sci*. 2008;85(9):867–872.

271. Ntola A. An Investigation of the Relationship Between Corneal Sensitivity and Blinking; *PhD Thesis*. *Cardiff: University of Cardiff;* 2006.

272. Doughty MJ, Naase T, Button NF. Frequent spontaneous eyeblink activity associated with reduced conjunctival surface (trigeminal nerve) tactile sensitivity. *Graefes Arch Clin Exp Ophthalmol*. 2009;247(7):939–946.

273. Varikooty J, Simpson TL. The interblink interval I: the relationship between sensation intensity and tear film disruption. *Invest Ophthalmol Vis Sci*. 2009;50(3):1087–1092.

274. Al-Abdulmunem M. Relation between tear breakup time and spontaneous blink rate. *Int Contact Lens Clin*. 1999;26(5):117–120.

275. Prause JU, Norn M. Relation between blink frequency and break-up time? *Acta Ophthalmologica*. 1987;65(1):19–22.

276. Tsubota K, Nakamori K. Effects of ocular surface area and blink rate on tear dynamics. *Arch Ophthalmol*. 1995;113(2):155–158.

277. Acosta MC, Gallar J, Belmonte C. The influence of eye solutions on blinking and ocular comfort at rest and during work at video display terminals. *Exp Eye Res*. 1999;68(6):663–669.

278. Holly FJ. Tear film physiology and contact lens wear. II. Contact lens-tear film interaction. *Am J Optom Physiol Opt*. 1981;58(4):331–341.

279. Carney LG, Hill RM. Variations in blinking bahaviour during soft lens wear. *Faculty of Health; Institute of Health and Biomedical Innovation*. 1984.

280. Hill RM, Carney LG. The effect of hard lens wear on blinking behaviour. *Faculty of Health; Institute of Health and Biomedical Innovation*. 1984.

281. Rushworth G. Observations on blink reflexes. *J Neurol Neurosurg Psychiatr*. 1962;25(2):93-108.

282. Bentivoglio AR, Daniele A, Albanese A, Tonali PA, Fasano A. Analysis of blink rate in patients with blepharospasm. *Mov Disord*. 2006;21(8):1225–1229.

283. Day RM. Ocular manifestations of thyroid disease. Current concepts. *Arch Ophthalmol*. 1960;64:324–341.

284. Vega J, Simpson T, Fonn D. A noncontact pneumatic esthesiometer for measurement of ocular sensitivity: a preliminary report. *Cornea*. 1999;18(6):675-681.

285. Purslow C, Wolffsohn JS. Ocular surface temperature. *Eye & Contact Lens: Science & Clinical Practice*. 2005;31(3):117–123.

286. Cornsweet TN. The staircase-method in psychophysics. *The American Journal of Psychology*. 1962;75(3):485.

287. Murphy PJ. An examination of human corneal sensitivity by non-invasive methods. *PhD Thesis, Glasgow University;* 1996:1–245.

288. Golebiowski B, Papas EB, Stapleton F. Factors affecting corneal and conjunctival sensitivity measurement. *Optom Vis Sci*. 2008;85(4):241–246.

289. Golebiowski B, Papas EB, Stapleton F. Corneal and conjunctival sensory function: the impact on ocular surface sensitivity of change from low to high oxygen transmissibility contact lenses. *Invest Ophthalmol Vis Sci*. 2012.

290. Navascues-Cornago M, Maldonado-Codina C, Morgan PB. Mechanical sensitivity of the human conjunctiva. *Cornea*. 2014;33(8):855–859.

291. Golebiowski B, Chim K, So J, Jalbert I. Lid margins: sensitivity, staining, meibomian gland dysfunction, and symptoms. *Optom Vis Sci*. 2012;89(10):1–7.

292. Roszkowska AM, Colosi P, Ferreri FM, Galasso S. Age-related modifications of corneal sensitivity. *Ophthalmologica*. 2004;218(5):350–355.

293. Millodot M, Larson W. New measurements of corneal sensitivity: a preliminary report. *American Journal of Optometry and archives of American Academy of Optometry*. 1969;46(4):261–265.

294. Velasco M, Bermúdez F, Romero J, Hita E. Variations in corneal sensitivity with hydrogel contact lenses. *Acta Ophthalmologica*. 1994;72(1):53–56.

295. Situ P, Simpson TL, Fonn D. Eccentric variation of corneal sensitivity to pneumatic stimulation at different temperatures and with CO2. *Exp Eye Res*. 2007;85(3):400–405.

296. Patel DV, Tavakoli M, Craig JP, Efron N, McGhee CNJ. Corneal sensitivity and slit scanning in vivo confocal microscopy of the subbasal nerve plexus of the normal central and peripheral human cornea. *Cornea*. 2009;28(7):735–740.

297. Brennan NA, Maurice DM. Brennan: Corneal aesthesiometry with a carbon dioxide laser (ARVO Abstract). *Invest Ophthalmol Vis Sci*. 1989;30(S148).

298. Draeger J, Schloot W, Wirt H. Interindividual differences of corneal sensitivity. genetic aspects. *Ophthalmic paediatrics and genetics*. 1985;6(1-2):291–295.

299. Bourcier T, Acosta MC, Borderie V, et al. Decreased corneal sensitivity in patients with dry eye. *Invest Ophthalmol Vis Sci*. 2005;46(7):2341–2345.

300. Murphy PJ, Patel S, Kong N, Ryder REJ, Marshall J. Noninvasive assessment of corneal sensitivity in young and elderly diabetic and nondiabetic subjects. *Invest Ophthalmol Vis Sci*. 2004;45(6):1737–1742.

301. Millodot M. The influence of age on the sensitivity of the cornea. *Invest Ophthalmol Vis Sci*. 1977;16(3):240–242.

302. Benítez-Del-Castillo JM, Acosta MC, Wassfi MA, et al. Relation between corneal innervation with confocal microscopy and corneal sensitivity with noncontact esthesiometry in patients with dry eye. *Invest Ophthalmol Vis Sci*. 2007;48(1):173–181.

303. De Paiva CS, Pflugfelder SC. Corneal epitheliopathy of dry eye induces hyperesthesia to mechanical air jet stimulation. *Am J Ophthalmol*. 2004;137(1):109–115.

304. Toit du R, Situ P, Simpson T, Fonn D. The effects of six months of contact lens wear on the tear film, ocular surfaces, and symptoms of presbyopes. *Optom Vis Sci*. 2001;78(6):455–462.

305. Millodot M. Diurnal variation of corneal sensitivity. *British Journal of Ophthalmology*. 1972;56(11):844–847.

306. Toit du R, Vega JA, Fonn D, Simpson T. Diurnal variation of corneal sensitivity and thickness. *Cornea*. 2003;22(3):205–209.

307. Millodot M, O'Leary DJ. Loss of corneal sensitivity with lid closure in humans.

Exp Eye Res. 1979;29(4):417–421.

308. Millodot M. Do blue-eyed people have more sensitive corneas than brown-eyed people? *Nature*. 1975;5504:151–152.

309. Guttridge NM. Changes in ocular and visual variables during the menstrual cycle. *Ophthalmic Physiol Opt*. 1994;14(1):38–48.

310. Stockhorst U, Pietrowsky R. Olfactory perception, communication, and the nose-to-brain pathway. *Physiol Behav*. 2004;83(1):3–11.

311. Blomqvist A. Sex hormones and pain: a new role for brain aromatase? *J Comp Neurol*. 2000;423(4):549–551.

312. Aloisi AM. Gonadal hormones and sex differences in pain reactivity. *Clin J Pain*. 2003;19(3):168–174.

313. Rosenberg ME, Tervo TM, Gallar J, et al. Corneal morphology and sensitivity in lattice dystrophy type II (familial amyloidosis, Finnish type). *Invest Ophthalmol Vis Sci*. 2001;42(3):634–641.

314. Rosenberg ME, Tervo TM, Immonen IJ, Müller LJ, Gronhagen-Riska C, Vesaluoma MH. Corneal structure and sensitivity in type 1 diabetes mellitus. *Invest Ophthalmol Vis Sci*. 2000;41(10):2915–2921.

315. Rosenberg ME, Tervo TMT, Müller LJ, Moilanen JAO, Vesaluoma MH. In vivo confocal microscopy after herpes keratitis. *Cornea*. 2002;21(3):265–269.

316. Vesaluoma MH, Sankila EM, Gallar J, et al. Autosomal recessive cornea plana: in vivo corneal morphology and corneal sensitivity. *Invest Ophthalmol Vis Sci*. 2000;41(8):2120–2126.

317. Dogru M, Yildiz M, Baykara M, Özçetin H, Ertürk H. Corneal sensitivity and ocular surface changes following preserved amniotic membrane transplantation for nonhealing corneal ulcers. *Eye*. 2003;17(2):139–148.

318. Schwartz DE. Corneal sensitivity in diabetics. *Arch Ophthalmol*. 1974;91(3):174–178.

319. Detorakis ET, Koukoula S, Chrisohoou F, Konstas AG, Kozobolis VP. Central corneal mechanical sensitivity in pseudoexfoliation syndrome. *Cornea*. 2005;24(6):688–691.

320. Adatia FA, Michaeli-Cohen A, Naor J, Caffery B, Bookman A, Slomovic A. Correlation between corneal sensitivity, subjective dry eye symptoms and corneal staining in Sjögren's syndrome. *Can J Ophthalmol*. 2004;39(7):767–771.

321. Xu KP, Yagi Y, Tsubota K. Decrease in corneal sensitivity and change in tear function in dry eye. *Cornea*. 1996;15(3):235–239.

322. Hoşal BM, Ornek N, Zilelioğlu G, Elhan AH. Morphology of corneal nerves and corneal sensation in dry eye: a preliminary study. *Eye (Lond)*. 2005;19(12):1276–1279.

323. Benitez-del-Castillo JM, del Rio T, Iradier T, Hernández JL, Castillo A, Garcia-Sanchez J. Decrease in tear secretion and corneal sensitivity after laser in situ keratomileusis. *Cornea*. 2001;20(1):30–32.

324. Tuisku IS, Konttinen YT, Konttinen LM, Tervo TM. Alterations in corneal sensitivity and nerve morphology in patients with primary Sjögren's syndrome. *Exp Eye Res*. 2008;86(6):879–885.

325. Situ P, Simpson TL, Fonn D, Jones LW. Conjunctival and corneal pneumatic sensitivity is associated with signs and symptoms of ocular dryness. *Invest Ophthalmol Vis Sci*. 2008;49(7):2971–2976.

326. Belmonte C, Aracil A, Acosta MC, Luna C, Gallar J. Nerves and sensations from the eye surface. *Ocul Surf*. 2004;2(4):248–253.

327. Lawrenson JG, Edgar DF, Tanna GK, Gudgeon AC. Comparison of the tolerability and efficacy of unit-dose, preservative-free topical ocular anaesthetics. *Ophthalmic Physiol Opt*. 1998;18(5):393–400.

328. Murphy PJ, Blades KJ, Patel S. Effect of 0.4% benoxinate hydrochloride on corneal sensitivity, measured using the non-contact corneal aesthesiometer (NCCA). *Optom Vis Sci*. 1997;74(12):1025–1029.

329. Acosta MC, Berenguer-Ruiz L, García-Gálvez A, Perea-Tortosa D, Gallar J, Belmonte C. Changes in mechanical, chemical, and thermal sensitivity of the cornea after topical application of nonsteroidal anti-inflammatory drugs. *Invest Ophthalmol Vis Sci*. 2005;46(1):282–286.

330. Kanellopoulos AJ, Pallikaris IG, Donnenfeld ED, Detorakis S, Koufala K, Perry HD. Comparison of corneal sensation following photorefractive keratectomy and laser in situ keratomileusis. *J Cataract Refract Surg*. 1997;23(1):34–38.

331. Pérez-Santonja JJ, Sakla HF, Cardona C, Chipont E, Alió JL. Corneal sensitivity after photorefractive keratectomy and laser in situ keratomileusis for low myopia. *Am J Ophthalmol*. 1999;127(5):497–504.

332. Murphy PJ, Corbett MC, O'Brart DP, Verma S, Patel S, Marshall J. Loss and recovery of corneal sensitivity following photorefractive keratectomy for myopia. *Journal of refractive surgery (Thorofare, NJ : 1995)*. 1999;15(1):38–45.

333. Gallar J, Acosta MC, Moilanen JAO, Holopainen JM, Belmonte C, Tervo TMT. Recovery of corneal sensitivity to mechanical and chemical stimulation after laser in situ keratomileusis. *Journal of refractive surgery (Thorofare, NJ : 1995)*. 2004;20(3):229–235.

334. Stapleton F, Hayward KB, Bachand N, et al. Evaluation of corneal sensitivity to mechanical and chemical stimuli after LASIK: a pilot study. *Eye & Contact Lens: Science & Clinical Practice*. 2006;32(2):88–93.

335. Tervo K, Latvala TM, Tervo TM. Recovery of corneal innervation following photorefractive keratoablation. *Arch Ophthalmol*. 1994;112(11):1466–1470.

336. Linna T, Tervo T. Real-time confocal microscopic observations on human corneal nerves and wound healing after excimer laser photorefractive keratectomy. *Current Eye Research*. 1997;16(7):640–649.

337. Linna TU, Pérez-Santonja JJ, Tervo KM, Sakla HF, Alió y Sanz JL, Tervo TM. Recovery of corneal nerve morphology following laser in situ keratomileusis. *Exp Eye Res*. 1998;66(6):755–763.

338. Ishikawa T, del Cerro M, Liang FQ, Loya N, Aquavella JV. Corneal sensitivity and nerve regeneration after excimer laser ablation. *Cornea*. 1994;13(3):225–231.

339. Latvala T, Linna T, Tervo T. Corneal nerve recovery after photorefractive keratectomy and laser in situ keratomileusis. *International Ophthalmology Clinics*. 1996;36(4):21.

340. Darwish T, Brahma A, O'Donnell C, Efron N. Subbasal nerve fiber regeneration after LASIK and LASEK assessed by noncontact esthesiometry and in vivo confocal microscopy: prospective study. *J Cataract Refract Surg*. 2007;33(9):1515–1521.

341. Richter A, Slowik C, Somodi S, Vick HP, Guthoff R. Corneal reinnervation following penetrating keratoplasty-correlation of esthesiometry and confocal microscopy. *Ger J Ophthalmol*. 1996;5(6):513–517.

342. Tervo T, Vannas A, Tervo K, Holden BA. Histochemical evidence of limited reinnervation of human corneal grafts. *Acta Ophthalmologica*. 1985;63(2):207–214.

343. Mathers WD, Jester JV, Lemp MA. Return of human corneal sensitivity after penetrating keratoplasty. *Arch Ophthalmol*. 1988;106(2):210–211.

344. Ruben M, Colebrook E. Keratoplasty sensitivity. *British Journal of Ophthalmology*. 1979;63(4):265–267.

345. Stamer L, Böhnke M, Draeger J. [Development of corneal sensitivity following keratoplasty]. *Fortschr Ophthalmol*. 1987;84(5):432–435.

346. Millodot M. Effect of the length of wear of contact lenses on corneal sensitivity. *Acta Ophthalmologica*. 1976;54(6):721–730.

347. Millodot M. Does the long term wear of contact lenses produce a loss of corneal sensitivity? *Experientia*. 1977;33(11):1475–1476.

348. Millodot M. Effect of long-term wear of hard contact lenses on corneal sensitivity. *Arch Ophthalmol*. 1978;96(7):1225–1227.

349. Lowther GE, Hill RM. Sensitivity threshold of the lower lid margin in the course of adaptation to contact lenses. *American Journal of Optometry and archives of American Academy of Optometry*. 1968;45(9):587–594.

350. Knoll HA, Williams J. Effects of hydrophilic contact lenses on corneal sensitivity. *American Journal of Optometry and archives of American Academy of Optometry*. 1970;47(7):561–563.

351. Bergenske PD, Polse KA. The effect of rigid gas permeable lenses on corneal sensitivity. *J Am Optom Assoc*. 1987;58(3):212–215.

352. Millodot M, O'Leary DJ. Effect of oxygen deprivation on corneal sensitivity. *Acta Ophthalmologica*. 1980;58(3):434–439.

353. Situ P, Simpson TL, Jones LW, Fonn D. Effects of silicone hydrogel contact lens wear on ocular surface sensitivity to tactile, pneumatic mechanical, and chemical stimulation. *Invest Ophthalmol Vis Sci*. 2010;51(12):6111–6117.

354. Murphy PJ, Patel S, Marshall J. The effect of long-term, daily contact lens wear on corneal sensitivity. *Cornea*. 2001;20(3):264–269.

355. Millodot M. Effect of soft lenses on corneal sensitivity. *Acta Ophthalmologica*. 1974;52(5):603–608.

356. Polse KA. Etiology of corneal sensitivity changes accompanying contact lens wear. *Invest Ophthalmol Vis Sci*. 1978;17(12):1202–1206.

357. Lum E, Golebiowski B, Gunn R, Babhoota M, Swarbrick H. Corneal sensitivity with contact lenses of different mechanical properties. *Optom Vis Sci*. 2013;90(9):954–960.

358. Brennan NA, Bruce AS. Esthesiometry as an indicator of corneal health. *Optom Vis Sci*. 1991;68(9):699–702.

359. Gallar J, Tervo T, Neira W, et al. Selective changes in human corneal sensation associated with herpes simplex keratitis. *Invest Ophthalmol Vis Sci*. 2010.

360. Tesón M, Calonge M, Fernandez I, Stern ME, González-García MJ. Characterization by Belmonte's gas esthesiometer of mechanical, chemical, and thermal corneal sensitivity thresholds in a normal population. *Invest Ophthalmol Vis Sci*. 2012;53(6):3154–3160.

361. Golebiowski B, Lim M, Papas E, Stapleton F. Understanding the stimulus of an air-jet aesthesiometer: computerised modelling and subjective interpretation. *Ophthalmic and Physiological Optics*. 2013;33(2):104–113.

362. Murphy PJ, Ntola AM. Prolonged corneal anaesthesia by proxymetacaine hydrochloride detected by a thermal cooling stimulus. *Cont Lens Anterior Eye*.

2009;32(2):84–87.

363. Murphy PJ, Lawrenson JG, Patel S, Marshall J. Reliability of the non-contact corneal aesthesiometer and its comparison with the Cochet-Bonnet aesthesiometer. *Ophthalmic and Physiological Optics*. 1998;18(6):532–539.

364. Millodot M. A review of research on the sensitivity of the cornea. *Ophthalmic Physiol Opt*. 1984;4(4):305–318.

365. Patel S, Farrell JC. Age-related changes in precorneal tear film stability. *Optom Vis Sci*. 1989;66(3):175–178.

366. Horven I. Corneal temperature in normal subjects and arterial occlusive disease. *Acta Ophthalmologica*. 1975;53(6):863–874.

367. Aliò J, Padron M. Influence of age on the temperature of the anterior segment of the eye. Measurements by infrared thermometry. *Ophthalmic Res*. 1982;14(3):153–159.

368. Girardin F, Orgül S, Erb C, Flammer J. Relationship between corneal temperature and finger temperature. *Arch Ophthalmol*. 1999;117(2):166–169.

369. Schiffman RM, Christianson MD, Jacobsen G, Hirsch JD, Reis BL. Reliability and validity of the Ocular Surface Disease Index. *Arch Ophthalmol*. 2000;118(5):615–621.

370. Patel S, Bevan R, Farrell JC. Diurnal variation in precorneal tear film stability. *Am J Optom Physiol Opt*. 1988;65(3):151–154.

371. Johnson ME, Murphy PJ. Changes in the tear film and ocular surface from dry eye syndrome. *Prog Retin Eye Res*. 2004;23(4):449–474.

372. Schwartz B. Environmental temperature and the ocular temperature gradient. *Arch Ophthalmol*. 1965;74:237–243.

373. Kolstad A. Corneal sensivity by low temperatures. *Acta Ophthalmologica*. 1970;48(4):789–793.

374. Freeman RD, Fatt I. Environmental influences on ocular temperature. *Investigative ophthalmology*. 1973;12(8):596–602.

375. Michel M. Bestimmung des kontaktlinsenrelevanten okulären Trockenheitsgrades anhand validierter und optimierter Patienten-Fragebögen und objektiver Tests. *Diplomarbeit, Fachhochschule Jena, SiTec, Studiengang Augenoptik;* 2008.

376. Himebaugh NL, Begley CG, Bradley A, Wilkinson JA. Blinking and tear break-up during four visual tasks. *Optom Vis Sci*. 2009;86(2):E106–14.

377. Walt JG, Rowe MM, Stern KL. Evaluating the functional impact of dry eye: the Ocular Surface Disease Index. *Drug Inf J*. 1997;31:1436.

378. Schiffman RM, Christianson MD, Jacobsen G, Hirsch JD, Reis BL. Reliability and validity of the ocular surface disease Index. *Arch Ophthalmol*. 2000;118(5):615–621.

379. Dougherty BE, Nichols JJ, Nichols KK. Rasch analysis of the ocular surface disease index (OSDI). *Invest Ophthalmol Vis Sci*. 2011;52(12):8630–8635.

380. Seddon JM, Sahagian CR, Glynn RJ, Sperduto RD, Gragoudas ES. Evaluation of an iris color classification system. The eye disorders case-control study group. *Invest Ophthalmol Vis Sci*. 1990;31(8):1592–1598.

381. Henderson L, Bond D, Simpson T. The association between eye color and corneal sensitivity measured using a Belmonte esthesiometer. *Optom Vis Sci*. 2005;82(7):629–632.

382. Hale BD, Landers DM, Snyder Bauer R, Goggin NL. Iris pigmentation and fractionated reaction and reflex time. *Biological Psychology*. 1980;10:57–67.

383. Guillon JP. Non-invasive Tearscope Plus routine for contact lens fitting. *Cont Lens Anterior Eye*. 1998;21 Suppl 1:S31–40.

384. Mengher LS, Bron AJ, Tonge SR, Gilbert DJ. Effect of fluorescein instillation on the pre-corneal tear film stability. *Current Eye Research*. 1985;4(1):9–12.

385. Patel S, Murray D, McKenzie A, Shearer DS, McGrath BD. Effects of fluorescein on tear breakup time and on tear thinning time. *Am J Optom Physiol Opt*. 1985;62(3):188–190.

386. Armstrong RA. When to use the Bonferroni correction. *Ophthalmic and Physiological Optics*. 2014;34(5):1-7.

387. Craig JP, Tomlinson A. Importance of the lipid layer in human tear film stability and evaporation. *Optometry & Vision Science*. 1997;74(1):8–13.

388. Craig JP, Purslow C, Murphy PJ, Wolffsohn JSW. Effect of a liposomal spray on the pre-ocular tear film. *Cont Lens Anterior Eye*. 2010;33(2):83–87.

389. Maïssa C, Guillon M. Tear film dynamics and lipid layer characteristics--effect of age and gender. *Contact Lens and Anterior Eye*. 2010;33(4):176–182.

390. Keeler. Introduction and guided tour to the benefits of the Keeler Tearscope-plus. 1998:1–22.

391. Yokoi N, Komuro A. Non-invasive methods of assessing the tear film. *Exp Eye Res*. 2004;78(3):399–407.

392. Isreb MA, Greiner JV, Korb DR, et al. Correlation of lipid layer thickness measurements with fluorescein tear film break-up time and Schirmer's test. *Eye (Lond)*. 2003;17(1):79–83.

393. Craig JP, Singh I, Tomlinson A, Morgan PB, Efron N. The role of tear

physiology in ocular surface temperature. *Eye (Lond)*. 2000;14 (Pt 4):635–641.

394. Ousler GW, Hagberg KW, Schindelar M, Welch D, Abelson MB. The ocular protection index. *Cornea*. 2008;27(5):509–513.

395. Yokoi N, Yamada H, Mizukusa Y, et al. Rheology of tear film lipid layer spread in normal and aqueous tear-deficient dry eyes. *Invest Ophthalmol Vis Sci*. 2008;49(12):5319–5324.

396. Belmonte C, Brock JA, Viana F. Converting cold into pain. *Experimental brain research Experimentelle Hirnforschung Expérimentation cérébrale*. 2009;196(1):13–30.

397. Morgan PB, Soh MP, Efron N, Tullo AB. Potential applications of ocular thermography. *Optom Vis Sci*. 1993;70(7):568–576.

398. Hamano H, Minami S, Sugimori Y. Experiments in thermometry of the anterior portion of the eye wearing a contact lens by means of infra-red thermometer. *Contacto*; 1969:12–22.

399. Fatt I, Chaston J. Temperature of a contact lens on the eye. *International Contact Lens Clinic*; 1980:195–198.

400. Hill RM, Leighton AJ. Temperature changes of human cornea and tears under a contact lens. II. Effects of intermediate lid apertures and gaze. *American Journal of Optometry and archives of American Academy of Optometry*. 1965;42:71–77.

401. Efron N, Young G, Brennan NA. Ocular surface temperature. *Current Eye Research*. 1989;8(9):901–906.

402. Rolando M, Refojo MF, Kenyon KR. Increased tear evaporation in eyes with keratoconjunctivitis sicca. *Arch Ophthalmol*. 1983;101(4):557–558.

403. Mathers WD, Binarao G, Petroll M. Ocular water evaporation and the dry eye: A new measuring device. *Cornea*. 1993;12(4):335.

404. Morgan PB, Tullo AB, Efron N. Infrared thermography of the tear film in dry eye. *Eye (Lond)*. 1995;9 (Pt 5):615–618.

405. Purslow C, Wolffsohn J. The relation between physical properties of the anterior eye and ocular surface temperature. *Optom Vis Sci*. 2007;84(3):197–201.

406. van den Berg TJ, Speert JK, de Waard PW. Dependence of intraocular straylight on pigmentation and light transmission through the ocular wall. *Vision Res*. 1991;31(7-8):1361–1367.

407. Yaar M, Eller MS, DiBenedetto P, et al. The trk family of receptors mediates nerve growth factor and neurotrophin-3 effects in melanocytes. *J Clin Invest*. 1994;94(4):1550–1562.

408. Davies AM. Neurotrophins: more to NGF than just survival. *Curr Biol*. 2000;10(10):R374–6.

409. Hensel H. Recent advances in thermoreceptor physiology. *Journal of thermal Biology*. 1983;8:3–6.

410. Belmonte C, Gallar J. Cold thermoreceptors, unexpected players in tear production and ocular dryness sensations. *Invest Ophthalmol Vis Sci*. 2011;52(6):3888–3892.

411. Parra A, Madrid R, Echevarria D, et al. Ocular surface wetness is regulated by TRPM8-dependent cold thermoreceptors of the cornea. *Nature Medicine*. 2010;16(12):1396–1399.

412. Hirata H, Oshinsky ML. Ocular dryness excites two classes of corneal afferent neurons implicated in basal tearing in rats: involvement of transient receptor potential channels. *J Neurophysiol*. 2012;107(4):1199–1209.

413. Pult H, Riede-Pult BH, Purslow C. A comparison of an eyelid-warming device to traditional compress therapy. *Optom Vis Sci*. 2012;89(7):E1035–41.

414. Purslow C. Evaluation of the ocular tolerance of a novel eyelid-warming device used for meibomian gland dysfunction. *Cont Lens Anterior Eye*. 2013.

415. Schäfer K, Braun HA, Kürten L. Analysis of cold and warm receptor activity in vampire bats and mice. *Pflugers Arch*. 1988;412(1-2):188–194.

416. Heinz M, Schäfer K, Braun HA. Analysis of facial cold receptor activity in the rat. *Brain Res*. 1990;521(1-2):289–295.

417. Shea VK, Perl ER. Sensory receptors with unmyelinated (C) fibers innervating the skin of the rabbit's ear. *J Neurophysiol*. 1985;54(3):491–501.

418. Gelber DA, Pfeifer MA, Broadstone VL, et al. Components of variance for vibratory and thermal threshold testing in normal and diabetic subjects. *J Diabetes Complicat*. 1995;9(3):170–176.

419. Fowler CJ, Carroll MB, Burns D, Howe N, Robinson K. A portable system for measuring cutaneous thresholds for warming and cooling. *J Neurol Neurosurg Psychiatr*. 1987;50(9):1211–1215.

420. Cohen J. A power primer. *Psychol Bull*. 1992;112(1):155–159.

421. Bilkhu PS, Naroo SA, Wolffsohn JS. Effect of a commercially available warm compress on eyelid temperature and tear film in healthy eyes. *Optom Vis Sci*. 2014;91(2):163–170.